Characterising the novel *MYB-TYK2* fusion gene in high-risk acute lymphoblastic leukaemia: oncogenic potential, effective therapeutic strategies and *in vitro* modelling of drug resistance mechanisms

Paniz Tavakoli Shirazi

B.Sc (Microbiology), MBIB (Biomedical)

Leukaemia Research Group

Precision Medicine Theme

South Australian Health and Medical Research Institute (SAHMRI)

School of Medicine

Faculty of Health and Medical Sciences

The University of Adelaide, South Australia

A thesis submitted in fulfilment of the requirements for the degree of Doctor of Philosophy 2021

Table of content

Abstract iv

Declaration vi

Acknowledgments vii

Publications ix

Conference abstracts and presentations x

Scholarships and awards xiii

Chapter1:Introduction 2

1.1. Acute Lymphoblastic Leukaemia 3

1.1.1. Clinical features of ALL 3

1.1.2. Immunophenotypic classification of ALL 4

1.1.3. Underlying biology of B-ALL 5

1.1.4. Genomic profiling and genomic subtypes of B-ALL 7

1.2. Ph-like ALL is a high-risk subtype 13

1.2.1. *JAK* family rearrangements 17

1.3. The role of Tyk2 in cancer 18

1.3.1. Can Aberrant Tyk2 levels cause leukaemia? 19

1.3.2. *TYK2* alterations occur in ALL patients 20

1.4. Cytokine signalling pathways 23

1.4.1. Tyk2 mediates cytokine signalling and activation of JAK/STAT pathway 24

1.4.2. Tyk2 mediates crosstalk with other oncogenic signalling pathways 25

1.4.3. The interplay in regulation and stabilisation of Tyk2 and STAT proteins 26

1.5. Potential therapeutic approaches in ALL 28

1.5.1. Conventional treatment regimen in ALL....28
1.5.2. Use of tyrosine kinase inhibitors and other small molecule inhibitors as targeted therapy can be of benefit in ALL....29
1.6. Development of TKI resistance, specifically to JAKi, occurs via reactivation of the JAK/STAT signalling pathway....32
1.6.1. Mechanism of resistance to ABLi....32
1.6.2. Mechanisms of resistance to JAKi....33
1.7. Concluding remarks....35
1.8. Summary and project aims....36
Chapter 2: Exploring the oncogenic and therapeutic target potential of the *MYB-TYK2* fusion gene in B-cell acute lymphoblastic leukemia....38
2.1 Supplementary Materials....84
Chapter 3: Constitutive JAK/STAT signaling is the primary mechanism of resistance to JAKi in *TYK2*-rearranged acute lymphoblastic leukemia....129
3.1 Supplementary Materials....165
4. Discussion and future direction....179
4.1 Introduction....180
4.2 Major findings....180
4.2.1 Expression of the MYB-TYK2 fusion gene induces B-ALL *in vivo*....181
4.2.2 The HDACi, vorinostat and the JAKi, cerdulatinib are efficacious against *MYB-TYK2*-altered disease....181
4.2.3 HDACi treatment can reverse the persistent JAK/STAT signalling in cerdulatinib resistant *MYB-TYK2*-altered disease....183

4.3 Limitations and future directions 184

4.3.1 Limitations of cerdulatinib and vorinostat incorporation into the treatment regimen of *TYK2*-rearranged ALL cases 184

4.3.2 Co-binding and transphosphorylation of Jak1 and Tyk2 and increased JAKi insensitivity in cells 185

4.3.3 *In vivo* modelling of JAKi resistance in *MYB-TYK2* mice and investigation of the pre-clinical efficacy of HDACi therapy against the resistance disease 186

4.3.4 Final Conclusions 186

References……188

Appendix……...213

Abstract

A growing number of *TYK2* activating alterations have been detected in acute lymphoblastic leukaemia (ALL) patients, including the *MYB-TYK2* fusion gene. *MYB-TYK2* was identified in a high risk (HR) Ph-ALL case and is associated with poor outcome. The transforming and leukaemogenic potential of activating *TYK2* alterations, including those of *MYB-TYK2*, requires clarification in the ALL setting. Tyk2 is a member of the JAK family of tyrosine kinases and similar to *JAK* fusions, may result in activation of JAK/STAT signalling, and potentially be amenable to JAK inhibitor (JAKi) therapy. In depth characterisation of the underlying mechanisms resulting in leukaemogenesis are warranted and will inform drug response and targetability potential. Moreover, since the development of clinical resistance to targeted therapies such as JAKi, broad investigation of effective small molecule inhibitors (SMIs) is essential. Exploration of the possible modes of drug resistance following long-term treatment and importantly, how to circumvent resistance development, will provide alternative therapies for JAKi resistance in *TYK2*-altered patients. Hence, this study aimed to 1) identify and characterise the mechanisms of oncogenicity and activated downstream signalling pathways in *MYB-TYK2* harbouring cells, 2) assess the efficacy of targeted therapeutics against *MYB-TYK2* altered disease and 3) determine the possible mechanisms of resistance to candidate therapy via *in vitro* models to inform alternative therapeutic approaches to overcome possible disease persistence and resistance.

In vitro and *in vivo* models were used to comprehensively model *MYB-TYK2*-altered disease. Depending on the downstream experiments, either cytokine-dependent Ba/F3 pro-B cells, *Arf*$^{-/-}$ pre-B primary mouse cells or NIH-3T3 cells, were retrovirally transduced with the *MYB-TYK2* fusion gene isolated from an ALL patient. The targetability of the *MYB-TYK2* fusion gene was investigated via high throughput screen (HTS) of 3088 cytotoxic and targeted compounds with further validation of candidates in pre-clinical models. Resistance modelling of the candidate JAKi cerdulatinib was achieved by gradual exposure of

cells expressing the *MYB-TYK2* fusion gene to increasing concentrations of cerdulatinib over several months.

This study elucidated the transformative ability and functional significance of the *MYB-TYK2* fusion gene to induce B-ALL *in vivo*. Results demonstrated the constitutive activation of JAK/STAT signalling due to expression of the *MYB-TYK2* fusion gene. HTS identified the HDACi, vorinostat and the HSP90i, tanespimycin as effective targeted therapeutics against cells harbouring the *MYB-TYK2* fusion gene *in vitro*. In addition, the sensitivity of the *MYB-TYK2* fusion gene was established to the novel JAKi, cerdulatinib. Both vorinostat and cerdulatinib demonstrated anti-leukaemic effects in pre-clinical *in vivo* models of the *MYB-TYK2* altered disease, resulting in a significantly reduced leukaemic burden. Further investigations into resistance following long-term exposure to cerdulatinib, indicated the likelihood of resistance to cerdulatinib therapy. Results suggested a persistent JAK/STAT activation despite Tyk2 inhibition via possible heterodimer formation with Jak1 and thus, Myb-Tyk2 trans-phosphorylation. This persistent signalling, however, was successfully reversed by HDACi treatment.

Overall, the findings presented in this thesis demonstrate, for the first time, the driving potential of *TYK2* activating alterations. Through robust modelling and rigorous testing of effective SMIs, this study identified novel therapeutic strategies using vorinostat and cerdulatinib against *MYB-TYK2*-altered disease. These results provide strong evidence for re-purposing of these drugs as an addition to a chemotherapy backbone for treatment of this highly aggressive subtype of B-ALL. Further insights into the resistance profile in response to cerdulatinib, as well as incorporation of targeted therapeutics to overcome this resistance, will assist high-risk patients in a clinical setting. These findings contribute to precision medicine approaches and will ultimately improve outcome and long-term survival for patients harbouring activating *TYK2* alterations.

Declaration

I certify that this work contains no material which has been accepted for the award of any other degree or diploma in my name, in any university or other tertiary institution and, to the best of my knowledge and belief, contains no material previously published or written by another person, except where due reference has been made in the text. In addition, I certify that no part of this work will, in the future, be used in a submission in my name, for any other degree or diploma in any university or other tertiary institution without the prior approval of the University of Adelaide and where applicable, any partner institution responsible for the joint-award of this degree.

I give permission for the digital version of my thesis to be made available on the web, via the University's digital research repository, the Library Search and also through web search engines, unless permission has been granted by the University to restrict access for a period of time.

Paniz Tavakoli Shirazi

02/02/2021

Acknowledgments

I would firstly like to express my sincerest appreciation and gratitude to Prof. Deborah White, Dr. Laura Eadie and Dr. Sue Heatley for their mentorship, expertise, guidance and tremendous support during the past 4 years. None of this would have been possible without you. Deb, thank you for all your priceless scientific insight and personal support, and for pushing me to become a more confident and independent researcher. Laura, thank you for showing me all the tips and tricks, especially with mouse techniques, and for your meticulous attention to detail in your feedback of my work and drafts, which prepared me for the level required in scientific research. Sue, thank you very much for being a moral support throughout my PhD. Your motivation and kind advice helped me through the ups and downs of a PhD. I am forever indebted to all of you.

To my Lab mates, Elly, Charlotte, Michelle and Stephanie, thank you for all the friendship and support throughout these years. Elly and Charlotte, what can I say! I am very fond of our cell culture room chats, drinks and nights out…so many memories here and interstate! I am very fortunate to share this PhD and academic journey with you! Special thanks to all Leukaemia Research Group members, in particular, Barb, for her assistance with cloning, Caitlin for her help with processing mouse tissues; Steph for persistently following up on orders, organising meetings and fun Lab events; to Bron for taking care of MTA and its logistics at the beginning of my PhD; to Verity for always helping me with my random questions and when I was looking for reagents to try out new experiments; and to Randall for his technical help and support with flow cytometry experiments.

I would also like to express my sincerest gratitude to Dr. Maxime François for his continuing support and insightful comments on immunofluorescence microscopy experiments and Dr John Bruning for his assistance with computational modelling experiments. I also express my warm thanks to Ms Swati Irani for her help with immunohistochemistry techniques; the staff of the University of Adelaide Histology

service, especially Ms. Kathryn Batra; the staff of Cell Screen SA, in particular Dr. Amanda Aloia, for their technical support in regard to slide preparation and high throughput drug screen experiments, respectively; and the staff of Bioresources Core Facility at SAHMRI for the technical support provided.

A special thank-you to my close friends. You have always been there for me throughout my PhD, celebrated achievements and highs with me, distracted me at lows and helped me to keep my spirit up through this roller-coaster. Finally, my very special thanks go to my parents and sister for supporting me unconditionally throughout my study and life in general; thank you for listening to my nagging when experiments failed, encouraging me to keep going during rough and stressful times, and getting as enthusiastic when I was talking about my exciting research results. I owe you everything.

Publications

Paniz Tavakoli Shirazi, Laura N Eadie, Susan L Heatley, Timothy P Hughes, David T Yeung and Deborah L White, The effect of co-occurring lesions on leukaemogenesis and drug response in T-ALL and ETP-ALL, *Br J Cancer* (2019) doi:10.1038/s41416-019-0647-7.

Paniz Tavakoli Shirazi, Laura N Eadie, Susan L Heatley, John B Bruning, and Deborah L White, Constitutive JAK/STAT signalling is the primary mechanism of resistance to JAKi in *TYK2*-rearranged acute lymphoblastic leukemia, *Cancer Letters* (2021) doi:10.1016/j.canlet.2021.04.027

Paniz Tavakoli Shirazi, Laura N Eadie, Susan L Heatley, and Deborah L White, TYK2 activating alterations in acute lymphoblastic leukemia: novel driver oncogenes with potential avenues for precision medicine?, *Journal of Cancer Science and Clinical Therapeutics* (2021) doi:10.26502/jcsct.5079112

*Submitted manuscripts:

Paniz Tavakoli Shirazi, Laura N Eadie, Susan L Heatley, Maxime François, David T Yeung, Timothy P Hughes and Deborah L White, Exploring the oncogenic and therapeutic target potential of the *MYB-TYK2* fusion gene in B-cell acute lymphoblastic leukemia, submitted to *Oncogene* Journal

Conference abstracts and presentations

Paniz Tavakoli Shirazi, Laura N Eadie, Susan L Heatley, John B Bruning, and Deborah L White, *Persistent Activation of JAK/STAT Signaling Plays an Important Role in In Vitro Jaki Resistance in TYK2-rearranged B-Cell Acute Lymphoblastic Leukaemia*, Annual Meeting of the American Society of Hematology December 2020, San Diego, California, USA (was held in virtual format due to COVID-19 pandemic), online publication doi:https://doi.org/10.1182/blood-2020-139048.

Paniz Tavakoli Shirazi, Laura N Eadie, Susan L Heatley, David T Yeung and Deborah L White. *Vorinostat treatment demonstrated efficacy against MYB-TYK2 altered B-cell acute lymphoblastic leukaemia in in vitro and in vivo models*. Australian Society for Medical Research (ASMR), November 2020, Adelaide, SA, Australia. **Oral presentation**

Paniz Tavakoli Shirazi, Laura N Eadie, Susan L Heatley and Deborah L White. 2020, *Oncogenic role and therapeutic targeting of the novel MYB-TYK2 fusion gene in high-risk acute lymphoblastic leukaemia*. Cancer in SA Translational Research Meeting, September 2020, Adelaide, SA, Australia. **Invited oral presentation**

Paniz Tavakoli Shirazi, Laura N Eadie, Susan L Heatley, David T Yeung and Deborah L White. *The MYB-TYK2 gene fusion induces B-cell acute lymphoblastic leukaemia in in vitro and in vivo models and can be effectively targeted by the dual SYK/JAK inhibitor, cerdulatinib.* 25th Congress of the European Hematology Association (EHA), June 2020, Germany (was held in virtual format due to COVID-19 pandemic). **Poster presentation**

Paniz Tavakoli Shirazi, Laura N Eadie, Susan L Heatley and Deborah L White. *The dual SYK/JAK inhibitor cerdulatinib demonstrates in vitro efficacy against a novel MYB-TYK2 fusion protein in acute*

lymphoblastic leukaemia cells. Cancer in SA Translational Research Meeting, July 2019, Adelaide, SA, Australia. **Invited oral presentation**

Paniz Tavakoli Shirazi, Laura N Eadie, Susan L Heatley and Deborah L White. *The dual SYK/JAK inhibitor cerdulatinib demonstrates in vitro efficacy against a novel MYB-TYK2 fusion protein in acute lymphoblastic leukaemia cells.* Australian and New Zealand Children's Haematology/Oncology Group Annual Scientific meeting, June 2019, Christchurch, New Zealand. **Oral presentation**

Paniz Tavakoli Shirazi, Laura N Eadie, Susan L Heatley and Deborah L White. *Characterising novel genomic lesions to develop a new combinational therapeutic strategy in high-risk acute lymphoblastic leukaemia, categorised by JAK fusions.* 2018 EMBL Australia Postgraduate Symposium, November 2018, Brisbane, QLD, Australia. **Oral presentation**

Paniz Tavakoli Shirazi, Laura N Eadie, Susan L Heatley and Deborah L White. *The dual SYK/JAK inhibitor cerdulatinib demonstrates in vitro efficacy against a novel MYB-TYK2 fusion protein in acute lymphoblastic leukaemia cells.* 2018 EMBL Australia Postgraduate Symposium, November 2018 Brisbane, QLD, Australia. **Poster presentation**

Paniz Tavakoli Shirazi, Laura N Eadie, Susan L Heatley and Deborah L White. *The dual SYK/JAK inhibitor cerdulatinib demonstrates in vitro efficacy against a novel MYB-TYK2 fusion protein in acute lymphoblastic leukaemia cells.* SAHMRI Annual Scientific Meeting, October 2018, Adelaide, SA, Australia. **Poster presentation**

Paniz Tavakoli Shirazi, Laura N Eadie, Susan L Heatley and Deborah L White. *The dual SYK/JAK inhibitor cerdulatinib demonstrates in vitro efficacy against a novel MYB-TYK2 fusion protein in acute*

lymphoblastic leukaemia cells. 12th Florey Postgraduate Conference, September 2018, Adelaide, SA, Australia. **Poster presentation**

Paniz Tavakoli Shirazi, Laura N Eadie, Susan L Heatley and Deborah L White. *The dual SYK/JAK inhibitor cerdulatinib demonstrates in vitro efficacy against a novel MYB-TYK2 fusion protein in acute lymphoblastic leukaemia cells.* Australian Society for Medical Research (ASMR), June 2018, Adelaide, SA, Australia. **Poster presentation**

Scholarships and awards

Recipient of travel grant to attend "25th Congress of the European Hematology Association (EHA)", Frankfurt, Germany. (2020)

Recipient of the "Betty Hartmann Leukaemia Research Supplementary Scholarship" to support the PhD and undertake research relating to the disease of Leukaemia, The University of Adelaide. (2019-2020)

Recipient of travel grant to attend "2018 EMBL Australia Postgraduate Symposium", Brisbane, QLD. (2018)

Invitation/acceptance to attend "2018 EMBL Australian PhD course", University of New South Wales, Sydney, Australia. (2018)

Recipient of the "Adelaide Graduate Research Scholarship" to undertake a PhD, The University of Adelaide. (2017-2020)

1. Chapter 1: Introduction

1.1. Acute Lymphoblastic Leukaemia

1.1.1. Clinical features of ALL

Acute lymphoblastic leukaemia (ALL) is the most common cancer in children, with a peak incidence between the age of 2 to 5 years, but is also an important cause of morbidity and mortality in adults (1, 2). ALL is divided into two key groups: B-cell (B-ALL; also known as B-cell precursor lymphoblastic leukemia) and T-cell (T-ALL) lineage, which respectively account for up to 85-75% and 15-25% of cases depending on the age group (childhood- adult ALL) (3-5). The predominant B-ALL group, in particular, accounts for approximately 88% and 75% in childhood and adult cases, respectively (6).

Clinical manifestation of ALL can be designated by accumulation of early lymphoid precursors in bone marrow, peripheral blood and also extramedullary sites due to deregulated transcription and maturation arrest of lymphoid lineage cells (7). Affected individuals suffer from symptoms related to bone marrow failure such as anaemia, and other common symptoms including inexplicable bleeding and repeated infections (7).

The diagnosis is generally determined by presence of lymphoblasts in blood and bone marrow. ALL patient's age, white cell count and cytogenetic analyses can be used to determine prognosis (3). These prognostic factors have been used to predict the risk of treatment failure and hence define standard-risk and high-risk (HR) ALL subtypes of B-ALL (4). Further evaluation consists of morphological analysis of malignant lymphocytes, immunophenotyping, treatment response to induction therapy and minimal residual disease (MRD) and more recently, assessment of genomic abnormalities by next generation sequencing (3, 4, 6). These analyses are critical for determining optimal risk stratification and treatment regimen. Involvement of the central nervous system (CNS) is an additional symptom that is associated with poor outcome and can increase the risk of relapse (8, 9). Several factors have been suggested to contribute to CNS involvement in ALL such as age, genomic profile (e.g. Philadelphia (Ph) chromosome

positivity) (10) and differentiation stage of malignant lymphocytes (9). Interestingly, it has recently been suggested that during the disease development in B-ALL, selection of leukaemic cells with specific genomic determinants can increase the risk of CNS disease (11). These observations emphasise the need for correct identification of patients at risk of CNS involvement.

Advances have been made in the treatment of ALL by improvements in haematopoietic stem cell transplantation (SCT), CNS directed treatment and optimisation of chemotherapy regimens (section 1.5). Current treatment regimens result in a 5-year event free survival rate of approximately 80% in childhood ALL cases (12, 13). However, relapsed or refractory ALL still occurs in approximately 20% of childhood cases, and for these patients, outcomes are very poor (12, 13). Therefore, this disorder remains a leading cause of non-traumatic death in children. In addition, the outcome for adult patients remains extremely poor with an overall 5-year survival rate of approximately 40% and of these, nearly 7% experience subsequent relapse (14-16).

1.1.2. Immunophenotypic classification of ALL

Immunophenotypic analysis of lymphocytes based on cluster of differentiation (CD) markers can classify ALL into 3 broad groups: B-ALL, mature B-ALL, and T-ALL. In B-ALL, CD24, CD22, CD20, CD19, CD34 and CD79a are the main markers for differential diagnosis while CD10 and cytoplasmic/surface membrane immunoglobulin M (IgM) are used for further differentiation into immunological groups (6, 17). Based on the proposed classification by the *European Group for the Immunological Characterization of Leukemias* (EGIL), B-ALL can be sub-divided into pro-, common, pre- and mature B-ALL Table 1-1 (17, 18).

Table 1-1.**Key differentiating CD antigen markers of B-ALL subtypes**. This table was modified based on information from references (17-19).

B-ALL subtypes	CD antigen markers	Approximate frequency (based on GMALL trial)
Pro- B-ALL (EGIL B-I)	TdT^+, $CD24^+$, $CD19^+$ and/or $CD79a^+$/$CD22^+$/$CD34^+$, $\underline{CD10^-}$, cytoplasmic immunoglobulin negative, dim CD45 and CD20	11%
Common ALL (EGIL B-II)	TdT^+, $CD24^+$, $CD19^+$, $CD79a^+$, $CD34^+$, $\underline{CD10^+}$, cytoplasmic immunoglobulin negative, increased CD45 and CD20	49%
Pre B-ALL	TdT^+, $CD22^+$, $CD10^+$, $CD19^+$, $CD79a^+$, $CD34^+$, $CD20^+$, $\underline{\text{cytoplasmic IgM}^+}$	12%
Mature B-ALL	TdT^-, $CD34^-$, $CD19^+$, $\underline{\text{surface IgM}^+}$	4%

Variable positivity in CD20 and CD22 has been reported in literature beyond pro-B-ALL. Main differentiator markers are underlined in each group. Abbreviations: B-ALL, B-cell acute lymphoblastic leukaemia; CD, cluster of differentiation; IgM, immunoglobulin M; TdT, terminal deoxynucleotidyl transferase.

1.1.3. Underlying biology of B-ALL

Although the exact cause of B-ALL is unknown, disease usually arises due to repopulation of the bone marrow with B-lymphoid precursors. This phenomenon is due to the acquisition of initiating lesions, including gene translocations that confer self-renewal, differentiation arrest and epigenetic reprogramming of lymphoid progenitors (1). Accumulation of additional secondary mutations and genomic alterations, affecting multiple cellular pathways, then contribute to the clinical manifestation of the disease (1, 2). Each ALL patient genome has approximately 10-20 alterations at the time of diagnosis and are often double this number at relapse (that may or may not contribute to disease pathogenesis and relapse) (20). Perturbated pathways comprise those governing lymphoid development, cell cycle regulation, tumour suppression, transcriptional regulation, epigenetic modification, Janus family of tyrosine kinases (JAK)/ signal transducer and activator of transcription (STAT) signalling,

phosphatidylinositol 3-kinase (PI3K)/mammalian target of rapamycin (mTOR) and RAS signalling Figure 1-1 (1, 2, 21).

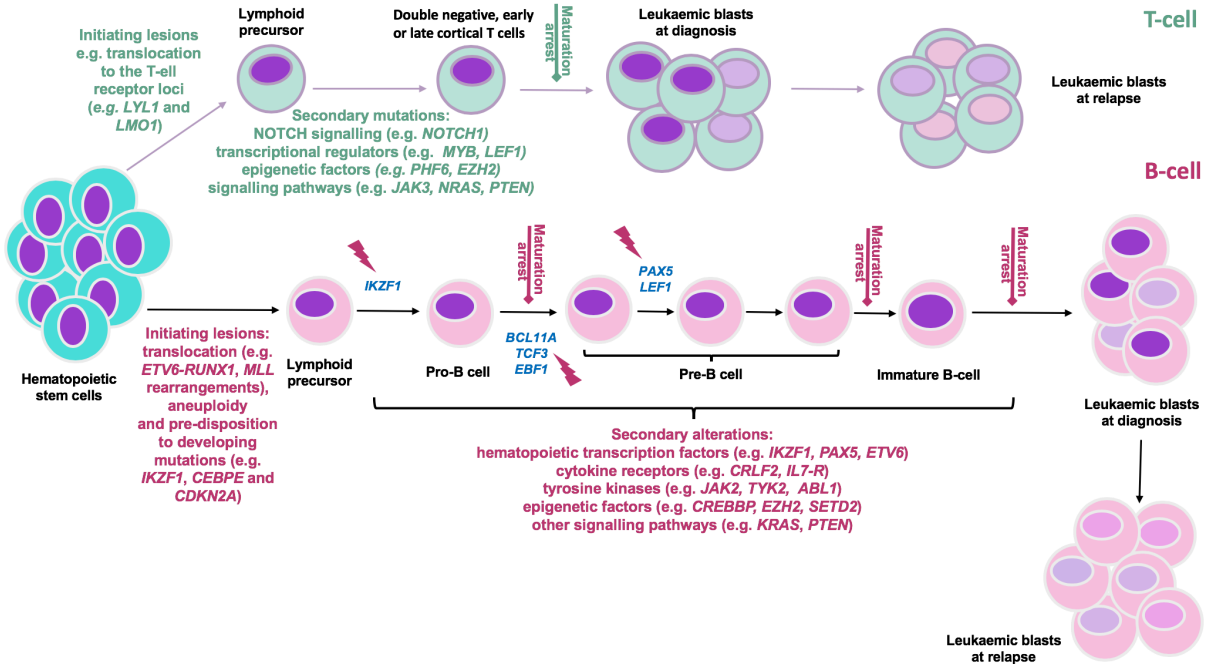

Figure 1-1. Predisposition and consequent development of ALL can be due to chronological acquisition of deleterious genomic alterations. The differentiation of haematopoietic cells into B- and T-lineage (represented in pink and green respectively) and their maturation is strictly regulated by transcription factors re-enforcing commitment to either fate. T-ALL initiation is mainly due to rearrangement of oncogenic transcription factors (e.g. *LYL1, LMO1)* into a position adjacent to T-cell receptor loci. In the B-ALL setting, changes in chromosome number (aneuploidy); acquisition of chromosomal rearrangements including translocations of genes that 1. control lymphoid development (e.g *ETV6, RUNX1*) 2. activate kinase signalling (e.g. *ABL1*) or oncogenes (e.g. *MYC*) 3. control epigenetic regulation (e.g. *MLL*(*KMT2A*)); and mutations in B-cell transcriptional regulator genes (e.g. *IKZF1, PAX5, EBF1, CEBPE*) and tumour suppressor genes (e.g, *CDKN2A/2B*) confer developmental arrest on lymphoid progenitors at various stages based on the altered genes (indicated by red flash). Subsequently, acquisition of additional co-operating events (as indicated) contribute to development of a genetically polyclonal disease. Selection or acquisition of further mutations can result in resistance to therapy and relapse. Adapted from (1, 2, 22).

1.1.4. Genomic profiling and genomic subtypes of B-ALL

ALL is a heterogeneous disorder that is commonly characterised by recurring chromosomal rearrangements, genetic alterations targeting common cellular pathways and insertion or deletion mutations (21, 23). Technologies such as gene expression profiling, single nucleotide polymorphism (SNP) analysis and recent studies utilising next generation sequencing (NGS) have significantly improved our understanding of the genomic basis of ALL. This led to identification of several main gene fusions, that may result in formation of chimeric proteins with leukaemogenic activity, and/or activation of cellular pathways that contribute to leukaemogenesis and disease relapse (24). Several of these alterations result in cryptic gene fusions that are undetectable with conventional methods such as karyotyping. However, introduction of cytogenetic analysis and next generation genomic techniques allowed identification of cryptic rearrangements, further refinement of the genomic classification and definition of HR subgroups, that may ultimately inform alternative targets for treatment.

Figure **1-2** represent the key subtypes of B- and T-ALL highlighting the risk stratification and frequency of their occurrence particularly in paediatrics and young adults (25).

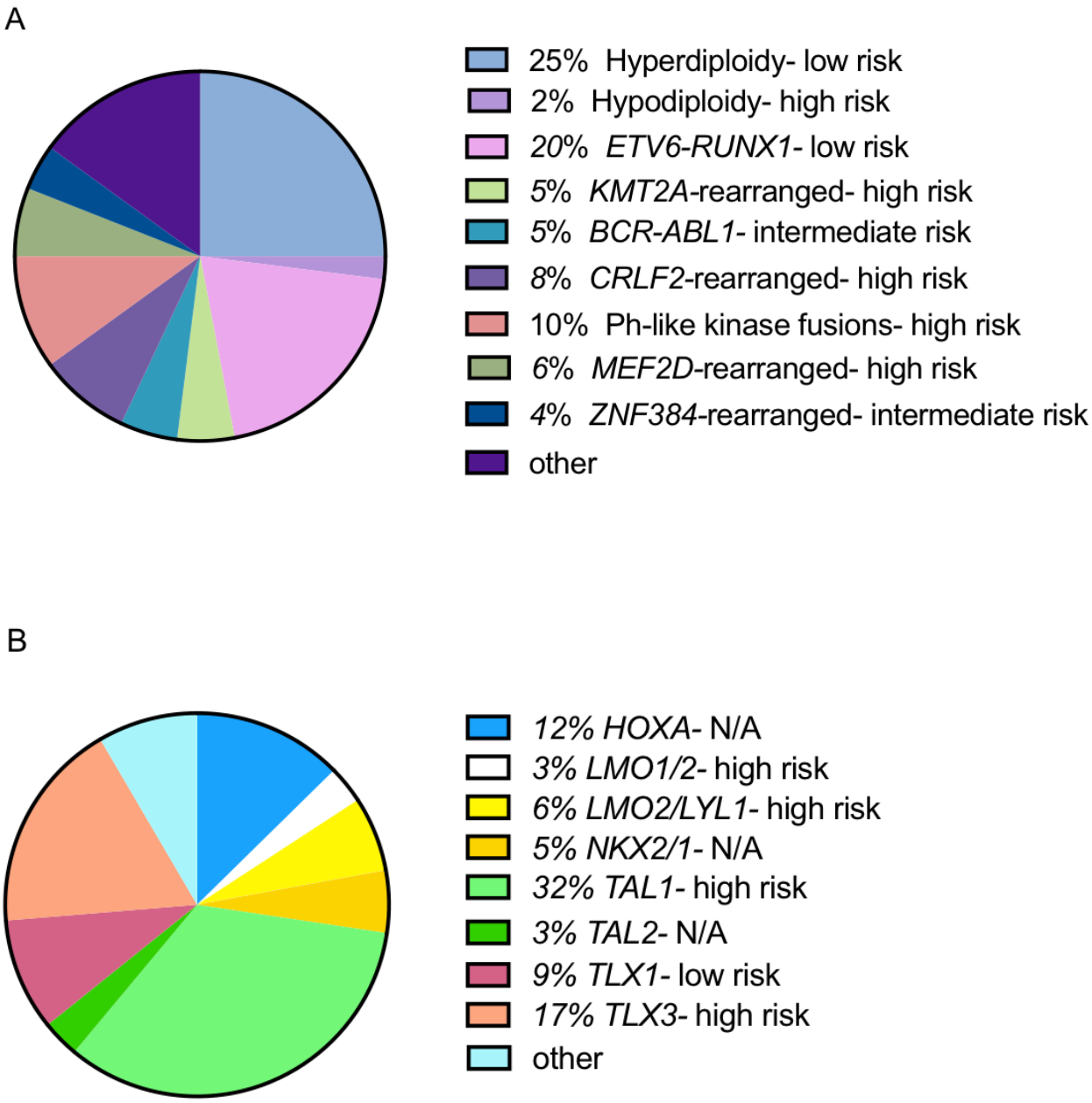

Figure 1-2. Key subtypes of childhood ALL. Relative incidence, approximate frequency and the prognosis of (A) B-ALL and (B) T-ALL subtypes. Adapted from (25, 26). Abbreviations: N/A, no data available.

B-ALL cases are mostly classified by chromosomal gains and losses within leukaemic cells (hyper- or hypodiploidy), recurrent chromosomal translocations and cryptic gene fusions (Figure 1-2 A) (25). B-ALL rearrangements (21) include but are not limited to:

- *BCR-ABL1* (*Breakpoint cluster region protein (BCR)-Abelson Tyrosine-Protein Kinase 1* (*ABL1*); also known as Philadelphia (Ph) chromosome)
- t(12;21)(p13;q22) *ETV6-RUNX1* (*ETS variant transcription factor 6-Runt-related transcription factor 1,* also known as *TEL-AML1*)
- *MYC* (*c-MYC,* gene regulator and proto-oncogene), multiple recurrent fusion partners
- *KMT2A (lysine methyltransferase 2A*, previously known as *MLL* (*mixed-lineage leukaemia*)), multiple recurrent fusion partners
- *CRLF2* (*cytokine receptor-like factor 2*), multiple recurrent fusion partners
- t(1;19)(q23;p13) *TCF3-PBX1* (*transcription factor 3-PBX homeobox 1*)
- *MEF2D* (*myocyte enhancer factor 2D*), multiple recurrent fusion partners
- *ZNF384* (*zinc finger protein 384*), multiple recurrent fusion partners
- *PAX5* (*paired box 5*), multiple recurrent fusion partners

Some of these lesions including *BCR-ABL1*, *ETV6-RUNX1* and *KMT2A* rearrangements, have long been identified in B-ALL cases by conventional methods (27), whereas *MEF2D* and *ZNF384* rearrangements have more recently been classified as subsets of childhood B-ALL (28). In addition, integration of gene expression analysis not only demonstrated a specific gene expression signature for these lesions (29, 30), but also resulted in identification of a new subgroup termed *BCR-ABL1*- or Ph-like ALL (31, 32). Patients with Ph-like ALL harbour a diverse range of genomic alterations responsible for cytokine receptor and kinase signalling (section 1.2) but do not have the *BCR-ABL1* oncogene (29, 31, 32). Identification of genomic alterations at diagnosis allows risk stratification and subsequent treatment selection. For example, high hyperdiploidy and the *ETV6-RUNX1* fusion gene, are generally associated with a good

clinical outcome (1, 33). In contrast, patients with alterations such as the *BCR-ABL1* fusion gene and hypodiploidy have less favourable outcomes (24, 34, 35).

In addition to the above-mentioned translocations, further recurrent alterations, including fusion genes and single nucleotide variants are often observed in B-ALL cases. These alterations frequently perturb important pathways and genes (Table 1-2) involved in: (21, 23, 32, 36-40).

- regulation of lymphoid development (e.g. *PAX5* and *IKZF1 (Ikaros family zinc finger 1*))
- cytokine receptor signalling (e.g. *CRLF2* and *IL-7R* (*interleukin-7 receptor*))
- tyrosine kinase signalling (e.g. *JAK1* (*Janus tyrosine kinase 1*), *JAK2*, *JAK3, TYK2* (*tyrosine kinase 2*) and *ABL1*)
- RAS signalling (e.g. the proto-oncogenes *NRAS* and *KRAS*)
- cell division and tumour suppression (e.g. *CDKN2A/B* (*cyclin-dependent kinase Inhibitor 2A* and *2B*))
- epigenetic regulation and chromatin modifications (e.g. *SETD2 (set domain containing 2)* and *EZH2* (*enhancer of zeste homolog 2*))

The prevalence of each mutation and/or alteration differs according to the B-ALL subtype and each may be a secondary or cryptic event in driving the disease (21). Utilisation of NGS and SNP analysis, highlighted the frequent occurrence of *IKZF1* alterations in Ph-like and Ph-positive B-ALL; *IKZF1* alterations are considered an indicator of poor outcome and are a hallmark of HR-ALL. (39). Similarly, other genomic alterations are observed with differing frequencies depending on the disease subtype and age group. The alterations most frequently observed in B-ALL are summarised in Table 1-2.

Table 1-2. Key genomic alterations observed in B-ALL. (adapted from Hunger *et al* (2015) (41))

Key mutations of high risk ALL	Disease/Frequency	Alteration	Activated signalling pathways and /or the outcome of mutation	Possible targeted therapy	Comments	Function	References
*JAK1/ 2**	• B-ALL • 18-35% DS ALL • 10% HR Ph-like ALL	Mutations in kinase or pseudokinase domain	Activation of JAK/STAT pathway	JAKi	*JAK* mutations often co-occur with alterations of *IKZF1* and *CDKN2A/B* in Ph-like ALL. *JAK*-mutated cases are associated with poor outcome	encodes members of the non-receptor family of tyrosine kinases that mediate cytokine signalling	(38, 42, 43)
Activating kinase fusion genes	• B-ALL • 30% HR Ph-like ALL	*ABL1/2* rearrangements*	Activation of cytokine receptor and kinase signalling pathways	ABLi	Demonstrates a Ph-like gene expression profile and is associated with high risk of relapse	encodes a non-receptor tyrosine kinase	(15, 25, 31, 44)
		CSF1R rearrangements		ABLi		encodes a transmembrane protein tyrosine kinase	
		EPOR rearrangements		JAK2i		encodes the EPOR cytokine receptor	
		TYK2 rearrangements		TYK2i		encodes a member of the Jak family of non-receptor kinases	
		JAK2 rearrangements*		JAK2i		as mentioned above	
		IL-7R mutation*		JAK2i		encodes a protein that functions as a cytokine receptor	
		FLT3 mutation*		FLT3i		encodes a tyrosine kinase receptor that is associated with haematopoiesis	
		SH2B3 deletion*		-		encodes a negative regulator of cytokine signalling	
CRLF2	• B-ALL • 50% Ph-like ALL • >50% DS ALL	*IGH-CRLF2, P2RY8-CRLF2*	Activation of JAK/STAT pathway	JAK2i	50% of the cases also harbour mutated *JAK*	encodes a cytokine receptor protein that is associated with haematopoiesis .	(37, 45-47)

RAS mutations*	• B-ALL and DS-ALL 30-50% of relapsed cases	*NRAS/ KRAS*	Activation of RAS signalling pathway	MEK-ERKi	Associated with poor outcome	encodes a membrane protein with intrinsic GTPase activity	(25, 48-52)
PAX5	B-ALL (30%)	Deletions, sequence mutations and rearrangements	Reduced DNA binding and activation of transcription factors	-	*PAX5* attenuation increases susceptibility to development of leukaemia.	encodes a transcription factor from paired box family proteins that is required for development of B-cells	(32, 53-55)
*IKZF1**	• B-ALL • 60% Ph-like ALL • 30% HR B-ALL	Deletions and sequence mutations	Loss of function	-	Associated with poor outcome	encodes a transcription factor that regulates haematopoietic cell differentiation	(15, 32, 39, 55)
*SETD2**	• B-ALL 12% of relapsed cases.	Sequence mutation	Impaired epigenetic transcriptional regulation	epigenetic inhibitors	High prevalence in hypodiploid ALL	encodes a H3K36 trimethyltransferase	(48, 52)
*CREBBP**	• B-ALL 19% of relapsed cases	Deletion, sequence mutation	Impaired transcriptional regulation and histone acetylation	epigenetic inhibitors	confers resistance to glucocorticoids	encodes CREB binding protein involved in activation of transcription factors and has intrinsic histone acetyltransferase activity	(48, 52)

Abbreviations: B-ALL, B-cell acute lymphoblastic leukaemia; Colony stimulating factor 1 receptor, (*CSF1R*); CREB Binding Protein, (*CREBBP*); DS, Down syndrome; Erythropoietin receptor, (*EPOR*); Fms Related Tyrosine Kinase 3, (*FLT3*); Philadelphia chromosome-like ALL, Ph like-ALL; SH2B Adaptor Protein 3, (*SH2B3*); i, inhibitors; *=also observed in T-ALL.

1.2. Ph-like ALL is a high-risk subtype

Ph-like ALL is a HR subtype of B-ALL which lacks the *BCR-ABL1* oncogene but demonstrates a similar gene expression profile to that of Ph-positive (*BCR-ABL1*+) ALL (31, 39). The incidence of Ph-like ALL increases with age, accounting for 15% of paediatric ALL and >20% of young adult and adult ALL (15). Patients with this HR subtype experience poor chemotherapy response, low survival rate and higher risk of relapse (56, 57).

Ph-like ALL, unlike several other ALL subtypes (e.g. Ph-positive ALL), is not founded by a single chromosomal rearrangement but is rather categorised by a diverse range of genomic alterations. The most prevalent alteration detected in Ph-like ALL is *IKZF1* (deletion mutations in approximately 60% of cases); Ph-like ALL is also characterised by alterations involving genes that are responsible for regulation of cytokine and kinase pathways (31, 39). These include rearrangements of *ABL1* and *ABL2, EPOR, CRLF2*, *JAKs* and mutations that result in constitutive activation of JAK/STAT signalling (24, 37). In addition, mutations activating RAS signalling pathways (e.g. *NRAS, PTPN11* and *KRAS)*, and signalling of other kinases such as *FLT3*, are recurrently detected in Ph-like ALL (24, 37). These alterations ultimately contribute to dysregulated B-cell proliferation, maturation and survival resulting in leukaemia. Figure 1-3 outlines the key Ph-like ALL subtypes.

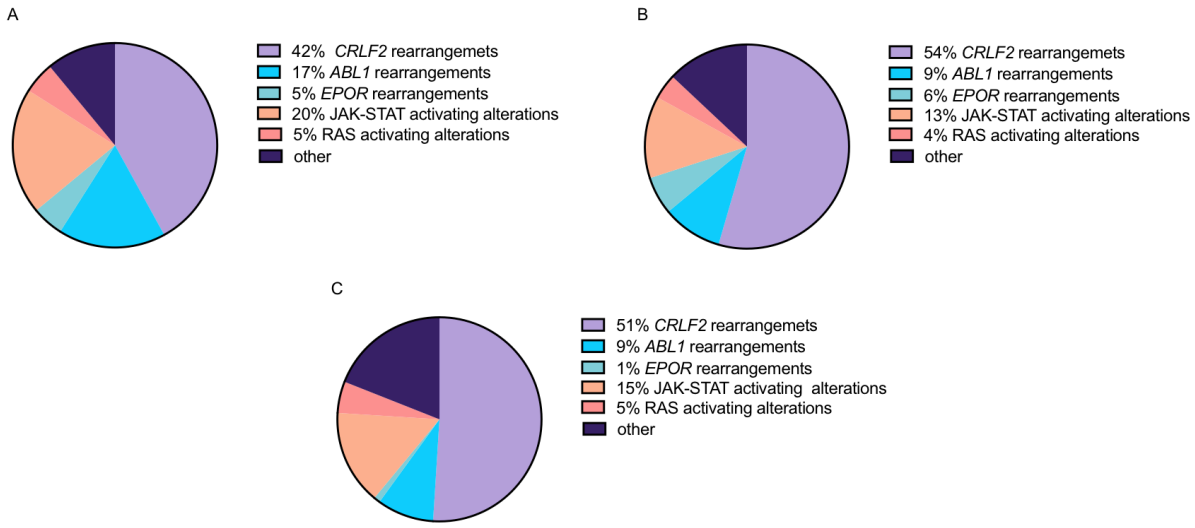

Figure 1-3. Key subtypes of Ph-like ALL. Approximate frequency of Ph-like ALL subtypes in (A) children, (B) adolescents and young adults (AYAs) (grouped together), and (C) adults. Adapted from Pui *et.al.* (2017) (58).

CRLF2 rearrangements (*CRLF2*-r), characterised by over expression of TSLP (thymic stromal lymphopoietin) protein (46, 59), are detected in approximately 50% of Ph-like ALL patients with two key fusion genes: *IGH-CRLF2* and *P2RY8-CRLF2* (24, 37, 60). *CRLF2*-rearranged cases can harbour additional activating mutations in IL-7-JAK/STAT pathway (e.g. *JAK1*, *JAK2, IL-7*) and RAS pathway genes (e.g. *NRAS* and *KRAS)* (37, 46, 61, 62) and are proposed to be amenable to treatments with JAK (JAKi), PI3K/mTOR (PI3K/mTORi) and BCL2 (BCL2i) inhibitors (63, 64). Another approximately 10% of Ph-like ALL cases harbour *ABL*-class fusion genes (24, 65). *ABL*-class fusions lead to aberrant expression of *ABL1*, *ABL2, CSF1R* (*colony stimulating factor 1 receptor)* or *PDGFRβ (platelet-derived growth factor receptor β)* genes and are responsive to ABL inhibitors (ABLi) (Table 1-3) (24, 65). The other dominant sub-group of Ph-like ALL comprises *JAK*-class fusion genes (approximately 12% of children and 15% of adolescents) (24, 65) and these may be amenable to JAKi (Table 1-3) (24, 63). Additional subsets of genomic alterations that lead to JAK/STAT activation in Ph-like cases include sequence mutation of *SH2B3*, *IL-7R*, *JAK1, JAK3* and *IL2Rβ (Interleukin 2 Receptor Subunit β)* rearrangements (collectively termed JAK/STAT activating lesions in Figure 1-3) (15, 24)

Table 1-3. Identified kinase rearrangements in Ph-like ALL. Adapted from Roberts *et al* (2017 and 2014) (15, 24) except where otherwise referenced.

3' kinase partner	Tyrosine Kinase Inhibitors	5' partner
ABL1	ABLi	*ETV6*, NUP214*, ZMIZ1*, RANBP2*, RCSD1, SNX2*, SFPQ (66)*
ABL2	ABLi	*PAG1*, RCSD1*, ZC3HAV1*
CSF1R	ABLi	*MEF2D (67), SSBP2**
PDGFRα	ABLi	*FIP1L1**
PDGFRβ	ABLi	*EBF1*, SSBP2, TNIP1, ZEB2, SNX29, ATF7IP** (68)
CRLF2	JAK2i	*IGH*, P2RY8**
JAK2	JAK2i	*ATF7IP*, BCR*, ETV6*, PAX5*, PPFIBP1, SSBP2 (69), SMU1, EBF1*, STRN3, TERF2, ZNF340, SPAG9* (70), RFX3 (44), USP25 (44), ZNF274 (44), OFD1 (71)*
EPOR	JAK2i	*IGH*, IGK*, THADA*
TYK2	TYK2i	*MYB*, SMARCA4, ZNF340*
FLT3	FLT3i	*ZMYM2*
NTRK3	NTRKi	*ETV6**
PTK2B	FAKi	*TMEM2, KDM6A, STAG2*
IL2Rβ	JAK1/2i	*MYH9**
BLNK	-	*DNTT*
CBL	-	*KANK1*

*=alterations with confirmed *in vitro* transforming ability (37, 47, 72-81). Potential ABLi, JAKi and FLT3i may include dasatinib, ruxolitinib and AC220. Abbreviations: Activating Transcription Factor 7 Interacting Protein, (*ATF7IP*); B Cell Linker, (*BLNK*); Cbl Proto-Oncogene, (*CBL*); Csk-Binding Protein, (*PAG1*); DNA Nucleotidylexotransferase, (*DNTT*); EBF Transcription Factor 1, (*EBF1*); FIP1-Like 1 Protein, (*FIP1L1*), Immunoglobulin Kappa Locus, (*IGK*); Immunoglobulin Heavy Locus, (*IGH*); KN Motif And Ankyrin Repeat Domains 1, (*KANK1*); Lysine Demethylase 6A, (*KDM6A*); MYB Proto-Oncogene, (*MYB*); Myocyte Enhancer Factor 2D, (*MEF2D*); Myosin Heavy Chain 9, (*MYH9*); Neurotrophic Receptor Tyrosine Kinase 3, (*NTRK3*); Nucleoporin 214, (*NUP214*); OFD1 Centriole And Centriolar Satellite Protein, (*OFD1*), PPFIA Binding Protein 1, (*PPFIBP1*); Protein Tyrosine Kinase 2 Beta, (*PTK2B*); RAN Binding Protein 2, (*RANBP2*); RCSD Domain Containing 1, (*RCSD1*); Regulatory Factor X3, (*RFX3*); Single Stranded DNA Binding Protein 2, (*SSBP2*); SMU1 DNA Replication Regulator And Spliceosomal Factor, (*SMU1*); Sorting Nexin 2, (*SNX2*); Sorting Nexin 29, (*SNX29*); Sperm Associated Antigen 9, (*SPAG9*); Splicing Factor Proline And Glutamine Rich, (*SFPQ*); Striatin 3, (*STRN3*); Stromal Antigen 2, (*STAG2*); SWI/SNF Related, Matrix Associated, Actin Dependent Regulator Of Chromatin, Subfamily A, Member 4, (*SMARCA4*); Telomeric Repeat Binding Factor 2, (*TERF2*); THADA Armadillo Repeat Containing, (*THADA*); TNFAIP3 Interacting Protein 1, (*TNIP1*); Transmembrane Protein 2, (*TMEM2*); Ubiquitin Specific Peptidase 25, (*USP25*); Zinc Finger And BTB Domain Containing 46, (*ZNF340*); Zinc Finger CCCH-Type Containing, Antiviral 1, (*ZC3HAV1*); Zinc Finger E-Box Binding Homeobox 2, (*ZEB2*); Zinc Finger MIZ-Type Containing 1, (*ZMIZ1*); Zinc Finger MYM-Type Containing 2, (*ZMYM2*); Zinc Finger Protein 274, (*ZNF274*).

Due to the introduction of NGS approaches, the underlying alterations of Ph-like ALL are now better understood. In addition, the presence of kinase alterations in Ph-like ALL, highlights the clinical importance of this subtype. Studies have suggested variable responses to available tyrosine kinase inhibitors (TKIs) in *in vitro* and *in vivo* pre-clinical and case studies (21, 63, 82, 83). However, given the ongoing discovery of novel alterations, the driving potential of each alteration to induce leukaemia alone and with co-occurring lesions, requires improved and updated *in vitro* and *in vivo* characterisation. This is also vital for identification of a targeted treatment approach against specific alterations to maximise patient outcomes.

1.2.1. JAK family rearrangements

JAK-class rearrangements include fusions activating Jak2 and Tyk2 proteins (Figure 1-4) (15, 24). Each *JAK*-class fusion gene has a variable 5' partner gene and breakpoints yet retains an in-frame kinase domain resulting in constitutive activity of the fusion protein (15, 24). Each fusion has an in-frame kinase domain (also known as JH1) and may or may not contain a disrupted pseudokinase domain (termed JH2), responsible for auto-inhibition of JAK kinase domain (24, 69, 84). In addition, the fusions lack the FERM (four-point one, erzrin, radixin, moesin) and SH-like (Src-homology) domains, which are involved in protein and cytokine receptor binding, respectively (84, 85). Despite the diversity of the 5' partner, they commonly harbour a DNA binding domain and facilitate the dimerisation and subsequent activation of JAKs (24, 69).

Since the identification of *JAK*-class fusion genes in leukaemic cases, several studies have investigated the transformative and/or leukaemogenic potential of a number of these fusions via *in vitro* and/or *in vivo* methods including *ETV6*(*TEL*)*-JAK2, PCM1-JAK2, BCR-JAK2, PAX5-JAK2* and *ATF7IP-JAK2* (65, 86-89). In addition, JAK mediated activation of the Stat5 protein has been documented in many of these

JAK-class fusion genes (discussed in section 1.4) (24, 65, 75, 89). *In vitro* sensitivity to ruxolitinib (Jak1/2 inhibitor) has been reported for *JAK*-class fusion genes such as *PAX5-JAK2, ATF7IP-JAK2* and *MYH9-IL2Rβ* (65). However, the functional role of other *JAK* rearranged fusion genes in leukaemia development, for instance those involving *TYK2,* and their targetability in *in vivo* and *in vitro* models is currently unknown and is the subject of this thesis.

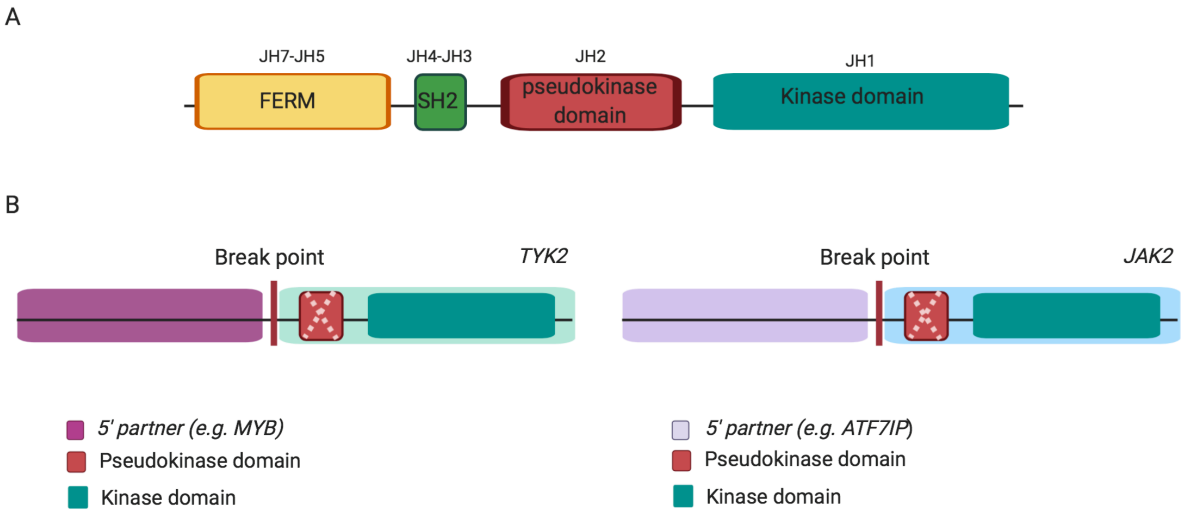

Figure 1-4. Schematic structure of wild type Jak protein, JAK2 and TYK2 alterations in Ph-like ALL. (A) Wild type Jak, each Jak protein consists of four domains including FERM, SH2, pseudokinase and kinase. (B) *TYK2* and *JAK2* alterations, *JAK*-class fusions exhibit an intact kinase domain with either a disrupted or absent (as indicated by crossed dashed lines) pseudokinase domain fused to variable 5' partner genes. Abbreviation: JH, Jak homology domain.

1.3. The role of Tyk2 in cancer

Four human JAKs including Jak1, Jak2, Jak3 and Tyk2 have been reported and are associated with activation of type I and II cytokines including both interleukin (IL) and interferon (IFN) receptors (84, 90). Tyk2 was the first member of the Jak family of tyrosine kinases to be described and linked to cytokine signalling and the downstream JAK/STAT pathway (91, 92). JAK/STAT is one of the most mutated signalling pathways in cancer; recognised as one of the twelve core cancer pathways (93, 94).

1.3.1. Can Aberrant Tyk2 levels cause leukaemia?

The involvement of Jak1-3 in inducing cancer have been intensively studied while Tyk2 was mainly studied in the setting of auto-immune and inflammatory diseases (95, 96). Studies reported impaired type I IFN and IL signalling due to Tyk2 deficiency in several mouse models (97) and very limited human cases (98, 99). Subsequent genome wide association analyses linked Tyk2 deficiency with auto-immune and inflammatory diseases (100). Furthermore, *ex vivo* analysis on bone marrow cells from wild type and Tyk2 deficient mice, demonstrated a reduced inhibition of B-cell lymphopoiesis upon IFNα stimulation in Tyk2 deficient cells (101). IFNα signalling can also inhibit B-cell differentiation and induce apoptosis in a normal setting (102). In addition, reduced Stat3 signalling and response to IFNβ-mediated apoptosis have been reported in Tyk2 deficient pro-B cells (103). Collectively, these findings highlighted a possible role for Tyk2 in regulation of B-cell apoptosis that may be related to B-cell leukaemia. Another study suggested an increased susceptibility of Tyk2 deficient mice to develop of B-cell lymphoid leukaemia/lymphoma and T-ALL induced by Abelson murine leukemia virus and *ETV6-JAK2* fusion gene, respectively (104). The greater incidence of disease in Tyk2 deficient mice compared to wild type controls, however, can possibly be explained by the tumour surveillance properties of Tyk2, as Tyk2-deficient animals also demonstrated reduced cytotoxic activity of T- and natural killer cells (100, 104). Interestingly, the immunosurveillance properties of Tyk2 are demonstrated to be independent of its canonical kinase activity since Tyk2 deficient mice expressing kinase inactive Tyk2 protein (harbouring *Tyk2-K923E* mutation) exhibited normal development of natural killer cells in bone marrow (105). The cytotoxic activity of these natural killer cells against a variety of tumour cells was also relatively restored upon expression of kinase inactive Tyk2 protein (105). These results highlight the potential benefit of TYK2 inhibitors (TYK2i) to treat cancers exhibiting higher Tyk2 levels and would not cause impairment of tumour surveillance.

Tyk2 overexpression and activation has been demonstrated to be associated with oncogenesis in various cancer cell lines and patient samples (breast, prostate and ovarian cancer) (102, 106-109). For instance, a study by Ide *et al.* (2008) demonstrated increased invasiveness of prostate tumour as a result of increased Tyk2 expression (107). Another study demonstrated invasion of malignant cells into the liver upon Tyk2 protein expression using *in vivo* transgenic mouse models of B-cell lymphoma co-expressing the *c-MYC* oncogene (107). The significance of increased Tyk2 expression in haematological malignancies was only recently highlighted in T-ALL and anaplastic large cell lymphoma (ALCL) (110, 111). *TYK2* gene knock down by small interfering RNA, resulted in impaired growth and increased cell apoptosis in more than 60% of patient derived T-ALL cells and cell lines (110). This observation was not reported in other *JAK* family genes and seems to be specific to *TYK2* (110). In addition, *TYK2* deletion in mouse models of *NPM-ALK*-induced ALCL and human primary ALCL cells demonstrated prolonged survival in mouse models and reduced growth/increased apoptosis in primary cells (111). Data from both studies also demonstrated the dependency of T-ALL and ALCL cell lines and patient samples on Tyk2 activation that leads to upregulation of Stat1/3 and consequently members of anti-apoptotic Bcl2 family (110, 111).

The importance of Tyk2 in cancer development and progression is complex. Tyk2 not only contributes to JAK/STAT activation which is the hallmark of many cancers (94, 112), but also depending on the cell type and context, displays tumour suppressive and oncogenic properties. This may be due to intrinsic and extrinsic involvement of the Tyk2 protein in multiple cellular functions including proliferation, apoptosis and invasion.

1.3.2. TYK2 alterations occur in ALL patients

Reports on gain of function or activating *TYK2* mutations and alterations in haematological malignancies have emerged only recently. In 2013, the first activating *TYK2* mutations (Table 1-4) were reported in T-

ALL cell lines and were shown to have transformative ability; affording IL-3 dependent pro-B murine Ba/F3 cells harbouring these mutations cytokine independent growth (111). A year later, the first case of a *TYK2* fusion gene was reported in Ph-like ALL (24). Furthermore, *TYK2* alterations have been reported in other blood cancers including acute myeloid leukaemia (AML), CD30-positive lymphoproliferative disorder (LPD) and ALCL (113-116). *In vitro* analysis of *NPM1*(*Nucleophosmin 1*)-*TYK2* and *NFKB2*(*nuclear factor of kappa light polypeptide gene enhancer in B cells 2*))-*TYK2* fusion genes, detected only in LPD and ALCL patients respectively, demonstrated constitutive auto- and trans-phosphorylation of Tyk2 and downstream activation of STAT family proteins (113, 114). However, the oncogenesis potential of these *TYK2* fusion genes in *in vivo* models is unknown. Table 1-4 highlights the key *TYK2* alterations and the current *in vitro* functional consequences in ALL.

Table 1-4. Key TYK2 mutations and rearrangements detected in ALL. Modified from Woss *et.al* (2019) (117) and St. Jude PeCan Data portal (118).

***TYK2* alterations**	**Disease**	**Known functional status**	**Domain**	**References**
TYK2 p.G271S	B-ALL	n.d. *	FERM	(119)
TYK2 p.V678L	B-ALL	n.d. *	Pseudokinase (JH2)	(119)
TYK2 p.P760L	B-ALL	increased Tyk2 autophosphorylation/ STATs activation	Pseudokinase (JH2)	(120)
MYB-TYK2	B-ALL (Ph-like)	cytokine independent growth	Intact kinase (JH1)	(24, 65)
SMARCA4-TYK2	B-ALL (Ph-like)	n.d. *	Intact kinase (JH1)	(15)
ZNF340-TYK2	B-ALL (Ph-like)	n.d. *	Intact kinase (JH1)	(15)
TYK2 p.G36D	T-ALL	cytokine independent growth	FERM	(111)
TYK2 p.S47N	T-ALL	cytokine independent growth	FERM	(111)
TYK2 p.R425H	T-ALL	failed cytokine independent growth	FERM	(111)
TYK2 p.V731I	T-ALL	cytokine independent growth	Pseudokinase (JH2)	(111)
TYK2 p.G761V	T-ALL	increased Tyk2 autophosphorylation/ STATs activation	Pseudokinase (JH2)	(120)
TYK2 p.E957D	T-ALL	cytokine independent growth / Weak STATs activation	Kinase (JH1)	(111, 120)
TYK2 p.M926V	T-ALL	no STATs activation	Kinase (JH1)	(120)
TYK2 p.R1027H	T-ALL	cytokine independent growth /Weak STATs activation	Kinase (JH1)	(111)

* These alterations are speculated to be gain of function and activating mutations and rearrangements, since no functional analyses are available. Abbreviations: n.d.=no data

As shown in Tables 1-3 and 1-4, three 5' partners have been identified for *TYK2* rearrangements in Ph-like ALL (*MYB*, *SMARCA4* (*SWI/SNF Related, Matrix Associated, Actin Dependent Regulator Of Chromatin, Subfamily A, Member 4*), *ZNF340* (*Zinc-finger protein 340*)) (24, 65). Apart from a single *in vitro* study that demonstrated the ability of the *MYB-TYK2* fusion gene to induce cytokine independent growth in pro-B murine Ba/F3 cells (65), significance of *TYK2* fusion genes as a driver oncogene in leukaemogenesis is unknown. It is not clear whether *TYK2* fusions are secondary events and the result of genomic instability, co-occurring events promoting the disease or capable of inducing the disease as a single driving alteration at earlier stages of leukaemogenesis. Likewise, the downstream signalling activated due to the presence of *TYK2* fusion genes in the B-ALL setting is currently not known.

1.4. Cytokine signalling pathways

The JAK/STAT signalling network is complex (Figure 1-5). The Tyk2 protein can induce signalling redundancy, alternate signalling through other pathways and interact with positive or negative regulatory components. This interplay delivers multiple therapeutic targets and emphasises the importance of careful study to find the appropriate inhibitors for each patient and disease context.

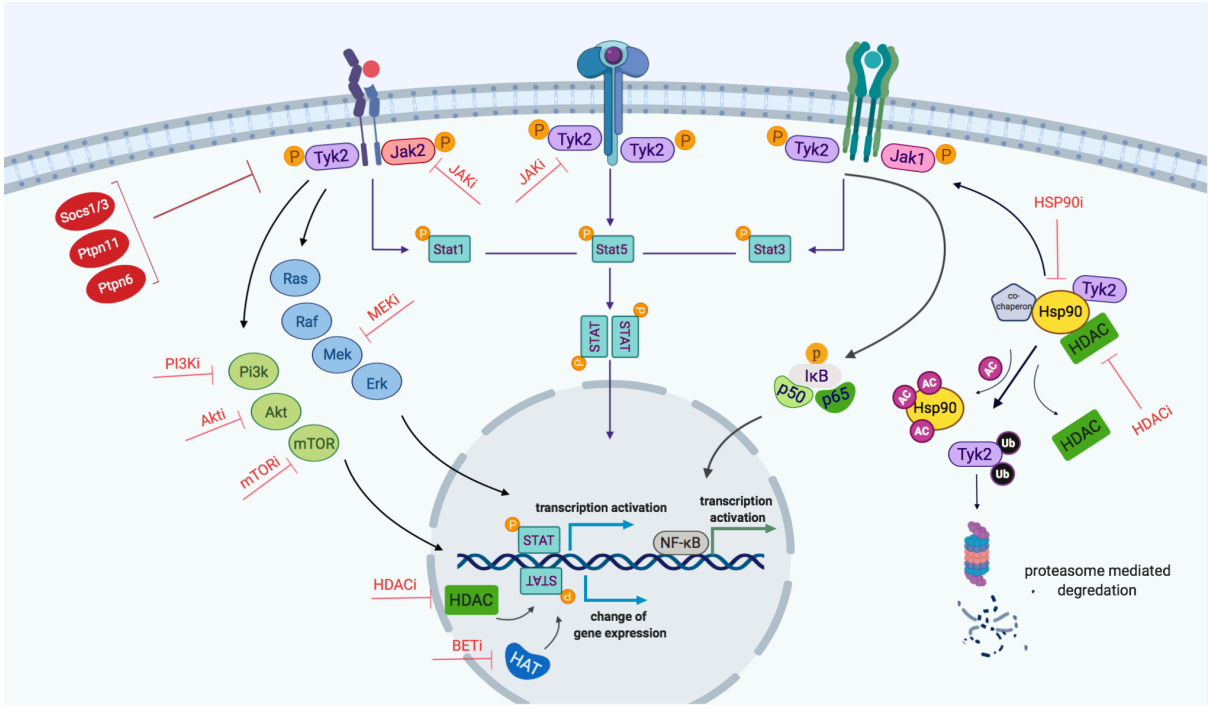

Figure 1-5. Schematic representation of Tyk2-mediated JAK/STAT signalling network. Binding of cytokine to the cytokine receptor complex results in dimerisation, which consequently phosphorylates JAK proteins as the cytokine receptor itself lacks intrinsic biological activity. Activated JAKs induce the phosphorylation of STATs which, following dimerisation, translocate into the nucleus and stimulate gene expression. STATs bind to the enhancer region of genes and by recruiting epigenetic modifiers (HDAC and HAT) to modulate the transcription of genes. JAKs activate other downstream signalling cascades including PI3K/mTOR, RAS and NF-κB. Furthermore, Hsp90 and its co-chaperones such as HDAC proteins play an important role in facilitating signalling and JAK protein stabilisation. Red proteins (e.g Socs1/3) are pathway regulators. Potential inhibitors of the proteins and pathways are indicated with red T-shaped lines. Abbreviations: AC, acetyl group; BET, Bromodomain and Extra-Terminal motif; HATs, histone acetyltransferases; HDAC, histone deacetylates; Ub, Ubiquitin; P, phosphorylation

1.4.1. Tyk2 mediates cytokine signalling and activation of JAK/STAT pathway

The cytokine superfamily is a group of glycoproteins that includes interleukins, chemokines and interferons. They are essential for regulating biological processes such as the development and maintenance of B and T lymphocytes (85). JAK family kinases mediate the signalling of over 50 cytokines (121). Binding of cytokines to the cytokine receptors on the cell surface results in dimerisation or conformational changes of the receptor complex and consequently leads to auto- and trans-

phosphorylation of JAK family protein dimers (122). Activation of JAKs results in phosphorylation of STAT family proteins enabling translocation into the nucleus ((122). STATs, as classic transcription factors, bind to DNA regulatory elements and facilitate the expression or modulation of target genes (97, 122). STAT family proteins consist of seven members: Stat1-4, 5a, 5b and 6 (123). Cytokine signalling is associated with cross-specificity in activation of overlapping JAKs and STATs (124). Apart from homo-dimerisation of JAK family proteins, hetero-dimerisation of these proteins can also lead to activation of the JAK/STAT pathway (121, 125). Tyk2 mediated cytokine signalling has been demonstrated, including type I, II and III IFNs (e.g. IFNα, β and λ) and ILs (e.g IL-6, IL-10, IL-12, IL-22 and IL-23) (117, 121), but importantly the capability of Tyk2 to activate all STAT proteins has also been defined (117). Various studies reported Tyk2 signalling in dimerisation with Jak1 and Jak2 in response to cytokines (92, 100, 121, 125-127). In haematological malignancies the association of Tyk2 with Jak1 and/or Jak2 has also been reported (114, 128-130). Constitutive Tyk2 auto- and trans-phosphorylation due to activating *TYK2* genomic alterations predominantly results in activation of Stat1, 3 and 5 in leukaemias (111, 113, 114, 116, 120). Therefore, dependent on the specific cell types, cytokines and also disease, multiple JAK and STAT family proteins can be activated in response to Tyk2 perturbation.

1.4.2. Tyk2 mediates crosstalk with other oncogenic signalling pathways

JAK signalling and STAT family protein activation can interact and induce activation of several other signalling pathways such as PI3K/mTOR and RAS (112, 117). RAS (family of small GTPases) and PI3K/mTOR signalling pathways are responsible for signal transmission from cytokine, B-cell receptors and tyrosine kinases (131). These signalling pathways are crucial for lineage commitment and proper development of B-cells in the bone marrow (131, 132). Crosstalk with other oncogenic pathways, has been demonstrated in the setting of B- and T-cell ALL where the aberrant expression of the *ETV6-JAK2* fusion gene resulted in constitutive activation of RAS, PI3K and also NF-κB signalling pathways (133). In particular, some *TYK2* activating alterations were reported to induce activation of extracellular signal-

regulated kinase (ERK) signalling in T-ALL, in addition to JAK/STAT activation (111). In other haematological malignancies activating mutations to the Tyk2 protein, resulted in aberrant signalling through additional pathways such as PI3K/mTOR, RAS and also PIM (proto-oncogene serine/threonine-protein kinases) (116, 128). Taken together, these results demonstrate the capability of the Tyk2 protein in inducing activation of additional oncogenic signalling pathways, depending on the specific cell type, mode of activation and disease context.

1.4.3. The interplay in regulation and stabilisation of Tyk2 and STAT proteins

The activity of JAK family proteins is negatively regulated by multiple intrinsic and extrinsic factors. The first intrinsic inhibitory feature includes the regulatory ability of the pseudokinase domain (JH2,Figure 1-4) to control the kinase domain activity (134-136). In addition, extrinsic negative regulation of JAK/STAT pathway relies mainly on the SH2 domain-containing suppressors of cytokine signalling (SOCSs) proteins and proteases (e.g. protein tyrosine phosphatases Ptpn1, Ptpn6 and Ptpn11) (121, 134). The SOCS family proteins promote ubiquitination and degradation of JAK family proteins while proteases dephosphorylate activated JAKs and cytokine receptors; both actions lead to attenuation of JAK/STAT signalling (134). Apart from the global role of these negative regulators, previous studies demonstrated that deactivation of Tyk2 signalling and acceleration of Tyk2 protein degradation is mainly due to direct protein-protein interaction of Socs1/3, Ptpn6 and Ptpn1 with activated Tyk2 (100, 137-140).

JAK and STAT family proteins are clients of heat shock proteins (HSP), in particular Hsp90 (141). The Hsp90 is a chaperone protein that plays an important role in maturation, stabilisation, folding and function of JAK and STAT proteins (141-143). Interestingly, Hsp90 is identified as the chaperone for various oncogenes (144, 145). It promotes the functional stability of malignant cells that would otherwise be disrupted due to acquired alterations and increases their adaptability to environmental factors such as treatment (144, 145). This function of Hsp90 is also vital in JAK/STAT dependent haematological

malignancies and *CRLF2*-rearranged and *JAK2*- and *JAK1*-mutated B-ALL (141, 146-148). In these cases inhibition of Hsp90 by small molecule inhibitors (SMIs) or RNA interference resulted in attenuation of STATs phosphorylation and degradation of JAK proteins (146-148). Proteomic analysis further confirmed the direct interaction of Hsp90 with Tyk2 protein enhancing its stability (117, 149). In addition, Hsp90 inhibition resulted in Tyk2 degradation and signal reduction in T-ALL cells harbouring wildtype and mutant *TYK2* (150).

Hsp90 functions through association with several proteins and co-chaperones and is subject to multiple regulatory mechanisms (142, 143). One of these negative regulatory mechanisms involves acetylation of lysine residues on Hsp90 that subsequently inhibits the binding of client and co-chaperone proteins leading to JAK proteins aggregation (143, 151). Therefore, histone deacetylases (HDACs) including Hdac1, 6 and 10 play an important role in facilitating Hsp90 activity (143, 151).

Moreover, STAT proteins interact with epigenetic co-factors such as histone acetyltransferases (HATs) and HDACs to modulate transcription of target genes (124). Historically, HDACs activity was believed to regulate transcriptional repression only, however, recent studies revealed that both HDACs and HATs can act as activators and/or repressors of STAT-mediated transcription (124, 152-154). HDAC mediated deacetylation of target gene's transcription activation sites upon Stat1, 2 and 5 binding to DNA, is essential to recruit the transcription machinery (e.g. RNA polymerase II) and initiate transcription (152, 155-159). Hence, silencing of HDAC activity through SMIs or small interfering RNAs results in decreased STATs phosphorylation levels and expression of target genes (152, 155-159). HDACs also play an important role in modulation of the acetylation balance of STAT proteins in co-operation with HATs that directly regulate STATs activity and protein stability (160). These data highlight the positive regulatory effect of HDACs. Growing evidence also indicates efficacy of HDAC inhibitors (HDACi) in haematological malignancies and other cancers (153, 161, 162). Of note, apart from direct effect on STATs, HDACi

display various mechanisms of actions that can include growth arrest, extrinsic or intrinsic apoptosis pathway, mitotic or ROS facilitated cell death and cell senescence (163).

1.5. Potential therapeutic approaches in ALL

1.5.1. Conventional treatment regimen in ALL

In the ALL setting, therapy is generally selected through a risk stratification process depending on age, white blood count, and primary genomic and/or karyotypic alterations; all of these factors are important indicators of prognosis (section 1.1.1) (164). Conventional chemotherapy treatment consists of 3 stages: induction, intensification (or consolidation) and long-term maintenance (1, 4). First line therapy aims to eliminate the maximum number of leukaemic cells. This includes the administration of glucocorticoids such as prednisone or dexamethasone with addition of asparaginase, vincristine and intrathecal chemotherapy (i.e. hydrocortisone, cytarabine and methotrexate) (4, 165). Following induction therapy, based on the risk groups to which patients are assigned, they may receive allogeneic SCT (HR and standard risk) or continue on to consolidation therapy (4, 165). Consolidation and maintenance therapy, depending on the protocol, can consist of methotrexate (DNA synthesis inhibitor) and other chemotherapeutics aiming to eradicate and reduce the possibility of disease recurrence (1). These regimens can also include CNS prophylaxis of intrathecal chemotherapy (4).

It is unlikely that the survival rate of refractory and/or relapsed disease can be sufficiently improved by intensified chemotherapy regimens, CNS directed treatment and/or SCT (4, 166, 167). Although combinational high dose chemotherapy has dramatically improved the survival rates, these aggressive treatment approaches are also associated with severe side effects such as osteonecrosis, pancreatitis, high infection rate and thrombosis (165, 168, 169). Furthermore, chemotherapy treatment can be associated with long term toxicity and secondary malignancies even in survivors (167, 170, 171). SCT, is also associated with substantial morbidity and mortality (172-174). In addition, SCT is limited by

availability of matched stem cell/bone marrow donors (166, 175). Several studies have demonstrated the poor outcome of patients with Ph-like ALL in response to conventional chemotherapy regimens (31, 39, 60). For instance, *in vitro* cytotoxicity assays demonstrated the significantly lower response of Ph-like ALL patients' cells to chemotherapeutics such as L-asparaginase and daunorubicin compared with other B-ALL cases (31). Further investigation using whole genome sequencing followed by complementary functional studies, demonstrated that mutations in *JAK1, IL-7R* and *NRAS* are associated with steroid resistance (176). *JAK1* and *RAS* mutated cases have been suggested to associate with chemoresistance through activation of AKT and MEK-ERK downstream signalling and demonstrated high risk of relapse and poor outcome (176, 177). Therefore, there is an unmet need for further targeted therapeutics that can improve the outcome for these high risk patients.

1.5.2. Use of tyrosine kinase inhibitors and other small molecule inhibitors as targeted therapy can be of benefit in ALL

The use of ABLi against the Bcr-Abl oncoprotein transformed treatment outcomes for patients with CML and Ph-positive ALL (178-181). These inhibitors demonstrated efficacy through binding to the ATP-pocket present in the Abl protein and blocking the downstream signalling (182, 183). In addition, administration of ABLi demonstrated a reduction of disease burden and reduced blast count in clinical case reports of Ph-like ALL patients harbouring *EBF1-PDGFRB*, *ATF7IP-PDGFRB* and *ETV6-ABL1* fusion genes (83, 184, 185). These observations warrant further investigation in larger cohorts and the efficacy of dasatinib (second generation Src/Abl inhibitor) in addition to chemotherapy is under investigation (NCT02883049, NCT02143414). The success of ABLi in targeting the oncoprotein and improving patients' outcome, highlighted a promising avenue for targeting other kinases such as JAK family proteins.

Ruxolitinib was the first JAK1/2i approved for treatment of patients with myeloproliferative disorders such as myeloproliferative neoplasms (MPN), polycythemia vera (PV) and essential thrombocythemia (ET), the majority of whom harboured the *JAK2* p.V617F mutation (186-189). Ruxolitinib, in comparison with other available regimens, is associated with reduced side effects (190), significant improvement of symptoms and reduced splenomegaly (191). *In vitro* and *in vivo* sensitivity to ruxolitinib has recently been demonstrated in several pre-clinical studies using Ph-like models harbouring *CRLF2* and *JAK2* alterations (24, 63, 65, 75). These studies provide a rationale for the use of JAKi in the clinical setting for Ph-like ALL cases carrying JAK/STAT activating alterations. Nevertheless, testing other potential JAKi is crucial due to the variable response to ruxolitinib reported in *in vivo* models and the differing potency of inhibitors in targeting different alterations (63, 65, 192, 193). For instance, a study by Akahane *et.al* (2017) demonstrated the superior *in vitro* anti-leukaemic and *in vivo* efficacy of NDI-031301 (Tyk2-specific inhibitor) compared with baricitinib (Jak1/2 inhibitor with little effect on Jak3 and Tyk2) and tofacitinib (Jak3/2/1 inhibitor) to induce cell death in human T-ALL lines and decrease tumour burden in mice (194). However, this could be due to a higher dependency of T-ALL cells on Tyk2 activation (111). Sensitivity to ruxolitinib has also been investigated via *in vivo* models of T-ALL with JAK/STAT over expression which demonstrated potential anti-leukaemic activity and prolonged survival (195, 196). The efficacy of adding ruxolitinib to conventional chemotherapy treatment is currently being investigated in clinical trials for HR-ALL *CRLF2*-rearranged patients with or without *JAK2* variants (NCT02420717, NCT02723994, NCT02723994) as well as newly diagnosed HR Ph-like ALL patients (NCT02420717, NCT02883049).

Furthermore, based on the genomic alterations, alternative signalling pathways such as PI3K/mTOR and RAS can be activated in Ph-like ALL cases (section 1.2). In addition, the underlying biology and signalling crosstalk of pathways involving JAK/STAT (section 1.4), provides other possible therapeutic targets. Table 1-5 summarises the SMIs that, thus far, have shown promising *in vitro* and *in vivo* efficacy in Ph-like ALL.

Table 1-5. Potential Small Molecule Inhibitors (SMIs) with demonstrated pre-clinical efficacy against Ph-like ALL.

modified from Kotb *et.al* (2018) (197)

SMIs	Class	Genomic alteration/ activated pathways	Clinical Status	Current trials in ALL	Reference
gedatolisib	dual PI3K/mTORi	*CRLF2* rearrangements, *JAK2, ABL1* and *PDGFRB* fusions	*in vitro* and *in vivo* alone or in combination with ruxolitinib	-	(198)
rapamycin	mTORi	*CRLF2* rearrangements, *JAK2* fusions and *IL7-R* mutations	*in vitro* and *in vivo*	In trial for relapsed ALL/lymphoma (NCT00874562 and NCT01162551)	(63)
selumetinib	MEK1/2i	*CRLF2* rearrangements	*in vitro* and *in vivo* (in combination with AZD1480 (Jak2 inhibitor))	In trial for ALL (NCT03705507)	(192)
givinostat	HDACi	*CRLF2* rearrangements	*in vitro* and *in vivo* (superior efficacy in comparison with ruxolitinib)	-	(199).
panobinostat	HDACi	Reh (pre-B cell line) and primary Ph-like ALL cells	*in vitro*	Previously in trial for relapsed ALL/AML (NCT00723203 terminated)	(200)
JQ1	BETi	*CRLF2* rearrangements	*in vitro* and *in vivo*	-	(201)
luminespib	HSP90i	*CRLF2* rearrangements	*in vitro* and *in vivo*	-	(146)

Abbreviations: i, inhibitor.

Taken together, these findings highlight the potential benefit of therapies targeted to specific genomic alterations that may improve the response to treatment and outcomes in patients. Currently there is an unmet need to widely investigate the efficacy of SMIs on other Ph-like ALL subtypes including *JAK* family fusion genes. In the era of precision medicine, it is essential to understand the activated pathways due to each underlying genomic alteration in patients. In addition, it is then crucial to identify therapeutics that specifically target activated pathways through robust pre-clinical models to test novel therapies and allow more alteration-specific clinical trials.

1.6. Development of TKI resistance, specifically to JAKi, occurs via reactivation of the JAK/STAT signalling pathway

1.6.1. Mechanism of resistance to ABLi

Unfortunately, despite the encouraging success of Abl TKIs in treatment of CML and Ph-positive ALL, a considerable number of patients develop resistance to therapy. The mechanisms of TKI resistance is well documented and, in brief, is usually a result of:

1) mutations in the kinase domain (commonly p.T315I) that result in inhibition of drug binding (202, 203),

2) increased expression of the *BCR-ABL1* oncogene that results in titration of available intracellular TKIs (204, 205),

3) alterations in expression and activity of drug transporter membrane proteins: increase in drug efflux transporters (e.g. members of the ATP-binding cassette (ABC) transporter superfamily) and decrease in drug influx transporters (e.g. organic cation transporter, member 1, Oct-1 (in the case of imatinib resistance) (206-208)

Resistance to imatinib (first generation Abl inhibitor) was considered as the most common cause of relapse and therapy resistance in Ph-positive ALL cases (181). Following this, second generation of ABLi (dasatinib and nilotinib), that bind to the active form of the Abl protein, were developed to overcome imatinib resistance and increase drug potency (181, 209-211). Dasatinib demonstrated initial activity against imatinib-resistant cases however, resistance to therapy and treatment failure occurred in Ph-positive ALL cases (181, 209, 210). Recently, the T315I mutation has also been reported by our laboratory in a relapsed Ph-like ALL patient harbouring an *ABL1* fusion gene after initial sensitivity to dasatinib (184). In cases of dasatinib failure, third generation TKI ponatinib or the novel allosteric ABLi, asciminib (that may soon become a frontline therapy; NCT03595917), will be administered for these patients (4, 212, 213). Of note, unlike for ALL, Abl TKIs have been used as monotherapy in the CML setting but failed to consistently result in treatment free remission in patients mainly due to intolerance or resistance (214). Development of resistance highlights the importance of ongoing inhibitor testing and the need for more effective therapeutic regimens; possibly through administration of a combination of inhibitors to prevent the outgrowth of resistant leukaemic clones due to single agent treatment. Efficacy of this combinational strategy was demonstrated in *in vitro* and pre-clinical models of CML (214).

1.6.2. Mechanisms of resistance to JAKi

In contrast to ABLi, the mechanisms of resistance to JAKi is not as well understood. Although, ruxolitinib treatment resulted in improved quality of life in MPN patients, the reduction in allelic burden by ruxolitinib in *JAK2* mutant MPN patients appears to be limited (191). In recent trials for myelofibrosis patients, long-term exposure to ruxolitinib led to loss of response in 50% of cases after 3 years of treatment (215, 216). The evidence of resistance mechanisms to JAKi are predominantly from *in vitro* studies on MPN and include:

1) acquisition of secondary kinase domain mutations that results in conformational changes in drug binding to the JAK protein (146, 217, 218),

2) persistent JAK/STAT signalling due to heterodimerisation and transactivation of JAK family proteins (219-221)

Although the presence of secondary kinase domain mutations have been reported to confer resistance to ATP competitive JAKi *in vitro* (146, 217, 218), these mutations have not been detected in any of the MPN patients that developed resistance to ruxolitinib (222). Conversely, reactivation of the JAK/STAT signalling upon long term exposure to ruxolitinib treatment has recently been reported in MPN patients (223). This effect thought to be due to transactivation of Jak2 with Jak1 and Tyk2 proteins (219, 220, 223). Ruxolitinib and other type I JAKi bind to the ATP binding site of JAK proteins to supress the JAK/STAT signalling, however, they also lead to stabilisation of JAK proteins and increased phosphorylation of the activation loop (224). Therefore, this may indicate that the lack of resistance-related *JAK* mutations in MPN patients is due to the likelihood of this persistence mechanism through increased JAK heterodimer development and reactivation of the JAK/STAT pathway.

The possibility of resistance development in Ph-like ALL patients harbouring *CRLF2* and *JAK* family alterations remains unclear as the addition of ruxolitinib to treatment regimens is recent and still under investigation. However, given the commonality of developing TKI resistance in CML, Ph-positive ALL and recently MPN patients, it is plausible that same resistance mechanisms will be a common route of therapy failure in Ph-like ALL cases. Thus, it is essential to employ pre-clinical models to anticipate and prevent the emergence of TKI-resistance and/or inform alternative treatments to overcome lack of response in ALL patients. This will ultimately ensure long term remission and potentially avert relapse.

1.7. Concluding remarks

The current use of NGS technology enabled the better understanding and identification of high risk subtypes of B-ALL such as Ph-like ALL that are of clinical importance due to potential targetability by TKIs. Yet, new lesions are reported frequently in studies investigating genome wide profiling of ALL (28, 60) that warrant further characterisation using laboratory models. Studies into large cohorts of Ph-like ALL cases demonstrated the presence of *TYK2* alterations such as *MYB-TYK2* as a high risk subtype (15, 65). Although, *TYK2* activating mutations and rearrangements have been reported in other haematological malignancies such as T-ALL, anaplastic large cell lymphoma (ALCL) and CD30-positive lymphoproliferative disorder patients (111, 113-116), to date there is no available literature providing a clear functional significance for these alterations in driving leukaemia pathogenesis. Given the recent report identifying *MYB-TYK2* as a novel alteration in HR Ph-like ALL, it is crucial to investigate the biological consequences of aberrant kinase expression as a result of this fusion gene.

Several studies highlighted the important role of the Tyk2 protein in activation of JAK/STAT signalling. In addition, based on the biological context, Tyk2 can mediate crosstalk to other oncogenic pathways and interact with regulatory complexes (100, 117). Therefore, this paradigm provides an avenue for discovering possible SMIs against *TYK2* altered disease. Considering that JAK/STAT signalling is expected to be the predominant signalling pathway activated by Tyk2 fusion proteins, Jak/Tyk2 inhibitors may be among the most promising candidate therapeutics against fusions involving these genes.

Although, incorporation of TKIs such as ABLi and ruxolitinib (JAKi) into Ph-positive ALL and myeloproliferative neoplasms (MPN) patients' respective treatment regimens appears promising, there is still cause for concern as relapse due to TKI resistance can occur (181, 209, 210, 215, 216). In addition, the mode of resistance varies depending on the TKI and possibly genomic alterations. Hence, it is important to identify the resistance mechanism that may arise due to long term exposure to specific TKIs

in the setting of *TYK2* alterations. This approach will identify alternate treatment strategies in order to overcome and avert treatment failure and relapse in patients.

1.8. Summary and project aims

In the B-ALL setting, the novel HR Ph-like *MYB-TYK2* fusion gene may be a potent driver lesion that remains to be fully characterised. Current literature does not convey a clear picture of the transforming and leukaemogenic potential of activating *TYK2* alterations in the ALL setting. Owing to the growing number of *TYK2* alterations detected in ALL patient samples, it is necessary to understand the underlying biology of this fusion with respect to changes in leukaemogenesis and activated signalling pathways. Moreover, there is an unmet need to inform drug response and targeted therapeutics against this fusion. Information from these studies combined with explorations of the possible modes of treatment resistance, and how to circumvent resistance development, will ultimately improve outcome in patients.

Hypothesis:

The *MYB-TYK2* alteration is a driver oncogene of B-ALL. The poor prognosis of *MYB-TYK2* rearranged ALL cases could be greatly improved via development of new targeted therapies based on a greater understanding of this lesion with respect to drug response and possible modes of therapy resistance.

Aims:

1. Generate *in vitro* and *in vivo* models of *MYB-TYK2* altered disease to identify and characterise the mechanisms of oncogenicity and activated downstream signalling pathways
2. Inform and assess the efficacy of targeted therapeutics against *MYB-TYK2* altered disease using *in vitro and in vivo* models

3. Determine the possible mechanisms of resistance to candidate therapy in *in vitro* models and inform alternative therapeutic approaches to overcome possible disease persistence and resistance

Results from this thesis elucidated the functional significance of the *MYB-TYK2* fusion gene in inducing leukaemia. Additionally, the downstream signalling pathways of the *MYB-TYK2* fusion gene were identified and targeted therapeutics against *MYB-TYK2* altered disease were investigated. Due to the likelihood of TKI-resistance development, this study also generated therapy-resistant cell lines in order to evaluate and predict possible resistance mechanisms that may occur as a result of long term treatment in patients. Understanding the driving potential of the *MYB-TYK2* fusion gene and drug response by establishing robust models of disease, like those described here, in order to rigorously test and narrow down effective SMIs will improve outcome for patients harbouring activating *TYK2* alterations. The approach presented here has the potential to be used against other genomic alterations and will assist in tailoring precision medicine for individual patients in order to improve long-term survival of HR ALL patients.

`

2. Chapter 2: Exploring the oncogenic and therapeutic target potential of the *MYB-TYK2* fusion gene in B-cell acute lymphoblastic leukemia

Statement of Authorship

Title of Paper	Exploring the oncogenic and therapeutic target potential of the *MYB-TYK2* fusion gene in B-cell acute lymphoblastic leukemia
Publication Status	☐ Published ☐ Accepted for Publication ☑ Submitted for Publication ☐ Unpublished and Unsubmitted work written in manuscript style
Publication Details	Paniz Tavakoli Shirazi, Laura N Eadie, Susan L Heatley, Maxime François, David T Yeung, Timothy P Hughes and Deborah L White, Exploring the oncogenic and therapeutic target potential of the *MYB-TYK2* fusion gene in B-cell acute lymphoblastic leukemia, submitted to Oncogene Journal

Principal Author

Name of Principal Author (Candidate)	Paniz Tavakoli Shirazi		
Contribution to the Paper	Conceived, designed, performed experiments, generated lines and reagents, interpreted/analysed data, wrote and revised the manuscript.		
Overall percentage (%)	90%		
Certification:	This paper reports on original research I conducted during the period of my Higher Degree by Research candidature and is not subject to any obligations or contractual agreements with a third party that would constrain its inclusion in this thesis. I am the primary author of this paper.		
Signature		Date	12/1/21

Co-Author Contributions

By signing the Statement of Authorship, each author certifies that:

i. the candidate's stated contribution to the publication is accurate (as detailed above);
ii. permission is granted for the candidate in include the publication in the thesis; and
iii. the sum of all co-author contributions is equal to 100% less the candidate's stated contribution.
iv.

Name of Co-Author	Laura Eadie		
Contribution to the Paper	Supervised, designed experiments and critically revised the manuscript.		
Signature		Date	12/01/21

Name of Co-Author	Susan Heatley		
Contribution to the Paper	Supervised, designed experiments and critically revised the manuscript.		
Signature		Date	12-1-21

Name of Co-Author	Maxime François		
Contribution to the Paper	Assisted with immunofluorescent microscopy experiments and provided reagents.		
Signature		Date	22.1.2021

Name of Co-Author	David Yeung		
Contribution to the Paper	Assisted with blood film and critically revised the manuscript.		
Signature		Date	12 JAN 2021

Name of Co-Author	Timothy Hughes		
Contribution to the Paper	Critically revised the manuscript.		
Signature		Date	12/1/2021

Name of Co-Author	Deborah White		
Contribution to the Paper	Supervised, designed experiments and critically revised the manuscript.		
Signature		Date	12/1/21

Exploring the oncogenic and therapeutic target potential of the *MYB-TYK2* fusion gene in B-cell acute lymphoblastic leukemia

Paniz Tavakoli Shirazi[1,2], Laura N Eadie[1,2], Susan L Heatley[1,2], Maxime François[4,5], Timothy P Hughes[1,2], David Yeung[1,2,3] and Deborah L White[1,2,3,4,6]

1. Cancer Program, Precision Medicine Theme, South Australian Health & Medical Research Institute (SAHMRI), Adelaide, Australia
2. Faculty of Health and Medical Sciences, University of Adelaide, Adelaide, Australia
3. Royal Adelaide Hospital, Adelaide, Australia
4. Faculty of Sciences, University of Adelaide, Adelaide, Australia
5. CSIRO Health and Biosecurity, Nutrition & Health program, Adelaide, Australia
6. Australian Genomics Health Alliance (AGHA)

Corresponding author:

Prof. Deborah White (PhD. FFSc(RCPA)).

Director: Cancer Program SAHMRI.

Deputy Theme Leader: Precision Medicine SAHMRI.

NHMRC RD Wright Research Fellow

Beat Cancer Project Principal Research Fellow

Professor: The Faculty of Health and Medical Science, University of Adelaide.

Professor: School of Biological Sciences. The Faculty of Sciences, University of Adelaide.

Cancer Program. Precision Medicine Theme, South Australian Health & Medical Research Institute (SAHMRI), Adelaide, Australia

Phone: +61 08

E-mail:

Abstract:

TYK2-rearrangements have recently been identified in high-risk acute lymphoblastic leukemia (HR-ALL) cases and are associated with poor outcome. Current understanding of the leukemogenic potential and therapeutic targetability of activating *TYK2* alterations in the ALL setting is unclear, thus further investigations are warranted. Consequently, we developed *in vitro,* and for the first time, *in vivo* models of B-cell ALL from a patient harboring the *MYB-TYK2* fusion gene. These models revealed JAK/STAT signaling activation and the oncogenic potential of the *MYB-TYK2* fusion gene in isolation. High throughput screening identified the HDAC inhibitor, vorinostat and the HSP90 inhibitor, tanespimycin plus the JAK inhibitor, cerdulatinib as the most effective agents against cells expressing the *MYB-TYK2* alteration. Evaluation of vorinostat and cerdulatinib in pre-clinical models of *MYB-TYK2*-rearranged ALL demonstrated that both drugs exhibited anti-leukemic effects and reduced the disease burden in treated mice. Importantly, these findings indicate that activating *TYK2* alterations can function as driver oncogenes rather than passenger or secondary events in disease development. In addition, our data provide evidence for use of vorinostat and cerdulatinib in the treatment regimens of patients with this rare yet aggressive type of high-risk ALL that warrants further investigation in the clinical setting.

Introduction:

Despite advances in treatment and management of acute lymphoblastic leukemia (ALL), High-Risk (HR-ALL) is still associated with increased risk of relapse and leukemia associated death (1, 2). As genomic drivers of the disease are progressively elucidated, incorporating precision therapeutics with specificity against these druggable targets may be the optimal approach to improve outcome. For instance, *JAK* activating mutations and rearrangements signal through the JAK/STAT signaling pathway and/or other

pathways due to the possible cross talk induced by JAK signaling (1, 3-5); to enhance cellular proliferation and survival, leading to a group of HR-ALL within cases classified as Ph-like ALL. These lesions may be amenable to therapeutic inhibition through small molecule inhibitors (SMIs). The efficacy of a number of such SMIs has been demonstrated in *in vitro* and pre-clinical *in vivo* models and case studies (6-12).

Following the recognition of the oncogenic driving potential of *TYK2*, gain of function mutations and rearrangements are reported with increasing frequency in different ALL subtypes (1, 13-15). These include high risk Ph-like ALL where*TYK2* rearrangements were identified in 1.5% of patients in a cohort of 194 Ph-like ALL cases (1). A full list of *TYK2* germline and somatic activating mutations and rearrangements identified in ALL has been reported recently by our group (16). Similar to other JAK family kinases, TYK2 facilitates cytokine signaling and the downstream JAK/STAT activation. However, little is known about its oncogenic potential, and its susceptibility to drug inhibition (17, 18). While the role of JAK1-3 in cancer has been intensively studied, TYK2 has mainly been studied in relation to auto-immune and inflammatory diseases (18, 19). In 2014, the first case of a *TYK2* fusion gene was reported in a HR B-ALL patient; subsequently, three 5' partner genes have been identified in association with *TYK2* fusions (*MYB*, *SMARCA4*, *ZNF340*) with similar breakpoints at exon 19 and 18 (12, 20). While the transforming ability of the *MYB-TYK2* fusion gene has previously been demonstrated in Ba/F3 cells (12), further characterization of *TYK2* fusion genes as drivers of leukemogenesis has not been described. Furthermore, *TYK2* alterations have been reported in other blood cancers including acute myeloid leukemia and lymphomas (21-24) demonstrating constitutive auto- and trans-phosphorylation of TYK2 and downstream activation of STAT family proteins (21, 22). Yet, it is not clear whether these fusions are secondary events, or the primary drivers of leukemogenesis. Furthermore, the potential for such lesions to affect downstream signaling in B-ALL, and its susceptibility to therapeutic intervention had been largely unexplored. This study examines the potential of *MYB-TYK2* as a leukemic driver, testing the hypotheses

that 1) this is achieved through constitutive JAK/STAT signaling; and 2) this interaction is susceptible to SMI inhibition.

Material and method

Retroviral constructs. The *MYB-TYK2* fusion gene, isolated from an ALL patient, was obtained from St. Jude Children's Research Hospital (Memphis, Tennessee, USA) in a pCR-Blunt II-TOPO® vector. The fusion gene was excised and ligated into the multiple cloning site of the Green Fluorescent Protein (GFP)-tagged p-Ruf-iG2 retroviral vector by a non-directional cloning using digest with *Eco*R1 restriction enzyme. The correct orientation and sequence of the fusion gene was verified by enzyme digestion and Sanger sequencing. Retroviral particles were used to generate Ba/F3-*MYB-TYK2*, *Arf*$^{-/-}$*-MYB-TYK2* and NIH-3T3-*MYB-TYK2* lines as detailed in supplementary methods.

***In vivo* mouse transplantation.** Retrovirally transduced *Arf*$^{-/-}$*-MYB-TYK2* cells (0.9-1x10^6 cells/mouse) and the EV counterpart (1.4-2x10^6 cells /mouse) were transplanted via tail vein injection into 6 week old sublethally irradiated (300 cGy) non-obese diabetic/severe combined immunodeficient NOD.Cg-*Prkdc*^{scid} *Il2rg*^{tm1Wjl}/SzJ (NSG) mice. Blood samples were collected fortnightly by tail vein bleed to assess the engraftment levels (GFP positive leukaemic cells). The mice were fed a standard rodent diet and water supplemented with 0.3 mg/mL Baytril *ad libitum*. Animals were monitored daily for clinical signs of leukemia (weight loss, hunching, ruffled fur, reluctance to move) and were humanly killed when moribund (20% weight loss and/or body score of 4). All experiments were performed according to institutional animal ethics.

Supplementary methods

Detailed methods undertaken for this study are provided in the supplemental appendices.

Results:

Expression of the *MYB-TYK2* fusion gene results in cytokine independence and activation of the JAK/STAT signaling pathway

The *MYB-TYK2* fusion gene was transduced into IL-3 dependent Ba/F3 pro-B cells, IL-7 dependent *Arf*$^{-/-}$ pre-B cells and NIH-3T3 fibroblasts (Figure 1A). *MYB-TYK2* mRNA expression was confirmed by RT-PCR (Supplementary Figure 1). The *MYB-TYK2* fusion gene consists of the 5' *MYB* retaining the DNA binding domain that facilitates dimerisation (20, 25), and the 3' *TYK2* kinase gene that has an in-frame kinase domain and disrupted pseudo kinase domain, responsible for kinase auto-inhibition (Figure 1A). Expression of the *MYB-TYK2* fusion gene facilitated both IL-3 dependent Ba/F3 and IL-7 dependent *Arf*$^{-/-}$ cells to proliferate in a cytokine independent manner offering a significant proliferative advantage (Figure 1B&C). Conversely the empty vector (EV) counterparts did not demonstrate cytokine independent growth. Immunofluorescence (IF) analysis for MYB and TYK2 in the NIH-3T3-*MYB-TYK2* cells demonstrated altered localization of both proteins compared with the locations of these proteins when endogenously expressed (nucleus and cytoplasm, respectively (26, 27); instead, ubiquitous expression of MYB-TYK2 was observed (Figure 1D&E and Supplementary Figure 2). This is while Tyk2 as a non-receptor tyrosine kinase and intracellular signal transducer can be mainly found in cytoplasm and membrane (27). Western blot analyses revealed constitutive activation of the intact TYK2 catalytic kinase domain in Ba/F3-*MYB-TYK2* cells (Supplementary Figure 3, panel A); MYB and total TYK2 analyses further confirmed the expression of the MYB-TYK2 fusion protein in these cells (Supplementary Figure 3, panel B and C). Phosphoflow cytometric analyses on Ba/F3 *MYB-TYK2* cells, in the absence of IL-3, support the oncogenic role of this fusion gene. MYB-TYK2 protein expression led to constitutive activation of JAK/STAT signaling via phosphorylation (p) of STAT3 and STAT5 in Ba/F3 *MYB-TYK2* cells compared with EV controls (MFI=833 vs 104, p=0.04 and 641 vs 427, p>0.05; Figure 1F). An increase in pERK

(MFI=166 vs 82, p=0.005; Figure 1G) and decrease in S6 phosphorylation (ribosomal protein which is an indicator of mTOR activity (28)) (MFI=4805 vs 8539, p=0.007; Figure 1G) was also observed in cells expressing the MYB-TYK2 fusion protein compared with EV control. There was no activation of STAT1 (Figure 1F) or other signaling pathways explored (Supplementary Figure 4A). Of note, expression of the *MYB-TYK2* fusion gene in Ba/F3 cells resulted in accumulation of histone acetylation when compared with EV controls, indicated by elevated levels of histone 3 lysine 9 acetylation (H3K9ac) (MFI=0.7 vs 0.3, p=0.003). No change in the level of H3 lysine 27 tri-methylation (H3K27me3) was detected (Supplementary Figure 4B).

The *MYB-TYK2* fusion gene induces B-cell ALL in *in vivo* models

NSG mice were transplanted with either *Arf*$^{-/-}$*-MYB-TYK2* or *Arf*$^{-/-}$-EV cells via tail vein injection (n=5 per cohort). Expression of the *MYB-TYK2* fusion gene led to development of leukemia with a median latency of 84 days post-transplantation compared with EV mice which were culled at 133 days post-transplantation with no signs of leukemia (p=0.002; n=5 vs n=5, respectively, Figure 2A). One of the *MYB-TYK2* mice was culled due to irradiation complications at day 12 and was censored from survival analysis. At end-stage disease, *MYB-TYK2* mice demonstrated splenomegaly (n=4, 269±42 mg; p=0.01) and a significant increase in liver weight (n=4, 1667±101 mg; p=0.03) compared with EV control mice (n=5, 86±13 and 1319±73 mg, respectively; Figure 2B). The presence of the *MYB-TYK2* fusion gene was confirmed in cells isolated from organs of *MYB-TYK2* mice by RT-PCR (Supplementary Figure 5 A&B). All *MYB-TYK2* mice demonstrated an average of 63% (±13%), 46% (±15%), 53% (±17%), 62% (±30%) infiltration of GFP positive leukemic *Arf*$^{-/-}$*-MYB-TYK2* cells in bone marrow, spleen, liver and peripheral blood, respectively, by flow cytometric analyses (Supplementary Figure 6). Bone marrow, spleen and liver sections stained with hematoxylin and eosin (H&E) and GFP antibody further confirmed the leukemic infiltration in the peripheral organs of *MYB-TYK2* mice (Figure 2C and Supplementary Figure

7). In addition, peripheral blood smears from *MYB-TYK2* mice stained with Giemsa-Wright Stain demonstrated the presence of blast cells (Figure 2D). At study end point, control mice exhibited engraftment of *Arf*$^{-/-}$-EV cells in the bone marrow, spleen, liver and peripheral blood with no onset of leukemia (average GFP expression, 7-11%; data not shown). This observation is in line with previous studies demonstrating the *CDKN2A* mutation alone is insufficient to cause robust engraftment and leukemia development (12, 29-31). GFP positive (MYB-TYK2 positive) cells isolated from bone marrow, spleen and liver demonstrated a pro/pre-B cell immunophenotype (CD45R/B220^{+}, CD43^{+}, CD19^{+}, CD24^{+}, BP1$^{+/-}$ and IgM^{-}; Figure 2E; (32)), and were negative for myeloid and erythroid markers (GR1, MAC1, TER119 and THY1). Collectively, these data demonstrate, for the first time, the leukemogenic potential of the *MYB-TYK2* fusion gene via *in vivo* models and highlight *MYB-TYK2* as a putative driver gene.

High throughput screen (HTS) identified HDAC inhibitors as potential targeted therapeutic candidates against MYB-TYK2

A primary HTS using two libraries consisting of 3088 cytotoxic agents and targeted inhibitors were assessed for their impact on Ba/F3-*MYB-TYK2* cell viability. Two replicate assays were performed with both passing quality assurance assessments (Supplementary Tables 3-4, Supplementary Figure 8-10). In the primary HTS, 162 compounds were identified as hits in both replicates (Supplementary Table 5), and a panel of compounds was selected for further assessment in a secondary dose-response HTS screen. This panel consisted of:

1) the top 30 compounds leading to <1% viability compared with DMSO control (unbiased selection)
2) 26 compounds selected based on preclinical and clinical literature, all leading to 1-15% viability in treated cells compared with DMSO control (Supplementary Table 6)

The Ba/F3-*MYB-TYK2* cells were exposed to different concentration ranges (10 nM-10 μM) of these 56 compounds and the estimated IC_{50} of each drug was calculated. From this panel, 6 compounds were identified as pan-assay interference compounds and were excluded from further analysis. From the remaining compounds, 34 had known bioavailability from human studies, and/or *in vivo* models; while the IC_{50} of 20 of these compounds were deemed clinically relevant (Figure 3, Supplementary Table 6). Of the 56 compounds present in the secondary HTS, sensitivity of Ba/F3-*MYB-TYK2* cells within a clinically achievable range was observed for 83% (clinically relevant vs total, 10 vs 12) of the HDACi (Supplementary Table 6). Other active compounds of note included inhibitors of HSP90 and BCL-2. With the exclusion of pacritinib, none of the kinase inhibitors showed efficacy against Ba/F3-*MYB-TYK2* cells within clinically acceptable ranges. However, pacritinib indicated 10,000x less potency in targeting TYK2 compared with JAK2 (e.g. *PAX5-JAK2*) as reported previously (12), and thus was excluded from further analysis. Bioavailability and pharmacokinetics for the JAKi TG101209 are not yet known, however, evaluated IC_{50} for Ba/F3-*MYB-TYK2* cells was higher than the IC_{50} range reported for *JAK*-rearranged ALL lines (33, 34). Considering the results from the second dose-response HTS, 7 candidates were selected for further *in vitro* experiments:

1) HDACi: belinostat, vorinostat, panobinostat (FDA approved) and CUDC-907 (selected due to the clinical status for treatment of B-cell lymphoma (35, 36) and pre-clinical status in treatment of hematological malignancies (37)).
2) HSP90i: geldanamycin and its analogue, tanespimycin was also included given its current status in clinical trials for various cancers (38)
3) Cepharanthine (multi-action inhibitor with demonstrated ability in inhibition of BCL2 in cancer cells (39))

Vorinostat and tanespimycin demonstrate *in vitro* activity against Ba/F3-*MYB-TYK2* cells, resulting in proliferation and JAK/STAT signaling inhibition

Selected compounds were further assessed with regards to TYK2 selectivity and JAK/STAT inhibition, using Ba/F3 cell lines harboring *PAX5-JAK2* and *ATF7IP-JAK2* as controls (12). Ba/F3-*MYB-TYK2* cells achieved IC_{50} within the clinically relevant range for all drugs (Supplementary Table 7). The variable responses to available tyrosine kinase inhibitors (TKIs) observed in previous *in vitro* and *in vivo* pre-clinical experiments and case studies (6, 7, 40, 41), highlight potential implications for the successful use of SMIs as a part of a targeted treatment approach in clinic. Thus, we selected inhibitors with a greater or similar efficacy against TYK2 versus JAK2 for further investigation. The drugs exhibited greater or similar selectivity against the *MYB-TYK2* harboring cells in comparison with *JAK2*-rearranged lines: 1) vorinostat (Ba/F3-*MYB-TYK2* vs -*PAX5-JAK2* or -*ATF7IP-JAK2*; IC_{50}=535 vs 637 nM, p=0.04 or 465 nM, p>0.05; Figure 4A), 2) tanespimycin (202 vs 90, p=0.03 or 134 nM, p>0.05; Figure 4B), 3) belinostat (148 vs 90 nM, p>0.05 or 124 nM; p>0.05; Supplementary Figure 11). Conversely, significantly decreased selectivity compared with Ba/F3-*PAX5-JAK2* was observed for cepharanthine (1549 vs 1116 nM, p=0.03; Supplementary Figure 11). Panobinostat, geldanamycin and CUCD-907 had significantly lower selectivity towards TYK2-mediated growth and were excluded from further analysis. Interestingly, vorinostat treatment of Ba/F3-*MYB-TYK2* cells resulted in a significant attenuation of JAK/STAT signaling –detected by a decrease in pSTAT5 levels at 60 and 120 mins, (DMSO vs vorinostat treated, 888 vs 662, p=0.01 and 783, p=0.01, respectively; Figure 4C), and pSTAT3 at 120 mins when compared with vehicle control (MFI=652 vs 627, p=0.03; Figure 4C). A similar trend was observed in Ba/F3-*MYB-TYK2* cells treated with tanespimycin (Figure 4D); a significant decrease in: 1) STAT5 activation after 60 and 120 mins treatment (DMSO vs tanespimycin, MFI= 888 vs 285, p=0.01 and 125, p=0.001, respectively) and 2) STAT3 activation upon 120 mins treatment (MFI=652 vs 99, p=0.01) compared with vehicle control. No significant decrease in the pSTAT5 or pSTAT3 levels was detected in response to other drug treatments

(Supplementary Figure 12). Vorinostat selectively inhibited Ba/F3-*MYB-TYK2* cells but not Ba/F3-*RCSD1-ABL1* cells with a three-fold difference in IC_{50} (IC_{50}=1738 vs 535 nM, p=0.006; Supplementary Figure 13A). Conversely, a differential sensitivity was not observed with tanespimycin treatment (IC_{50}=274 vs 202 nM, p>0.05; Supplementary Figure 13B), though its activity against Ba/F3-*RCSD1-ABL1* has previously been reported. (42, 43).

Cerdulatinib treatment inhibits proliferation and attenuates the activation of JAK/STAT associated proteins in Ba/F3-*MYB-TYK2* cells

Given the central role of the JAK/STAT pathway in the MYB-TYK2 fusion protein signaling, it was important to screen inhibitors that are specific for, or able to strongly target, the TYK2 protein. Recent studies demonstrated the potency of cerdulatinib to inhibit TYK2 via kinase assays (44, 45). The current status of cerdulatinib in clinical trial development for Chronic Lymphocytic Leukemia (NCT01994382) (46, 47), prompted further investigation into its efficacy against the *MYB-TYK2* fusion. Cerdulatinib inhibited growth of our Ba/F3-*MYB-TYK2* cells with an IC_{50} of 799 nM; this is within the clinically achievable range (1-2 μM plasma concentration with 40-65 mg daily dosing (47); Figure 5A). Sensitivity of Ba/F3-*PAX5-JAK2* cells to cerdulatinib was also observed (IC_{50}=602 nM; Figure 5A), demonstrating the ability of cerdulatinib to inhibit other JAKs (44, 45). In contrast, cerdulatinib had no effect on the proliferation of NALM-19 cells (IC_{50} >10 μM; Figure 5A), a human B-ALL line that is not dependent on JAK/STAT signaling for growth. Treatment with 1 μM cerdulatinib for 1 h resulted in significant inhibition of STAT5 and STAT3 activity in Ba/F3-*MYB-TK2* cells compared with vehicle (DMSO) control (cerdulatinib treated vs DMSO; MFI=104 vs 655, p=0.003 and 146 vs 615, p=0.0004, respectively; Figure 5B). A time dependent decrease in STAT5 and STAT3 activation was detected after only 5 min cerdulatinib treatment in Ba/F3-*MYB-TYK2* cells in comparison with vehicle treated cells (MFI=994 vs 494, p=0.001 and 1186 vs 522, p=0.01, pSTAT5 and pSTAT3, respectively; Supplementary Figure 14). As Ba/F3-*MYB-TYK2*

cells are insensitive to ruxolitinib (12), ruxolitinib treatment was used as a negative control with results as expected.

While previous experiments demonstrated the effect of vorinostat and cerdulatinib on inhibition of proliferation and JAK/STAT signaling, the ability of these inhibitors to induce apoptosis in Ba/F3-*MYB-TYK2* cells was unknown. Ba/F3-*MYB-TYK2* cells displayed an increase in Caspase 3/7 levels (required for the final execution of apoptosis (48, 49)) upon 24 and 48 h treatment with increasing concentrations of cerdulatinib or vorinostat compared with vehicle (DMSO treated) controls (Figure 5C). This escalation was most significant when cells were treated with 1 μM of cerdulatinib for 48 h (DMSO vs cerdulatinib treated, RLU=3026 vs 25967, $p<0.0001$; Figure 5C). Likewise, 1 μM vorinostat treatment significantly induced Caspase3/7 activation after 48 h treatment (DMSO vs vorinostat treated, RLU=2880 vs 31813, $p=0.04$; Figure 5C).

Cerdulatinib and vorinostat treatment effectively decreases the leukemic burden in *in vivo* models of *MYB-TYK2* B-ALL

To assess the potential of cerdulatinib and vorinostat in preclinical models of *MYB-TYK2* B-ALL, secondary recipient NSG mice were transplanted with mononuclear cells derived from the *MYB-TYK2* primagrafts. A robust secondary engraftment and faster repopulation of *MYB-TYK2* GFP positive leukemic cells (~40%) in peripheral blood was achieved by 3 weeks compared with ~1% primary engraftment of cells in week 4 (Supplementary Figure 15). Mice were randomized to receive vorinostat (70 mg/kg/day, i.p; n=10), cerdulatinib (35 mg/kg/day, oral gavage; n=10) and vehicle (n=5), 12-16 days post-transplantation with an average peripheral blood engraftment of 44% GFP positive cells (range=21-77%). Mice were treated for up to 12 days. At harvest, cerdulatinib treated mice demonstrated decreased spleen (n=10, 123±14 mg, $p=0.0007$) and liver (n=10, 1199±143, $p=0.0008$) weight compared with mice

receiving the vehicle (n=5, 215±26 mg and 1550±191 mg, respectively; Figure 6A). Vorinostat treatment resulted in a similar trend: a significant decrease in spleen weight of treated mice (n=10, 166±25, p=0.009) was observed in comparison to vehicle control animals (n=5, 215±26; Figure 6A). Cerdulatinib treated *MYB-TYK2* mice demonstrated a significantly lower infiltration of GFP positive leukemic cells in bone marrow (GFP (%) = 37 vs 75, p=0.0005) and spleen (GFP (%) = 39 vs 59, p=0.01) versus vehicle treated animals (Figure 6B and Supplementary Figure 16) measured by flow cytometry. Similar results were observed in vorinostat treated mice (Figure 6B and Supplementary Figure 16). Flow cytometric analysis also demonstrated a significant decrease of GFP positive leukemic cells in the peripheral blood of mice receiving either cerdulatinib or vorinostat in comparison with vehicle (GFP (%) = 46 and 23 vs 41, p=0.02 and p=0.01, respectively; Figure 6B).

Bone marrow and spleen sections stained with H&E and GFP antibody further confirmed the reduced leukemic infiltration in the peripheral organs of drug treated *MYB-TYK2* mice (Figure 6C). While the level of GFP positive leukemic cells in the liver indicated only a minor reduction between drug treated and vehicle *MYB-TYK2* mice (cerdulatinib and vorinostat treated vs vehicle, GFP (%) = 69 and 63 vs 82, p>0.05 for both), liver sections indicated reduced formation of tumor islands within the tissue (Figure 6C). Furthermore, all *MYB-TYK2* mice demonstrated a fully penetrant leukemia with infiltration of leukemic cells into the spine and/or spinal cord, however, no significant difference was observed in the level of GFP positive cells in spine/spinal cord tissue sections between the drug treated and vehicle control mice after 12 days of treatment (Supplementary Figure 17). In addition, cells isolated from the bone marrow and peripheral blood of mice from each treatment cohort, were stained with the selected panel markers (as Figure 2E) to inspect any immunophenotypic changes in the *MYB-TYK2* expressing leukemic cells in secondary transplant animals and/or due to drug treatment. No difference was observed between the treatment cohorts, with GFP positive leukemic cells displaying a pro/pre-B cell immunophenotype

(CD45R/B220+, CD43+, CD19+, CD24+, BP1+/- and IgM-; Supplementary Figure 18); (32)). Cells were negative for myeloid and erythroid markers (GR1, MAC1, TER119 and THY1). Collectively, these data demonstrate, for the first time, that *MYB-TYK2* B-ALL can be effectively targeted by either the JAKi, cerdulatinib or the HDACi, vorinostat, in *in vivo* pre-clinical models.

Addition of vorinostat or dexamethasone enhanced the efficacy of cerdulatinib treatment in Ba/F3-*MYB-TYK2* cells

To inform the efficacy of combination therapy with cerdulatinib and vorinostat or each agent with conventional chemotherapy, the synergistic effect of selected agents was evaluated in Ba/F3-*MYB-TYK2* cells treated with a range of dose combinations. Notably, sequential dose combinations of cerdulatinib and vorinostat exhibited synergy (ZIP score=2.07±1.44, Figure 7A). A higher degree of synergy was achieved at lower concentrations of vorinostat (ZIP score of the most synergistic area=11.4) with proliferation inhibition significantly greater than cerdulatinib as a single agent even in the presence vorinostat concentrations as low as 200 nM (IC50=992 nM vs 473 nM, p=0.006, Figure 7B). A synergistic effect was also observed between cerdulatinib and the chemotherapy agent, dexamethasone (ZIP=6.4±1.2; Figure 7C). Interestingly, while Ba/F3-*MYB-TYK2* cells demonstrate minimal sensitivity to dexamethasone as a single agent used at low concentrations (Supplementary Figure 19A), treatment with dexamethasone in combination with vorinostat resulted in significantly enhanced vorinostat sensitivity (ZIP score of the most synergistic area=19.6). A significantly reduced vorinostat IC50 was observed in the presence of 80 and 100 nM dexamethasone compared with vorinostat as a single agent (IC50=304 nM, p=0.04 and 30 nM, p=0.04 respectively vs 902 nM). The interaction between vorinostat and dexamethasone was most likely additive (ZIP score=-2.24±1.39; Supplementary Figure 19B). However, a low degree of synergy was detected at vorinostat concentrations less than 200 nM (ZIP score

of the most synergistic area=2.9) with an associated significant reduction in IC50 of Ba/F3-*MYB-TYK2* cells treated with 200 nM dexamethasone (IC50=654 nM vs 400 nM, p=0.03; Supplementary Figure 19C).

Discussion:

The TYK2 protein and its role in immunity, immunosurveillance and inflammation, has been studied over the last two decades, but its oncogenic potential has remained controversial owing to the lack of functional studies (17). Recent genomic studies in B-ALL, particularly with respect to whole transcriptomic analysis, revealed an increasing number cases putatively driven by *TYK2* rearrangements and mutations (1, 13-15, 20). Importantly, other reported *TYK2* rearrangements exhibit similar breakpoints at exon 19 or 18 of the *TYK2* gene, that result in an intact kinase domain and a disrupted pseudokinase domain. Since depending on the inhibitors class, compounds affect either TYK2 or downstreatm JAK/STAT signalling proteins. It is plausible that all rearrangements and activating mutations that leave the kinase domain unaffected or mutations that disrupt pseudokinase domain display similar oncogenic potential and drug responsiveness. Identifying the underlying biological and pathological consequences of these alterations in B-ALL is a pre-requisite for defining effective treatment approaches for *TYK2*-rearranged B-ALL patients.

We demonstrated the functional and leukemogenic significance of *TYK2* fusion genes in B-ALL, by comprehensive modelling of the *MYB-TYK2* fusion gene, isolated from a HR Ph-like ALL patient. The *MYB-TYK2* fusion gene conferred cytokine independent growth in Ba/F3 and $Arf^{-/-}$ cells, consistent with a previous report (12). Kinase alterations in *JAK* family fusion genes constitutively activate signaling pathways via aberrant kinase activation that are otherwise strictly regulated in normal hemopoiesis, to promote growth and oncogenicity regardless of the presence of cytokines (5, 12, 20, 34, 50). The detected levels of pTYK2 in Ba/F3-*MYB-TYK2* cells here indicated that the fusion governs a similar

mechanism of oncogenicity via aberrant TYK2 activation. Supporting this hypothesis, we observed constitutive JAK/STAT signaling due to activation of TYK2 kinase leading to phosphorylation of the downstream effectors, STAT3 and STAT5. Activation of JAK family proteins can induce activation of other downstream oncogenic pathways (5, 18). Crosstalk with other signaling pathways such as PI3K/mTOR, RAS/ERK and PIM due to overexpression or activation of TYK2 has been previously demonstrated in other hematological malignancies, such as acute myeloid leukemia and lymphomas, and is independent of *de novo* JAK/STAT activation (14, 24, 51). Thus, depending on the disease context, activating alterations and cell type, TYK2 may co-operate with proteins in other oncogenic signaling pathways and induce their activation. In this model, constitutive phosphorylation of the MYB-TYK2 fusion protein also mediated crosstalk, inducing activation of the ERK signaling pathway evidenced by high levels of pERK.

Investigation of the sub-cellular localization of MYB-TYK2 revealed both cytoplasmic and nuclear distribution. MYB is a nuclear transcription activator (26), and TYK2, as a non-receptor tyrosine kinase and intracellular signal transducer mainly observed in the cytoplasm and cell membrane (27). It has been suggested that nuclear localization of TYK2 is achievable, involves the presence of a motif region in the FERM domain and correlates with sustained interferon mediated signaling (52). Immunoprecipitation of nuclear JAK demonstrated its interaction with STAT3 upon stimulation with growth factors (53). The association of nuclear JAK family proteins with STAT proteins such as STAT3, may be a contributing factor to the downstream activation of these proteins in cells expressing *TYK2* activating alterations (14, 15, 22). However, this noncanonical function of JAK proteins remains to be fully elucidated. Previous IF analysis of the *NFKB2-TYK2* fusion gene similarly demonstrated both cytoplasmic and nuclear distribution of the fusion protein while *NPM1-TYK2* localized to the cytoplasm only (both fusions detected in lymphoma cases) (21, 22). These discrepancies, however, may be due to the variable 5' partner genes or the TYK2 breakpoints and further investigations are required.

The results of this study, and another by Roberts *et al,* (2017) (12), confirmed the oncogenic properties of the *MYB-TYK2* fusion gene *in vitro*. We extended previous experimentation to answer the question of whether TYK2 activation is a driver or a passenger alteration in ALL patients, and demonstrated TYK2 oncogenicity in a pre-B *Arf*$^{-/-}$ cell murine model. This model recapitulates features of human B-ALL, including frequent mutations in *CDKN2A/*B that are reported in more than 50% of Ph-like ALL cases particularly in combination with kinase alterations (1). The transplantation of *MYB-TYK2*-expressing *Arf*$^{-/-}$ cells into NSG mice, induced development of B-ALL with an immunophenotype consistent with arrest at the pro/pre-B cell differentiation stage (32) and invasion of leukemic cells to niche locations (bone marrow and central nervous system). Successful development of this animal model allowed for testing of small molecular inhibitor candidates that we identified through HTS. Elevated levels of histone acetylation due to expression of the *MYB-TYK2* oncogene suggested a potential epigenetic target for treatment with HDACi. This was further supported by identification of HDACi as the most effective class of inhibitors against Ba/F3-*MYB-TYK2* cells in our high throughput drug screening. HDACi display various mechanisms of action including growth arrest, induction of extrinsic or intrinsic apoptosis pathways, mitotic or ROS-facilitated cell death, cell senescence and interaction with proteins responsible for activation of transcription and signaling pathways (54). We demonstrated the ability of HDACi, including vorinostat, to inhibit the growth of Ba/F3-*MYB-TYK2* cells. The attenuation of JAK/STAT signaling we observed upon vorinostat treatment is in line with a previous T-cell lymphoma model indicating vorinostat treatment decreased activation of proteins involved in JAK/STAT and Pi3K signaling (55). Moreover, increasing evidence suggests that HDACs act as activators of STAT-mediated transcription (56-58). It has been proposed that deacetylation of transcription activation sites upon binding of STATs (i.e. STAT1, 2 and 5) to target genes is required for recruitment of transcription machinery (e.g. RNA polymerase II) and thus inhibition of HDAC activity results in decreased STAT-mediated transcription and reduced

expression of their target genes (57, 59-61). HDACs also play an important role in modulation of the acetylation balance of STATs proteins in co-operation with histone acetyltransferases that directly regulate STATs activity and protein stability (62). Of note, the effect of acetylation/deacetylation on transcription can be cell type or condition specific. For instance, activation of STAT3 mediated transcription is associated with either acetylation in response to type I interferon stimulation in a normal setting (63, 64) or deacetylation in B-cell lymphomas (65). Importantly, this may explain the lack of reduction in JAK/STAT signaling in Ba/F3-EV cells upon treatment with vorinostat (Supplementary Figure 20) and great efficacy of vorinostat toward cells expressing the *MYB-TYK2* fusion gene. Vorinostat effectively depleted the bone marrow and spleen of *MYB-TYK2* leukemic cells in mice, and is in agreement with the growing evidence of HDACi efficacy in hematological malignancies (58, 66), in particular, in *CRLF2*-rearranged ALL) (10).

Among the HTS candidate panel, tanespimycin (HSP90i) also demonstrated efficacy against Ba/F3-*MYB-TYK2* cells. The co-operation and vital role of the HSP90 protein in scaffolding JAK and STAT proteins is well documented (18, 67, 68). Thus, the sensitivity of cells expressing the MYB-TYK2 fusion protein to tanespimycin highlights the potential role of HSP90 in MYB-TYK2 fusion protein stabilization and subsequently JAK/STAT signaling. Efficacy of HSP90i has been previously reported in *in vitro* and *in vivo* models of hematological malignancies including *TYK2*- and *JAK2*-mutated leukemias (67, 69-71). Findings in this study support the *in vitro* efficacy of HSP90i against the *MYB-TYK2* fusion protein. However, this remains to be confirmed in additional pre-clinical models of *TYK2*-rearranged B-ALL.

Our HTS did not identify any JAKi that may have activity against the *MYB-TYK2* fusion gene, consistent with previous reports (12). Although, due to high levels of homology in the kinase (JH1) domain of JAK family proteins, ATP competitive JAKi are not specific for a single JAK family protein (72, 73). Yet, JAKi

demonstrate different potency and efficacy towards each JAK protein (72, 73). Therefore, the lack of sensitivity observed here may be due to the lower potency of the JAKi included in our HTS towards TYK2. Considering the number of ATP competitive JAKi currently progressing in the clinic, relatively few of these inhibitors show selectivity in TYK2 targeting (72, 73). The dual SYK/JAK inhibitor, cerdulatinib, however, is among the few inhibitors documented to display promising *in vitro* results in targeting the TYK2 protein (44, 45). Importantly, Ba/F3-*MYB-TYK2* cells demonstrated sensitivity to cerdulatinib within the clinically achievable range. Cerdulatinib treatment of Ba/F3-*MYB-TYK2* cells resulted in significant attenuation of JAK/STAT signaling and induction of apoptosis *in vitro* as well as significantly reduced leukemic burden in our *MYB-TYK2* mouse model. Of note, the synergistic effect of cerdulatinib in combination with vorinostat or dexamethasone in *MYB-TYK2* expressing cells, indicates the translational potential of this inhibitor as an addition to a chemotherapy backbone. Together, these results highlight, for the first time, the efficacy of the JAKi, cerdulatinib against *TYK2* activating alterations.

Although this study utilized a short drug administration cycle, significant anti-leukemic effects as a result of both cerdulatinib and vorinostat treatments were observed. Infiltration of disease into the central nervous system (CNS) prevented more robust disease eradication as it is known that SMIs do not penetrate the CNS when used as a single agents (12, 74). However, the results presented here provide compelling evidence for use of these SMIs in combination with chemotherapy and further *in vivo* studies are warranted. Additionally, the pharmacological experiments undertaken in this study were limited to mouse leukemia cells due to unavailability of patient material and further validation in patient cells and/or patient-derived xenograft models would be beneficial.

In conclusion, our findings characterize the downstream signaling activation due to expression of the *MYB-TYK2* fusion gene. These data demonstrate the leukemogenic potential of *MYB-TYK2* to induce B-

ALL in *in vitro* and *in vivo* models. Importantly, this is the first mouse model of *TYK2*-rearranged disease which provides evidence that activating *TYK2* alterations are driver oncogenes rather than passengers in the disease development. Furthermore, this study revealed the *in vitro* and *in vivo* efficacy of cerdulatinib and vorinostat against *MYB-TYK2*-rearranged B-ALL, as well as a synergistic effect of cerdulatinib in combination with vorinostat and dexamethasone *in vitro*. These novel findings identify potential therapeutics against this rare yet aggressive type of high-risk ALL and contribute significantly to the current literature on *TYK2*-altered disease. Incorporation of these two targeted inhibitors into treatment regimens may be of benefit against other *TYK2* fusions reported in HR Ph-like ALL such as *SMARCA4-TYK2* and *ZNF340-TYK2* (12). The pre-clinical data presented here, and the established safety profile of these inhibitors, warrants further evaluation of these inhibitors in combination with a chemotherapy backbone in order to achieve improved treatment outcomes in patients with high-risk *TYK2*-rearranged leukemia.

Acknowledgement:

Funding of this study was provided by NHMRC, Beat Cancer and LFA. PT was supported by an AGR University of Adelaide scholarship and Betty Hartmann Leukaemia Research Supplementary Scholarship. Flow cytometry analysis and cell sorting was performed at the South Australian Health Medical Research Institute (SAHMRI) in the ACRF Cellular Imaging and Cytometry Core Facility. The Facility is generously supported by the Detmold Hoopman Group, Australian Cancer Research Foundation and Australian Government through the Zero Childhood Cancer Program. Animal models were performed in the Bioresources Core Facility at SAHMRI and we would like to acknowledge the technical support provided. HTS was performed at Cell Screen SA, Flinders Centre for Innovation in Cancer and we would like to thank Dr. Amanda Aloia and Dr Bracho Granado for assisting with assay optimization.

Conflict of Interest:

Authors declare no conflict of interest in relation to the work described.

Contributions:

PT conceived the study, performed the experiments, analyzed the data and wrote the manuscript. LE contributed to the study design. EP helped in performing the experiments. LE, SH and DW supervised the research. All authors critically read and revised the manuscript.

Figures:

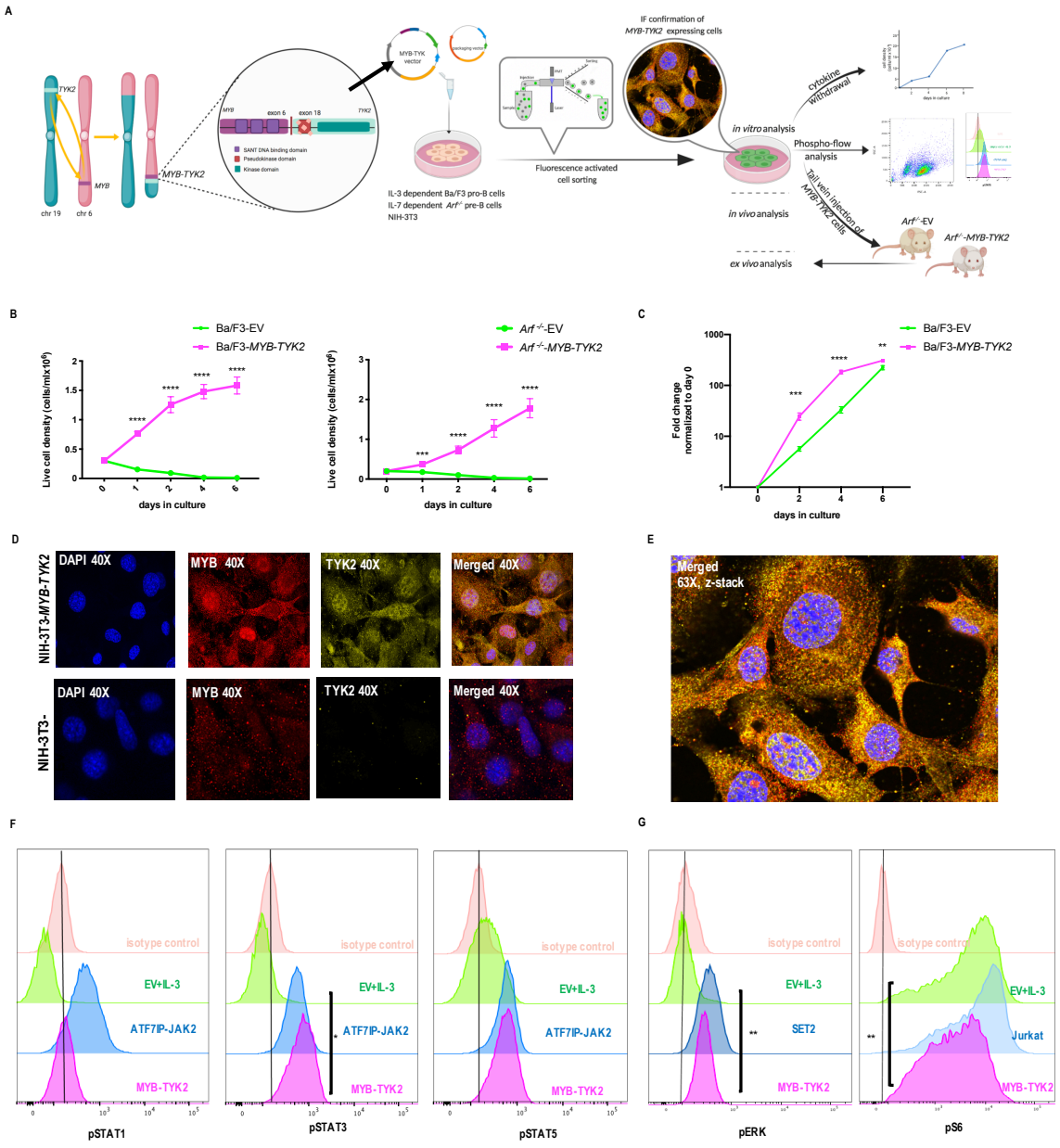
A
TYK2
MYB
chr 19
chr 6
MYB-TYK2
exon 6
exon 18
SANT DNA binding domain
Pseudokinase domain
Kinase domain
MYB-TYK vector
IL-3 dependent Ba/F3 pro-B cells
IL-7 dependent Arf-/- pre-B cells
NIH-3T3
Fluorescence activated cell sorting
IF confirmation of MYB-TYK2 expressing cells
in vitro analysis
cytokine withdrawal
Phospho-flow analysis
in vivo analysis
Tail vein injection of MYB-TYK2 cells
ex vivo analysis
Arf-/--EV
Arf-/--MYB-TYK2
B
Ba/F3-EV
Ba/F3-MYB-TYK2
Live cell density (cells/mlx10^6)
days in culture
Arf -/--EV
Arf -/--MYB-TYK2
C
Fold change normalized to day 0
D
NIH-3T3-MYB-TYK2
NIH-3T3-
DAPI 40X
MYB 40X
TYK2 40X
Merged 40X
E
Merged 63X, z-stack
F
isotype control
EV+IL-3
ATF7IP-JAK2
MYB-TYK2
pSTAT1
pSTAT3
pSTAT5
G
SET2
Jurkat
pERK
pS6

Figure 1. The *MYB-TYK2* fusion gene demonstrated transformative potential in *in vitro* models. (A) Schematic summary of experimental approach used to investigate transformative and leukemogenic potential of the *MYB-TYK2* fusion gene created by BioRender.com. (B) Ba/F3-*MYB-TYK2* and *Arf*$^{-/-}$-*MYB-TYK2* cells plus their empty vector (EV) controls were cultured in the absence of cytokines. Cell growth was monitored for the indicated period at two day intervals by trypan blue exclusion assay. (C) Ba/F3-*MYB-TYK2* and EV cells were cultured in starved (IL-3 free) and media supplemented with IL-3, respectively. Cell growth was monitored in two day intervals by CellTiter Glo assay. ATP-based luminescence readout is proportional to the number of viable cells. Background values at day 0 were measured and deducted from each day's corresponding readout values. (D) Immunofluorescence analysis of NIH-3T3-*MYB-TYK2* and NIH-3T3-EV cells. Cells were stained with TYK2 (yellow signal), MYB (red signal) antibodies, counter-stained with DAPI (blue signal) for nuclei visualization. (E) single plane of z-stacked image from NIH-3T3-*MYB-TYK2* cells. Images captured at 40X and 63X magnification as indicated by Confocal Microscopy and processed by NIS Elements Viewer software. (F&G) Representative histograms of phosphoflow cytometric analyses. Ba/F3 cells transduced with EV, *MYB-TYK2* and *ATF7IP-JAK2* fusion gene vectors, were stained for pSTAT1, 3 and 5 that are the main activated signaling proteins in response to TYK2 kinase activity (17), and their respective IgG isotype controls. Ba/F3-*ATF7IP-JAK2* cells were used as a positive control for STATs activation. Ba/F3-*MYB-TYK2* and EV cells were also assessed for phosphorylation of S6 and ERK. Jurkat and SET2 cells were used as positive controls as indicated. Three biological replicates were screened per condition for phosphoflow analysis. Negative MFI normalised to the IgG control values were considered as zero for statistical analysis. All interactions were measured by un-paired student's t-test. Error bars represent mean ±SD of three biological replicates. Abbreviations: IF, immunofluorescence. MFI, mean fluorescence intensity. RLU, relative luminescence units. *p<0.05, *** p<0.001, **** p<0.0001.

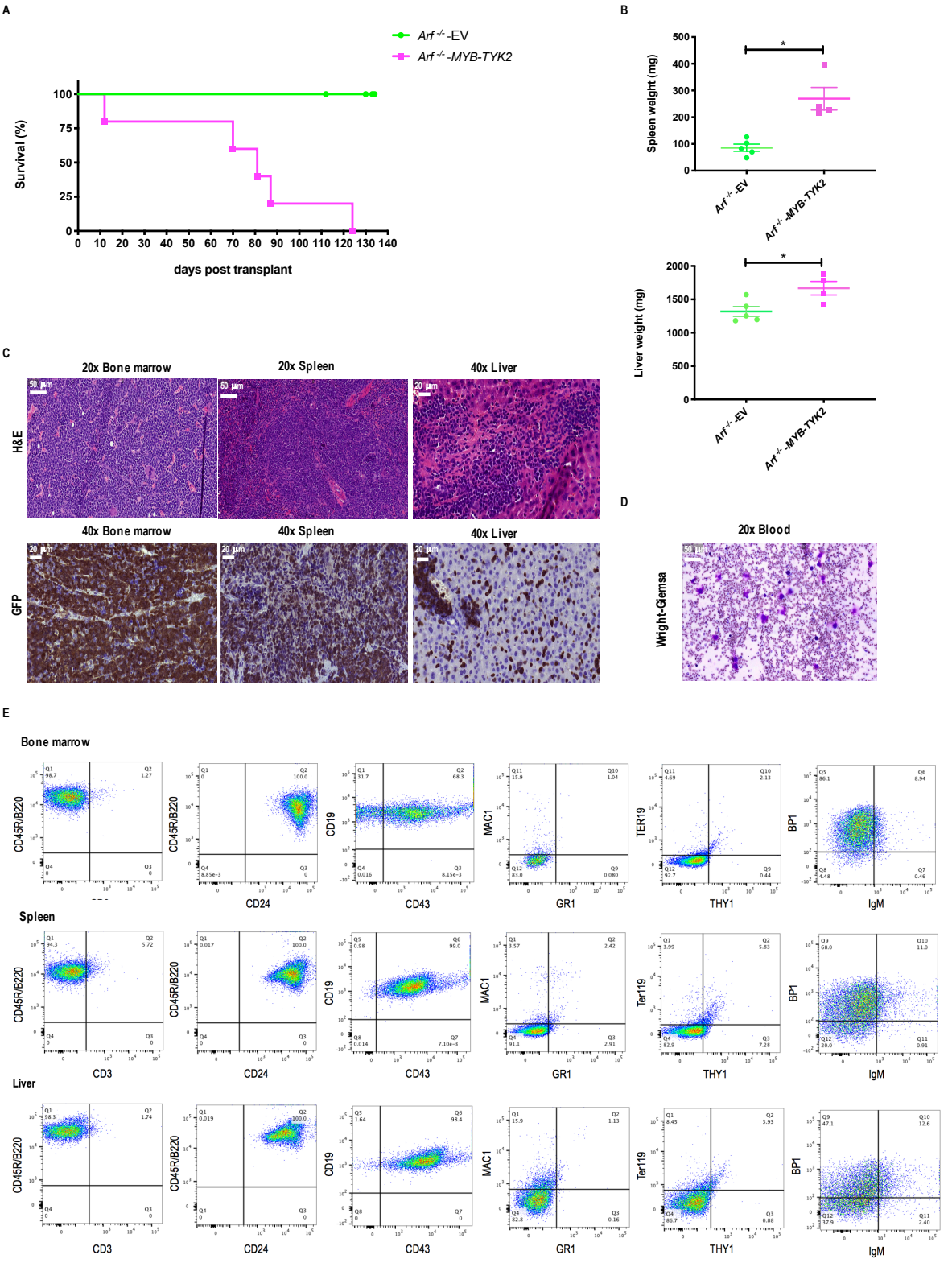
A
Arf -/- -EV
Arf -/- -MYB-TYK2
Survival (%)
days post transplant
B
Spleen weight (mg)
Liver weight (mg)
C
20x Bone marrow
20x Spleen
40x Liver
H&E
40x Bone marrow
40x Spleen
40x Liver
GFP
D
20x Blood
Wright-Giemsa
E
Bone marrow
Spleen
Liver
CD45R/B220
CD24
CD19
CD43
MAC1
GR1
TER119
THY1
BP1
IgM
CD3
Ter119

Figure 2. Mice transplanted with cells expressing the *MYB-TYK2* fusion gene developed leukemia with a median latency of 84 days. (A) Kaplan-Meier curves of *Arf*$^{-/-}$*-MYB-TYK2* mice (n=4) compared with control (empty vector) mice (n=5), p=0.003; interaction as measured by log-rank test. (B) Spleen and liver weight of *Arf*$^{-/-}$*-MYB-TYK2* (n=4) and empty vector control mice (n=5). (C) H&E (top) and GFP (bottom) staining of bone marrow, spleen and liver sections of a representative MYB-TYK2 mouse (n=3). (D) Peripheral blood smear of a single *MYB-TYK2* mouse. The blood film was stained with Giemsa and Wright Stain. Scale bars represent 50 µm and 20 µm at 20X and 40X magnification, respectively. (E) Flow cytometric analyses of *Arf*$^{-/-}$*-MYB-TYK2* leukemic cells isolated from bone marrow, spleen and liver of a *MYB-TYK2* mouse demonstrated an immunophenotype consistent with maturation arrest at pro/pre-B cell stage. The plots represent *Arf*$^{-/-}$*-MYB-TYK2* GFP positive cells (live cells only as determined by DAPI staining) expressing indicated CD or lineage markers. Quadrant gates were applied and compensated based on the fluorescence minus one (FMO) technique and unstained controls. Interactions were measured by un-paired student's t-test. All indicated error bars represent mean ±SD. *p<0.05.

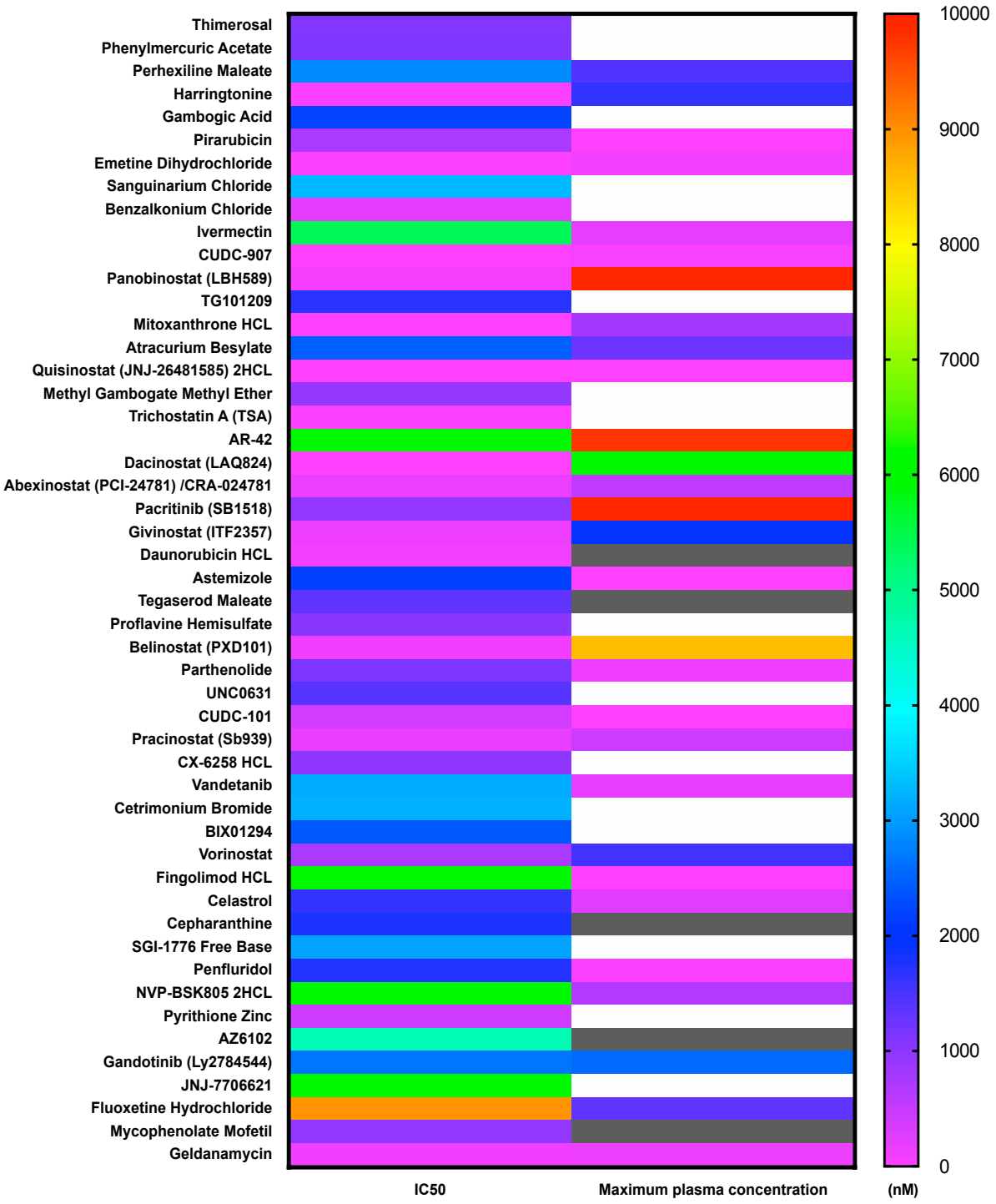
Thimerosal
Phenylmercuric Acetate
Perhexiline Maleate
Harringtonine
Gambogic Acid
Pirarubicin
Emetine Dihydrochloride
Sanguinarium Chloride
Benzalkonium Chloride
Ivermectin
CUDC-907
Panobinostat (LBH589)
TG101209
Mitoxanthrone HCL
Atracurium Besylate
Quisinostat (JNJ-26481585) 2HCL
Methyl Gambogate Methyl Ether
Trichostatin A (TSA)
AR-42
Dacinostat (LAQ824)
Abexinostat (PCI-24781) /CRA-024781
Pacritinib (SB1518)
Givinostat (ITF2357)
Daunorubicin HCL
Astemizole
Tegaserod Maleate
Proflavine Hemisulfate
Belinostat (PXD101)
Parthenolide
UNC0631
CUDC-101
Pracinostat (Sb939)
CX-6258 HCL
Vandetanib
Cetrimonium Bromide
BIX01294
Vorinostat
Fingolimod HCL
Celastrol
Cepharanthine
SGI-1776 Free Base
Penfluridol
NVP-BSK805 2HCL
Pyrithione Zinc
AZ6102
Gandotinib (Ly2784544)
JNJ-7706621
Fluoxetine Hydrochloride
Mycophenolate Mofetil
Geldanamycin
IC50
Maximum plasma concentration
10000
9000
8000
7000
6000
5000
4000
3000
2000
1000
0
(nM)

Figure 3. Heat map representation of potential IC_{50} of selected compounds in the secondary HTS. IC_{50} was estimated relative to DMSO control (n=1). The estimation of maximum plasma concentration for each drug was calculated based on the C_{max}, AUC_{0-24} or $AUC_{0-\infty}$ of the maximum tolerated dose (MTD) or the recommended dose as per references in Supplementary Table 6. Color bar indicates the concentration of compounds within the range of 0-10000 nM. Gray boxes indicate values higher than 10000 nM. Blank boxes indicate compound with no known bioavailability in human trials and/or animal models.

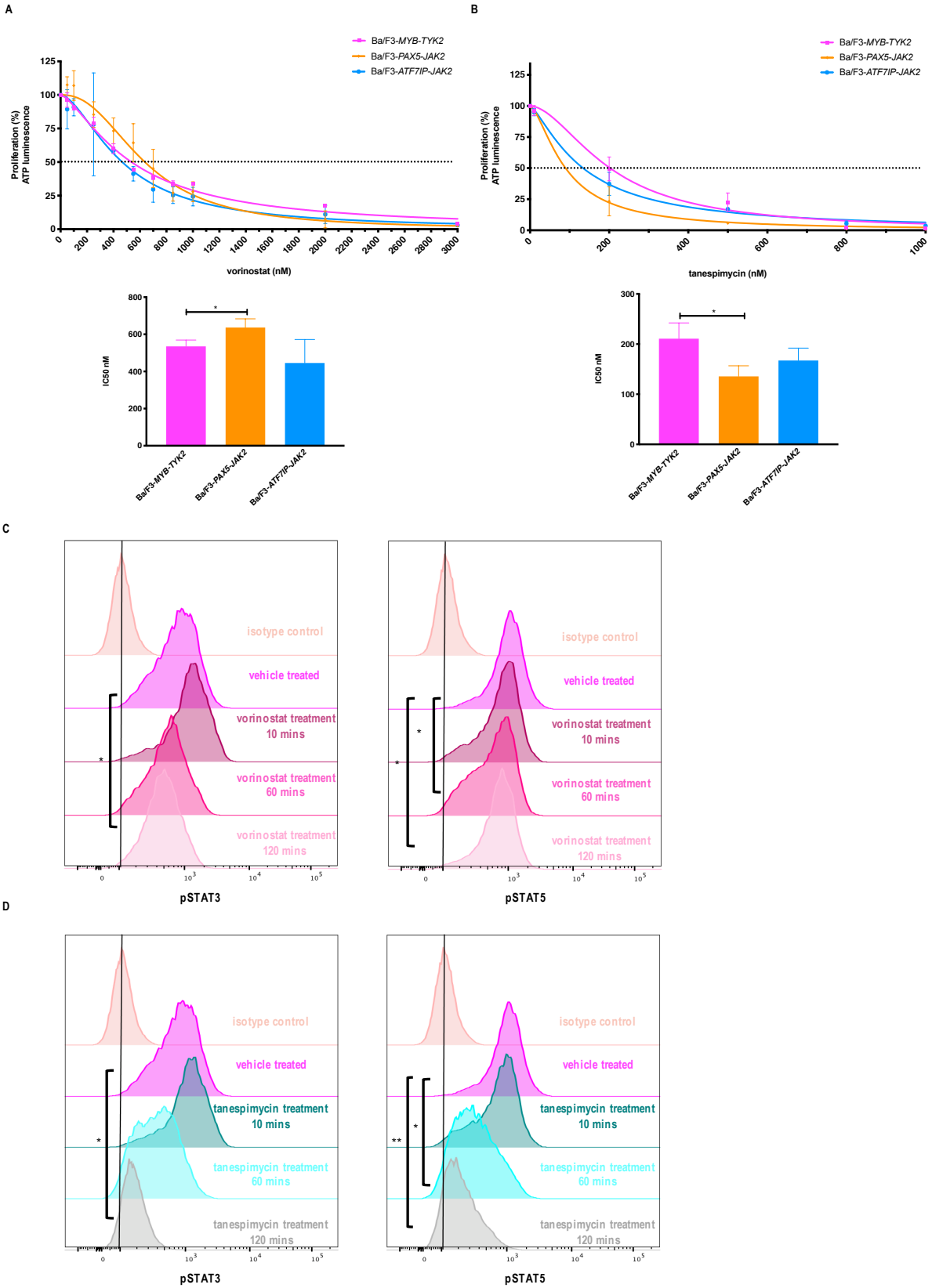
A
Ba/F3-MYB-TYK2
Ba/F3-PAX5-JAK2
Ba/F3-ATF7IP-JAK2
Proliferation (%) ATP luminescence
vorinostat (nM)
IC50 nM
B
tanespimycin (nM)
C
isotype control
vehicle treated
vorinostat treatment 10 mins
vorinostat treatment 60 mins
vorinostat treatment 120 mins
pSTAT3
pSTAT5
D
tanespimycin treatment 10 mins
tanespimycin treatment 60 mins
tanespimycin treatment 120 mins

Figure 4. Ba/F3 cells expressing the *MYB-TYK2* fusion gene demonstrated sensitivity to vorinostat and tanespimycin. (A&B) Proliferation analysis of Ba/F3-*MYB-TYK2*, -*PAX5-JAK2* and -*ATF7IP-JAK2* cells cultured in the presence of increasing concentrations of vorinostat and tanespimycin for 48 h. ATP-based luminescence readout is proportional to the number of viable cells. The percentage of proliferation was calculated relative to DMSO control of each line. Dotted line indicates the 50% inhibition of proliferation. IC_{50} values were estimated by nonlinear regression analysis using GraphPad Prism and are indicated in the panel below. Representative histograms of Ba/F3-*MYB-TYK2* cells' flow cytometric analyses (n=3) for pSTAT5 and pSTAT3 when treated with DMSO (vehicle), (C) 1 μM vorinostat and (D) 0.5 μM tanespimycin for the indicated period. Statistical analyses were measured by paired student's t-test for flow cytometry and un-paired student's t-test for proliferation assay analyses with error bars representing mean ±SD of 3 biological replicates. *p<0.05, **p<0.01.

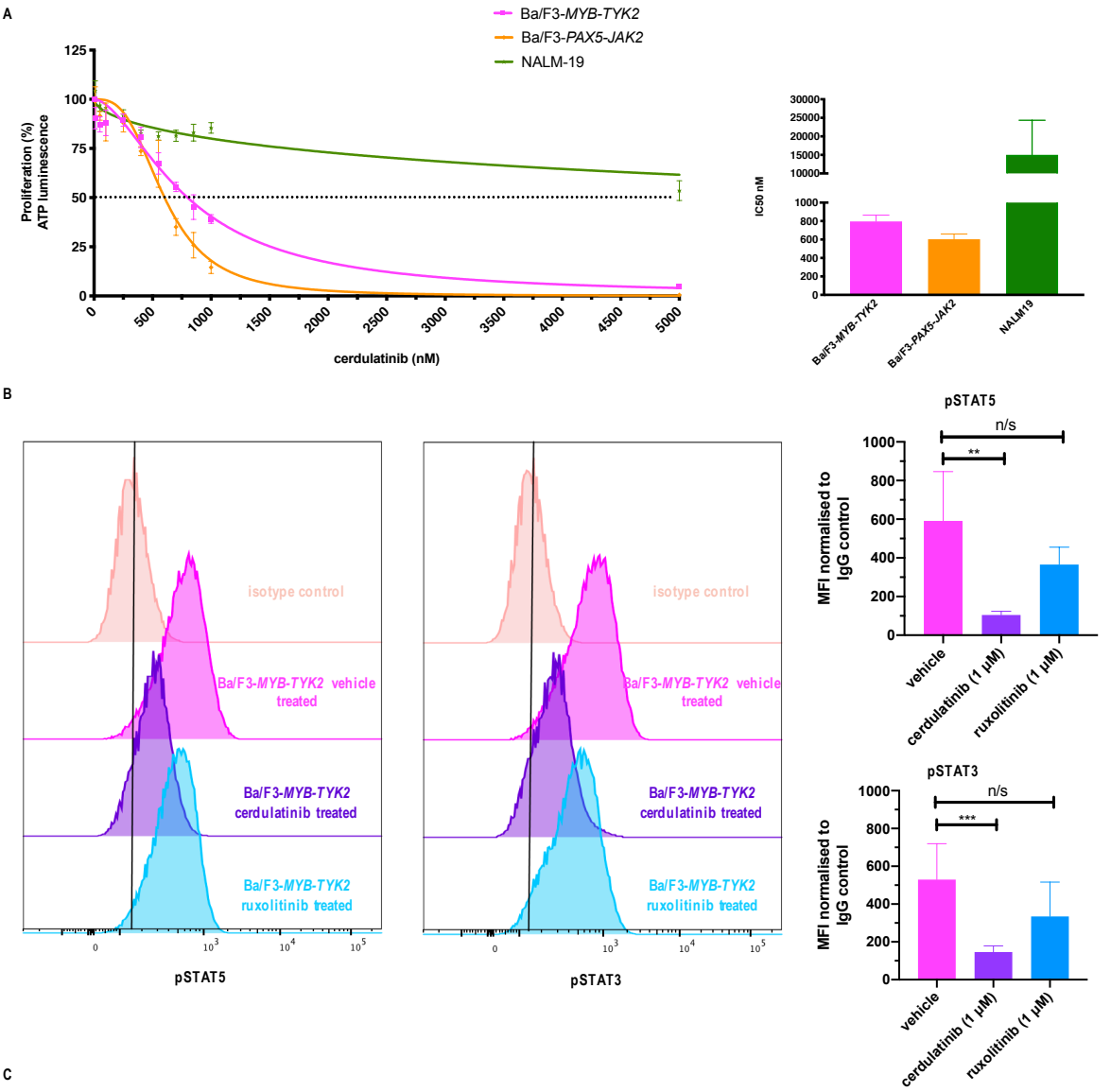
A
Ba/F3-MYB-TYK2
Ba/F3-PAX5-JAK2
NALM-19
Proliferation (%) ATP luminescence
cerdulatinib (nM)
IC50 nM
Ba/F3-MYB-TYK2
Ba/F3-PAX5-JAK2
NALM19
B
isotype control
Ba/F3-MYB-TYK2 vehicle treated
Ba/F3-MYB-TYK2 cerdulatinib treated
Ba/F3-MYB-TYK2 ruxolitinib treated
pSTAT5
pSTAT3
MFI normalised to IgG control
n/s
vehicle
cerdulatinib (1 µM)
ruxolitinib (1 µM)
C
vehicle
100 nM cerdulatinib
400 nM cerdulatinib
700 nM cerdulatinib
1 µM cerdulatinib
100 nM vorinostat
400 nM vorinostat
700 nM vorinostat
1 µM vorinostat
Caspase 3/7 activity (RLU)
24 h
48 h
treatment duration

Figure 5. Cerdulatinib demonstrated efficacy against Ba/F3 *MYB-TYK2* cells. (A) Dose-response curve of Ba/F3-*MYB-TYK2*, Ba/F3-*PAX5-JAK2* and NALM-19 cells treated with increasing concentrations of cerdulatinib for a duration of 48 h. Percent proliferation was estimated relative to DMSO vehicle control via CellTiter Glo assay. Dotted line indicates the 50% inhibition of proliferation. IC_{50} values were estimated by nonlinear regression analysis using GraphPad Prism and are indicated in the right panel. (B) Phosphoflow analysis of STAT5 and STAT3. Ba/F3-*MYB-TYK2* cells were treated with vehicle (DMSO) or 1 μM cerdulatinib for a duration of 1 h. Ruxolitinib treatment was used as a negative control (n=2). Cells were then stained for pSTAT5 and isotype control; p-values as measured by paired student's t-test. (C) Ba/F3-*MYB-TYK2* cells were incubated in the presence of different concentrations of cerdulatinib or vorinostat. Caspase 3/7 activation was measured by Caspase-Glo 3/7 assay at 24 and 48 h. Luminesce readout is proportional to the amount of Caspase 3 and 7 activity. Background values at day 0 were measured and deducted from each day's corresponding readout values. All statistical analyses were measured by un-paired student's t-test unless otherwise indicated. All indicated error bars represent mean ±SD of at least 3 separate experiments unless otherwise specified. Abbreviation: RLU, relative luminescence unit. *p<0.05, **p<0.01, ***p<0.001 and ****p<0.0001.

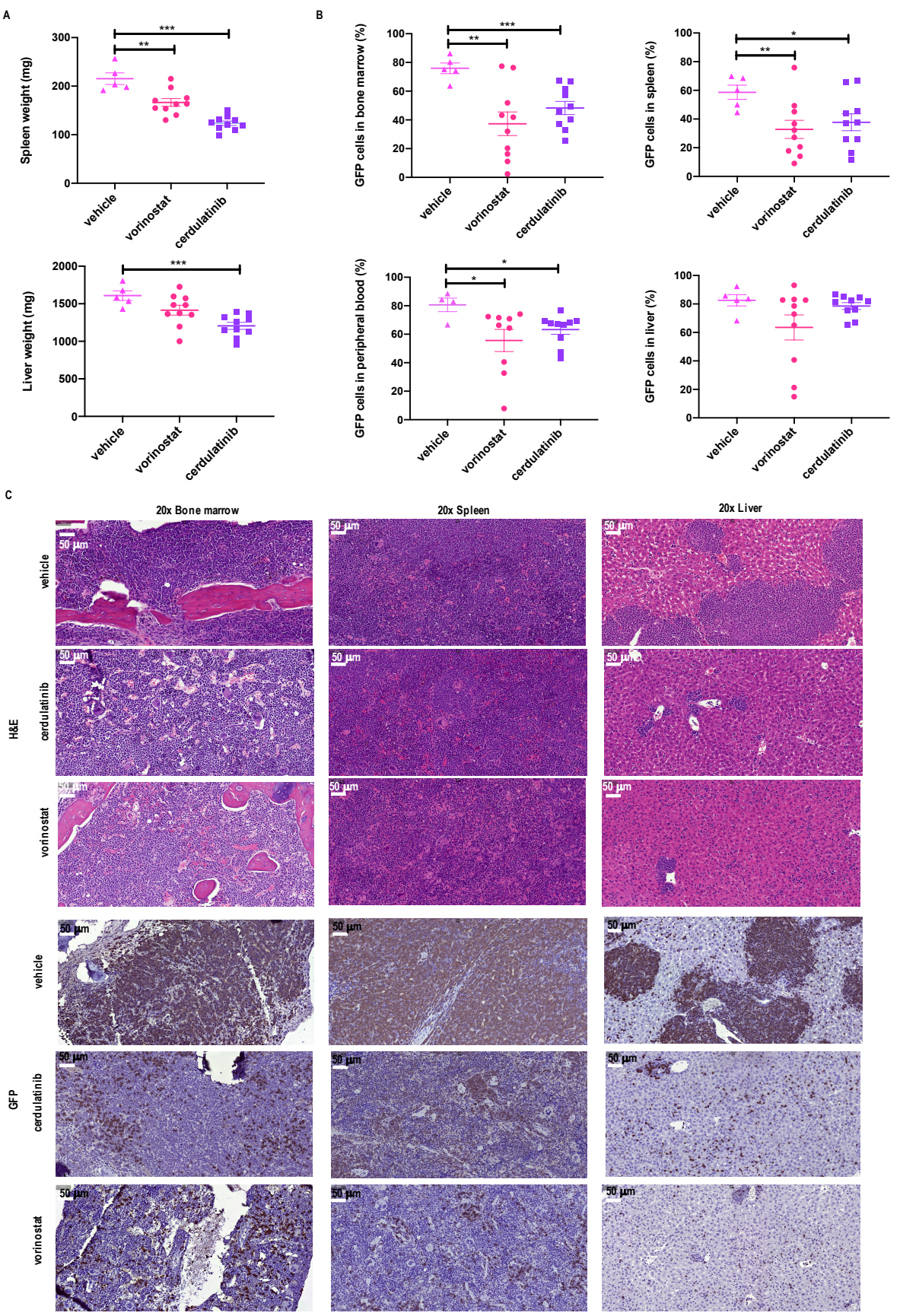
A
Spleen weight (mg)
Liver weight (mg)
vehicle
vorinostat
cerdulatinib
B
GFP cells in bone marrow (%)
GFP cells in spleen (%)
GFP cells in peripheral blood (%)
GFP cells in liver (%)
C
20x Bone marrow
20x Spleen
20x Liver
H&E
GFP
50 µm

Figure 6. The *MYB-TYK2* mice treated with cerdulatinib and vorinostat exhibit reduced B-ALL burden. (A) Spleen and liver weight of cerdulatinib (n=10) and vorinostat (n=10) vs vehicle treated (n=5) *Arf*$^{-/-}$*-MYB-TYK2* mice. (B) Levels of *Arf*$^{-/-}$*-MYB-TYK2* leukemic cells in bone marrow, spleen, liver and peripheral blood of mice in cohorts receiving cerdulatinib, vorinostat or vehicle, measured by GFP positivity of cells derived from mouse tissues via flow cytometric analysis. (C) H&E (top) and GFP (bottom) staining of tissue sections of representative mice from each cohort (n=3). Scale bars represent 50 μm at 20X magnification. All interactions were measured by un-paired student's t-test. All indicated error bars represent mean ±SD. *p<0.05, **p<0.01, ***p < 0.001.

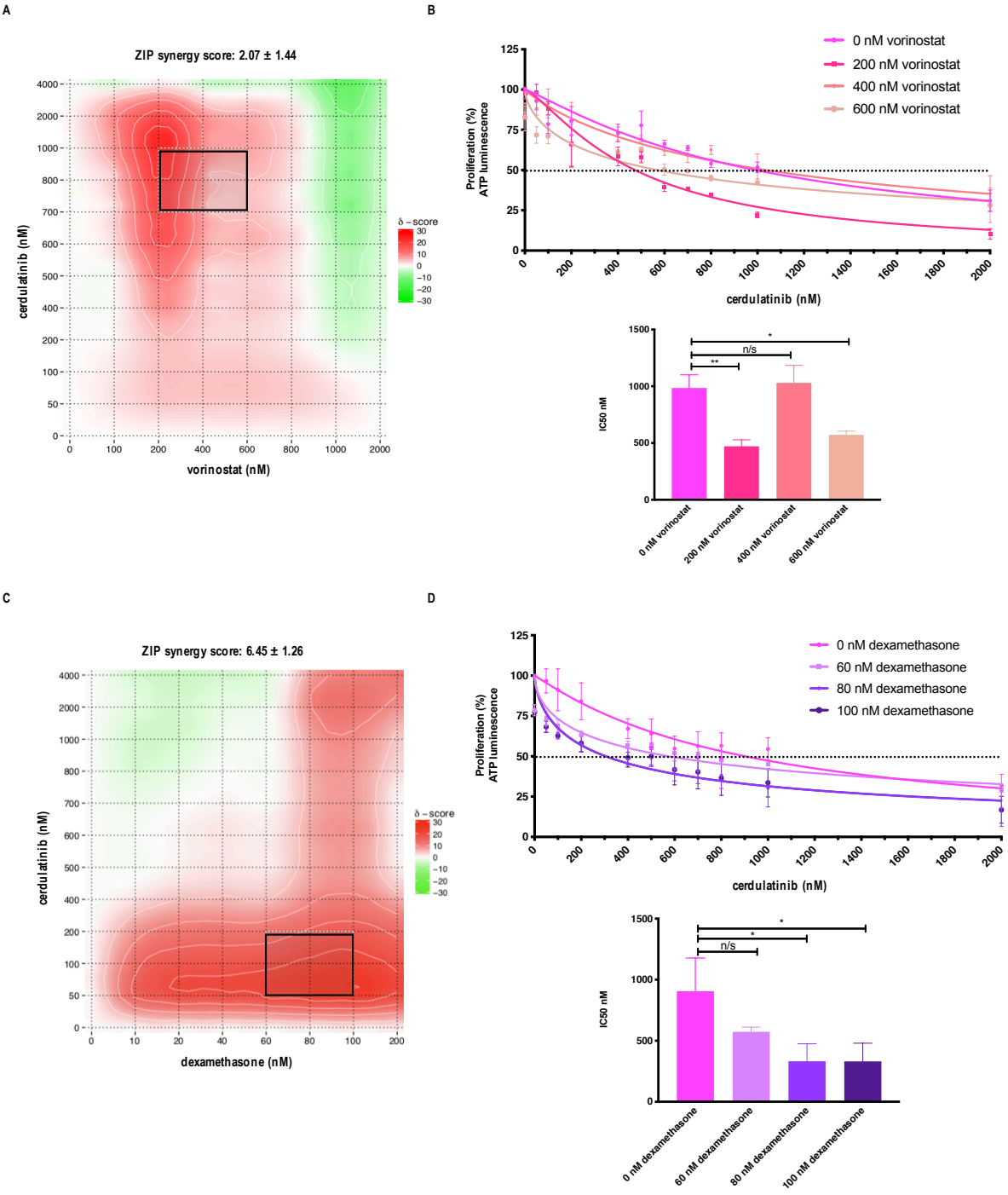
A
ZIP synergy score: 2.07 ± 1.44
cerdulatinib (nM)
vorinostat (nM)
δ – score
B
0 nM vorinostat
200 nM vorinostat
400 nM vorinostat
600 nM vorinostat
Proliferation (%) ATP luminescence
cerdulatinib (nM)
IC50 nM
n/s
C
ZIP synergy score: 6.45 ± 1.26
cerdulatinib (nM)
dexamethasone (nM)
δ – score
D
0 nM dexamethasone
60 nM dexamethasone
80 nM dexamethasone
100 nM dexamethasone
Proliferation (%) ATP luminescence
cerdulatinib (nM)
IC50 nM
n/s

Figure 7. Cerdulatinib demonstrated synergy when used in combination with vorinostat or dexamethasone. (A) Heatmap representation of sequential dose combinations of cerdulatinib and vorinostat. (B) Dose-response curve of Ba/F3-*MYB-TYK2* cells cultured in the presence of increasing concentrations of cerdulatinib in combination with 0, 200, 400, 800 nM dexamethasone. IC50 values as indicated in the panel below. (C) Heat map representation of sequential dose combinations of cerdulatinib and dexamethasone. (D) Dose-response curve of Ba/F3-*MYB-TYK2* cells cultured in the presence of increasing concentrations of cerdulatinib in combination with 0, 60, 80 and 100 nM dexamethasone. IC50 values as indicated in the panel below. Synergy is calculated based on ZIP method and is representative of three biological replicates. The black box indicates the most synergistic area as determined by the SynergyFinder 2.0 software. The proliferation (%) was calculated relative to DMSO vehicle control of each line after 48 h incubation with drugs and the IC50 is denoted by a horizontal dotted line. All interactions were measured by un-paired student's t-test. Error bars represent mean ±SD of 3 biological replicates. *p<0.05, **p<0.01, ns=not significant.

References:

1. Roberts KG, Gu Z, Payne-Turner D, McCastlain K, Harvey RC, Chen IM, et al. High Frequency and Poor Outcome of Philadelphia Chromosome-Like Acute Lymphoblastic Leukemia in Adults. *J Clin Oncol*. 2017;35(4):394-401.

2. Terwilliger T, Abdul-Hay M. Acute lymphoblastic leukemia: a comprehensive review and 2017 update. *Blood Cancer J*. 2017;7(6):e577.

3. Mullighan CG, Zhang J, Harvey RC, Collins-Underwood JR, Schulman BA, Phillips LA, et al. JAK mutations in high-risk childhood acute lymphoblastic leukemia. *Proc Natl Acad Sci U S A*. 2009;106(23):9414-8.

4. Nguyen MH, Ho JM, Beattie BK, Barber DL. TEL-JAK2 mediates constitutive activation of the phosphatidylinositol 3'-kinase/protein kinase B signaling pathway. *J Biol Chem*. 2001;276(35):32704-13.

5. Vainchenker W, Constantinescu SN. JAK/STAT signaling in hematological malignancies. *Oncogene*. 2013;32(21):2601-13.

6. Roberts KG, Mullighan CG. Genomics in acute lymphoblastic leukaemia: insights and treatment implications. *Nat Rev Clin Oncol*. 2015;12(6):344-57.

7. Maude SL, Tasian SK, Vincent T, Hall JW, Sheen C, Roberts KG, et al. Targeting JAK1/2 and mTOR in murine xenograft models of Ph-like acute lymphoblastic leukemia. *Blood*. 2012;120(17):3510-8.

8. Tasian SK, Teachey DT, Li Y, Shen F, Harvey RC, Chen IM, et al. Potent efficacy of combined PI3K/mTOR and JAK or ABL inhibition in murine xenograft models of Ph-like acute lymphoblastic leukemia. *Blood*. 2017;129(2):177-87.

9. Suryani S, Bracken LS, Harvey RC, Sia KC, Carol H, Chen IM, et al. Evaluation of the in vitro and in vivo efficacy of the JAK inhibitor AZD1480 against JAK-mutated acute lymphoblastic leukemia. *Mol Cancer Ther*. 2015;14(2):364-74.

10. Savino AM, Sarno J, Trentin L, Vieri M, Fazio G, Bardini M, et al. The histone deacetylase inhibitor givinostat (ITF2357) exhibits potent anti-tumor activity against CRLF2-rearranged BCP-ALL. *Leukemia*. 2017.

11. Ott CJ, Kopp N, Bird L, Paranal RM, Qi J, Bowman T, et al. BET bromodomain inhibition targets both c-Myc and IL7R in high-risk acute lymphoblastic leukemia. *Blood*. 2012;120(14):2843-52.

12. Roberts KG, Yang YL, Payne-Turner D, Lin W, Files JK, Dickerson K, et al. Oncogenic role and therapeutic targeting of ABL-class and JAK-STAT activating kinase alterations in Ph-like ALL. *Blood Adv*. 2017;1(20):1657-71.

13. Ma X, Liu Y, Liu Y, Alexandrov LB, Edmonson MN, Gawad C, et al. Pan-cancer genome and transcriptome analyses of 1,699 paediatric leukaemias and solid tumours. *Nature*. 2018;555(7696):371-6.

14. Sanda T, Tyner JW, Gutierrez A, Ngo VN, Glover J, Chang BH, et al. TYK2-STAT1-BCL2 pathway dependence in T-cell acute lymphoblastic leukemia. *Cancer Discov*. 2013;3(5):564-77.

15. Waanders E, Scheijen B, Jongmans MC, Venselaar H, van Reijmersdal SV, van Dijk AH, et al. Germline activating TYK2 mutations in pediatric patients with two primary acute lymphoblastic leukemia occurrences. *Leukemia*. 2017;31(4):821-8.

16. Tavakoli Shirazi P, Eadie LN, Heatley SL, White DL. TYK2 Activating Alterations in Acute Lymphoblastic Leukemia: Novel Driver Oncogenes with Potential Avenues for Precision Medicine? *Journal of Cancer Science and Clinical Therapeutics*. 2021;5:201-19.

17. Leitner NR, Witalisz-Siepracka A, Strobl B, Muller M. Tyrosine kinase 2 - Surveillant of tumours and bona fide oncogene. *Cytokine*. 2017;89:209-18.

18. Woss K, Simonovic N, Strobl B, Macho-Maschler S, Muller M. TYK2: An Upstream Kinase of STATs in Cancer. *Cancers (Basel)*. 2019;11(11).

19. O'Shea JJ, Holland SM, Staudt LM. JAKs and STATs in immunity, immunodeficiency, and cancer. *N Engl J Med*. 2013;368(2):161-70.

20. Roberts KG, Li Y, Payne-Turner D, Harvey RC, Yang YL, Pei D, et al. Targetable kinase-activating lesions in Ph-like acute lymphoblastic leukemia. *N Engl J Med*. 2014;371(11):1005-15.

21. Velusamy T, Kiel MJ, Sahasrabuddhe AA, Rolland D, Dixon CA, Bailey NG, et al. A novel recurrent NPM1-TYK2 gene fusion in cutaneous CD30-positive lymphoproliferative disorders. *Blood*. 2014;124(25):3768-71.

22. Crescenzo R, Abate F, Lasorsa E, Tabbo F, Gaudiano M, Chiesa N, et al. Convergent mutations and kinase fusions lead to oncogenic STAT3 activation in anaplastic large cell lymphoma. *Cancer Cell*. 2015;27(4):516-32.

23. Tomasson MH, Xiang Z, Walgren R, Zhao Y, Kasai Y, Miner T, et al. Somatic mutations and germline sequence variants in the expressed tyrosine kinase genes of patients with de novo acute myeloid leukemia. *Blood*. 2008;111(9):4797-808.

24. Tron AE, Keeton EK, Ye M, Casas-Selves M, Chen H, Dillman KS, et al. Next-generation sequencing identifies a novel ELAVL1-TYK2 fusion gene in MOLM-16, an AML cell line highly sensitive to the PIM kinase inhibitor AZD1208. *Leuk Lymphoma*. 2016;57(12):2927-9.

25. Poitras JL, Dal Cin P, Aster JC, Deangelo DJ, Morton CC. Novel SSBP2-JAK2 fusion gene resulting from a t(5;9)(q14.1;p24.1) in pre-B acute lymphocytic leukemia. *Genes Chromosomes Cancer*. 2008;47(10):884-9.

26. Klempnauer KH, Sippel AE. Subnuclear localization of proteins encoded by the oncogene v-myb and its cellular homolog c-myb. *Mol Cell Biol*. 1986;6(1):62-9.

27. Behrmann I, Smyczek T, Heinrich PC, Schmitz-Van de Leur H, Komyod W, Giese B, et al. Janus kinase (Jak) subcellular localization revisited: the exclusive membrane localization of endogenous Janus

kinase 1 by cytokine receptor interaction uncovers the Jak.receptor complex to be equivalent to a receptor tyrosine kinase. *J Biol Chem*. 2004;279(34):35486-93.

28. Dunlop EA, Tee AR. Mammalian target of rapamycin complex 1: signalling inputs, substrates and feedback mechanisms. *Cell Signal*. 2009;21(6):827-35.

29. Williams RT, Roussel MF, Sherr CJ. Arf gene loss enhances oncogenicity and limits imatinib response in mouse models of Bcr-Abl-induced acute lymphoblastic leukemia. *Proc Natl Acad Sci U S A*. 2006;103(17):6688-93.

30. Mullighan CG, Williams RT, Downing JR, Sherr CJ. Failure of CDKN2A/B (INK4A/B-ARF)-mediated tumor suppression and resistance to targeted therapy in acute lymphoblastic leukemia induced by BCR-ABL. *Genes Dev*. 2008;22(11):1411-5.

31. Notta F, Mullighan CG, Wang JC, Poeppl A, Doulatov S, Phillips LA, et al. Evolution of human BCR-ABL1 lymphoblastic leukaemia-initiating cells. *Nature*. 2011;469(7330):362-7.

32. Patton DT, Plumb AW, Abraham N. The survival and differentiation of pro-B and pre-B cells in the bone marrow is dependent on IL-7Ralpha Tyr449. *J Immunol*. 2014;193(7):3446-55.

33. Pardanani A, Hood J, Lasho T, Levine RL, Martin MB, Noronha G, et al. TG101209, a small molecule JAK2-selective kinase inhibitor potently inhibits myeloproliferative disorder-associated JAK2V617F and MPLW515L/K mutations. *Leukemia*. 2007;21(8):1658-68.

34. Cuesta-Dominguez A, Ortega M, Ormazabal C, Santos-Roncero M, Galan-Diez M, Steegmann JL, et al. Transforming and tumorigenic activity of JAK2 by fusion to BCR: molecular mechanisms of action of a novel BCR-JAK2 tyrosine-kinase. *PLoS One*. 2012;7(2):e32451.

35. Oki Y, Kelly KR, Flinn I, Patel MR, Gharavi R, Ma A, et al. CUDC-907 in relapsed/refractory diffuse large B-cell lymphoma, including patients with MYC-alterations: results from an expanded phase I trial. *Haematologica*. 2017;102(11):1923-30.

36. Younes A, Berdeja JG, Patel MR, Flinn I, Gerecitano JF, Neelapu SS, et al. Safety, tolerability, and preliminary activity of CUDC-907, a first-in-class, oral, dual inhibitor of HDAC and PI3K, in patients with relapsed or refractory lymphoma or multiple myeloma: an open-label, dose-escalation, phase 1 trial. *Lancet Oncol*. 2016;17(5):622-31.

37. Li X, Su Y, Hege K, Madlambayan G, Edwards H, Knight T, et al. The HDAC and PI3K dual inhibitor CUDC-907 synergistically enhances the antileukemic activity of venetoclax in preclinical models of acute myeloid leukemia. *Haematologica*. 2021;106(5):1262-77.

38. Talaei S, Mellatyar H, Asadi A, Akbarzadeh A, Sheervalilou R, Zarghami N. Spotlight on 17-AAG as an Hsp90 inhibitor for molecular targeted cancer treatment. *Chem Biol Drug Des*. 2019;93(5):760-86.

39. Bailly C. Cepharanthine: An update of its mode of action, pharmacological properties and medical applications. *Phytomedicine*. 2019;62:152956.

40. Lengline E, Beldjord K, Dombret H, Soulier J, Boissel N, Clappier E. Successful tyrosine kinase inhibitor therapy in a refractory B-cell precursor acute lymphoblastic leukemia with EBF1-PDGFRB fusion. *Haematologica*. 2013;98(11):e146-8.

41. Weston BW, Hayden MA, Roberts KG, Bowyer S, Hsu J, Fedoriw G, et al. Tyrosine kinase inhibitor therapy induces remission in a patient with refractory EBF1-PDGFRB-positive acute lymphoblastic leukemia. *J Clin Oncol*. 2013;31(25):e413-6.

42. Khajapeer KV, Baskaran R. Hsp90 Inhibitors for the Treatment of Chronic Myeloid Leukemia. *Leuk Res Treatment*. 2015;2015:757694.

43. Hawkins LM, Jayanthan AA, Narendran A. Effects of 17-allylamino-17-demethoxygeldanamycin (17-AAG) on pediatric acute lymphoblastic leukemia (ALL) with respect to Bcr-Abl status and imatinib mesylate sensitivity. *Pediatr Res*. 2005;57(3):430-7.

44. Coffey G, Betz A, DeGuzman F, Pak Y, Inagaki M, Baker DC, et al. The novel kinase inhibitor PRT062070 (Cerdulatinib) demonstrates efficacy in models of autoimmunity and B-cell cancer. *J Pharmacol Exp Ther*. 2014;351(3):538-48.

45. Ma J, Xing W, Coffey G, Dresser K, Lu K, Guo A, et al. Cerdulatinib, a novel dual SYK/JAK kinase inhibitor, has broad anti-tumor activity in both ABC and GCB types of diffuse large B cell lymphoma. *Oncotarget*. 2015;6(41):43881-96.

46. Coffey GP, Feng J, Betz A, Pandey A, Birrell M, Leeds JM, et al. Cerdulatinib Pharmacodynamics and Relationships to Tumor Response Following Oral Dosing in Patients with Relapsed/Refractory B-cell Malignancies. *Clin Cancer Res*. 2019;25(4):1174-84.

47. Flinn I, Hamlin PA, Strickland DK, Pandey A, Birrell M, Coffey G, et al. Phase 1 open-label dose escalation study of the dual SYK/JAK inhibitor cerdulatinib (PRT062070) in patients with relapsed/refractory B-cell malignancies: Safety profile and clinical activity. *Journal of Clinical Oncology*. 2015;33(15_suppl):8531-.

48. McIlwain DR, Berger T, Mak TW. Caspase functions in cell death and disease. *Cold Spring Harb Perspect Biol*. 2013;5(4):a008656.

49. Slee EA, Adrain C, Martin SJ. Executioner caspase-3, -6, and -7 perform distinct, non-redundant roles during the demolition phase of apoptosis. *J Biol Chem*. 2001;276(10):7320-6.

50. dos Santos NR, Ghysdael J. A transgenic mouse model for TEL-JAK2-induced B-cell lymphoma/leukemia. *Leukemia*. 2006;20(1):182-5.

51. Staerk J, Kallin A, Demoulin JB, Vainchenker W, Constantinescu SN. JAK1 and Tyk2 activation by the homologous polycythemia vera JAK2 V617F mutation: cross-talk with IGF1 receptor. *J Biol Chem*. 2005;280(51):41893-9.

52. Ragimbeau J, Dondi E, Vasserot A, Romero P, Uze G, Pellegrini S. The receptor interaction region of Tyk2 contains a motif required for its nuclear localization. *J Biol Chem*. 2001;276(33):30812-8.

53. Ram PA, Waxman DJ. Interaction of growth hormone-activated STATs with SH2-containing phosphotyrosine phosphatase SHP-1 and nuclear JAK2 tyrosine kinase. *J Biol Chem*. 1997;272(28):17694-702.

54. Xu WS, Parmigiani RB, Marks PA. Histone deacetylase inhibitors: molecular mechanisms of action. *Oncogene*. 2007;26(37):5541-52.

55. Wozniak MB, Villuendas R, Bischoff JR, Aparicio CB, Martinez Leal JF, de La Cueva P, et al. Vorinostat interferes with the signaling transduction pathway of T-cell receptor and synergizes with phosphoinositide-3 kinase inhibitors in cutaneous T-cell lymphoma. *Haematologica*. 2010;95(4):613-21.

56. Schindler C, Levy DE, Decker T. JAK-STAT signaling: from interferons to cytokines. *J Biol Chem*. 2007;282(28):20059-63.

57. Nusinzon I, Horvath CM. Unexpected roles for deacetylation in interferon- and cytokine-induced transcription. *J Interferon Cytokine Res*. 2005;25(12):745-8.

58. Buchwald M, Kramer OH, Heinzel T. HDACi--targets beyond chromatin. *Cancer Lett*. 2009;280(2):160-7.

59. Rascle A, Johnston JA, Amati B. Deacetylase activity is required for recruitment of the basal transcription machinery and transactivation by STAT5. *Mol Cell Biol*. 2003;23(12):4162-73.

60. Sakamoto S, Potla R, Larner AC. Histone deacetylase activity is required to recruit RNA polymerase II to the promoters of selected interferon-stimulated early response genes. *J Biol Chem*. 2004;279(39):40362-7.

61. Klampfer L, Huang J, Swaby LA, Augenlicht L. Requirement of histone deacetylase activity for signaling by STAT1. *J Biol Chem*. 2004;279(29):30358-68.

62. Zhuang S. Regulation of STAT signaling by acetylation. *Cell Signal*. 2013;25(9):1924-31.

63. Wang R, Cherukuri P, Luo J. Activation of Stat3 sequence-specific DNA binding and transcription by p300/CREB-binding protein-mediated acetylation. *J Biol Chem*. 2005;280(12):11528-34.

64. Yuan ZL, Guan YJ, Chatterjee D, Chin YE. Stat3 dimerization regulated by reversible acetylation of a single lysine residue. *Science*. 2005;307(5707):269-73.

65. Gupta M, Han JJ, Stenson M, Wellik L, Witzig TE. Regulation of STAT3 by histone deacetylase-3 in diffuse large B-cell lymphoma: implications for therapy. *Leukemia*. 2012;26(6):1356-64.

66. Tambaro FP, Dell'aversana C, Carafa V, Nebbioso A, Radic B, Ferrara F, et al. Histone deacetylase inhibitors: clinical implications for hematological malignancies. *Clin Epigenetics*. 2010;1(1-2):25-44.

67. Bocchini CE, Kasembeli MM, Roh SH, Tweardy DJ. Contribution of chaperones to STAT pathway signaling. *JAKSTAT*. 2014;3(3):e970459.

68. Prodromou C. Mechanisms of Hsp90 regulation. *Biochem J*. 2016;473(16):2439-52.

69. Schoof N, von Bonin F, Trumper L, Kube D. HSP90 is essential for Jak-STAT signaling in classical Hodgkin lymphoma cells. *Cell Commun Signal*. 2009;7:17.

70. Kucine N, Marubayashi S, Bhagwat N, Papalexi E, Koppikar P, Sanchez Martin M, et al. Tumor-specific HSP90 inhibition as a therapeutic approach in JAK-mutant acute lymphoblastic leukemias. *Blood*. 2015;126(22):2479-83.

71. Akahane K, Sanda T, Mansour MR, Radimerski T, DeAngelo DJ, Weinstock DM, et al. HSP90 inhibition leads to degradation of the TYK2 kinase and apoptotic cell death in T-cell acute lymphoblastic leukemia. *Leukemia*. 2016;30(1):219-28.

72. Gadina M, Johnson C, Schwartz D, Bonelli M, Hasni S, Kanno Y, et al. Translational and clinical advances in JAK-STAT biology: The present and future of jakinibs. *J Leukoc Biol*. 2018;104(3):499-514.

73. Vainchenker W, Leroy E, Gilles L, Marty C, Plo I, Constantinescu SN. JAK inhibitors for the treatment of myeloproliferative neoplasms and other disorders. *F1000Res*. 2018;7:82.

74. Ebadi M, Wasko J, Weisdorf DJ, Gordon PM, Rashidi A. Ruxolitinib combined with chemotherapy can eradicate chemorefractory central nervous system acute lymphoblastic leukaemia. *Br J Haematol*. 2019;187(1):e24-e7.

2.1 Supplementary Materials

Exploring the oncogenic and therapeutic target potential of the *MYB-TYK2* fusion gene in B-cell acute lymphoblastic leukemia

Paniz Tavakoli Shirazi[1,2], Laura N Eadie[1,2], Susan L Heatley[1,2], Maxime François[4,5], Timothy P Hughes[1,2], David Yeung[1,2,3] and Deborah L White[1,2,3,4,6]

1. Cancer Program, Precision Medicine Theme, South Australian Health & Medical Research Institute (SAHMRI), Adelaide, Australia
2. Faculty of Health and Medical Sciences, University of Adelaide, Adelaide, Australia
3. Royal Adelaide Hospital, Adelaide, Australia
4. Faculty of Sciences, University of Adelaide, Adelaide, Australia
5. CSIRO Health and Biosecurity, Nutrition & Health program, Adelaide, Australia
6. Australian Genomics Health Alliance (AGHA)

This PDF file include:

Supplementary Material and Methods

Supplementary Figure 1-20

Supplementary Table 6

Supplementary references

Supplementary Table 1-5 and 7 are included in the attached excel file:

https://figshare.com/s/86c059e05ab7d4b7f1a3

Material and methods:

***Arf*$^{-/-}$ cells generation.** *Arf*$^{-/-}$ cells are Pre-B-cells derived from bone marrow progenitors and were generated as described by Randle *et.al* (2001) (73). In brief, bone marrow cells were harvested from 5-7 week old *Arf*$^{-/-}$ donor mice (Jackson Laboratory, Maine, United States). Red cells were lysed, and the remainder of cells resuspended and fed with RPMI supplemented with 5% fetal bovine serum (Hyclone FBS, Fisher-Scientific, CAT# SH3007003), 4 mM L-Glutamine (Sigma-Aldrich, CAT#G7513), 1% (v/v) penicillin/streptomycin (Sigma-Aldrich, CAT#P4333) and 55 μM 2-Mercaptoethanol (Gibco, CAT#21985-023). Bone marrow derived pre-B cells were established on irradiated NIH-3T3 stromal cells (30 Gy) in the presence of saturating levels of IL-7 (50 ng/mL; Peprotech, CAT#217-17). Clusters of cells released into the media were transferred to liquid culture at day 6-7 post culture on stromal cells and then at 3-4 day intervals. More than 90% of cells transferred to liquid culture exhibited double B220/CD45R and CD24 positivity indicative of "common lymphoid progenitor cells" (74). The established pre-B *Arf*$^{-/-}$ cell line was maintained in similar culture media, with the addition of 10% FBS and 10 ng/mL IL-7.

Cell line generation, transduction and cell culture. Retroviral particles of p-Ruf-iG2-*MYB-TYK2*-GFP were packaged into HEK-293T (obtained fron ATCC, Virginia, USA) cells using Lipofectamine™ 2000 (Thermo Fisher Scientific, CAT# 11668-019) and the packaging vector pEQ-Eco. The harvested supernatant was used to infect IL-3 dependent parental Ba/F3 pro-B cells (ATCC, Virginia, USA), IL-7 dependent *Arf*$^{-/-}$ cells and NIH-3T3 cells. For *Arf*$^{-/-}$ cells, viral supernatant was centrifuged onto RetroNectin coated plates (30 μg per well, TaKaRa, CAT#T202) for 1.5 h at 2000 rpm. Supernatant was then removed, replaced with $3x10^5$ cells/mL, followed by spinfection of cells for 1 h at 1600 rpm. Ba/F3 target cells were resuspended in viral supernatant and spinfected at 1800 rpm for 1 h using polybrene (4 μg/mL, Sigma-Aldrich, CAT#TR-1003). Viral supernatant harvest and spinfection was carried out at 24

and 48 h post-transfection of HEK-293T cells. Cells harboring the *MYB-TYK2* fusion gene were GFP selected using fluorescence activated cell sorting (FACS) 72 h post-transduction to generate stable cell lines. Expression of the *MYB-TYK2* fusion was confirmed by RT-PCR. Cell lines harbouring the p-Ruf-iG2-GFP empty vector (EV) were similarly generated as experimental controls. Ba/F3 cells were maintained in RPMI1640 medium (Sigma-Aldrich, CAT#R0883) supplemented with 10% Fetal Calf Serum (FCS CellSera, BATCH#F21701), 2 mM L-glutamine, 0.6% (v/v) penicillin/streptomycin plus 5% WEHI-3B (source of IL-3) for Ba/F3-EV and parental cells or 10 ng/mL IL-7 for *Arf*$^{-/-}$-EV cells. Parental cell lines were tested negative for mycoplasma according to MycoAlert™ Mycoplasma Detection Kit (Lonza, Basel, Switzerland) and PCR test (performed at COMPATH, Gilles Plains, South Australia) before transfection/transduction procedure. NIH-3T3 cells were cultured in cytokine-free Dulbecco's Modified Eagle's Medium (DMEM, Sigma-Aldrich, CAT#D6046) with above-mentioned supplements. For cytokine independent growth, Ba/F3-*MYB-TYK2* and *Arf*$^{-/-}$*-MYB-TYK2* cells were washed (x3) via centrifugation and resuspension in cytokine-free media and then cultured in the absence of cytokines.

RT-PCR. For total RNA extraction, 1-2x10^6 primary cells and 5x10^6 cell lines were collected, pelleted and resuspended in 1 mL TRIzol® solution (Life Technologies, CAT#15596-018). Upon attaining a homogenous mixture, chloroform was added to each tube prior to centrifugation at 1200x g for 15 min. Total RNA was then pelleted by addition of isopropanol and 1 μg glycogen (Roche, CAT#10901393001) and washed with 75% ethanol prior to rehydration in NF-H_2o. The RNA quality was measured using a Nanodrop™ 8000 spectrophotometer. cDNA was synthesized using Quantitect Reverse Transcription Kit (Qiagen, CAT#205313). RT-PCR was performed with RT² SYBR Green ROX qPCR Mastermix (Qiagen, CAT#330523) with the following primers designed to amplify over the *MYB-TYK2* fusion gene break point region and housekeeping control: human *MYB*, 5'-CTACAGCTCAACTCCCTGCC-3' (forward) and human *TYK2*, 5'-CGGTGCTGCCTCTGGTAG-3' (reverse), mouse *Beta-actin*, 5'-

TTGCTGACAGGATGCAGAAG-3' (forward) and 5'-AAGGGTGTAAAACGCAGCTC-3' (reverse). Amplification was performed on the QuantStudio™ 7 Flex system (ThermoFisher) with the annealing/extention temperature at 60°C x 40 cycles. Data were quantified by Ct values and presented as $2^{\Delta Ct}$ fold change normalized to *Beta-actin* expression.

Compounds. Cerdulatinib (CAT# S7634), vorinostat (CAT#S1047), panobinostat (CAT# S1030), CUDC-907 (CAT# S2759), belinostat (CAT# S1085), cepharanthine (CAT#S4238), geldanamycin (CAT# S2713) and tanespimycin (17-AAG, CAT#S1141) were purchased from Selleckchem. For *in vitro* use, 10 mM inhibitor stocks were diluted in DMSO prior to use. Dilutions were prepared so that the final concentration of DMSO was 0.2% in culture media and assays. For *in vivo* use, the required volume of inhibitors according to the animals' weights, were prepared daily. Cerdulatinib, was dissolved in 0.5% Methyl Cellulose 400 Solution (CAT#131-17811, Wako Pure Chemical Industries) complemented with 2% DMSO and administered orally (oral gavage) at 35 mg/kg/day. Vorinostat was reconstituted in a solvent consisting of Milli-Q, 30% PEG300 (CAT# 91462, Sigma-Aldrich), 5% Tween 80 (CAT# S6702, SelleckChem) and 2%DMSO and administered via peritoneal injection (i.p.) at 70 mg/kg/day. The drug dose and route of administrations were selected based on previous studies (75-77).

***In vitro* proliferation, apoptosis and inhibitor assays.** For growth analysis, cells were plated at $1x10^4$ cells per mL in 24 well-plates in triplicates. At each indicated time point, 25 μL of cells was transferred to black 384-well ViewPlates (PerkinElmer, CAT#6007460) and viability was assessed via luminescence-based CellTiter Glo® 2.0 Assay (Promega, CAT# G9242) as per manufacturer protocol. Results were normalized to day 0 readout. A media only control was used to ensure minimal assay interaction with medium and to evaluate the background luminesence. For dose-response curves, cells were washed, plated in duplicate at 3000 cells/well in black 384-well ViewPlates in the presence of increasing drug

concentrations for 48 h prior to addition of CellTiter Glo reagent. For synergy analysis the SynergyFinder 2.0: visual analytics of multi-drug combination synergies software was used (78). Synery was calculated based on the Zero Interaction Potency (ZIP) model (79). A ZIP synergy value has been calculated for each combination considering all doses in addition to a ZIP score of the most synergistic area based on the percentage of viable cells after treatment normalized to DMSO control. Values greater than 10 indicate synergy between two drugs; values between 10 and -10 indicate an additive interaction; values less than -10 indicate antagonistic interactions. For apoptosis analysis, $1.2x10^4$ cells/well were seeded in a 96-well plate in triplicate. At day 0 or after 24 and/or 48 h incubation in the presence of increasing concentrations of drug, 25 μL of cells was transferred to black 384-well ViewPlates and apoptosis was assessed via luminescence Caspase-Glo® 3/7 assay (Promega, CAT#G091) according to the manufacturer protocol. Luminescence levels were assessed via VICTOR™ X Multilabel Plate Reader (PerkinElmer, Inc).

Phosphoflow analyses. Cells were washed (x1) via centrifugation and resuspension in RPMI1640 media with cell concentration adjusted to $5x10^5$ cells per tube. For evaluation of the effect of drug treatments, cells were resuspended in media supplemented with inhibitors at the indicated concentrations or DMSO for 1 h. Cells were then fixed with 100 μL of 16% paraformaldehyde per 1 mL of sample, incubated for 10 min at room temperature and washed via centrifugation once in 1xPBS. Permeabilization was carried out by dropwise addition of ice-cold 80% methanol to cell pellet while vortexing at low speed (600 rpm) to allow resuspension. Samples were stored at -20°C overnight and washed with phosphoflow buffer (1xPBS/1% BSA) prior to staining with antibodies for pSTAT5 (pY694, #CAT612567), pSTAT3 (pY705, #CAT562072), pERK1/2 (pT202/pY204, CAT#612566), pAKT (pS473, CAT#560378), pSYK (pY348, CAT#558529), pS6 (CAT# 14733, Cell Signaling Technology (CST)) or the isotype controls IgG_1 (CAT#555749) and IgG_2 (CAT#559319) at concentrations recommended by the manufacturer. All

antibodies were purchased from BD Biosciences unless otherwise indicated. For global histone methylation and acetylation analysis, cells were stained with antibodies H3 (CAT#12230), H3K27me3 (CAT#12158) and H3K9ac (CAT#66070) purchased from CST. Cells were stained with each antibody for 1 h in the dark at room temperature. Cells were analyzed on a BD FACSCanto II (BD Bioscience) except were indicated.

Western blotting. For total lysates, $1x10^6$ cells per cell line were lysed in NP-40 buffer containing 10 mM Tris-HCl (pH 7.4), 137 mM NaCl, 10% Glycerol and 1% NP-40 (Igepal™, Thermo Fisher Scientific, CAT#85124) supplemented with phosphatase and protease inhibitors (Complete mini EDTA-free protease inhibitors Cocktail, Roche, CAT# 04693132001). Lysates were pelleted, a sample of supernatant taken for protein quantification and to the remainder, addition of 1/3 volume of 4x loading buffer (0.25 M Tris-HCl (pH 6.8), 8% (w/v) SDS, 40% (v/v) glycerol, 20% (v/v) 2-merchaptoehtanol and 0.05% (w/v) bromophenol blue) prior to boiling at 100°C for 10 min. Protein quantification was determined by the DC Protein Assay (Bio-Rad, CAT#500-0116) based on the manufacturer's protocol. Total protein (70 μg) was separated by SDS-PAGE electrophoresis on Criterion™ TGX Precast gels (Bio-Rad, CAT# 5678084) with the Precision Plus Protein Kaleidoscope Standard (Bio-Rad, CAT#161-0375) used to determine protein size. The protein was transferred to LF-PVDF membrane (Bio-Rad, CAT#170-4275) via the Trans-Blot Turbo Transfer System (Bio-Rad Laboratories Inc., California, USA) using the midi blot and high molecular weight manufacturer settings. The membrane was then incubated with Intercept Blocking Buffer (LI-COR, CAT#927-70001) for 1 h at room temperature, prior to staining with primary antibody. Primary antibodies against TYK2 (CAT#14193), pTYK2 (CAT#68790), MYB (CAT#12319) and GAPDH (CAT#2118) were purchased from CST. Membranes were probed overnight at 4°C with primary antibodies diluted at 1:1000 in Intercept Blocking Buffer, washed 5x in TBST and stained with donkey-anti-rabbit IRDye 800CW (1:10000; Li-Core, CAT#925-32213) secondary antibody for 1 h at room

temperature. Membranes were washed 5x times and analysed on the Li-Cor Odyssey CLx Imaging System (LI-COR Biosciences, Nebraska, USA). Immunoblot image analysis was performed using ImageStudio software version 5.2.5.

Immunofluorescent analysis. Immunofluorescent imaging was carried out as previously described with slight modifications (80). Briefly, $1x10^5$ NIH-3T3-*MYB-TYK2* cells and their EV counterparts were seeded on coverslips overnight, fixed with 4% paraformaldehyde in PBS and permeabilized in 0.1% Triton X-100 prior to 1 h incubation in blocking buffer (10% FCS in PBS) in a humidified chamber. Cells were then stained with MYB (Origene, CAT# AP31223PU-N) and TYK2 (Santa Cruz Biotechnology, CAT# sc-5271) antibodies at 1:100 dilution in blocking buffer overnight. Cells were then washed and stained with secondary goat anti-rabbit Alexa Fluor 568 (ThermoFisher Scientific, CAT# A11036) and goat anti-mouse Alexa Fluor 647 (ThermoFisher Scientific, CAT# A21235) diluted at 1:200 in TBST, incubated at 37°C for 1.5 h and counter stained with DAPI (0.4 μg/mL). Cells were rinsed in 4xSSC and sealed on to slides after treatment with antifade mounting medium (ThermoFisher, CAT# P36930). Images were captured by Nikon A1 confocal microscope and processed by NIS Elements Viewer (v4.1).

***Ex vivo* GFP positivity and immunophenotyping analysis via flow cytometry.** At experimental endpoint, mice were culled and bone marrow, spleen, liver and brain harvested. Organs were transferred to a 70 μM filter and cells isolated in ice cold PBS supplemented with 2% FCS. Reb blood cells were lysed in buffer containing 0.1 M NH_4Cl and NH_4HCO_3 in MilliQ water. For GFP positivity analysis, cells were washed by centrifugation and resuspended in FACS fix (1% formaldehyde, 111 mM D-glucose, 0.02%Sodium Azide in 1x PBS). Liver cells were blocked in buffer containing 0.5% BSA, 2% FCS and PBS for 15 min and stained with LIVE/DEAD™ Fixable Blue Dead Cell Stain Kit (ThermoFisher,

CAT#L23105) for 30 min prior to fixation. For immunophenotyping, cells were blocked as previously and stained with CD45R/B220 (CAT# 553090), CD43 (CAT#553271), CD19 (CAT#563235), CD24 (CAT#562349), CD3 (CAT#565643), IgM (CAT#552867), BP1 (CAT#740485), MAC1 (CAT#553311), GR1 (CAT# 561083), THY1 (CAT#561409), TER119 (CAT#561071) purchased from BD Biosciences, for 1h in the dark. Cells were then washed in 0.5% BSA/PBS and fixed. In addition to an unstained control, anti-mouse Ig,κ compensation beads (BD Biosciences, CAT#5528843) were used to optimize compensation settings for the flow cytometric analysis. For differentiation between live and dead cells in bone marrow, spleen and peripheral blood samples, cells were stained with DAPI (0.4 μg/mL) prior to analysis on a BD FACSCanto II or BD LSRFortessa X-20 (BD Biosciences).

Immunohistochemistry. Mouse tissues were fixed in formalin at least 24 h prior to paraffin embedding. Tissue processing, embedding, sectioning of tissues at 5 μm and hematoxylin and eosin (H&E) staining was performed by the Histology Service at the University of Adelaide, Australia. For immunohistochemistry, tissue sections were heated and rehydrated in xylene treatment followed by brief ethanol treatment. Antigen retrieval occured through heat induced epitope retrieval using citrate buffer at pH 6 at 110°C in a pressurised decloaking chamber (Biocare Medical). Slides were then washed in 1xPBS and exposed to 0.3% H_2O_2 (30% w/v) in methanol for 10 min and washed prior to 1 h blocking with 5% goat serum in PBST (0.5% Tween). Tissue slides were stained with GFP antibody (CST, CAT#2956) diluted at 1:200 in 5% goat serum/PBST overnight in a humidified chamber. The next day, slides were washed and stained with goat anti-rabbit IgG H&L (HRP) (Abcam, CAT#ab205718) at 1:10000 prior to DAB exposure using SignalStain® DAB Substrate Kit (CST, CAT#8059) according to manufacturer's protocol. Tissues were counter stained with Mayer's hematoxylin and dehydrated prior to scanning and analysis with Slide Scanner (Pannoramic, 3DHistech) and CaseViewer (3DHistech, v2.6).

***In vivo* treatment studies.** Cells isolated from organs of *MYB-TYK2* primagrafts (approximately $2x10^5$ cells per mouse) were transplanted into sublethally irradiated (200 cGy) secondary NSG recipients via tail vein injection. Engraftment was monitored by assessment of GFP in the peripheral blood from two weeks post-transplant. Treatment commenced based on engraftment levels (%GFP positive leukemic cells) and mice were randomized to receive either cerdulatinib (35mg/kg/day; n=10), vorinostat (70mg/kg/day; n=10) or vehicle (0.5% methylcellulose+2% DMSO (n=2) and Milli-Q+30% PEG300+5% Tween 80+2% DMSO (n=3). Treatment was continued for up to 12 days. Body weight was measured daily. Animals were monitored daily for clinical signs of leukemia and were humanely killed when moribund. Bone marrow, spleen, liver and spine were harvested and cardiac puncture performed at experimental endpoint.

High Throughput Screen (HTS). The two libraries, Microsource Spectrum FDA-approved drugs library and SelleckChem Epigenetics library, were purchased and plated at Compound Australia (Griffith University, QLD, Australia) at 50 nL/well in black 384-well plates (View Plate, Perkin Elmer Cat#6007460). Controls were similarly plated, with the positive control being 1μM daunorubicin, a DNA synthesis inhibitor that is regularly used in ALL patients' chemotherapy regimen (81)). DMSO was used as a negative control (at final concentration of 0.2%). The HTS was performed at Cell Screen SA (Center for Innovation in Cancer, Flinders University, SA, Australia). Ba/F3-*MYB-TYK2* cells were seeded in a HEPA-filtered air environment, at 5000 cells/25 μL per well using a BioTek 406 washer/dispenser (achieving final concentration of 10 μM per compound). Plates were centrifuged for 3 sec and incubated for 24 h at 37°C/5% CO_2. CellTiter-Glo reagent was added at 25 μL/well via a plate:handler workstation (Perkin Elmer), using the BioTek406 after the plates were equilibrated to RT (Liconic room temperature plate

hotel). After 45 min incubation in the presence of CellTiter-Glo reagent, luminescence was measured on the EnSight™ Multimode Plate Reader (Perkin Elmer). Files containing plate layouts (Compounds Australia) and data from luminescence readings were imported independently into Spotfire data tables (TIBCO® Spotfire® Analyst 7.6.1.17). The data from all wells was cross-matched to drug codes, negative and positive controls, according to well coordinates. The median and median absolute deviation (MAD) from negative and positive control wells on each plate were used to calculate the robust z-prime values. Data for every compound treated well were normalized against the overall compound median and MAD on a per plate basis using the robust z-scores. The percentage of every compound value relative to the negative control on the plate was also calculated. Compounds were considered hits when corresponding data showed z-scores <-5 or <-2 (for the MicroSource Spectrum and Selleckchem libraries, respectively) and at least 50% reduction of the median of DMSO treated well (negative control). Control wells were used to estimate the coefficient of variation and consistency of the screening. Results were visualized in relevant graphics and final output data tables were exported to Excel files (Supplementary Tables 3-5). A standard method to identify outliers was used according to the distribution of the data in which first and third quartile, interquartile range (IQR), upper and lower outlier boundaries values were calculated for removal of outliers. Outliers were then identified as any data value that fell over Upper Inner Fence (UIF) and Lower Inner Fence (LIF). For secondary dose-response screen, selected compounds (Supplementary Table 5 and 6, Figure 3) were plated at Compound Australia at 50 nL/well in black 384-well plates backfilled to achieve the final concentration of 0.01 to 10 μM. Cells were seeded at 5000 cells/25 uL per well and incubated in the presence of drug for 48 h. Plates were equilibrated, incubated with CellTiter-Glo reagent and luminescence measured as previously. Percentage viability normalized to DMSO control was calculated for each concentration of compound and used to calculate IC50 value per compound using non-linear regression analysis. DMSO was maintained at a final concentration of 0.2% for all wells. PAINS (pan assay interference compounds) were excluded from the compound list. A

SMILES file (simplified molecular-input line-entry system) describing the Microsource drug library from Compounds Australia was analyzed with Match_PAINS_v12 script, in Vortex (Dotmatics Software). This script identifies PAINS based on descriptions previously described (82-85).

Statistical Analysis. All statistical analyses were performed in GraphPad Prism v8 (GraphPad Software, Inc). Paired and un-paired student's t-tests were performed for collected data as indicated and $p<0.05$ was considered statistically significant. The IC_{50} values were calculated by non-linear regression. All flow cytometry analyzes were analyzed using FlowJo analysis software™ v10 (FlowJo, LLC).

Supplementary Figures and Table

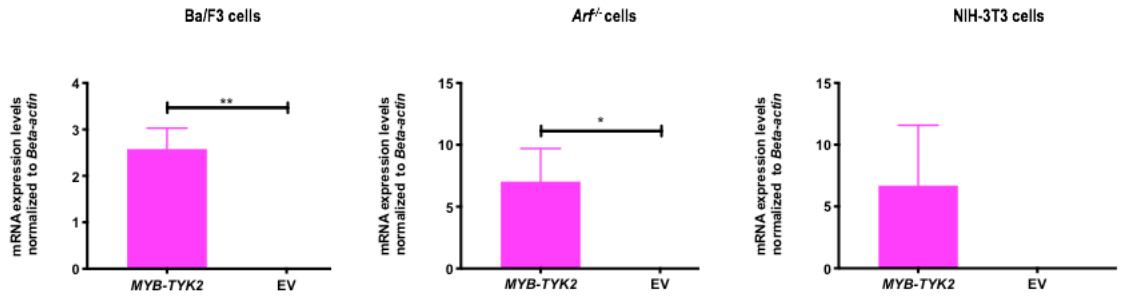

Supplementary Figure 1. RT-PCR validation of the *MYB-TYK2* fusion gene expression in transduced cell lines. RNA expression levels of the *MYB-TYK2* fusion gene in transduced Ba/F3, *Arf*$^{-/-}$ and NIH-3T3 cells compared with their corresponding empty vector controls. Primers were designed to amplify over the *MYB-TYK2* breakpoint region. Data are presented as fold change normalized to the *Beta-actin* expression. Three biological replicates were screened per line in duplicate. All indicated error bars represent mean ±SD. * $p<0.05$, ** $p<0.01$. EV=empty vector



Supplementary Figure 2. No primary antibody control of NIH-3T3-*MYB-TYK2* and NIH-3T3-EV cells. Cells were stained with secondary anti-rabbit Alexa Fluor 568 (Alexa 568R) and anti-mouse Alexa Fluor 647 (Alexa 647M) alone and counter-stained with DAPI (blue signal) for nuclei visualization. Images captured at 40X and 63X magnification as indicated by Confocal Microscopy and processed by ImageJ software.

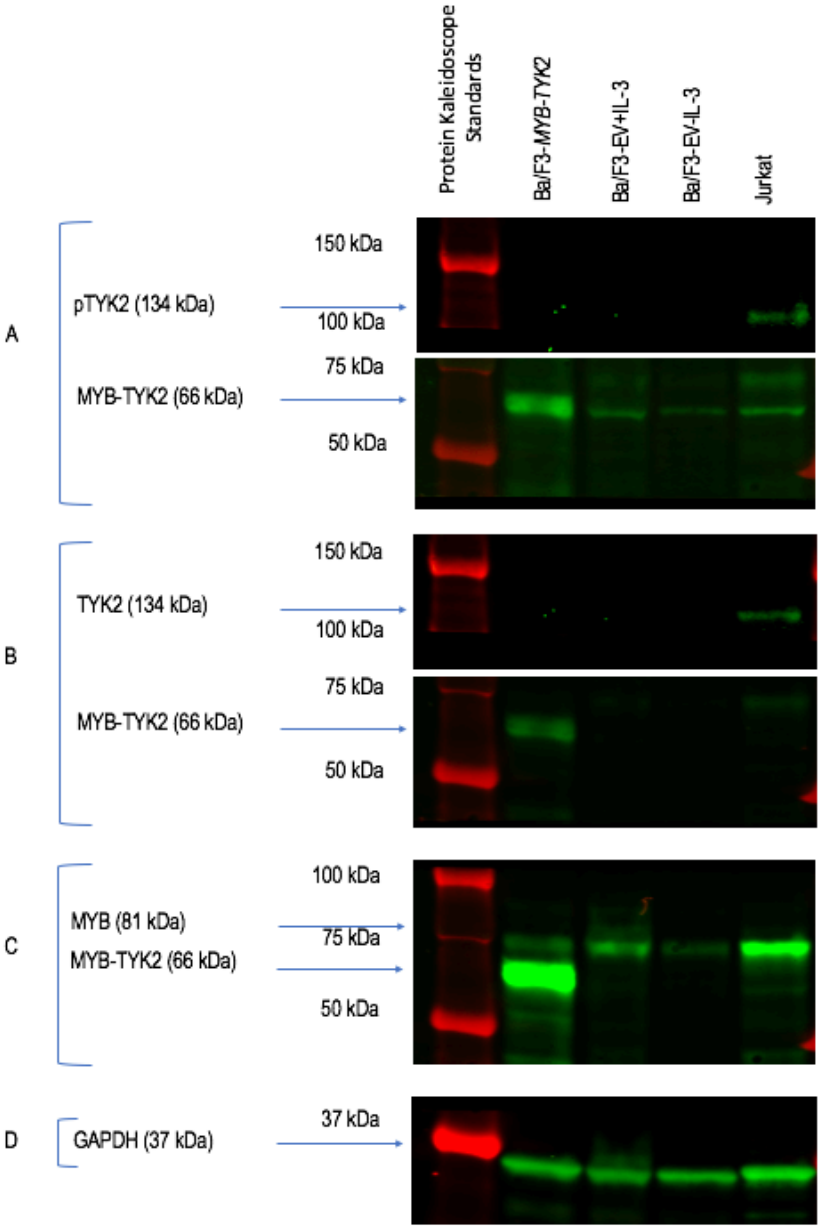
Protein Kaleidoscope Standards
Ba/F3-MYB-TYK2
Ba/F3-EV+IL-3
Ba/F3-EV-IL-3
Jurkat
A
pTYK2 (134 kDa)
MYB-TYK2 (66 kDa)
150 kDa
100 kDa
75 kDa
50 kDa
B
TYK2 (134 kDa)
MYB-TYK2 (66 kDa)
150 kDa
100 kDa
75 kDa
50 kDa
C
MYB (81 kDa)
MYB-TYK2 (66 kDa)
100 kDa
75 kDa
50 kDa
D
GAPDH (37 kDa)
37 kDa

Supplementary Figure 3. The truncated TYK2 protein partner present in Ba/F3-*MYB-TYK2* cells demonstrates kinase activity. Immunoblots were stained for pTYK2 (A), total TYK2 (B) and total MYB (C). GAPDH(D) was used as loading control. The presence of the fusion protein in Ba/F3-*MYB-TYK2* cells is indicated by the expression of both 5' and 3' partners (panels B and C). The Jurkat cell line was used as positive control for both MYB and TYK2 expression. Molecular weight of *MYB-TYK2* (66 kDa) was estimated based on the sequence length of the fusion gene (1860 bp). EV cells (plus or minus IL-3) were used as negative controls to account for any effect of the vector backbone or presence of IL-3 on phosphorylation of TYK2. No endogenous TYK2 expression (134 kDa) or phosphorylation was detected in Ba/F3 cells (-*MYB*-TYK2 and -EV (plus and minus IL-3)) (panels A and C), as expected. It should be noted that while non-specific bands were detected in all samples when staining with pTYK2 (due to inherent binding selectivity/specificity issues of the antibody), the intensity of these bands is lower than the fusion-specific band. The western blot shown is representative of 3 separate experiments.

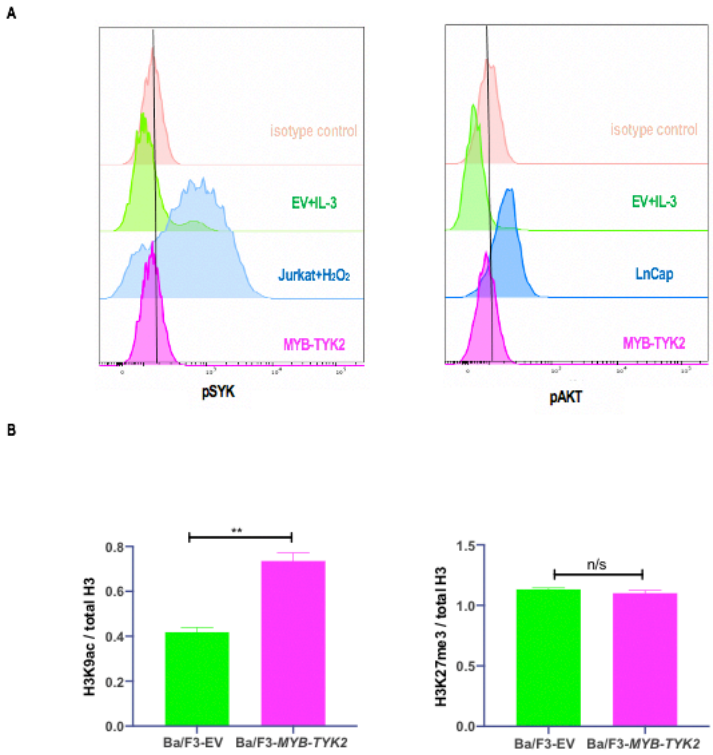

Supplementary Figure 4. The MYB-TYK2 fusion protein does not induce activation of the PI3K/mTOR signaling pathway or B-cell receptor signaling. (A) Representative histograms of phosphoflow cytometric analyses. Ba/F3-*MYB-TYK2* and EV cells were stained and assessed for phosphorylation of SYK (mediator of B-cell receptor signaling) and AKT (PI3K/mTOR pathway protein). LnCap cells were used as positive controls for pAKT as indicated. In order to trigger SYK phosphorylation, Jurkat cells were stimulated with 5 mM H_2O_2 for 15 min. Three biological replicates were screened per condition. (B) Fold change in H3K9ac and H3K27me3 levels in Ba/F3-*MYB-TYK2* and EV control cells as measured by flow cytometric analysis. All MFI values were normalized to the total H3 of each cell line. Indicated error bars represent mean ±SD of 3 separate experiments. **p<0.01.

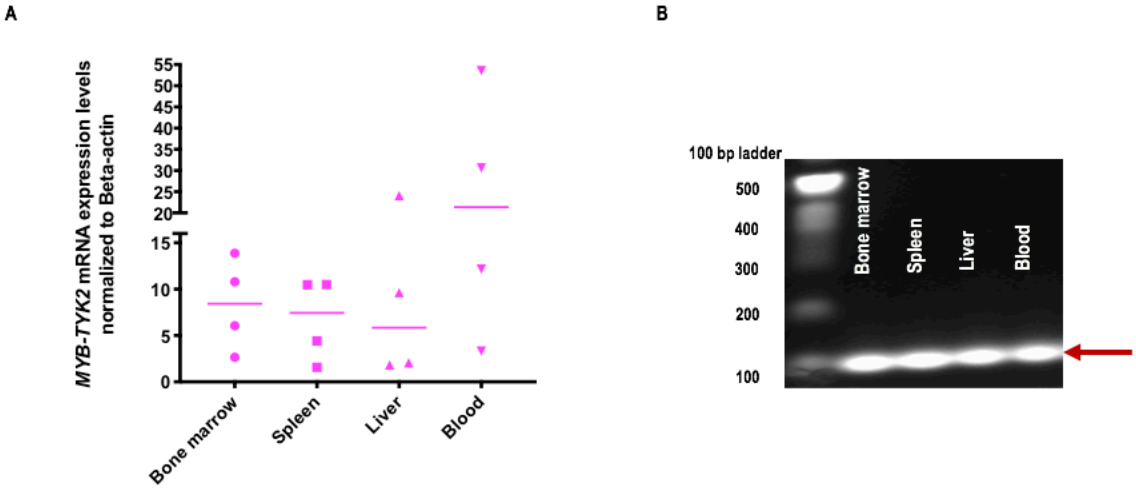

Supplementary Figure 5. RT-PCR confirmed expression of the *MYB-TYK2* fusion gene in cells isolated from *Arf*$^{-/-}$*-MYB-TYK2* mice. (A) RNA expression levels of *MYB-TYK2* fusion gene in cells isolated from *MYB-TYK2* mice (n=4). Horizontal lines indicate median (B) A representative DNA agarose gel of amplified PCR product over the breakpoint region of the *MYB-TYK2* fusion gene with expected size of 109 bp. Cells were isolated from the organs of *MYB-TYK2* mice (n=4). All indicated error bars represent mean ±SD.

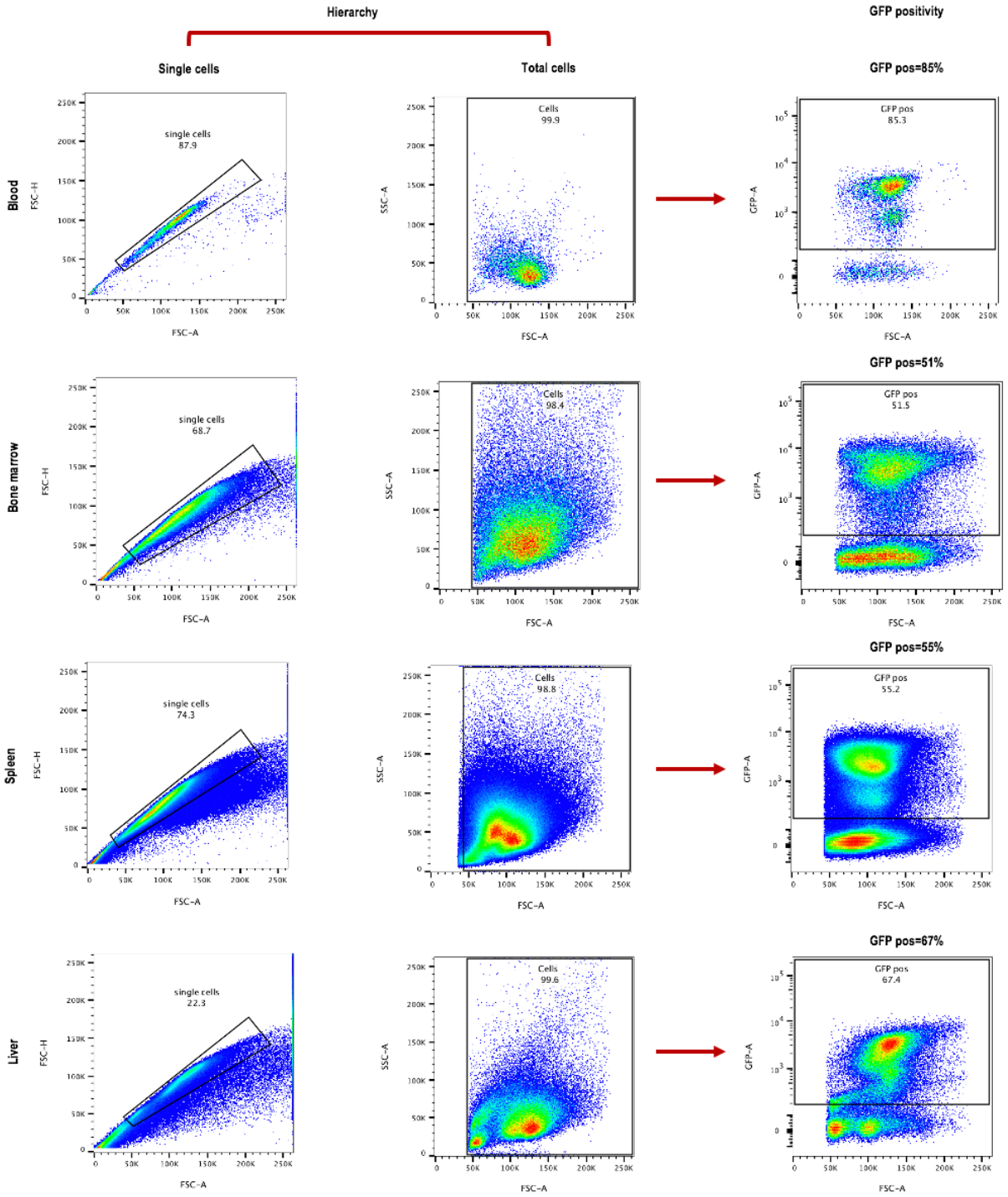

Supplementary Figure 6. Mice transplanted with *Arf*$^{-/-}$*-MYB-TYK2* cells demonstrated infiltration of GFP positive leukemic cells in peripheral blood, bone marrow, spleen and liver. A representative flow cytometric analysis, demonstrating the percentage of GFP positive cells isolated from blood, bone marrow, spleen and liver of *MYB-TYK2* mice (n=4). Left and middle plots display the gating hierarchy of the GFP positive cell population. Abbreviations: pos, positive.

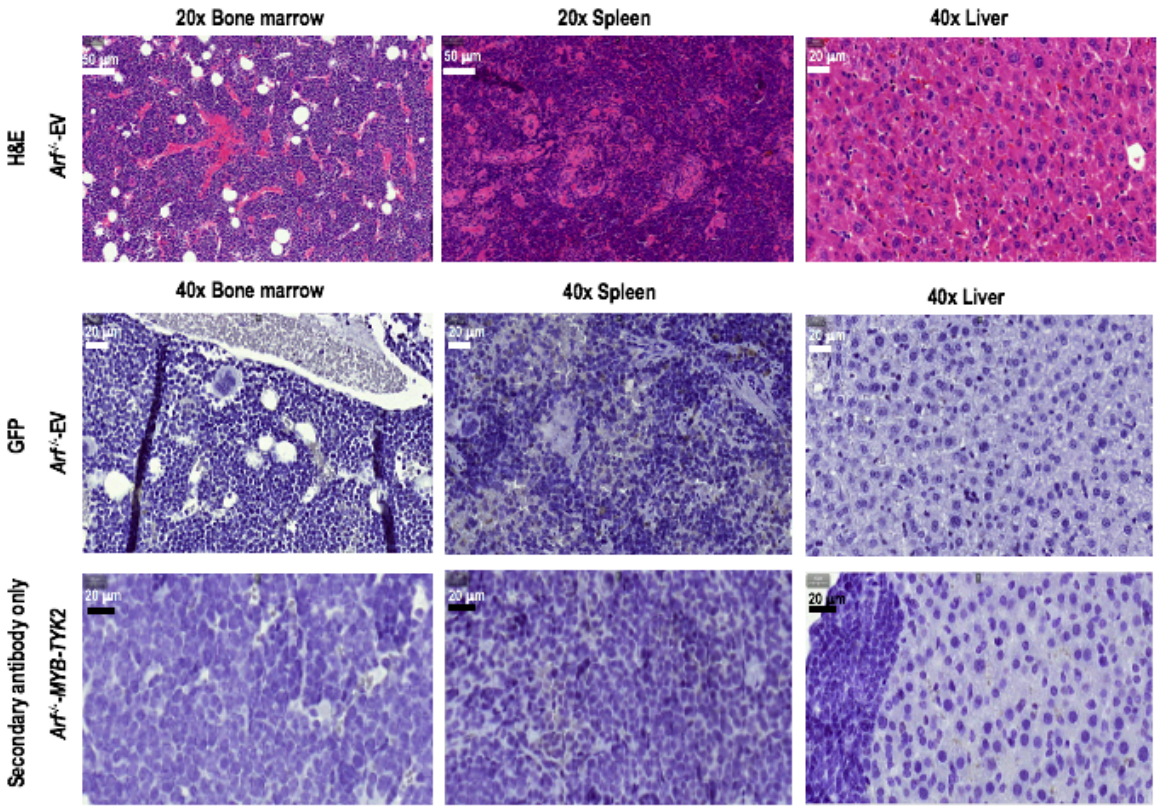

Supplementary Figure 7. Mice transplanted with *Arf*$^{-/-}$-EV cells demonstrated normal bone marrow, spleen and liver structure and no evidence of leukemia infiltration. H&E (top) and GFP (bottom) staining of bone marrow, spleen and liver sections of representative EV mice (n=3). Lower bottom panel demonstrates negative GFP staining from a representative *MYB-TYK2* mouse stained with secondary anti-rabbit IgG H&L (HRP) only. Scale bars represent 50 µm and 20 µm at 20X and 40X magnifications, respectively.

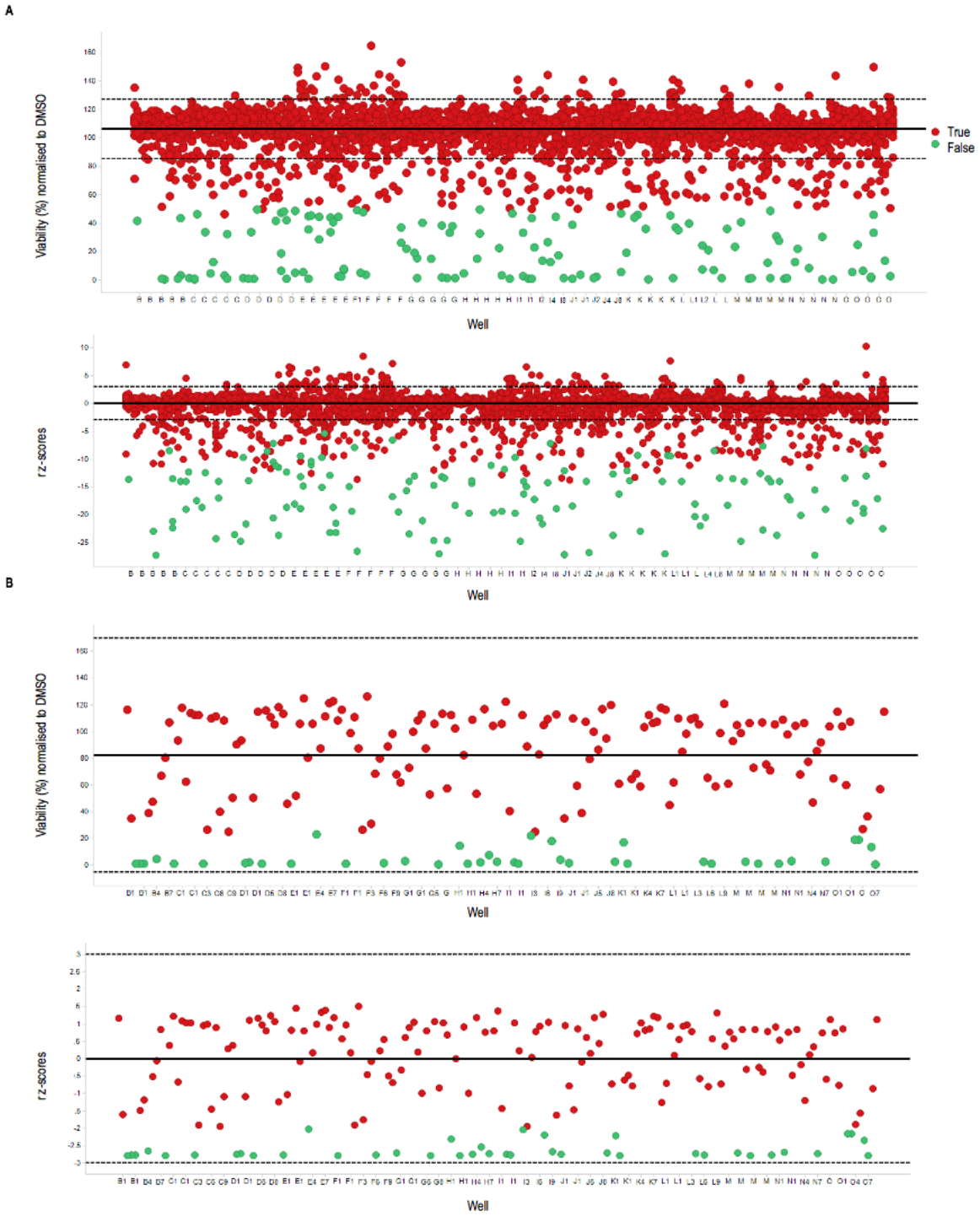
A
Viability (%) normalised to DMSO
True
False
Well
rz-scores
Well
B
Viability (%) normalised to DMSO
Well
rz-scores
Well

Supplementary Figure 8. Data distribution determined the threshold for defining the total hits based on robust z-score and percentage viability to DMSO values for every compound. A representative scatterplot of (A) the MicroSource Spectrum and (B) Selleckchem screened libraries. Robust z-score and percentage viability were determined for each compound. Scatterplots of screened compounds displayed adequate separation based on robust z-score and percentage viability compared to DMSO. The bold line represents the median and the dotted lines 3 times +/-MAD. Based on these graphics, total hits were defined as those compounds with 1) robust z-score of <-5 and <-2 for the MicroSource Spectrum and Selleckchem libraries, respectively (denoted by green circles) and 2) percentage viability (to DMSO) <50%. Abbreviations: MAD, median absolute deviation; rZ-score, robust z-score.

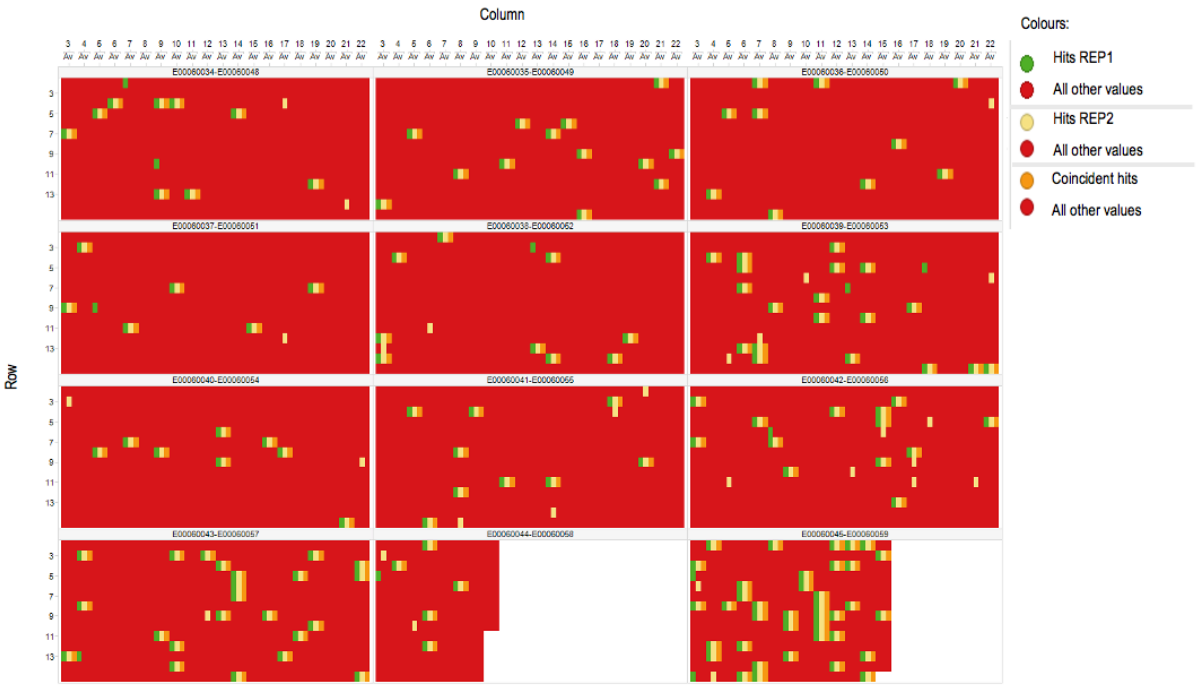

Supplementary Figure 9. Compiled replicate plate maps displayed distribution of hits across all screened plates. Heat map representation of hits detected in HTS assay with orange signal indicating hits in both replicates (coincident hits), green representing hits in only replicate 1 and yellow representing hits in replicate 2. This heat map representation demonstrated that total hits were spread across all plates indicating that no systematic errors occurred. Plate maps were the same for both plates. Abbreviations: REP, replicate.

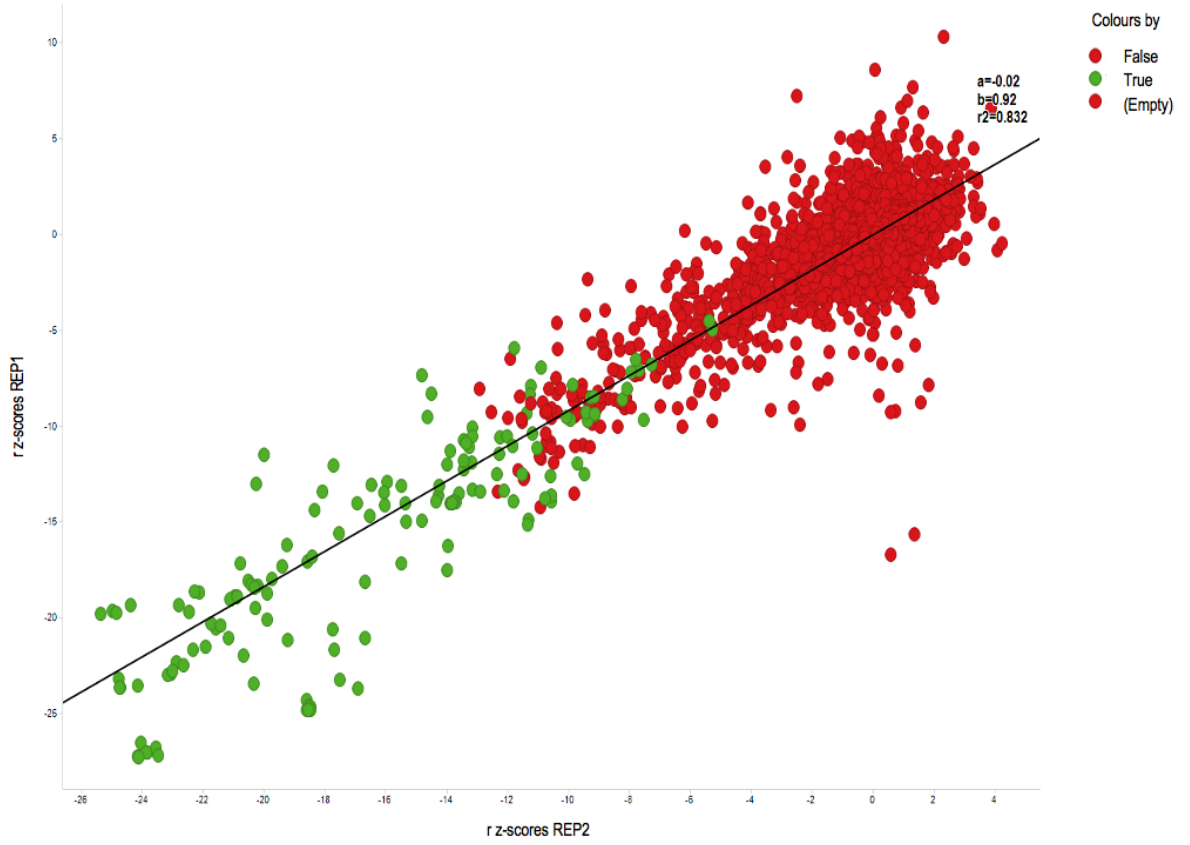

Supplementary Figure 10. Z-score comparisons of replicate 1 and 2 demonstrated adequate distribution of compounds. Comparison of z-score values from compounds in replicates 1 and 2 demonstrated well correlated data (r-squared (r^2) = 0.83). Green signal demonstrates the (True) hits defined by robust z-score of <-5 (and <-2 for SelleckChem library) and <50% viability compared with DMSO. The data linearity was measured by r-squared coefficient of variation. Abbreviations: REP, replicate; rZ-score, robust z-score, REP, replicate.

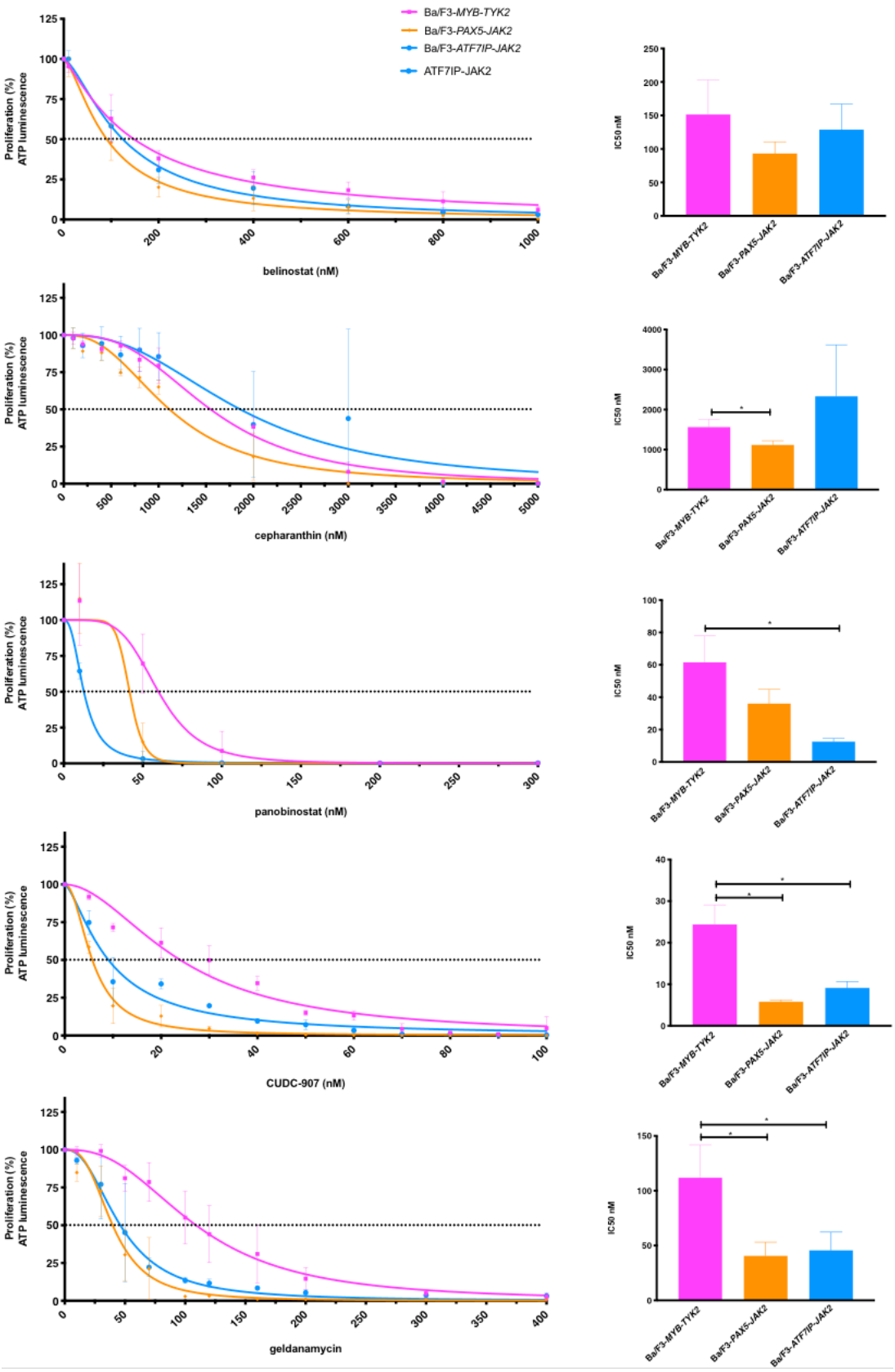
Ba/F3-MYB-TYK2
Ba/F3-PAX5-JAK2
Ba/F3-ATF7IP-JAK2
ATF7IP-JAK2
Proliferation (%) ATP luminescence
belinostat (nM)
cepharanthin (nM)
panobinostat (nM)
CUDC-907 (nM)
geldanamycin
IC50 nM

Supplementary Figure 11. Growth inhibitory activity of HTS candidates against Ba/F3-*MYB-TYK2* cells and other JAK/STAT signaling driven Ba/F3 cell lines. Ba/F3-*MYB-TYK2*, -*PAX5-JAK2* and -*ATF7IP-JAK2* cells cultured in the presence of increasing concentrations of each HTS candidate for 48 h for proliferation analysis. ATP-based luminescence readout is proportional to the number of viable cells. The percentage of proliferation was calculated relative to DMSO control of each line. Dotted line indicates the 50% inhibition of proliferation. IC50 values were estimated by nonlinear regression analysis using GraphPad Prism and are indicated in the right panel. All interactions were measured by un-paired student's t-test with error bars representing mean ±SD of 3 biological replicates. *p<0.05.

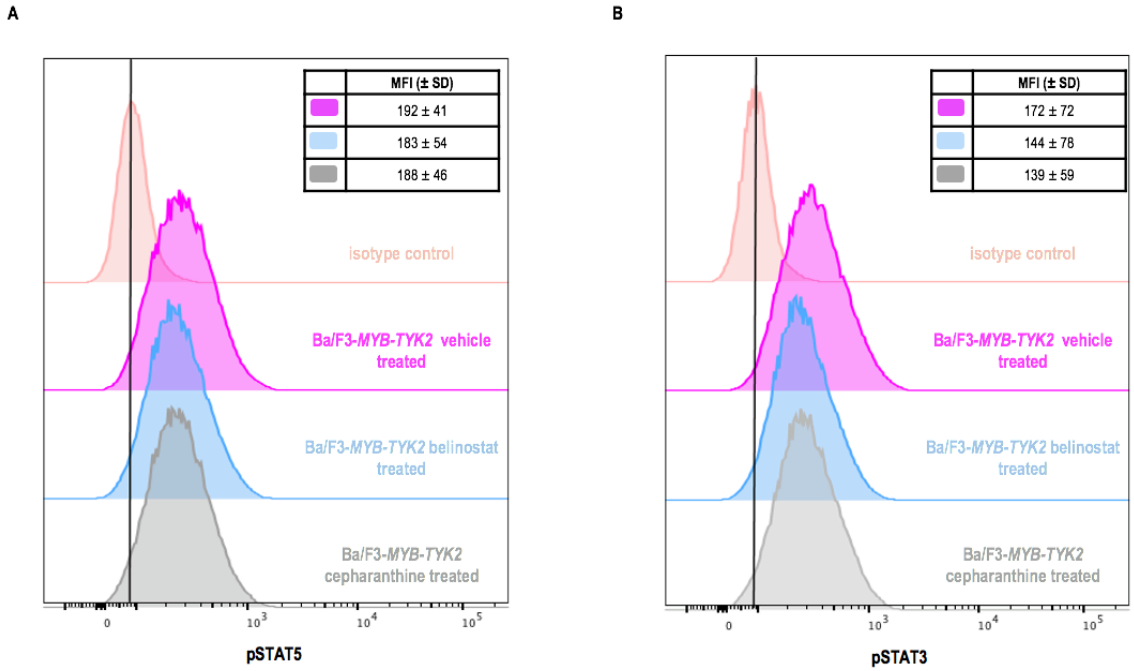

Supplementary Figure 12. Belinostat and cepharanthine did attenuate JAK/STAT signaling in Ba/F3-*MYB-TYK2* cells. Representative histograms of phosphoflow cytometric analyses for (A) pSTAT5 and (B) pSTAT3. Ba/F3-*MYB-TYK2* cells were treated with DMSO (vehicle), 0.2 μM belinostat or 2 μM cepharanthine for 1 h prior to fixation. Cells were stained for pSTAT5, pSTAT3 and isotype control. Three biological replicates were screened per condition.

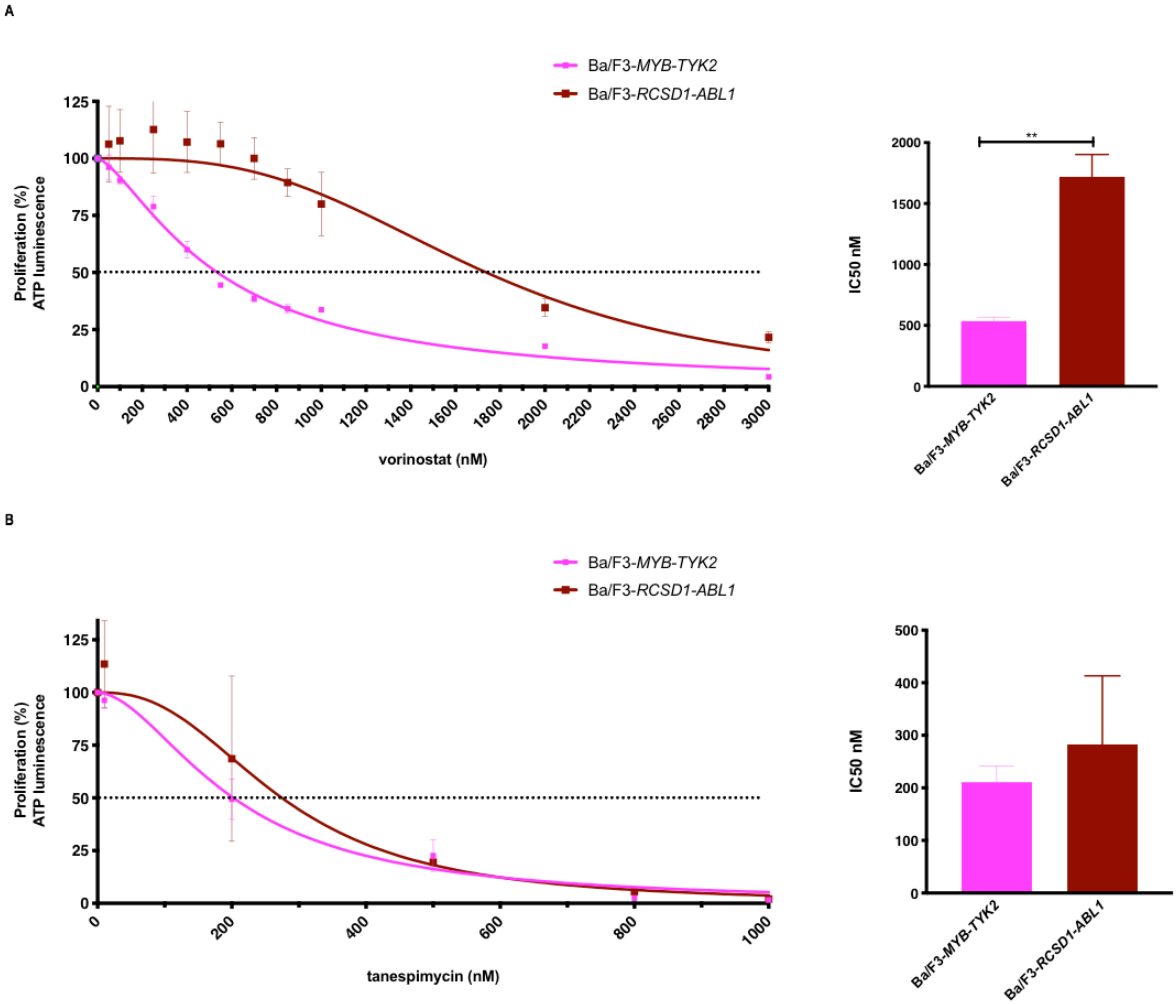

Supplementary Figure 13. Vorinostat selectively inhibits proliferation of Ba/F3-*MYB-TYK2* cells. Dose-response curve of Ba/F3-*MYB-TYK2* and -*RCSD1-ABL1* cells cultured in the presence of increasing concentrations of (A) vorinostat and (B) tanespimycin. The proliferation (%) was calculated relative to DMSO vehicle control of each line. IC50 values as indicated in the right panel. Nonlinear regression analysis was used to evaluate the IC50 of each line. All interactions were measured by un-paired student's t-test. Error bars represent mean ±SD of 3 biological replicates. **p<0.01.

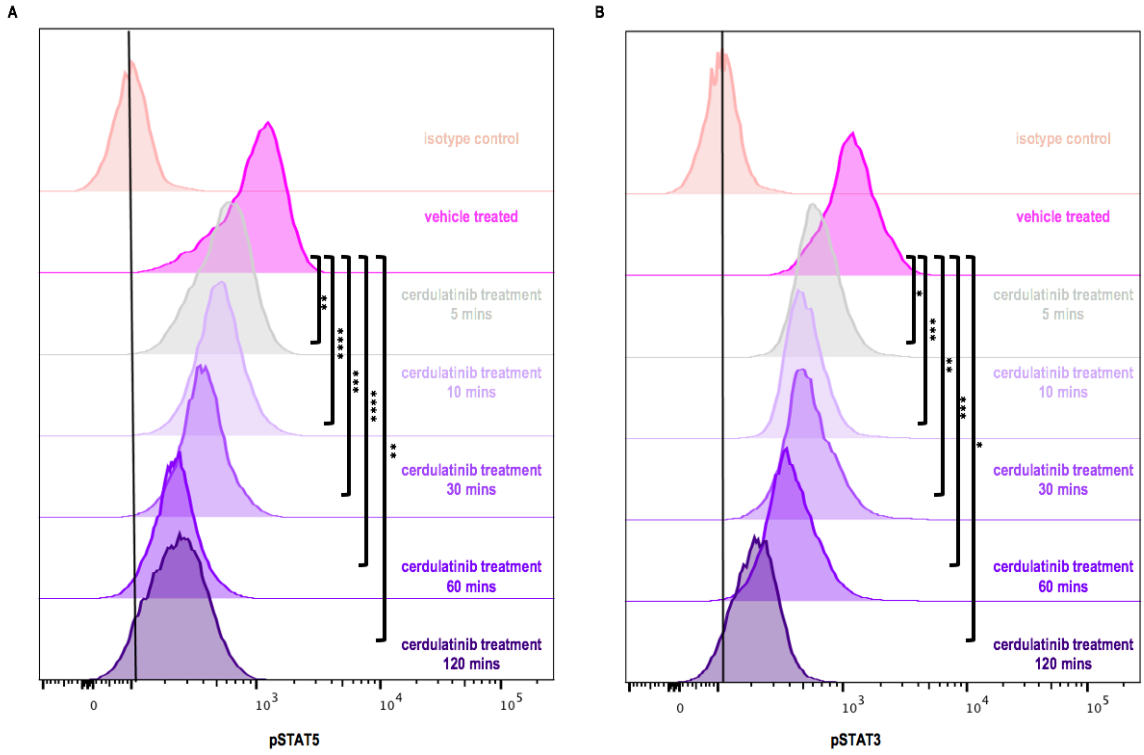

Supplementary Figure 14. A time-dependent reduction in activation of the JAK/STAT downstream effector proteins, STAT5 and STAT3 was identified in Ba/F3-*MYB-TYK2* cells upon cerdulatinib treatment. Representative histograms of flow cytometric analyses for (A) pSTAT5 and (B) pSTAT3 in Ba/F3-*MYB-TYK2* cell when treated with 1 μM cerdulatinib and vehicle for the indicated period. All interactions were measured by paired student's t-test. At least three biological replicates were screened per condition for phosphoflow analysis. *p<0.05, **p<0.01, ***p<0.001 and ****p<0.0001.

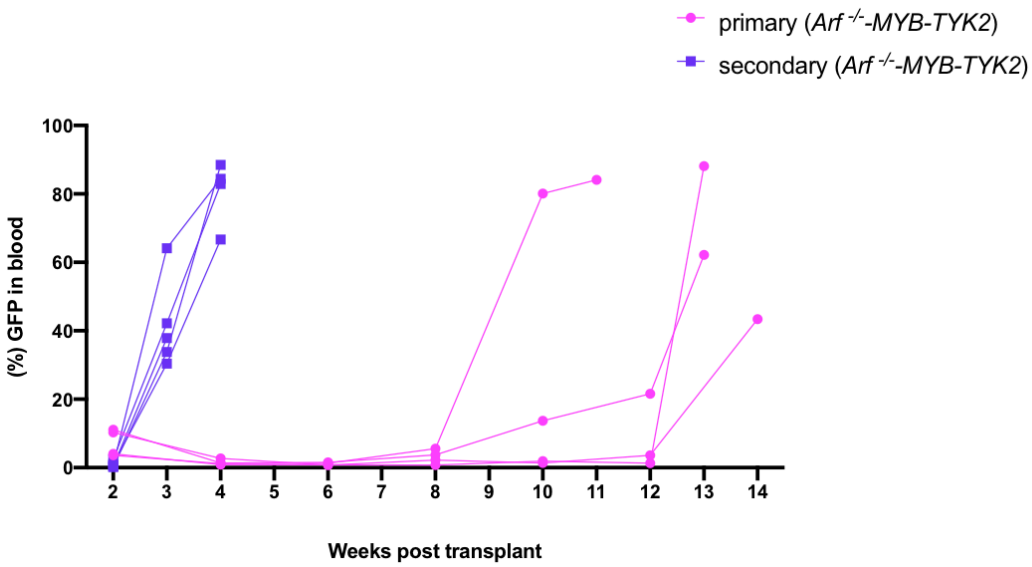

Supplementary Figure 15. Secondary engraftment of mice transplanted with Arf$^{-/-}$*-MYB-TYK2* cells resulted in a rapid onset of leukemia. Comparison of primary vs secondary (n=5) engraftment of Arf$^{-/-}$*-MYB-TYK2* cells measured by %GFP in peripheral blood. The percentage (%) of GFP positive cells was obtained via flow cytometric analysis from live cells only as determined by DAPI staining.

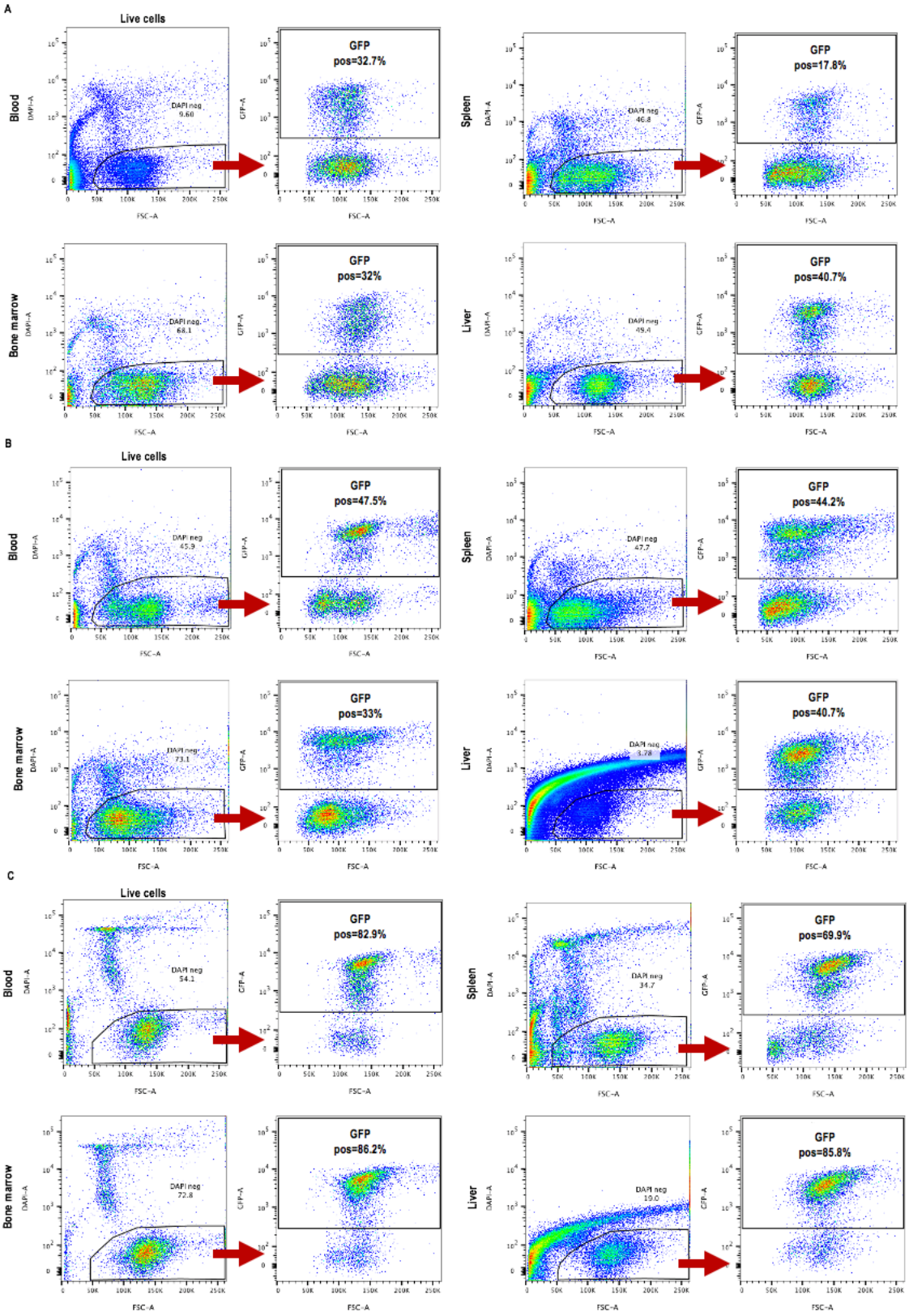
A
Live cells
Blood
DAPI neg
9.60
GFP
pos=32.7%
Spleen
DAPI neg
46.8
GFP
pos=17.8%
Bone marrow
DAPI neg
68.1
GFP
pos=32%
Liver
DAPI neg
49.4
GFP
pos=40.7%
B
Live cells
Blood
DAPI neg
45.9
GFP
pos=47.5%
Spleen
DAPI neg
47.7
GFP
pos=44.2%
Bone marrow
DAPI neg
73.1
GFP
pos=33%
Liver
DAPI neg
8.78
GFP
pos=40.7%
C
Live cells
Blood
DAPI neg
54.1
GFP
pos=82.9%
Spleen
DAPI neg
34.7
GFP
pos=69.9%
Bone marrow
DAPI neg
72.8
GFP
pos=86.2%
Liver
DAPI neg
19.0
GFP
pos=85.8%
DAPI-A
GFP-A
FSC-A

Supplementary Figure16. *MYB-TYK2* mice treated with cerdulatinib and vorinostat displayed reduced GFP positive leukaemic cells in organs. A representative flow cytometric analysis, investigating the percentage of GFP positive cells derived from blood, bone marrow, spleen and liver of *MYB-TYK2* mice treated with (A) vorinostat, (B) cerdulatinib and (C) vehicle. The pseudocolour plots on the left-hand side display the gating hierarchy of the GFP positive cell population; gated on live cells only as determined by DAPI (or LIVE/DEAD Fixable Blue Dead Cell Staining Kit for liver cells, read by the same excitation and channel as DAPI). Abbreviation: pos, positive.

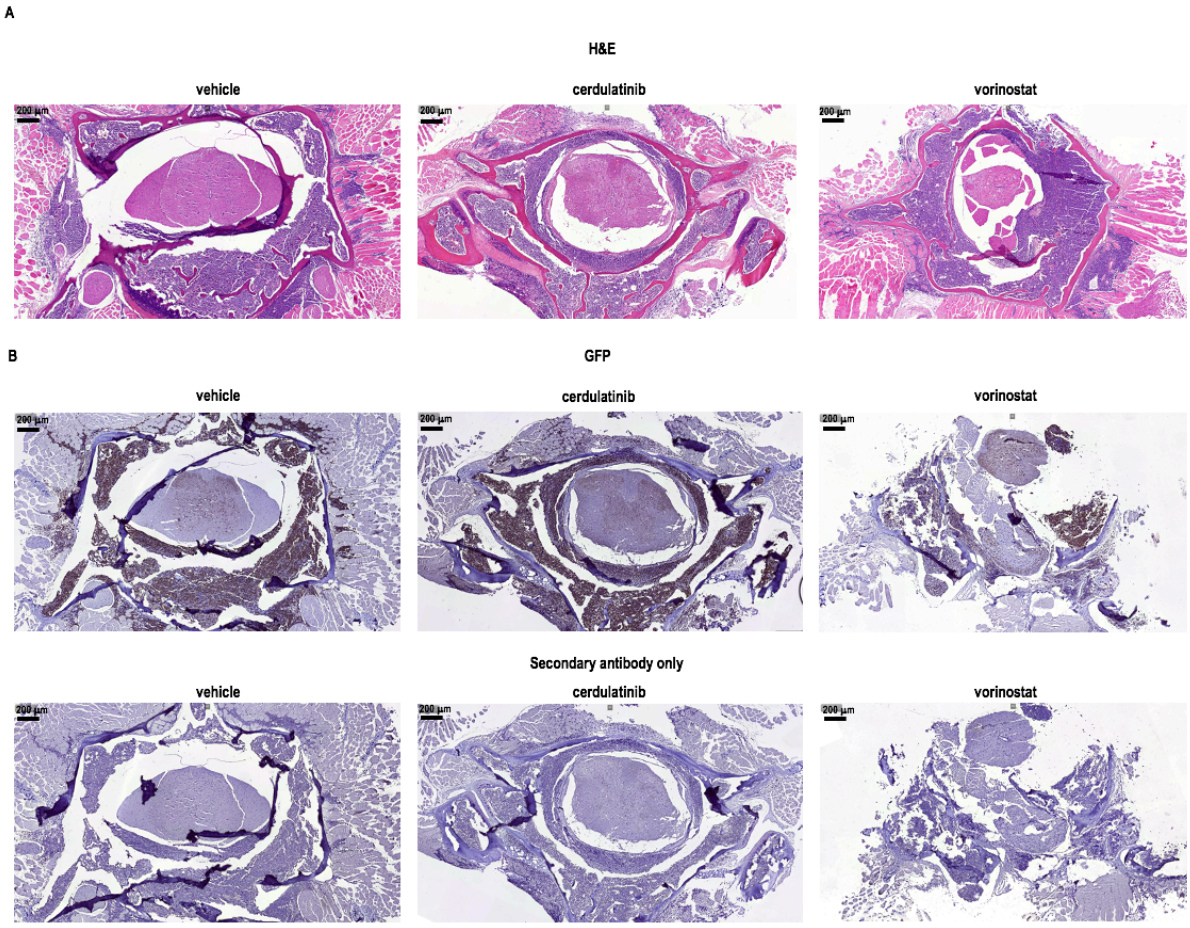

Supplementary Figure 17. Secondary transplanted *MYB-TYK2* mice exhibited a fully penetrant leukemia with aggressive infiltration of cells into the spine. (A) H&E and (B) GFP staining of spine/spinal cord tissue of a representative mouse per treatment cohort. Scale bars represent 200 µm at 5X magnification.

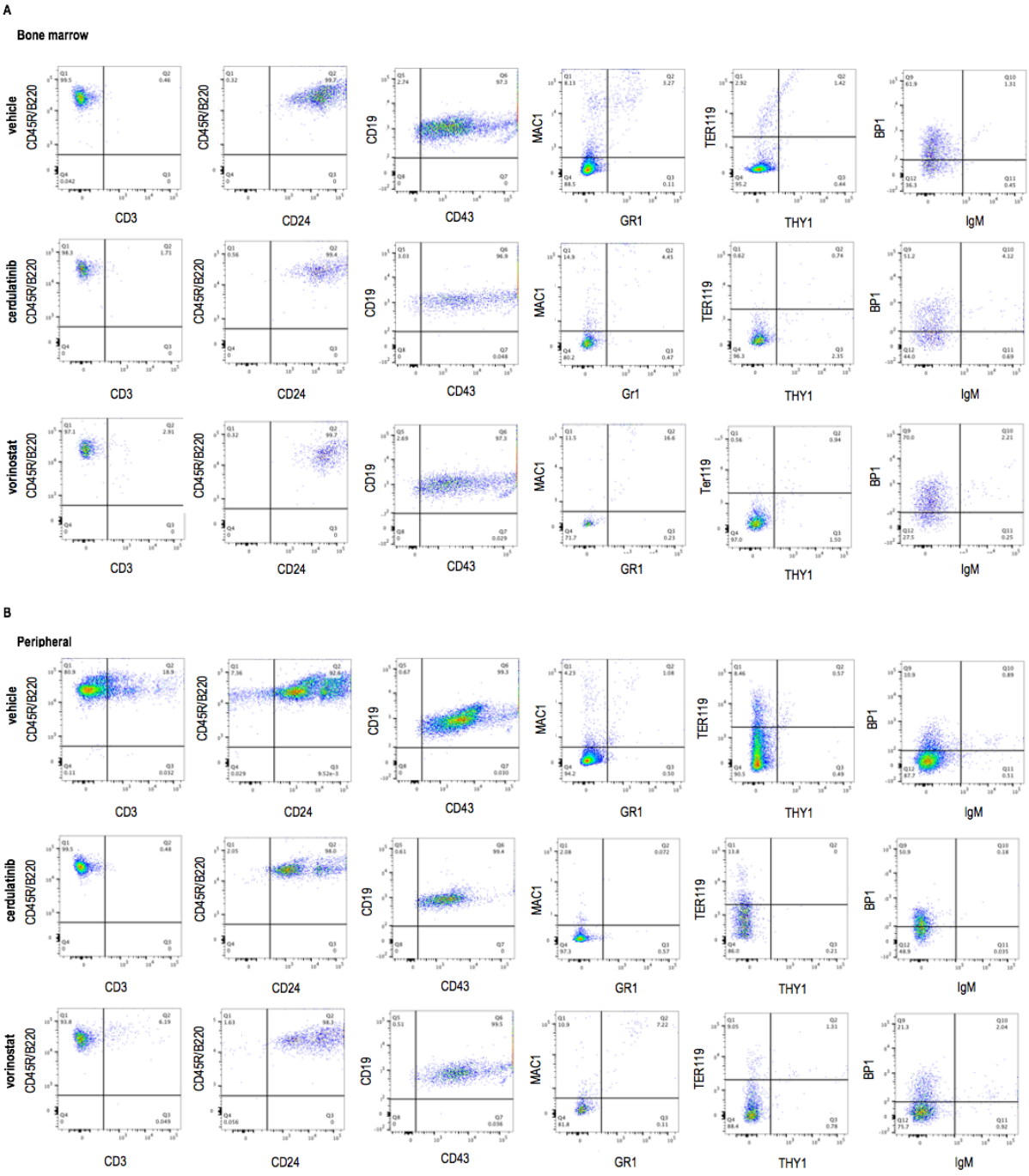

Supplementary Figure 18. Secondary transplanted animals demonstrated an immunophenotype consistent with arrest at pro/pre-B cell developmental stage. Representative flow cytometric analyses of *Arf*$^{-/-}$*-MYB-TYK2* leukemic cells isolated from (A) bone marrow and (B) peripheral blood of *MYB-TYK2* mice (n=3) from cerdulatinib, vorinostat and vehicle treatment cohorts. The plots represent *Arf*$^{-/-}$*-MYB-TYK2* GFP positive cells (live cells only as determined by DAPI staining) expressing indicated markers. Quadrant gates were applied and compensated based on the fluorescence minus one (FMO) technique and unstained controls.

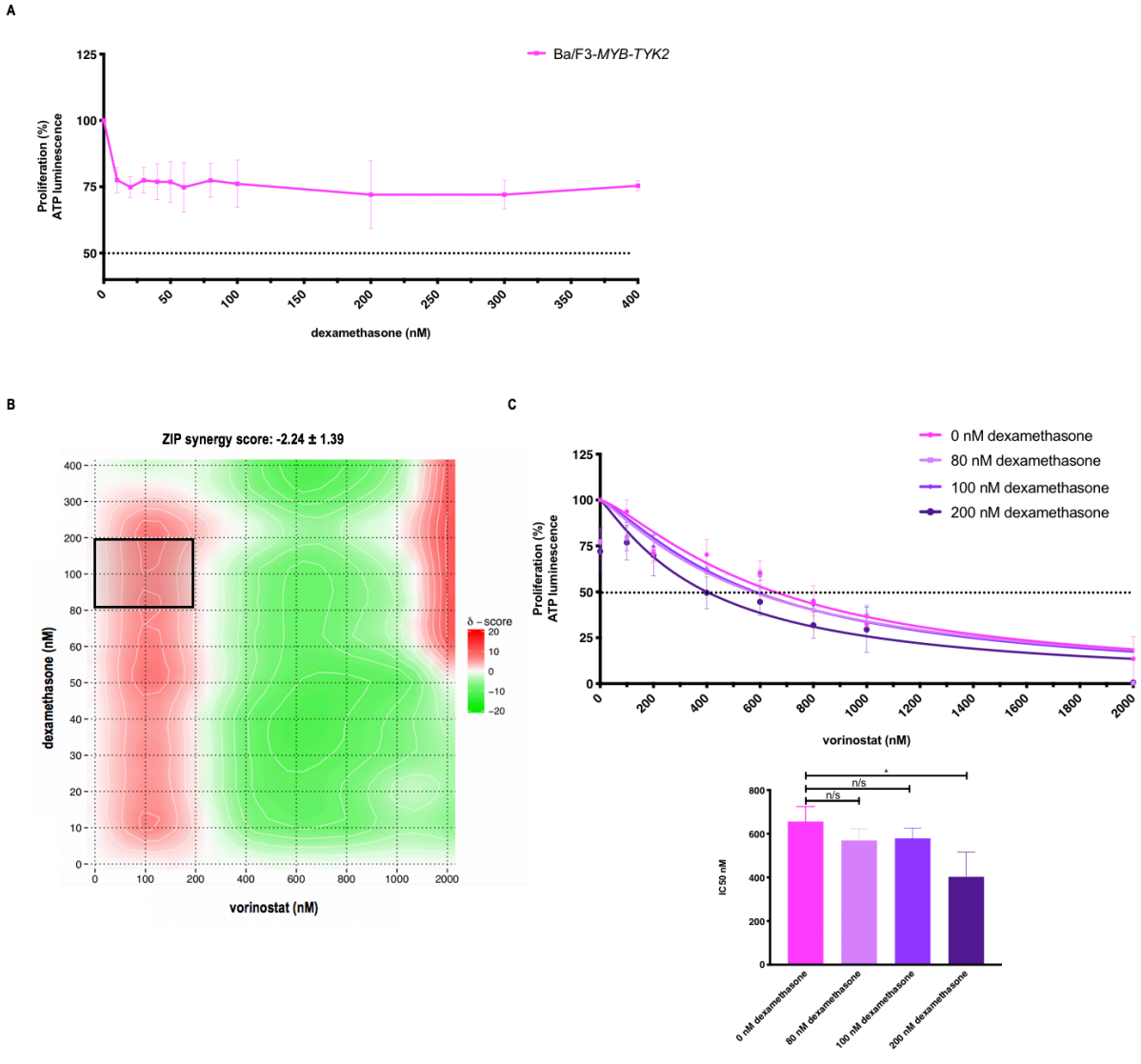

Supplementary Figure 19. Vorinostat demonstrated minimal synergy in combination with dexamethasone. (A) Proliferation analysis of Ba/F3-*MYB*-TYK2 cells cultured in the presence of increasing concentrations of dexamethasone. (B) Heatmap representation of sequential dose combinations of vorinostat and dexamethasone. The black box indicates the most synergistic area as determined by the SynergyFinder 2.0 software. (C) Dose-response curve of Ba/F3-*MYB-TYK2* cells cultured in the presence of increasing concentrations of vorinostat in combination with 0, 80, 100 and 200 nM dexamethasone. IC50 values as indicated in the panel below. The proliferation (%) was calculated relative to DMSO vehicle control of each line after 48 h incubation with drugs and the IC50 is denoted by a horizontal dotted line. IC50 values as indicated in the panel below. Synergy is calculated based on ZIP method and is representative of three biological replicates. All interactions were measured by un-paired student's t-test. Error bars represent mean ±SD of 3 biological replicates. *p<0.05, ns=not significant.

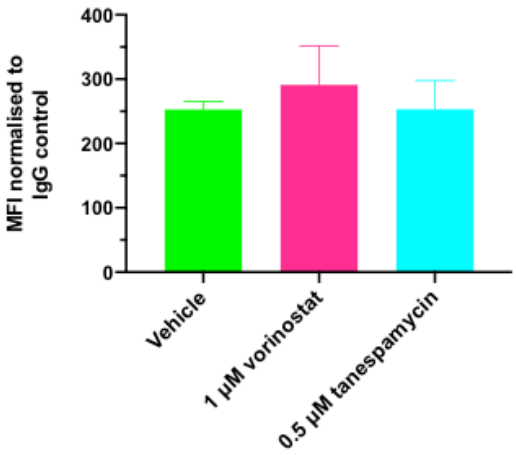

Supplementary Figure 19. Vorinostat and/or tanespimycin treatment does not result in attenuation of STAT5 signaling in Ba/F3-EV cells. Expression levels of pSTAT5 in Ba/F3-EV cells stained for pSTAT5 and isotype control. Cells were cultured in presence of IL-3 and treated with indicated inhibitors or vehicle control for 1 h prior to fixation. All indicated error bars represent mean ±SD of at least 3 separate experiments.

Supplementary Table 6. Activity of selected compounds in the secondary HTS screen.

Treatment ID	Treatment	Class	Comments	Approx. calculated IC50 (based on secondary HTS) (nM)	Approx. maximum plasma concentration (nM)	Reference
SN01004535	Thimerosal	antiseptic	possible antineoplastic properties	1140	N/A	
SN01004576	Phenylmercuric Acetate	antiseptic	antifungal properties	1160	N/A	
SN01004847	Perhexiline Maleate	antianginal	KCHN2 inhibition	2904	1500	(86)
SN00846426	Harringtonine	chemotherapeutic	alkylator	43	1700	(87)
SN01005951	Gambogic Acid	BCL-2i	BCL-2 inhibition/ HSP90i, possible antineoplastic properties	2269	N/A	(88, 89)
SN01730782	Pirarubicin	chemotherapeutic	topoisomerase II inhibition	800	13	(90)
SN01004313	Emetine Dihydrochloride	anti-protozoal	protein synthesis inhibition	46	135	(91)

SN01004179	Sanguinarium Chloride	antiseptic/anti-inflammatory	glutamate decarboxylase inhibition	3335	N/A	
SN01004897	Benzalkonium Chloride	antiseptic	antimicrobial properties	288.9	N/A	
SN01005408	Ivermectin	antiparasitic	GABA family agonist	5431	274	(92)
SN01730815	CUDC-907	HDACi	HDAC1/2/3/10 and Pi3k inhibition	15	74	(93)
SN01730749	Panobinostat (LBH589)	HDACi	pan-HDAC inhibition	104	9988	(94)
SN01730809	TG101209	JAKi	JAK2 inhibition	1766	N/A	
SN00852733	Mitoxanthrone HCL	chemotherapeutics	topoisomerase II inhibition	10.39	860	Daily med
SN01005282	Atracurium Besylate	Neuromuscular agents	possible antineoplastic properties	2509	1300	Daily med
SN01730759	Quisinostat (JNJ-26481585) 2HCL	HDACi	HDAC1/2/4/10/11	16	34	(95)
SN01006163	Methyl Gambogate Methyl Ether	others	N/A	994	N/A	
SN01730750	Trichostatin A (TSA)	HDACi	HDAC inhibition	51	N/A	
SN01730804	AR-42	HDACi	pan-HDAC inhibition	6171	9800	(96)

SN01730758	Dacinostat (LAQ824)	HDACi	pan-HDAC inhibition	28	6000	(97)
SN01730757	Abexinostat (PCI-24781) /CRA-024781	HDACi	pan-HDAC inhibition	217	600	(98)
SN01730909	Pacritinib (SB1518)	JAKi	JAK2 and FLT3 inhibition	1022	10000	(99)
SN01730798	Givinostat (ITF2357)	HDACi	pan-HDAC inhibition	203	2000	(100)
SN00852681	Daunorubicin HCL	chemotherapeutic	topoisomerase II inhibition	129	41000	(101)
SN00846412	Astemizole	anti-allergic agent	possible antineoplastic properties	2226	7	(102, 103)
SN00846275	Tegaserod Maleate	gastrointestinal agent	possible antineoplastic properties	1399	15000	(104, 105)
SN01005639	Proflavine Hemisulfate	antiseptic	possible antineoplastic properties	1080	N/A	
SN01730755	Belinostat (PXD101)	HDACi	pan-HDAC inhibition	184	8600	(106)
SN01005833	Parthenolide	antineoplastic agent	NF-κB signalling inhibition	1178	169	(107)
SN01730882	UNC0631	DNMTi	histone methyltransferase G9a inhibition	1464	N/A	
SN01730775	CUDC-101	HDACi	pan-HDAC inhibition	461	22	(108)

SN01730790	Pracinostat (Sb939)	HDACi	pan-HDAC inhibition	241	500	(109)
SN01730837	CX-6258 HCL	PIMi	pan-PIM inhibition	1029	N/A	
SN00852838	Vandetanib	VEGFRi	VEGFR2/3 and EGFR inhibition	3199	262	(110)
SN01005579	Cetrimonium Bromide	antiseptic	possible antineoplastic properties	3259	N/A	
SN01730904	BIX01294	DNMTi	histone methyltransferase G9a inhibition	2466	N/A	
SN00852845	Vorinostat	HDACi	pan-HDAC inhibition	785	1600	(111)
SN00852819	Fingolimod HCL	immunosuppressive agent	possible antineoplastic properties	6171	8.7	(112, 113)
SN01006361	Celastrol	anti-inflammatory agent	possible antineoplastic properties/ Hsp90-mediated and NF-κB signalling inhibition	1713	300*	(114)
SN00852803	Cepharanthine	antineoplastic agent	apoptosis/ multiple context-based signalling inhibition/ BCL-2 inhibition	1836	224000	(115, 116)
SN01730801	SGI-1776 Free Base	PIMi	PIM1 and FLT3 inhibition	3126	N/A	

SN01004894	Penfluridol	antipsychotic	possible antineoplastic properties	1801	47	(117)
SN01730808	NVP-BSK805 2hcl	JAKi	JAK2 inhibition	6171	742*	(118)
SN01004304	Pyrithione Zinc	antiseptic	possible antineoplastic properties	492	N/A	
SN01730894	AZ6102	TNKS1/2i	WNT signalling inhibition	4698	63000	(119)
SN01730800	Gandotinib (Ly2784544)	JAKi	JAK2 and STAT3 inhibition	2717	2600	(120)
SN01730779	JNJ-7706621	CDKi	pan-CDK inhibitor	6110	N/A	
SN01004988	Fluoxetine Hydrochloride	antipsychotic	possible antineoplastic properties	8983	1400	(121)
SN00852736	Mycophenolate Mofetil	immunosuppressive agent	purine biosynthesis/ possible antineoplastic properties	1009	18600	(122-124)
SN00852840	Geldanamycin	antiseptic	HSP90 inhibition/ tanespimycin (17-AAG)	170	178*	(124, 125)

Approx. IC_{50} was calculated relative to DMSO control. Information about compounds were compiled from: 1. https://dailymed.nlm.nih.gov/dailymed/ 2. https://pubchem.ncbi.nlm.nih.gov/ 3. https://drugs.ncats.io/drug/ unless otherwise referenced. The maximum plasma concentrations were calculated based on the C_{max}, AUC_{0-24} or $AUC_{0-\infty}$ of the maximum tolerated dose (MTD) or the recommended dose. (*) indicates the compounds with bioavailability calculated based on *in vivo* models. Abbreviations: AUC, area under the curve; C_{max}, maximum serum concentration; CDK, cyclin-dependent kinase; EGFR, Epidermal Growth Factor Receptor; GABA, gamma-aminobutyric acid receptors; KCHN2, Potassium Voltage-Gated Channel Subfamily H Member 2; N/A, not applicable, VEGFR, vascular endothelial growth factor receptor.

References:

73. Randle DH, Zindy F, Sherr CJ, Roussel MF. Differential effects of p19(Arf) and p16(Ink4a) loss on senescence of murine bone marrow-derived preB cells and macrophages. *Proc Natl Acad Sci U S A*. 2001;98(17):9654-9.

74. Cheng H, Zheng Z, Cheng T. New paradigms on hematopoietic stem cell differentiation. *Protein Cell*. 2020;11(1):34-44.

75. Jing B, Jin J, Xiang R, Liu M, Yang L, Tong Y, et al. Vorinostat and quinacrine have synergistic effects in T-cell acute lymphoblastic leukemia through reactive oxygen species increase and mitophagy inhibition. *Cell Death Dis*. 2018;9(6):589.

76. Ishikawa C, Senba M, Mori N. Anti-adult Tcell leukemia/lymphoma activity of cerdulatinib, a dual SYK/JAK kinase inhibitor. *Int J Oncol*. 2018;53(4):1681-90.

77. Coffey G, Betz A, DeGuzman F, Pak Y, Inagaki M, Baker DC, et al. The novel kinase inhibitor PRT062070 (Cerdulatinib) demonstrates efficacy in models of autoimmunity and B-cell cancer. *J Pharmacol Exp Ther*. 2014;351(3):538-48.

78. Ianevski A, Giri AK, Aittokallio T. SynergyFinder 2.0: visual analytics of multi-drug combination synergies. *Nucleic Acids Res*. 2020;48(W1):W488-W93.

79. Yadav B, Wennerberg K, Aittokallio T, Tang J. Searching for Drug Synergy in Complex Dose-Response Landscapes Using an Interaction Potency Model. *Comput Struct Biotechnol J*. 2015;13:504-13.

80. Tavakoli Shirazi P, Leifert WR, Fenech MF, Francois M. Folate modulates guanine-quadruplex frequency and DNA damage in Werner syndrome. *Mutat Res Genet Toxicol Environ Mutagen*. 2018;826:47-52.

81. Terwilliger T, Abdul-Hay M. Acute lymphoblastic leukemia: a comprehensive review and 2017 update. *Blood Cancer J*. 2017;7(6):e577.

82. Baell JB, Holloway GA. New substructure filters for removal of pan assay interference compounds (PAINS) from screening libraries and for their exclusion in bioassays. *J Med Chem*. 2010;53(7):2719-40.

83. Dahlin JL, Nissink JW, Strasser JM, Francis S, Higgins L, Zhou H, et al. PAINS in the assay: chemical mechanisms of assay interference and promiscuous enzymatic inhibition observed during a sulfhydryl-scavenging HTS. *J Med Chem*. 2015;58(5):2091-113.

84. Schorpp K, Rothenaigner I, Salmina E, Reinshagen J, Low T, Brenke JK, et al. Identification of Small-Molecule Frequent Hitters from AlphaScreen High-Throughput Screens. *J Biomol Screen*. 2014;19(5):715-26.

85. Brenke JK, Salmina ES, Ringelstetter L, Dornauer S, Kuzikov M, Rothenaigner I, et al. Identification of Small-Molecule Frequent Hitters of Glutathione S-Transferase-Glutathione Interaction. *J Biomol Screen*. 2016;21(6):596-607.

86. Kitoh H, Achiwa M, Kaneko H, Mishima K, Matsushita M, Kadono I, et al. Perhexiline maleate in the treatment of fibrodysplasia ossificans progressiva: an open-labeled clinical trial. *Orphanet J Rare Dis*. 2013;8:163.

87. Levy V, Zohar S, Bardin C, Vekhoff A, Chaoui D, Rio B, et al. A phase I dose-finding and pharmacokinetic study of subcutaneous semisynthetic homoharringtonine (ssHHT) in patients with advanced acute myeloid leukaemia. *Br J Cancer*. 2006;95(3):253-9.

88. Zhou Z, Wang JJCNDJ. Phase I human tolerability trial of gambogic acid. 2007;16(1):79.

89. Yang LJ, Chen Y. New targets for the antitumor activity of gambogic acid in hematologic malignancies. *Acta Pharmacol Sin*. 2013;34(2):191-8.

90. Marchiset-Leca D, Leca FR, Galeani A, Noble A, Catalin J. Pharmacokinetics and metabolism of pirarubicin in humans: correlation with pharmacodynamics. *Cancer Chemother Pharmacol*. 1995;36(3):239-43.

91. Regenthal R, Krueger M, Koeppel C, Preiss R. Drug levels: therapeutic and toxic serum/plasma concentrations of common drugs. *J Clin Monit Comput*. 1999;15(7-8):529-44.

92. Guzzo CA, Furtek CI, Porras AG, Chen C, Tipping R, Clineschmidt CM, et al. Safety, tolerability, and pharmacokinetics of escalating high doses of ivermectin in healthy adult subjects. *J Clin Pharmacol*. 2002;42(10):1122-33.

93. Younes A, Berdeja JG, Patel MR, Flinn I, Gerecitano JF, Neelapu SS, et al. Safety, tolerability, and preliminary activity of CUDC-907, a first-in-class, oral, dual inhibitor of HDAC and PI3K, in patients with relapsed or refractory lymphoma or multiple myeloma: an open-label, dose-escalation, phase 1 trial. *Lancet Oncol*. 2016;17(5):622-31.

94. DeAngelo DJ, Spencer A, Bhalla KN, Prince HM, Fischer T, Kindler T, et al. Phase Ia/II, two-arm, open-label, dose-escalation study of oral panobinostat administered via two dosing schedules in patients with advanced hematologic malignancies. *Leukemia*. 2013;27(8):1628-36.

95. Venugopal B, Baird R, Kristeleit RS, Plummer R, Cowan R, Stewart A, et al. A phase I study of quisinostat (JNJ-26481585), an oral hydroxamate histone deacetylase inhibitor with evidence of target modulation and antitumor activity, in patients with advanced solid tumors. *Clin Cancer Res*. 2013;19(15):4262-72.

96. Sborov DW, Canella A, Hade EM, Mo X, Khountham S, Wang J, et al. A phase 1 trial of the HDAC inhibitor AR-42 in patients with multiple myeloma and T- and B-cell lymphomas. *Leuk Lymphoma*. 2017;58(10):2310-8.

97. de Bono JS, Kristeleit R, Tolcher A, Fong P, Pacey S, Karavasilis V, et al. Phase I pharmacokinetic and pharmacodynamic study of LAQ824, a hydroxamate histone deacetylase inhibitor with a heat shock protein-90 inhibitory profile, in patients with advanced solid tumors. *Clin Cancer Res*. 2008;14(20):6663-73.

98. Evens AM, Balasubramanian S, Vose JM, Harb W, Gordon LI, Langdon R, et al. A Phase I/II Multicenter, Open-Label Study of the Oral Histone Deacetylase Inhibitor Abexinostat in Relapsed/Refractory Lymphoma. *Clin Cancer Res*. 2016;22(5):1059-66.

99. Verstovsek S, Odenike O, Singer JW, Granston T, Al-Fayoumi S, Deeg HJ. Phase 1/2 study of pacritinib, a next generation JAK2/FLT3 inhibitor, in myelofibrosis or other myeloid malignancies. *J Hematol Oncol*. 2016;9(1):137.

100. Furlan A, Monzani V, Reznikov LL, Leoni F, Fossati G, Modena D, et al. Pharmacokinetics, safety and inducible cytokine responses during a phase 1 trial of the oral histone deacetylase inhibitor ITF2357 (givinostat). *Mol Med*. 2011;17(5-6):353-62.

101. Lowis S, Lewis I, Elsworth A, Weston C, Doz F, Vassal G, et al. A phase I study of intravenous liposomal daunorubicin (DaunoXome) in paediatric patients with relapsed or resistant solid tumours. *Br J Cancer*. 2006;95(5):571-80.

102. Janssens MML. Astemizole. *Clinical Reviews in Allergy*. 1993;11(1):35-63.

103. Shah RR, Stonier PD. Repurposing old drugs in oncology: Opportunities with clinical and regulatory challenges ahead. *J Clin Pharm Ther*. 2019;44(1):6-22.

104. Appel-Dingemanse S. Clinical pharmacokinetics of tegaserod, a serotonin 5-HT(4) receptor partial agonist with promotile activity. *Clinical pharmacokinetics*. 2002;41(13):1021-42.

105. Liu W, Stachura P, Xu HC, Umesh Ganesh N, Cox F, Wang R, et al. Repurposing the serotonin agonist Tegaserod as an anticancer agent in melanoma: molecular mechanisms and clinical implications. *Journal of experimental & clinical cancer research : CR*. 2020;39(1):38.

106. Steele NL, Plumb JA, Vidal L, Tjornelund J, Knoblauch P, Buhl-Jensen P, et al. Pharmacokinetic and pharmacodynamic properties of an oral formulation of the histone deacetylase inhibitor Belinostat (PXD101). *Cancer Chemother Pharmacol*. 2011;67(6):1273-9.

107. Curry EA, 3rd, Murry DJ, Yoder C, Fife K, Armstrong V, Nakshatri H, et al. Phase I dose escalation trial of feverfew with standardized doses of parthenolide in patients with cancer. *Invest New Drugs*. 2004;22(3):299-305.

108. Shimizu T, LoRusso PM, Papadopoulos KP, Patnaik A, Beeram M, Smith LS, et al. Phase I first-in-human study of CUDC-101, a multitargeted inhibitor of HDACs, EGFR, and HER2 in patients with advanced solid tumors. *Clin Cancer Res*. 2014;20(19):5032-40.

109. Abaza YM, Kadia TM, Jabbour EJ, Konopleva MY, Borthakur G, Ferrajoli A, et al. Phase 1 dose escalation multicenter trial of pracinostat alone and in combination with azacitidine in patients with advanced hematologic malignancies. *Cancer*. 2017;123(24):4851-9.

110. Martin P, Oliver S, Kennedy SJ, Partridge E, Hutchison M, Clarke D, et al. Pharmacokinetics of vandetanib: three phase I studies in healthy subjects. *Clin Ther*. 2012;34(1):221-37.

111. Kadia TM, Yang H, Ferrajoli A, Maddipotti S, Schroeder C, Madden TL, et al. A phase I study of vorinostat in combination with idarubicin in relapsed or refractory leukaemia. *Br J Haematol*. 2010;150(1):72-82.

112. David OJ, Kovarik JM, Schmouder RL. Clinical pharmacokinetics of fingolimod. *Clinical pharmacokinetics*. 2012;51(1):15-28.

113. White C, Alshaker H, Cooper C, Winkler M, Pchejetski D. The emerging role of FTY720 (Fingolimod) in cancer treatment. *Oncotarget*. 2016;7(17):23106-27.

114. Zhang J, Li CY, Xu MJ, Wu T, Chu JH, Liu SJ, et al. Oral bioavailability and gender-related pharmacokinetics of celastrol following administration of pure celastrol and its related tablets in rats. *J Ethnopharmacol*. 2012;144(1):195-200.

115. Bailly C. Cepharanthine: An update of its mode of action, pharmacological properties and medical applications. *Phytomedicine*. 2019;62:152956.

116. Jiang Y, Liu M, Liu H, Liu S. A critical review: traditional uses, phytochemistry, pharmacology and toxicology of Stephania tetrandra S. Moore (Fen Fang Ji). *Phytochem Rev*. 2020:1-41.

117. Tuan NM, Lee CH. Penfluridol as a Candidate of Drug Repurposing for Anticancer Agent. *Molecules*. 2019;24(20).

118. Baffert F, Regnier CH, De Pover A, Pissot-Soldermann C, Tavares GA, Blasco F, et al. Potent and selective inhibition of polycythemia by the quinoxaline JAK2 inhibitor NVP-BSK805. *Mol Cancer Ther*. 2010;9(7):1945-55.

119. de Vicente J, Tivitmahaisoon P, Berry P, Bolin DR, Carvajal D, He W, et al. Fragment-Based Drug Design of Novel Pyranopyridones as Cell Active and Orally Bioavailable Tankyrase Inhibitors. *ACS Med Chem Lett*. 2015;6(9):1019-24.

120. Verstovsek S, Mesa RA, Salama ME, Li L, Pitou C, Nunes FP, et al. A phase 1 study of the Janus kinase 2 (JAK2)(V617F) inhibitor, gandotinib (LY2784544), in patients with primary myelofibrosis, polycythemia vera, and essential thrombocythemia. *Leuk Res*. 2017;61:89-95.

121. Bibbo S, Lamolinara A, Capone E, Purgato S, Tsakaneli A, Panella V, et al. Repurposing a psychoactive drug for children with cancer: p27(Kip1)-dependent inhibition of metastatic neuroblastomas by Prozac. *Oncogenesis*. 2020;9(1):3.

122. Jacobson P, El-Massah SF, Rogosheske J, Kerr A, Long-Boyle J, DeFor T, et al. Comparison of two mycophenolate mofetil dosing regimens after hematopoietic cell transplantation. *Bone Marrow Transplant*. 2009;44(2):113-20.

123. Majd N, Sumita K, Yoshino H, Chen D, Terakawa J, Daikoku T, et al. A Review of the Potential Utility of Mycophenolate Mofetil as a Cancer Therapeutic. *Journal of Cancer Research*. 2014;2014:423401.

124. Supko JG, Hickman RL, Grever MR, Malspeis L. Preclinical pharmacologic evaluation of geldanamycin as an antitumor agent. *Cancer Chemother Pharmacol*. 1995;36(4):305-15.

125. Gorska M, Popowska U, Sielicka-Dudzin A, Kuban-Jankowska A, Sawczuk W, Knap N, et al. Geldanamycin and its derivatives as Hsp90 inhibitors. *Front Biosci (Landmark Ed)*. 2012;17:2269-77.

3. Chapter 3: Constitutive JAK/STAT signaling is the primary mechanism of resistance to JAKi in *TYK2*-rearranged acute lymphoblastic leukemia

Statement of Authorship

Title of Paper	Constitutive JAK/STAT signaling is the primary mechanism of resistance to JAKi in *TYK2*-rearranged acute lymphoblastic leukemia
Publication Status	☑ Published ☐ Accepted for Publication ☐ Submitted for Publication ☐ Unpublished and Unsubmitted work written in manuscript style
Publication Details	Tavakoli Shirazi P, Eadie LN, Page EC, Heatley SL, Bruning JB, White DL. Constitutive JAK/STAT signaling is the primary mechanism of resistance to JAKi in TYK2-rearranged acute lymphoblastic leukemia. *Cancer Lett.* 2021;512:28-37.

Principal Author

Name of Principal Author (Candidate)	Paniz Tavakoli Shirazi
Contribution to the Paper	Conceived, designed and performed experiments, generated lines and reagents, interpreted/analysed data, wrote and revised manuscript.
Overall percentage (%)	90%
Certification:	This paper reports on original research I conducted during the period of my Higher Degree by Research candidature and is not subject to any obligations or contractual agreements with a third party that would constrain its inclusion in this thesis. I am the primary author of this paper.
Signature	Date 17/5/21

Co-Author Contributions

By signing the Statement of Authorship, each author certifies that:

i. the candidate's stated contribution to the publication is accurate (as detailed above);
ii. permission is granted for the candidate in include the publication in the thesis; and
iii. the sum of all co-author contributions is equal to 100% less the candidate's stated contribution.
iv.

Name of Co-Author	Laura Eadie
Contribution to the Paper	Supervised, designed experiments and critically revised the manuscript.
Signature	Date: 12/01/21

Name of Co-Author	Susan Heatley
Contribution to the Paper	Supervised, designed experiments and critically revised the manuscript.
Signature	Date: 12-1-21

Name of Co-Author	John Bruning		
Contribution to the Paper	Performed the computational modelling and critically revised the manuscript		
Signature		Date	13-1-2020

Name of Co-Author	Deborah White		
Contribution to the Paper	Supervised, designed experiments and critically revised the manuscript		
Signature		Date	12/1/21

Name of Co-Author	Elyse Page		
Contribution to the Paper	Helped in performing experiments		
Signature		Date	17/5/21

Constitutive JAK/STAT signaling is the primary mechanism of resistance to JAKi in *TYK2*-rearranged acute lymphoblastic leukemia

Paniz Tavakoli Shirazi[1,2], Laura N Eadie[1,2], Elyse C Page[1], Susan L Heatley[1,2], John B Bruning[3] and Deborah L White[1,2,3,4]

1.Cancer Program, Precision Medicine Theme, South Australian Health & Medical Research Institute (SAHMRI), Adelaide, Australia

2.Faculty of Health and Medical Sciences, University of Adelaide, Adelaide, Australia

3. Faculty of Sciences, University of Adelaide, Adelaide, Australia

4. Australian Genomics Health Alliance (AGHA)

Corresponding author:

Prof. Deborah White (corresponding author) PhD. FFSc(RCPA).

Director: Cancer Program SAHMRI.

Deputy Theme Leader: Precision Medicine SAHMRI.

NHMRC RD Wright Research Fellow

Beat Cancer Project Principal Research Fellow

Professor: The Faculty of Health and Medical Science, University of Adelaide.

Professor: School of Biological Sciences. The Faculty of Sciences, University of Adelaide.

Cancer Program. Precision Medicine Theme, South Australian Health & Medical Research Institute (SAHMRI), Adelaide, Australia

Phone: +61 08

E-mail:

Abstract:

Activating *TYK2*-rearrangements have recently been identified and implicated in the leukemogenesis of high-risk acute lymphoblastic leukemia (HR-ALL) cases. Pre-clinical studies indicated the JAK/TYK2 inhibitor (JAKi), cerdulatinib, as a promising therapeutic against *TYK2*-rearranged ALL, attenuating the constitutive JAK/STAT signaling resulting from the TYK2 fusion protein. However, following a period of clinical efficacy, JAKi resistance often occurs resulting in relapse. In this study, we modeled potential mechanisms of JAKi resistance in *TYK2*-rearranged ALL cells *in vitro* in order to recapitulate possible clinical scenarios and provide a rationale for alternative therapies. Cerdulatinib resistant B-cells, driven by the *MYB-TYK2* fusion oncogene, were generated by long-term exposure to the drug. Sustained treatment of *MYB-TYK2*-rearranged ALL cells with cerdulatinib led to enhanced and persistent JAK/STAT signaling, co-occurring with JAK1 overexpression. Hyperactivation of JAK/STAT signaling and JAK1 overexpression was reversible as cerdulatinib withdrawal resulted in re-sensitization to the drug. Importantly, histone deacetylase inhibitor (HDACi) therapies were efficacious against cerdulatinib-resistant cells demonstrating a potential alternative therapy for use in *TYK2*-rearranged B-ALL patients who have lost response to JAKi treatment regimens.

Key words: Acute Lymphoblastic Leukemia, *TYK2* rearrangements, JAKi, resistance, HDACi

Introduction:

Acute lymphoblastic leukemia (ALL) patients harboring *JAK* alterations experience poor outcomes and have a high risk of relapse (1). Specifically, *JAK*-rearranged adult cases demonstrate an inferior 5-year event free and overall survival compared with cases harboring *ABL1/2*-rearrangements (2). Currently targeted therapeutics are considered the best approach to overcome chemotherapy refractoriness and improve patient outcomes. They are therefore a promising option in JAK/STAT driven high-risk (HR)

subtypes of ALL (1-5). In recent years, sensitivity to JAK inhibitors (JAKi) has been demonstrated in several *in vitro* and *in vivo* models of JAK/STAT activating alterations (e.g. *JAK*-class and *CRLF2* rearrangements) (6-13). Clinical trials investigating the efficacy of concomitant ruxolitinib with conventional chemotherapy in *CRLF2*-rearranged patients with or without *JAK2* mutations (NCT02420717, NCT02723994, NCT02723994) as well as newly diagnosed HR Ph-like ALL patients (NCT02420717, NCT02883049) are underway. We have also recently demonstrated, in pre-clinical investigations, the sensitivity of the aggressive *MYB-TYK2* fusion gene to the dual SYK/JAKi, cerdulatinib (14).

JAKi therapy has noticeably improved the treatment outcome for patients with myeloproliferative neoplasms (MPN) (15-18). Ruxolitinib was the first JAK1/2 inhibitor (JAK1/2i) approved for the treatment of MPNs where the majority of cases harbored the gain of function, *JAK2* p.V617F mutation, and thus demonstrated constitutive activation of JAK/STAT signaling (15-18). However, the reduction in allelic burden by ruxolitinib in *JAK2* mutant MPN patients appears to be limited (19) and due to the limited curative potential, extended treatment periods are usually required (20). Long-term exposure to ruxolitinib is of clinical concern as it has led to loss of response and insensitivity to JAKi in 50% of cases after 2-3 years of treatment (21-23), indicating the development of resistance in leukemic cells. Consequently, the outcome for MPN patients after acquisition of ruxolitinib resistance is poor. Very limited alternative treatment options exist for these patients (24-26), highlighting the unmet need to model potential resistance mechanisms and identify additional tailored treatment regimens.

Currently, the evidence describing possible resistance mechanisms to JAKi is limited and mainly from *in vitro* studies in MPNs. The proposed mechanisms in these models include: 1) acquired secondary mutations in the *JAK2* kinase domain that often effect drug binding (27-29) and 2) persistent JAK/STAT signaling due to heterodimerization and transactivation of JAK family proteins (i.e. JAK1, JAK2, JAK3

and TYK2) (30-32). Conversely, the only study investigating the effect of long-term exposure to ruxolitinib in B-ALL cells harboring *CRLF2r/JAK2* mutations suggests that adaptation to prolonged JAK2 inhibition is due to up-regulation of c-MYC expression rather than persistent activation of JAK/STAT signaling, highlighting that JAKi-resistance development may be dependent on biological context (33).

The *TYK2* gene fusions were recently identified in large cohort studies in ALL patients with different 5' partners including *MYB*, *SMARCA4*, *ZNF340* (2, 11, 12). However, their role in leukemogenesis was not established (2, 12). We have now demonstrated that *MYB-TYK2* harboring cells cause the onset of leukemia in mice and are sensitive to cerdulatinib treatment *in vitro* and *in vivo* (14). In this current study, we generated cerdulatinib-resistant *MYB-TYK2*-rearranged B-ALL cells in order to recapitulate the potential clinical scenario. We identified a novel *TYK2* kinase domain mutation that developed in response to JAKi (cerdulatinib) treatment. Cerdulatinib-resistant *MYB-TYK2*-rearranged cells also demonstrated hyperactive JAK/STAT signaling. Importantly, we demonstrated sensitivity to alternative therapeutics that may be used in the clinic should a patient develop resistance to cerdulatinib, providing evidence for a precision medicine approach in the treatment of these high-risk patients.

Methods:

Cell line generation and culture. Ba/F3-*MYB-TYK2* cells were generated by retroviral transduction of parental Ba/F3 pro-B cells with a plasmid construct containing the *MYB-TYK2* fusion gene isolated from an ALL patient as described previously (14). Cells were maintained in normal media: RPMI1640 medium (Sigma-Aldrich, CAT#R0883) supplemented with 10% Fetal Calf Serum (FCS, CellSera, BATCH#F21701), 2 mM L-glutamine (Sigma-Aldrich, CAT#G7513) and 1% (v/v) penicillin/streptomycin (Sigma-Aldrich, CAT#P4333). The cerd^{res} Ba/F3-*MYB-TYK2* cells were generated by gradual exposure of cells to increasing concentrations of cerdulatinib to 3 μM for a period of 144-151 days. This

concentration is equivalent to 3-1.5x the clinically achievable plasma levels of 1-2 μM (34, 35) and 3.7x the half maximal inhibitory concentration (IC_{50}) of cerdulatinib naïve Ba/F3-*MYB-TYK2* in *in vitro* proliferation assay (14). The $cerd^{res}$ Ba/F3-*MYB-TYK2* cells were grown in the presence of 3 μM cerdulatinib at all times. Control Ba/F3-*MYB-TYK2* cells were maintained in parallel and cultured in media containing vehicle (dimethyl sulfoxide, DMSO). For all luminescence and flow drug treatment assays, resistant and control cells were washed three times via centrifugation and incubated in inhibitor-free media at least 1 h prior to set up. For re-sensitization experiments, cerdulatinib was completely withdrawn by thorough washout (3x centrifugation and resuspension in normal media) from the media and cells were cultured in cerdulatinib free media for a period of 5 weeks.

Compounds. Cerdulatinib (CAT# S7634), vorinostat (CAT#S1047), panobinostat (CAT# S1030) and tanespimycin (17-AAG, CAT#S1141) were purchased from Selleckchem. For use, 10 mM inhibitor stocks were diluted in DMSO prior to use. Dilutions were prepared so that the final concentration of DMSO was 0.2% in culture media and assays at all times.

Statistical Analysis. All statistical analyses were performed in GraphPad Prism v8 (GraphPad Software, Inc). Paired and un-paired student's t-test were performed for collected data as indicated and $p<0.05$ was considered statistically significant. The IC_{50} values were calculated by non-linear regression.

Supplementary methods

Detailed methods undertaken for this study are provided in the supplemental appendices.

Results:

Prolonged exposure of *MYB-TYK2*-rearranged B-ALL cells to cerdulatinib induced drug resistance while maintaining proliferation suppression

To investigate potential mechanisms of JAKi resistance in *TYK2*-rearranged B-ALL, Ba/F3-*MYB-TYK2* cells were treated with increasing concentrations of cerdulatinib over a period of 151 days. Cerdulatinib-exposed Ba/F3-*MYB-TYK2* cells (cerd^{res} Ba/F3-*MYB-TYK2*) survived and proliferated in cerdulatinib concentrations sufficient for growth inhibition and death of control cells. Cerd^{res} Ba/F3-*MYB-TYK2* cells exhibited an 8.7-fold increase in IC_{50} compared to control cells (IC_{50}=6508 vs 739 nM, p=0.001; Figure 1A). The resistant cells demonstrated 3.3- and 2.4-fold decrease in Annexin V positivity compared to control cells, when exposed to high micromolar concentrations of cerdulatinib (% Annexin V positivity=21% vs 69%, p=0.0003 and 30% vs 74%, p=0.00006; 6 and 8 μM respectively; Figure 1B). Interestingly, following prolonged TYK2 inhibition in the cerd^{res} Ba/F3-MYB-TYK2 cells, the growth rate was reduced resulting in lower numbers of leukemic cells proliferating compared with control (Figure 1C). This lowered proliferation capacity in the cerd^{res} Ba/F3-*MYB-TYK2* cells was further validated with additional cell cycle analysis via CellTrace Violet, indicating a significant reduction in number of cell division cycles in resistant cells compared with control (cell cycles=9 vs 13, p=0.002; Figure 1D). Of note, previous studies reported the transient accumulation of histone modifications (acetylation and/or methylation) in cancer cells to enable survival in response to drug exposure (36-38). Indeed, cerd^{res} Ba/F3-*MYB-TYK2* cells displayed elevated levels of tri-methylation of lysine 27 on H3 (H3K27me3) compared with control cells (MFI=1.1 vs 1.6, p=0.02, Supplementary Figure 1A). No change in the level of acetylation of lysine 9 on H3 (H3K9ac) was detected (Supplementary Figure 1A).

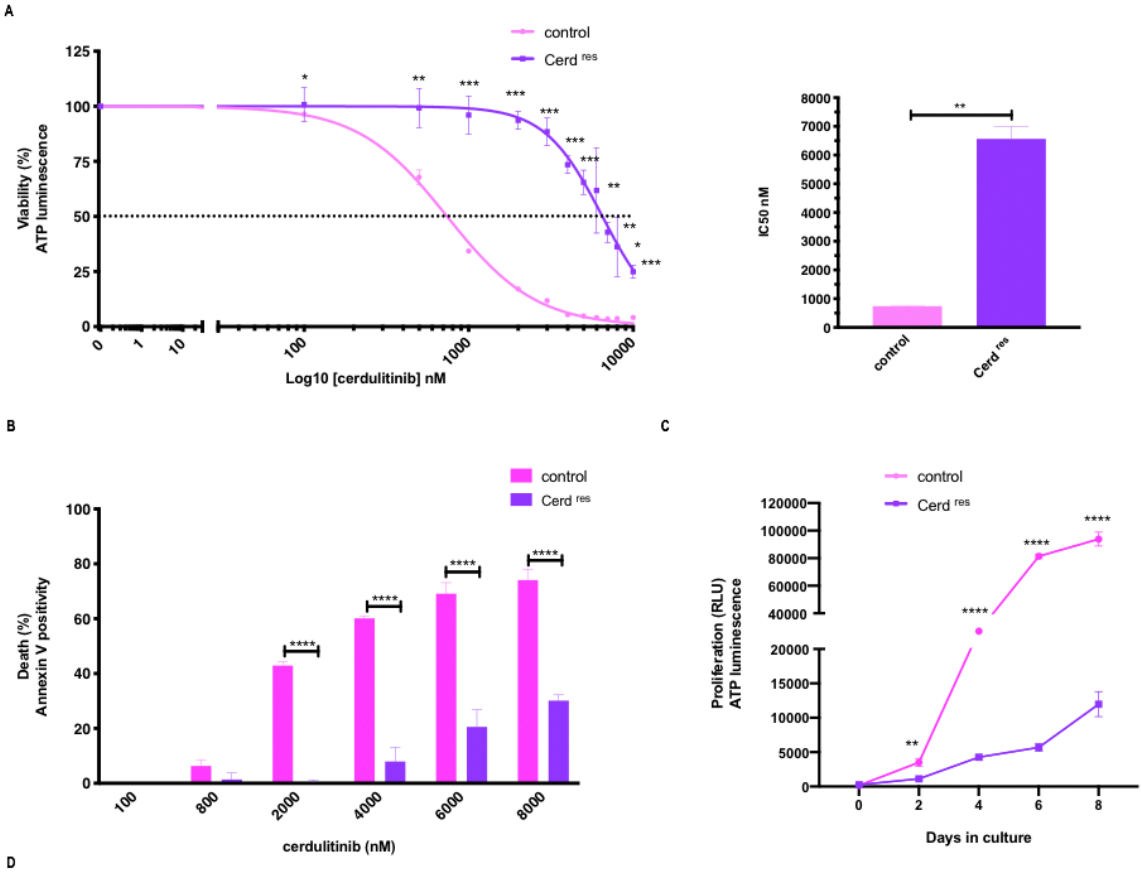

Cell Lines	Number of peaks (n=3)	Average number of cell cycles
Cerd^{res}	10	9
	9	
	9	
Control	12	13
	13	
	13	

Figure 1. Prolonged cerdulatinib exposure rendered Ba/F3-*MYB-TYK2* cells insensitive to treatment. (A) Viability analysis of cerd^{res} Ba/F3-*MYB-TYK2* and control cells cultured in the presence of the indicated concentrations of cerdulatinib for 48 h. Viability was calculated relative to no drug control for each line. IC_{50} values for cerdulatinib as indicated in the right panel. (B) Cell death analysis. Cerd^{res} Ba/F3-*MYB-TYK2* and control cells were cultured in presence of different cerdulatinib concentrations. After 48 h, cells were stained and assessed for percentage Annexin V positivity via f flow cytometric analyses. Values are normalized to no drug control for each line. (C) Proliferation levels of cerd^{res} Ba/F3-*MYB-TYK2* cells compared with control, monitored in 2-day intervals. CellTiter Glo assay luminescence readout is proportional to number of viable cells with day 0 background values deducted from each day's corresponding readout values. (D) Daily cell cycle analysis of Cerd^{res} Ba/F3-*MYB-TYK2* and control cells for the duration of 4 days. Cell were stained with CellTrace violet. The peaks, indicated by black arrows, in the histograms are representative of successive generations of live cells. All statistical analyses were measured by un-paired student's t-test. All indicated error bars represent mean ±SD (n=3). Abbreviation: RLU, relative luminescence unit. *p<0.05, **p<0.01, ***p<0.001, ****p < 0.0001.

Mutation of the TYK2 kinase domain does not confer resistance to cerdulatinib in *MYB-TYK2* driven cells

Mutations in the kinase domain of JAK tyrosine kinases are suggested to be the most common route of resistance in patients receiving JAKi therapy (20, 27-29). To assess whether resistance to cerdulatinib in the setting of *TYK2* alteration occurs due to mutation, Sanger sequencing was performed over the full length *MYB-TYK2* fusion gene. The presence of a novel mutation was discovered in the kinase domain of *TYK2* (p.R987Q, c.3338G>A) in approximately 60% of cerd^{res} Ba/F3-*MYB-TYK2* cells. However, *de novo* introduction of *MYB-TYK2* p.R987Q into the parental Ba/F3 cells (Ba/F3-*MYB-TYK2*$^{p.R987Q}$) did not render the cells resistant to cerdulatinib with these cells displaying similar drug tolerability compared with control (IC_{50}=1200 vs 739nM, p>0.05; Figure 2A) and significantly decreased IC_{50} compared with cerd^{res} Ba/F3-*MYB-TYK2* (IC_{50}=1200 vs 6505, p=0.0001). Additionally, expression of the p.R987Q mutation did not alter the proliferation rate of Ba/F3-*MYB-TYK2*$^{p.R987Q}$ cells compared to control (Supplementary Figure 2A). Computational modeling demonstrated that the substitution of arginine for glutamine in the TYK2 p.R987Q protein resulted in 180º reversal of cerdulatinib binding in the ATP binding pocket of the

mutated kinase (Figure 2B and Supplementary Figure 2B). While, the mutation does not inhibit drug binding, the modeling indicates less favorable binding of cerdulatinib to mutated TYK2 (TYK2 p.R987Q vs TYK2, binding score= -18.6 vs -23.4) validating the slight increase in the IC_{50} observed in these cells compared with control cells (Figure 2A). An accumulation of cerd^{res} Ba/F3-*MYB-TYK2* cells carrying the TYK2 p.R9887Q mutation over the period of exposure to different cerdulatinib concentrations was detected that decreased upon cerdulatinib withdrawal (Supplementary Figure 2C and D). This suggests that the generation of kinase domain mutations may act as a reversible and initial resistance mechanism *in vitro* but are not sufficient to confer robust resistance alone.

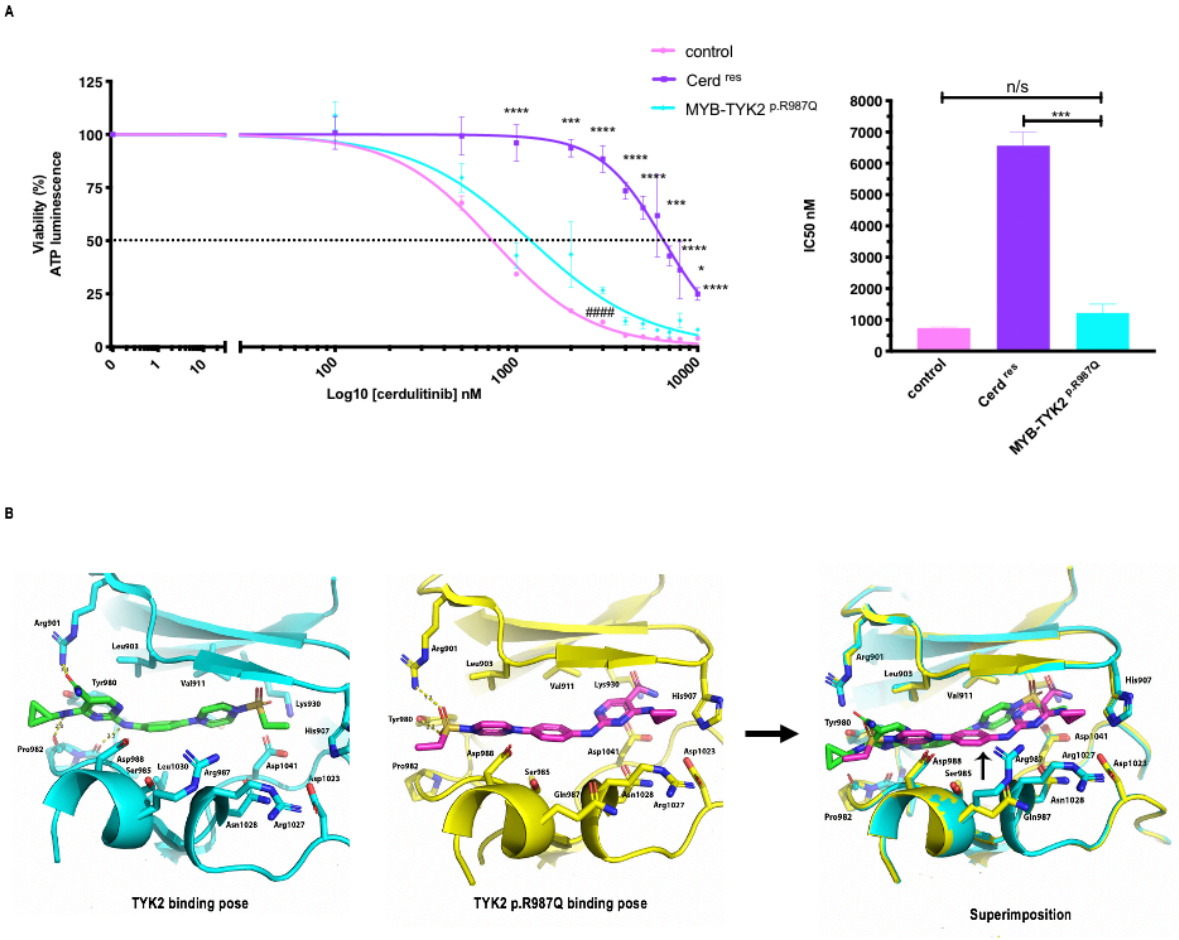

Protein	Score	VLS Score	Strain	Steric	Torsion	Electro	H bond	Hyrdoph	Surface
TYK2	-23.45	-36.67	13.21	-37.89	3	4.457	-4.278	-6.287	15.36
TYK2 p.R987Q	-18.67	-26.42	7.756	-40.6	3	15	-2.151	-6.639	16.49

Figure 2. The p.R987Q point mutation in TYK2 kinase domain is not sufficient to confer resistance to cerdulatinib. (A) Viability analysis of cerd^{res} Ba/F3-*MYB-TYK2*, Ba/F3-*MYB-TYK2*$^{p.R987Q}$ and control cells cultured in the presence of increasing concentrations of cerdulatinib for 48 h. Viability was calculated relative to no drug control for each line. IC_{50} values for cerdulatinib as indicated in the right panel. (B) Computational modeling indicating the binding orientation and affinity of cerdulatinib in the kinase domain of wild type TYK2 and TYK2 p.R987Q proteins. All interactions were measured by un-paired student's t-test. (*) indicates Cerd^{res} Ba/F3-*MYB-TYK2* vs Ba/F3-*MYB-TYK2*$^{p.R987Q}$; (#) indicates Ba/F3-*MYB-TYK2*$^{p.R987Q}$ vs control. All indicated error bars represent mean ±SD of 3 biological replicates. *p<0.05, ***p < 0.001. ****p< 0.0001. Abbreviation: n/s, not significant.

MYB-TYK2-rearranged cells developed constitutive activation of JAK/STAT signaling in response to long-term cerdulatinib exposure

Given the inability of the p.R987Q kinase domain mutation alone to confer resistance in Ba/F3-*MYB-TYK2* cells, combined with the persistent growth of cerd^{res} Ba/F3-*MYB-TYK2* cells in presence of cerdulatinib, it was necessary to investigate additional resistance mechanisms. Activation of proteins in key signaling pathways were evaluated by flow cytometric analyses in cerd^{res} Ba/F3-*MYB-TYK2* cells. Phosphoflow analysis indicated increased JAK/STAT signaling via hyperactivation of STAT5 in cerd^{res} Ba/F3-*MYB-TYK2* cells compared with control cells (MFI=324 vs 202, p=0.003; Figure 3A). No statistical difference was detected in pSTAT3 (MFI= 305 vs 261; p>0.05; Figure 3A) between cerd^{res} Ba/F3-*MYB-TYK2* cells and control cells. There was a reduced pERK expression (RAS pathway; cerd^{res} Ba/F3-*MYB-TYK2* vs control, MFI= 26 vs 54, p=0.001; Supplementary Figure 3) in resistant cells whilst no activation of PI3K/mTOR activation or B-cell receptor signaling was evident in control or cerd^{res} Ba/F3-*MYB-TYK2* cells (Supplementary Figure 3).

JAK/STAT signaling was sustained in cerd^{res} Ba/F3-*MYB-TYK2* cells following treatment with a clinically relevant concentration of cerdulatinib (1 μM) (pSTAT5, vehicle vs cerdulatinib-treated MFI=45 vs 37, p>0.05; pSTAT3, vehicle vs cerdulatinib-treated 13 vs 9, p>0.05). Conversely, 1 μM cerdulatinib was

sufficient to attenuate pSTAT5 and pSTAT3 signaling in control cells (pSTAT5, vehicle vs cerdulatinib treated, MFI= 31 vs 12, p=0.001; pSTAT3, vehicle vs cerdulatinib treated MFI=10 vs 0, p=0.02, Figure 3B&C). The decrease observed in the level of JAK/STAT signaling in cerd^{res} Ba/F3-*MYB-TYK2* cells upon treatment with a higher cerdulatinib concentration (3 μM) was expected due to the retained ability of drug to bind and slow MYB-TYK2 downstream signaling. This was despite the cells' capacity to bypass the effect of drug, predominantly via persistent STAT5 activation.

Cerd^{res} Ba/F3-*MYB-TYK2* cells as well as control cells demonstrated sensitivity against CDDO-Im, an inhibitor of STAT5/3 (39, 40) (IC50= 81 vs 61, respectively; p>0.05; Supplementary Figure 4A). Interestingly, pharmacological inhibition of STAT5 and 3 with concentrations of CDDO-Im, as low as 10 and 80 nM, resulted in an increased proliferation inhibition of cerd^{res} Ba/F3-*MYB-TYK2* cells compared to non-CDDO-Im treated cells when exposed to increasing concentrations of cerdulatinib (Supplementary Figure 4B). The basal (10 and/or 80 nM) CDDO-Im treatment in combination with cerdulatinib resulted in a 1.2- and 4.9- fold decrease in IC50 of cerd^{res} Ba/F3-*MYB-TYK2* cells, respectively (non- vs 10 nM or 80 nM CDDO-Im-treated cells, IC50= 6804 vs 5541, p>0.05 or vs 131, p=0.0006; Supplementary Figure 4C); lowering the IC50 of cerd^{res} Ba/F3-*MYB-TYK2* cells to levels exhibited by control cells. This data further validated the increased JAK/STAT signalling via STAT5 as a resistance mechanism.

Western blot analysis confirmed hyperphosphorylation of the MYB-TYK2 fusion protein in cerd^{res} Ba/F3-*MYB-TYK2* cells in comparison to control cells (p=0.01; Figure 3D&E). Despite the recent evidence defining the accumulation of activation-loop phosphorylation in JAK family members upon type I JAKi exposure (41, 42), increased pTYK2 was also detected in drug naïve Ba/F3-*MYB-TYK2*$^{p.R987Q}$ (p>0.05; Supplementary Figure 5A). However, the persistent STAT5 activation detected in cerd^{res} Ba/F3-*MYB-TYK2* cells was not due to expression of p.R987Q mutation since there was no difference in pSTAT5 expression in control vs Ba/F3-*MYB-TYK2*$^{p.R987Q}$ (p>0.05; Supplementary Figure 5B). Given that previous

studies demonstrated TYK2 signaling via heterodimer formation with other JAK family proteins (i.e. JAK1, JAK2 and JAK3) in response to various cytokines (43-48) the persistence mechanism detected here may be associated with trans-phosphorylation of MYB-TYK2 via other JAKs. To investigate this phenomenon further, JAK1/2 expression levels in cerd^{res} Ba/F3-*MYB-TYK2* cells were determined (Figure 3D). Interestingly, a JAK1 expression was significantly increased in the cerd^{res}Ba/F3-*MYB-TYK2* cells compared with control (p=0.0008; Figure 3E). This association of elevated JAK1 with the MYB-TYK2 fusion protein was only detectable in cerd^{res}Ba/F3-*MYB-TYK2* cells and not the inhibitor naïve Ba/F3-*MYB-TYK2*$^{p.R987Q}$ cells (Supplementary Figure 5A). No significant difference in the level of JAK2 expression (Figure 3D), and no JAK3 expression (data not shown), was detected in cerd^{res}Ba/F3-*MYB-TYK2* cells.

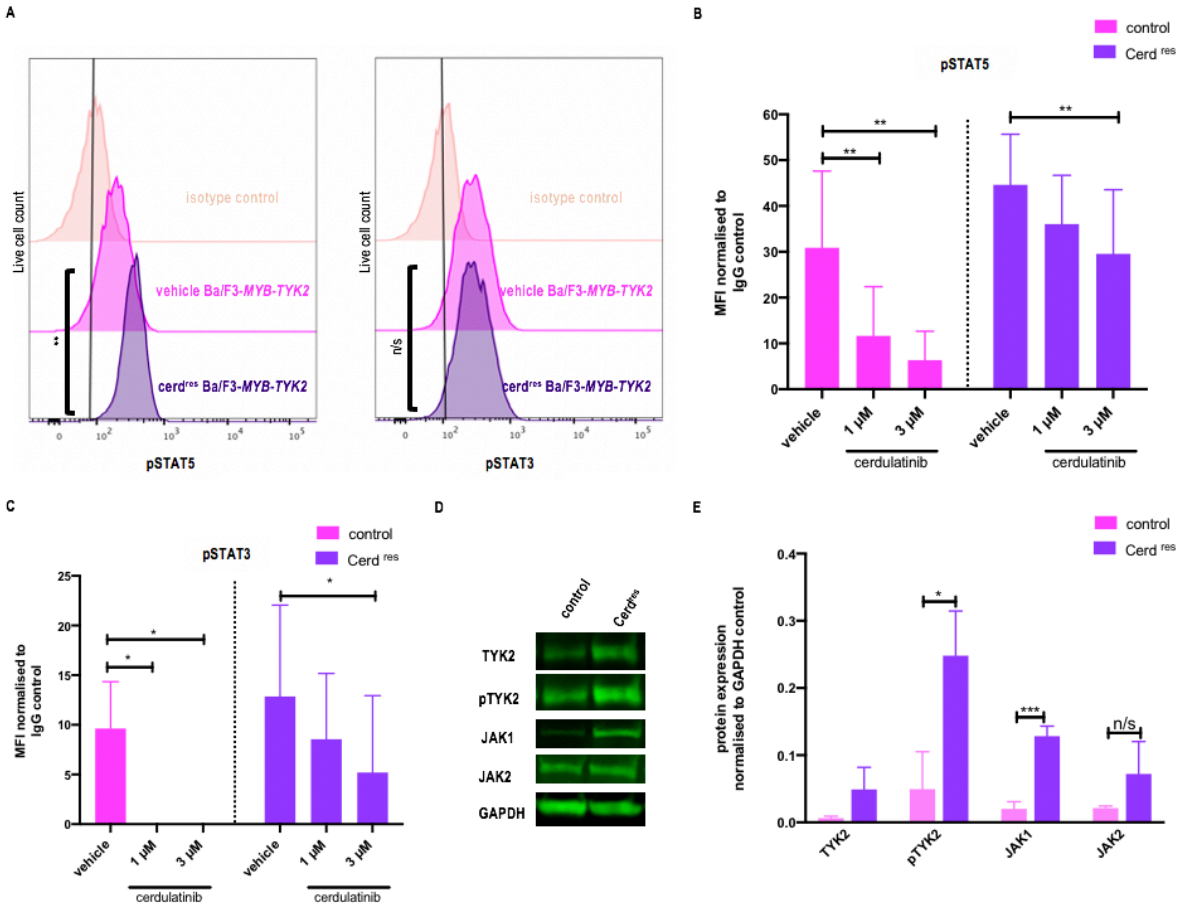

Figure 3. Persistent activation of the JAK/STAT signaling pathway via association with JAK1 promotes development of cerdulatinib resistance in Ba/F3-*MYB-TYK2* cells. (A) Representative histograms of flow cytometric analyses for pSTAT5 and pSTAT3 investigating JAK/STAT signaling activation in cerdulatinib resistant cells vs controls. Expression levels of (B) pSTAT5 and (C) pSTAT3 in cerd^{res} Ba/F3-*MYB-TYK2* and control cells when treated with indicated cerdulatinib concentrations and vehicle for 1 h prior to fixation. P-values were calculated by paired student's t-test. Negative MFI values following normalization were considered as zero. (D) Representative western blotting for cerd^{res} Ba/F3-*MYB-TYK2* and control cells when probed for TYK2, pTYK2 (Y1054/1055), JAK1, JAK2 and GAPDH loading control. (E) Relative expression of pTYK2, total TYK2, JAK2 and JAK1 in cerd^{res} Ba/F3-*MYB-TYK2* compared with control cells. P-values were calculated by un-paired student's t-test. All indicated error bars represent mean ±SD of at least 3 biological replicates. Abbreviation: MFI, mean fluorescence intensity. *p<0.05, **p<0.01, ***p<0.001.

Cerdulatinib withdrawal resulted in re-sensitization of cerd^{res} Ba/F3-*MYB-TYK2* cells to cerdulatinib treatment

In order to investigate reversibility of the persistent JAK/STAT signaling exhibited by cerd^{res} Ba/F3-*MYB-TYK2* cells, cerdulatinib was completely removed from the media, and cells were cultured for 5 weeks. Re-sensitized *MYB-TYK2*-rearranged cells (cerd^{resen} Ba/F3-*MYB-TYK2*) exhibited re-established sensitivity to cerdulatinib treatment as evidenced by dose dependent proliferation inhibition in comparison with cerd^{res} Ba/F3-*MYB-TYK2* cells (Figure 4A). Cerdulatinib treatment also resulted in attenuated pSTAT5 and pSTAT3 (vehicle vs cerdulatinib treated, MFI=258 vs 14, p=0.0002 and 92.5 vs 24.1, p=0.002; Figure 4B) in cerd^{resen} Ba/F3-*MYB-TYK2* cells. While Cerd withdrawal resulted in a significant decrease in IC_{50} (cerd^{res} vs cerd^{resen}, 6508 vs 2603 nM, p=0.0003; Supplementary Figure 6A), the IC_{50} did not decrease to that observed in control cells (cerd^{resen} vs control, 2603 vs 739nM, p=0.01; Supplementary Figure 6A). Instead, cerdulatinib withdrawal resulted in a significant reduction of H3K27me3 levels in cerd^{res} Ba/F3-*MYB-TYK2* cells (cerd^{res} vs cerd^{resen}, MFI=1.6 vs 1.2, p=0.04) back to levels comparable with that of control cells (Supplementary Figure 1A). Moreover, Cerdulatinib removal led to significantly decreased TYK2 phosphorylation levels (cerd^{res} vs cerd^{resen}, p=0.01; Supplementary Figure 5A) and a decrease in JAK1 levels (cerd^{res} vs cerd^{resen}, p=0.01, Supplementary Figure 5A).

Interestingly, JAK1 expression in cerd^{resen} Ba/F3-*MYB-TYK2* cells was still significantly increased compared with control cells (control vs cerd^{resen}, p=0.03) which may explain slightly higher IC_{50} values seen in re-sensitized cells.

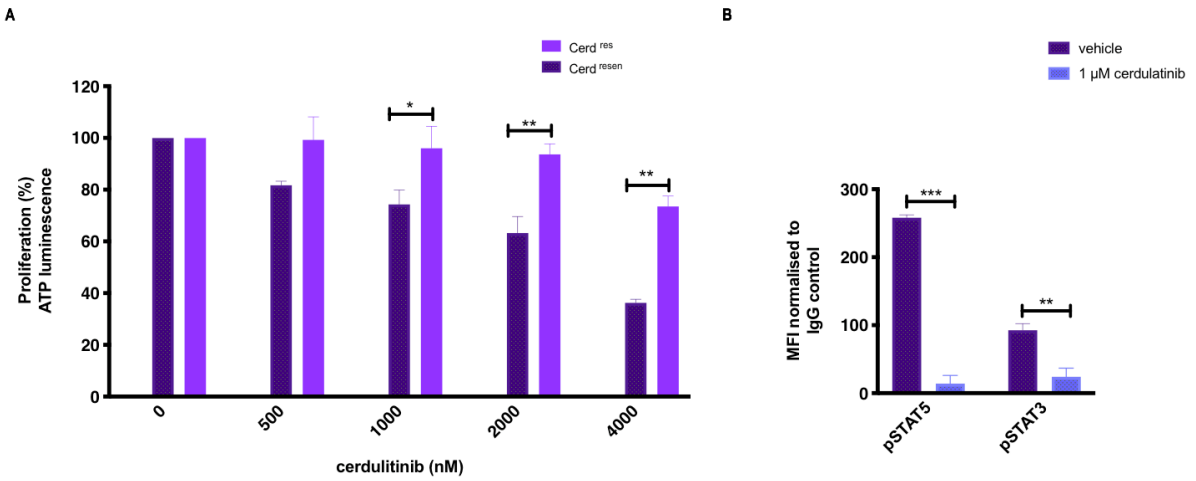

Figure 4. Cerdulatinib withdrawal results in re-sensitization of cerd^{res} Ba/F3-*MYB-TYK2* cells to treatment. (A) Percent viability of cerd^{res} Ba/F3-*MYB-TYK2* and cerd^{resen} Ba/F3-*MYB-TYK2* cells upon treatment with different cerdulatinib concentrations for 48 h. Viability was estimated relative to vehicle control via CellTiter Glo assay. (B) Flow cytometric analysis of cerd^{resen} Ba/F3-*MYB-TYK2* treated with vehicle or 1 μM cerdulatinib for a duration of 1 h. Negative MFI values following normalization were considered as zero. All indicated error bars represent mean ±SD of 3 separate experiments.

Cerdulatinib resistant *MYB-TYK2*-rearranged cells can be effectively targeted by HDACi

Since these data indicated JAKi resistance occurs in the setting of *TYK2*-rearranged ALL, it was necessary to identify alternative therapeutic approaches to target and reverse the constitutive JAK/STAT signaling in cerd^{res} Ba/F3-*MYB-TYK2*. We have recently demonstrated sensitivity of parental Ba/F3-*MYB-TYK2* cells to HSP90 and histone deacetylases (HDAC) inhibition in *in vitro* and/or pre-clinical models of *MYB-TYK2* disease (14). Elevated levels of histone acetylation due to expression of the *MYB-TYK2* oncogene (14) signified a potential epigenetic target for treatment with HDACi, further supported by our high throughput drug screening indicating HDACi as the most predominant class of inhibitors effective

against Ba/F3-*MYB-TYK2* cells. In addition, the reported ability of HSP90i to overcome JAKi resistance (27, 30) prompted further assessment of these small molecule inhibitors (SMIs) in our current model. *MYB-TYK2*-rearranged resistant cells exhibited cross-resistance to HSP90 inhibition by tanespimycin. Tanespimycin treatment failed to inhibit growth and decrease pSTAT5 levels in cerd^{res} Ba/F3-*MYB-TYK2* while the control cells retained sensitivity (Supplementary Figure 7A and B). However, no changes in the expression level of HSP90 protein were detected in cerd^{res} Ba/F3-*MYB-TYK2* cells compared with controls (Supplementary Figure 7C). This cross-resistance to HSP90i may be due to overactivation of JAK/STAT signaling in cerd^{res} Ba/F3-*MYB-TYK2* cells. Intriguingly, cerdulatinib resistant cells maintained sensitivity to histone deacetylase inhibitors (HDACi). Vorinostat and panobinostat demonstrated equal efficacy against cerd^{res} Ba/F3-*MYB-TYK2* and control cells, inhibiting growth within clinically relevant ranges (cerdulatinib resistant vs control, IC_{50}=513 and 45 nM vs 530 and 61, vorinostat and panobinostat, respectively, Figure 5A). Similar sensitivity to HDACi treatment was observed in cerd^{resen} Ba/F3-*MYB-TYK2* cells (IC50=478 nM, Supplementary Figure 6B). Efficient inhibition of STAT5 activation in response to HDACi treatment (i.e. vorinostat) was subsequently confirmed in cerd^{res} Ba/F3-*MYB-TYK2* (p=0.01; Figure 5B). Notably, vorinostat treatment resulted in increased acetylation levels of H3 measured by the H3K9ac marker in cerd^{res} Ba/F3-*MYB-TYK2* and control cells (vehicle vs vorinostat treated, MFI= 0.7 vs 1.4, p=0.002 and MFI= 0.7 vs 1.1, p=0.004, respectively; Supplementary Figure 1B). A similar trend was observed for methylation levels of H3, marked by H3K27me3 (vehicle vs vorinostat treated, MFI=1.6 vs 1.8, p>0.05 and MFI=1.1 vs 1.3, p=0.04, respectively; Supplementary Figure 1B).

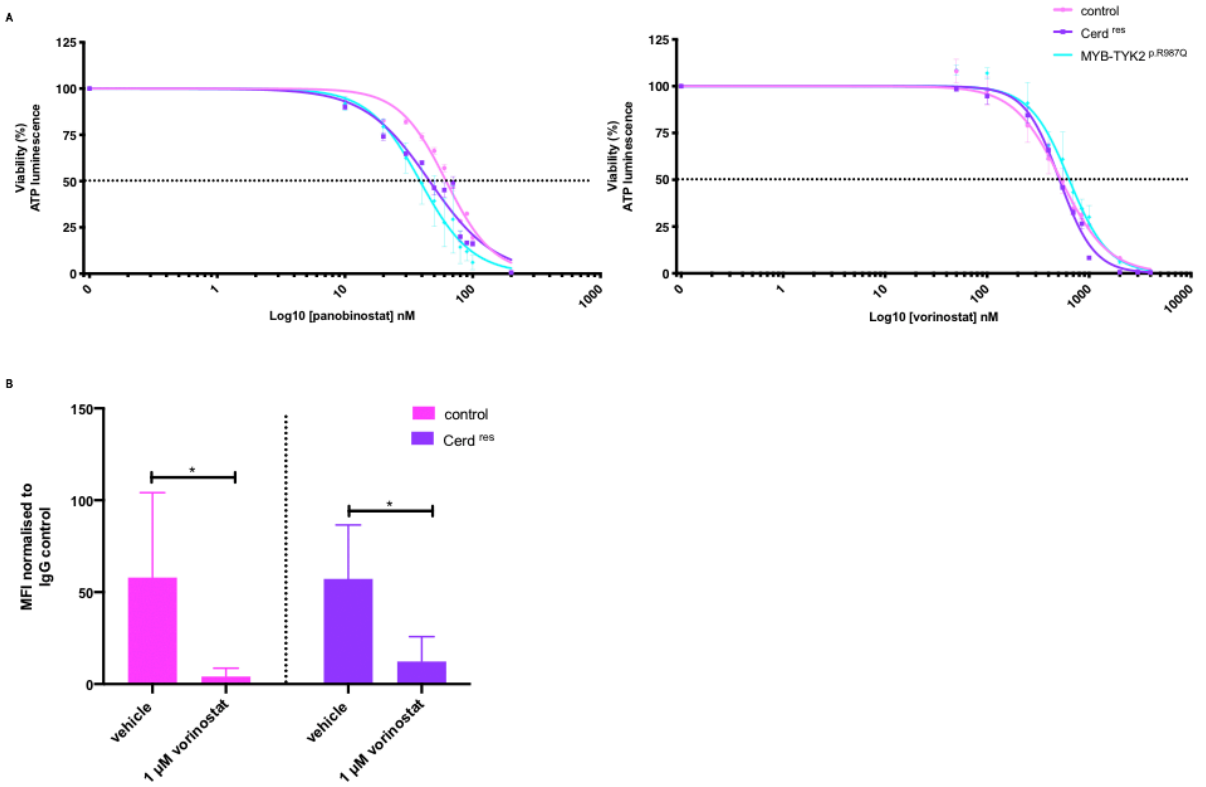

Figure 5. HDACi treatment inhibits growth and attenuates JAK/STAT signaling in cerd^{res} Ba/F3-*MYB-TYK2* cells. (A) Dose response curve of cerd^{res} Ba/F3-*MYB-TYK2,* Ba/F3-*MYB-TYK2*$^{p.R987Q}$ and control cells treated with increasing concentrations of vorinostat and panobinostat for 48 h. Viability was estimated relative to vehicle control of each line. (B) pSTAT5 levels in cerd^{res} Ba/F3-*MYB-TYK2* and control cells when incubated in the presence of 1 µM vorinostat for 1 h. All interactions were measured by paired student's t-test. Negative MFI values following normalization were considered as zero. All indicated error bars represent mean ±SD of at least 3 biological replicates. *p<0.05.

Discussion:

Identification of rearrangements that lead to constitutively active *TYK2* in HR-ALL cases (2, 11) and their driving oncogenic potential (14), highlight TYK2 as a promising therapeutic target and rationalize the use of JAKi with TYK2 specificity in these cases. Although, there is no doubt that the use of JAKi such as ruxolitinib offers improved outcomes for MPN patients, the lengthy treatment has become a clinical concern due to loss of sensitivity and relapse in half of JAKi-treated patients (21-23). Hence, it is critical to elucidate the relevance of acquired resistance to JAKi therapy in B-ALL, specifically the cases with *TYK2*-rearranged disease.

Despite the variability of 5' partner genes reported in *TYK2* rearrangements, they mostly harbor DNA binding domain and facilitate dimerization of TYK2 protein (2, 12). Whilst TYK2 retains an intact kinase domain resulting in constitutive activity of the fusion protein (2, 12). This study, for the first time, recapitulated the possible JAKi resistance scenarios in *TYK2*-rearranged B-ALL via long-term exposure of Ba/F3 cells expressing the *MYB-TYK2* fusion gene to the SYK/JAK inhibitor, cerdulatinib. Considering the high level of homology between the kinase domain (also known as JH1) of JAK family proteins and the drug binding pocket (49, 50), including TYK2, parallel JAKi resistance mechanisms may also be applicable to other JAK family proteins. Initially, a TYK2 p.R987Q kinase domain mutation was detected in more than 50% of clones that had a negligible effect on the drug binding affinity. However, *de novo* modeling of the mutation suggests the unlikelihood of it being responsible for resistance (Figure 2). Although, our finding is in contrast with previous studies (27-29) that suggest an important role for secondary JAK2 kinase domain mutations in conferring resistance to JAKi. These studies report that JAK2 kinase domain mutations induce conformational changes weakening/reducing drug binding. It is critical to note that the reported mutations were randomly mutagenized into cells already harboring JAK2 p.V617F or p.R683G and did not develop under long-term pharmacological inhibition of the protein. Moreover, there have been no reports of secondary mutations developing in the JAK2 kinase domain in any of the MPN patients who develop resistance to ruxolitinib (23). This is in agreement with our finding highlighting the insufficiency of TYK2 p.R987Q to confer overt resistance in isolation.

The *MYB-TYK2* fusion gene (Supplementary Figure 8) has an in-frame kinase domain and contains a disrupted pseudokinase domain (termed JH2), responsible for auto-inhibition of JAK kinase domain (12, 51, 52). In addition, this fusion, similarly to other *JAK* family fusions, lacks the FERM (four-point one, erzrin, radixin, moesin) and SH-like (Src-homology) domains, which are required for protein and cytokine receptor binding, respectively (52, 53). Previous studies have demonstrated the ability of type I JAKi to

induce accumulation of JAK activation-loop phosphorylation in MPN and B-ALL cases harboring a mutant JAK2 (i.e. JAK2 p.V617F or p.R683G, respectively), despite the suppression of downstream STATs activation (10, 27, 33, 41). However, a study by Andraos *et.al.* (2012), suggested this phenomenon was context based and dependent on 1) specific genomic alterations 2) the affected domain in JAKs (i.e. FERM, JH1 or JH2 domains) and 3) receptor complex interactions (42). For instance, cells harboring the *ETV6-JAK2* fusion gene displayed no augmented JAK2 phosphorylation due to ruxolitinib treatment. The ruxolitinib-induced activation-loop phosphorylation plausibly requires an interplay between JH1 and JH2 domains that is lacking in the ETV6-JAK2 fusion protein (42). It is also important to note that different JAK mutations may favor stabilization of the protein into active or inactive conformations (42, 54). Our current study highlights significant hyperphosphorylation of TYK2 in cerd^{res} Ba/F3-*MYB-TYK2* cells and minimally enhanced phosphorylation of TYK2 in drug naïve Ba/F3-*MYB-TYK2*$^{p.R987Q}$ cells (Figure 3 and Supplementary Figure 5) suggesting that the *TYK2* p.R987Q mutation may favor the active conformation of the kinase, although this requires further investigation.

Intriguingly, chronic suppression of TYK2 activity by cerdulatinib in cells expressing the *MYB-TYK2* fusion gene reduced the proliferative capability of these oncogenic cells (Figure 1C and D), leading to persistent JAK/STAT signaling via transphosphorylation of MYB-TYK2 by JAK1 (Figure 3). This suggests co-operation between JAK1 and MYB-TYK2 as the primary resistance mechanism in this model of *TYK2*-rearranged disease. This persistent signaling and cerdulatinib-insensitivity occurred via a reversible mechanism since drug withdrawal re-sensitized cells (Figure 4). This drug-mediated pressure resulting in persistent JAK/STAT signaling through alternate heterodimerization with JAKs and its reversibility have been reported as a mode of JAKi resistance in previous studies in MPN patients on long term ruxolitinib treatment (20, 30, 31). Whilst, there is no report of changes in the proliferation rate of JAKi-resistant cells in the MPN setting (30, 31), CRLF2-rearranged/*JAK2* p.R683G mutant B-ALL cells proliferated more slowly, with lower numbers of leukemic cells entering the cell cycle, despite no evidence of persistent

JAK/STAT signaling upon prolonged JAKi exposure (33). These discrepancies may be explained by the initial/intrinsic level of JAKi sensitivity of the different cells used in each study. *JAK2* p.V617F MPN cells exhibit more rapid ruxolitinib-suppressed growth as opposed to CRLF2/*JAK2* p.R683G cells (33, 55, 56) and are thus more prone to exhibit overt resistance as opposed to acquiring an adoptive bypass/persistence mechanism. *MYB-TYK2*-rearranged cells in our current study appear to also display these previously reported mechanisms of JAKi resistance as well as the novel *TYK2* p.R987Q point mutation.

Several studies have suggested that dynamic but transient epigenetic modifications may play a role in adaptability of sub populations of cells to stress induced by drug exposure in addition to activation of signalling cascades (36, 37, 57). Investigation of global histone modification in this model displayed a significant increase in H3K37me3 levels in resistant cells while H3K9ac marker remained unchanged (Supplementary Figure 1A). The increased H3K27me3 levels has previously been associated with multi-drug resistance in solid cancers (36). In line with a previous study by Sreenath *et al* (2010) (37), the methylation mark was reversed upon cerdulatinib withdrawal implicating transient acquisition of epigenetic modifications as a strategy for drug tolerance. In addition, the high level of repressive H3K27me3 observed in cerdulatinib resistant cells may also explain the lower proliferative capacity detected (Figure 1C); resistant cells likely conserved energy by repressing genes responsible for cell cycle division. However, further validation of this hypothesis is required and is outside the scope of this study.

The data presented here suggest that JAKi resistance can occur in the setting of *TYK2*-rearranged ALL. The TYK2 protein (similar to its JAK family counterparts) is a client of heat shock (HSP) proteins (58-60). Furthermore, HSP90 function is regulated by several proteins and co-chaperons. Acetylation of lysine residues on HSP90 is a negative regulatory mechanism that leads to aggregation of client proteins such

as JAKs (58, 61). Thus, HDAC proteins play an essential role in facilitating HSP90 activity (58, 61). Nevertheless, HDACs can also regulate STATs activity (58, 62). HDACs induce deacetylation of the transcription activation sites, essential for recruitment of transcription machinery (e.g. RNA polymerase II) and activation of STATs mediated transcription (62-69). Thus, HDACi may offer an attractive target for the JAK-mutated JAKi resistant cells as they circumvent the requirement for direct JAK protein targeting with JAKi. Targeting HSP90 chaperones and/or the HDAC family of proteins have proven effective in leukemias with activated JAK/STAT signaling (27, 70-73). These observations, plus the intrinsic sensitivity of Ba/F3-*MYB-TYK2* cells to HSP90 and HDAC inhibition (14), provide a rationale for the use of these small molecule inhibitors against JAKi-resistant cells. JAKi resistance induced cross-resistance to HSP90i in *MYB-TYK2*-rearranged cells (Supplementary Figure 7); although this observation was contradictory to previous reports demonstrating the sensitivity of JAKi resistant JAK2-driven cells to HSP90i due to induced protein degradation (27, 30). This may be explained by growing evidence suggesting JAK/STAT activation is a contributing mechanism of resistance to HSP90i (74, 75). The JAK/STAT-induced resistance to HSP90i is suggested to be reversed by JAKi therapy in solid tumors (75). However, this remains to be confirmed in our current model. Conversely, HDACi retain the ability to inhibit proliferation and attenuate the persistent signaling of *MYB-TYK2* resistant cells through inhibition of pSTAT5 and pSTAT3 (Figure 5). This is in line with increasing evidence that supports the functional role of HDACs in activation of gene transcription and signalling meditated by STATs (62-69). Studies(36, 76) have suggested vorinostat's anti-cancer effect acts via epigenetic modifications including: 1) increased acetylation 2) context dependent methylation regulation inducing transcription activation of tumour suppressor genes and repression of oncogenes. In our model, vorinostat increased global histone acetylation as well as methylation, in addition to reducing activation of STAT5 and STAT3. These dynamic changes in histone modifications and STATs, suggest activation and repression of genes that lead to proliferation inhibition and cell death. Moreover, efficacy of HDACi has been demonstrated in

hematological malignancies (65, 77) and JAK/STAT driven *in vitro* and *in vivo* models of ALL (72, 78) and are currently clinically available.

Taken together, we demonstrate that JAKi resistance can occur via constitutive but reversible JAK/STAT signaling as a result of TYK2 transphosphorylation via JAK1 in *TYK2*-rearranged ALL. We also characterize the novel *TYK2* p.R987Q kinase domain mutation. Importantly, the acquired resistance observed in our models was overcome by HDACi therapy. Our data indicate alternative targeted therapeutics and contribute to the growing body of evidence for precision medicine approaches. We provide a rationale for the use of HDACi therapy in JAKi exposed patients with *TYK2*-rearranged ALL and our findings warrant further investigation in preclinical models.

Acknowledgement:

Funding of this study was provided by NHMRC, Beat Cancer and LFA. PT was supported by an AGR University of Adelaide scholarship and Betty Hartmann Leukaemia Research Supplementary Scholarship. The *MYB-TYK2* fusion gene, isolated from an ALL patient, was a gift from Charles Mullighan, St. Jude Children's Research Hospital (Memphis, Tennessee, USA). Flow cytometry analysis was performed at the South Australian Health Medical Research Institute (SAHMRI) in the ACRF Cellular Imaging and Cytometry Core Facility. The Facility is generously supported by the Detmold Hoopman Group, Australian Cancer Research Foundation and Australian Government through the Zero Childhood Cancer Program.

Conflict of Interest:

Authors declare no conflict of interest in relation to the work described.

Contributions:

PT conceived the study, performed the experiments, analyzed the data and wrote the manuscript. EP helped in performing the experiments. LE, SH and DW supervised the research. JB performed the computational modeling. All authors critically read and revised the manuscript.

References:

1. Mullighan CG, Zhang J, Harvey RC, Collins-Underwood JR, Schulman BA, Phillips LA, et al. JAK mutations in high-risk childhood acute lymphoblastic leukemia. *Proc Natl Acad Sci U S A*. 2009;106(23):9414-8.

2. Roberts KG, Gu Z, Payne-Turner D, McCastlain K, Harvey RC, Chen IM, et al. High Frequency and Poor Outcome of Philadelphia Chromosome-Like Acute Lymphoblastic Leukemia in Adults. *J Clin Oncol*. 2017;35(4):394-401.

3. Roberts KG, Morin RD, Zhang J, Hirst M, Zhao Y, Su X, et al. Genetic alterations activating kinase and cytokine receptor signaling in high-risk acute lymphoblastic leukemia. *Cancer Cell*. 2012;22(2):153-66.

4. Heatley SL, Sadras T, Kok CH, Nievergall E, Quek K, Dang P, et al. High prevalence of relapse in children with Philadelphia-like acute lymphoblastic leukemia despite risk-adapted treatment. *Haematologica*. 2017;102(12):e490-e3.

5. Reshmi SC, Harvey RC, Roberts KG, Stonerock E, Smith A, Jenkins H, et al. Targetable kinase gene fusions in high-risk B-ALL: a study from the Children's Oncology Group. *Blood*. 2017;129(25):3352-61.

6. Maude SL, Dolai S, Delgado-Martin C, Vincent T, Robbins A, Selvanathan A, et al. Efficacy of JAK/STAT pathway inhibition in murine xenograft models of early T-cell precursor (ETP) acute lymphoblastic leukemia. *Blood*. 2015;125(11):1759-67.

7. Treanor LM, Zhou S, Janke L, Churchman ML, Ma Z, Lu T, et al. Interleukin-7 receptor mutants initiate early T cell precursor leukemia in murine thymocyte progenitors with multipotent potential. *J Exp Med*. 2014;211(4):701-13.

8. Maude SL, Tasian SK, Vincent T, Hall JW, Sheen C, Roberts KG, et al. Targeting JAK1/2 and mTOR in murine xenograft models of Ph-like acute lymphoblastic leukemia. *Blood*. 2012;120(17):3510-8.

9. Suryani S, Bracken LS, Harvey RC, Sia KC, Carol H, Chen IM, et al. Evaluation of the in vitro and in vivo efficacy of the JAK inhibitor AZD1480 against JAK-mutated acute lymphoblastic leukemia. *Mol Cancer Ther*. 2015;14(2):364-74.

10. Wu SC, Li LS, Kopp N, Montero J, Chapuy B, Yoda A, et al. Activity of the Type II JAK2 Inhibitor CHZ868 in B Cell Acute Lymphoblastic Leukemia. *Cancer Cell*. 2015;28(1):29-41.

11. Roberts KG, Yang YL, Payne-Turner D, Lin W, Files JK, Dickerson K, et al. Oncogenic role and therapeutic targeting of ABL-class and JAK-STAT activating kinase alterations in Ph-like ALL. *Blood Adv*. 2017;1(20):1657-71.

12. Roberts KG, Li Y, Payne-Turner D, Harvey RC, Yang YL, Pei D, et al. Targetable kinase-activating lesions in Ph-like acute lymphoblastic leukemia. *N Engl J Med*. 2014;371(11):1005-15.

13. Iacobucci I, Li Y, Roberts KG, Dobson SM, Kim JC, Payne-Turner D, et al. Truncating Erythropoietin Receptor Rearrangements in Acute Lymphoblastic Leukemia. *Cancer Cell*. 2016;29(2):186-200.

14. Tavakoli Shirazi P, Eadie LN, Heatley SL, François M, Hughes TP, Yeung DT, et al. Exploring the oncogenic and therapeutic target potential of the *MYB-TYK2* fusion gene in B-cell acute lymphoblastic leukemia

. *Oncogene* 2021;under revision.

15. Harrison C, Kiladjian JJ, Al-Ali HK, Gisslinger H, Waltzman R, Stalbovskaya V, et al. JAK inhibition with ruxolitinib versus best available therapy for myelofibrosis. *N Engl J Med*. 2012;366(9):787-98.

16. Verstovsek S, Kantarjian H, Mesa RA, Pardanani AD, Cortes-Franco J, Thomas DA, et al. Safety and efficacy of INCB018424, a JAK1 and JAK2 inhibitor, in myelofibrosis. *N Engl J Med*. 2010;363(12):1117-27.

17. Verstovsek S, Mesa RA, Gotlib J, Levy RS, Gupta V, DiPersio JF, et al. A double-blind, placebo-controlled trial of ruxolitinib for myelofibrosis. *N Engl J Med*. 2012;366(9):799-807.

18. Mascarenhas J, Hoffman R. Ruxolitinib: the first FDA approved therapy for the treatment of myelofibrosis. *Clin Cancer Res*. 2012;18(11):3008-14.

19. Harrison C, Vannucchi AM. Ruxolitinib: a potent and selective Janus kinase 1 and 2 inhibitor in patients with myelofibrosis. An update for clinicians. *Ther Adv Hematol*. 2012;3(6):341-54.

20. Meyer SC. Mechanisms of Resistance to JAK2 Inhibitors in Myeloproliferative Neoplasms. *Hematol Oncol Clin North Am*. 2017;31(4):627-42.

21. Verstovsek S, Mesa RA, Gotlib J, Levy RS, Gupta V, DiPersio JF, et al. Efficacy, safety, and survival with ruxolitinib in patients with myelofibrosis: results of a median 3-year follow-up of COMFORT-I. *Haematologica*. 2015;100(4):479-88.

22. Cervantes F, Vannucchi AM, Kiladjian JJ, Al-Ali HK, Sirulnik A, Stalbovskaya V, et al. Three-year efficacy, safety, and survival findings from COMFORT-II, a phase 3 study comparing ruxolitinib with best available therapy for myelofibrosis. *Blood*. 2013;122(25):4047-53.

23. Andreoli A, Verger E, Robin M, Raffoux E, Zini J-M, Rousselot P, et al. Clinical Resistance To Ruxolitinib Is More Frequent In Patients Without MPN-Associated Mutations and Is Rarely Due To Mutations In The JAK2 Kinase Drug-Binding Domain. *Blood*. 2013;122(21):1591-.

24. Pardanani A, Tefferi A. How I treat myelofibrosis after failure of JAK inhibitors. *Blood*. 2018;132(5):492-500.

25. Shanavas M, Popat U, Michaelis LC, Fauble V, McLornan D, Klisovic R, et al. Outcomes of Allogeneic Hematopoietic Cell Transplantation in Patients with Myelofibrosis with Prior Exposure to Janus Kinase 1/2 Inhibitors. *Biol Blood Marrow Transplant*. 2016;22(3):432-40.

26. Harrison CN, Schaap N, Mesa RA. Management of myelofibrosis after ruxolitinib failure. *Ann Hematol*. 2020;99(6):1177-91.

27. Weigert O, Lane AA, Bird L, Kopp N, Chapuy B, van Bodegom D, et al. Genetic resistance to JAK2 enzymatic inhibitors is overcome by HSP90 inhibition. *J Exp Med*. 2012;209(2):259-73.

28. Deshpande A, Reddy MM, Schade GO, Ray A, Chowdary TK, Griffin JD, et al. Kinase domain mutations confer resistance to novel inhibitors targeting JAK2V617F in myeloproliferative neoplasms. *Leukemia*. 2012;26(4):708-15.

29. Hornakova T, Springuel L, Devreux J, Dusa A, Constantinescu SN, Knoops L, et al. Oncogenic JAK1 and JAK2-activating mutations resistant to ATP-competitive inhibitors. *Haematologica*. 2011;96(6):845-53.

30. Koppikar P, Bhagwat N, Kilpivaara O, Manshouri T, Adli M, Hricik T, et al. Heterodimeric JAK-STAT activation as a mechanism of persistence to JAK2 inhibitor therapy. *Nature*. 2012;489(7414):155-9.

31. Meyer SC, Keller MD, Chiu S, Koppikar P, Guryanova OA, Rapaport F, et al. CHZ868, a Type II JAK2 Inhibitor, Reverses Type I JAK Inhibitor Persistence and Demonstrates Efficacy in Myeloproliferative Neoplasms. *Cancer Cell*. 2015;28(1):15-28.

32. Lim K-H, Chang Y-C, Chiang Y-H, Lin H-C, Huang L, Wang W-T, et al. Acquired Resistance to JAK Inhibitors in Calr-Mutated Myeloproliferative Neoplasms. *Blood*. 2019;134(Supplement_1):2970-.

33. Kim SK, Knight DA, Jones LR, Vervoort S, Ng AP, Seymour JF, et al. JAK2 is dispensable for maintenance of JAK2 mutant B-cell acute lymphoblastic leukemias. *Genes Dev*. 2018;32(11-12):849-64.

34. Flinn I, Patel MR, Wagner-Johnston ND, Pandey A, Coffey G, Leeds J, et al. Pharmacokinetics and pharmacodynamics of the dual syk/jak inhibitor PRT062070 (cerdulatinib) in patients with advanced B-cell malignancies. 2014;32(15_suppl):2619-.

35. Flinn I, Hamlin PA, Strickland DK, Pandey A, Birrell M, Coffey G, et al. Phase 1 open-label dose escalation study of the dual SYK/JAK inhibitor cerdulatinib (PRT062070) in patients with relapsed/refractory B-cell malignancies: Safety profile and clinical activity. *Journal of Clinical Oncology*. 2015;33(15_suppl):8531-.

36. Yang C, Zhang J, Ma Y, Wu C, Cui W, Wang L. Histone methyltransferase and drug resistance in cancers. *Journal of experimental & clinical cancer research : CR*. 2020;39(1):173.

37. Sharma SV, Lee DY, Li B, Quinlan MP, Takahashi F, Maheswaran S, et al. A chromatin-mediated reversible drug-tolerant state in cancer cell subpopulations. *Cell*. 2010;141(1):69-80.

38. Menon DR, Das S, Krepler C, Vultur A, Rinner B, Schauer S, et al. A stress-induced early innate response causes multidrug tolerance in melanoma. *Oncogene*. 2015;34(34):4545.

39. Brachet-Botineau M, Polomski M, Neubauer HA, Juen L, Hedou D, Viaud-Massuard MC, et al. Pharmacological Inhibition of Oncogenic STAT3 and STAT5 Signaling in Hematopoietic Cancers. *Cancers (Basel)*. 2020;12(1).

40. Liby K, Voong N, Williams CR, Risingsong R, Royce DB, Honda T, et al. The synthetic triterpenoid CDDO-Imidazolide suppresses STAT phosphorylation and induces apoptosis in myeloma and lung cancer cells. *Clin Cancer Res*. 2006;12(14 Pt 1):4288-93.

41. Tvorogov D, Thomas D, Liau NPD, Dottore M, Barry EF, Lathi M, et al. Accumulation of JAK activation loop phosphorylation is linked to type I JAK inhibitor withdrawal syndrome in myelofibrosis. *Sci Adv*. 2018;4(11):eaat3834.

42. Andraos R, Qian Z, Bonenfant D, Rubert J, Vangrevelinghe E, Scheufler C, et al. Modulation of activation-loop phosphorylation by JAK inhibitors is binding mode dependent. *Cancer Discov*. 2012;2(6):512-23.

43. Hammaren HM, Virtanen AT, Raivola J, Silvennoinen O. The regulation of JAKs in cytokine signaling and its breakdown in disease. *Cytokine*. 2019;118:48-63.

44. Ghoreschi K, Laurence A, O'Shea JJ. Janus kinases in immune cell signaling. *Immunol Rev*. 2009;228(1):273-87.

45. Bacon CM, McVicar DW, Ortaldo JR, Rees RC, O'Shea JJ, Johnston JA. Interleukin 12 (IL-12) induces tyrosine phosphorylation of JAK2 and TYK2: differential use of Janus family tyrosine kinases by IL-2 and IL-12. *J Exp Med*. 1995;181(1):399-404.

46. Velazquez L, Fellous M, Stark GR, Pellegrini S. A protein tyrosine kinase in the interferon alpha/beta signaling pathway. *Cell*. 1992;70(2):313-22.

47. Muller M, Briscoe J, Laxton C, Guschin D, Ziemiecki A, Silvennoinen O, et al. The protein tyrosine kinase JAK1 complements defects in interferon-alpha/beta and -gamma signal transduction. *Nature*. 1993;366(6451):129-35.

48. Leitner NR, Witalisz-Siepracka A, Strobl B, Muller M. Tyrosine kinase 2 - Surveillant of tumours and bona fide oncogene. *Cytokine*. 2017;89:209-18.

49. Vainchenker W, Leroy E, Gilles L, Marty C, Plo I, Constantinescu SN. JAK inhibitors for the treatment of myeloproliferative neoplasms and other disorders. *F1000Res*. 2018;7:82.

50. Gadina M, Johnson C, Schwartz D, Bonelli M, Hasni S, Kanno Y, et al. Translational and clinical advances in JAK-STAT biology: The present and future of jakinibs. *J Leukoc Biol*. 2018;104(3):499-514.

51. Poitras JL, Dal Cin P, Aster JC, Deangelo DJ, Morton CC. Novel SSBP2-JAK2 fusion gene resulting from a t(5;9)(q14.1;p24.1) in pre-B acute lymphocytic leukemia. *Genes Chromosomes Cancer*. 2008;47(10):884-9.

52. Ihle JN, Gilliland DG. Jak2: normal function and role in hematopoietic disorders. *Curr Opin Genet Dev*. 2007;17(1):8-14.

53. Valentino L, Pierre J. JAK/STAT signal transduction: regulators and implication in hematological malignancies. *Biochem Pharmacol*. 2006;71(6):713-21.

54. Ungureanu D, Wu J, Pekkala T, Niranjan Y, Young C, Jensen ON, et al. The pseudokinase domain of JAK2 is a dual-specificity protein kinase that negatively regulates cytokine signaling. *Nat Struct Mol Biol*. 2011;18(9):971-6.

55. Wernig G, Kharas MG, Okabe R, Moore SA, Leeman DS, Cullen DE, et al. Efficacy of TG101348, a selective JAK2 inhibitor, in treatment of a murine model of JAK2V617F-induced polycythemia vera. *Cancer Cell*. 2008;13(4):311-20.

56. Geron I, Abrahamsson AE, Barroga CF, Kavalerchik E, Gotlib J, Hood JD, et al. Selective inhibition of JAK2-driven erythroid differentiation of polycythemia vera progenitors. *Cancer Cell*. 2008;13(4):321-30.

57. Emran AA, Marzese DM, Menon DR, Hammerlindl H, Ahmed F, Richtig E, et al. Commonly integrated epigenetic modifications of differentially expressed genes lead to adaptive resistance in cancer. *Epigenomics*. 2019;11(7):732-7.

58. Prodromou C. Mechanisms of Hsp90 regulation. *Biochem J*. 2016;473(16):2439-52.

59. Taipale M, Krykbaeva I, Koeva M, Kayatekin C, Westover KD, Karras GI, et al. Quantitative analysis of HSP90-client interactions reveals principles of substrate recognition. *Cell*. 2012;150(5):987-1001.

60. Woss K, Simonovic N, Strobl B, Macho-Maschler S, Muller M. TYK2: An Upstream Kinase of STATs in Cancer. *Cancers (Basel)*. 2019;11(11).

61. Kramer OH, Mahboobi S, Sellmer A. Drugging the HDAC6-HSP90 interplay in malignant cells. *Trends Pharmacol Sci*. 2014;35(10):501-9.

62. Rascle A, Johnston JA, Amati B. Deacetylase activity is required for recruitment of the basal transcription machinery and transactivation by STAT5. *Mol Cell Biol*. 2003;23(12):4162-73.

63. Schindler C, Levy DE, Decker T. JAK-STAT signaling: from interferons to cytokines. *J Biol Chem*. 2007;282(28):20059-63.

64. Nusinzon I, Horvath CM. Unexpected roles for deacetylation in interferon- and cytokine-induced transcription. *J Interferon Cytokine Res*. 2005;25(12):745-8.

65. Buchwald M, Kramer OH, Heinzel T. HDACi--targets beyond chromatin. *Cancer Lett*. 2009;280(2):160-7.

66. Nusinzon I, Horvath CM. Interferon-stimulated transcription and innate antiviral immunity require deacetylase activity and histone deacetylase 1. *Proc Natl Acad Sci U S A*. 2003;100(25):14742-7.

67. Chang HM, Paulson M, Holko M, Rice CM, Williams BR, Marie I, et al. Induction of interferon-stimulated gene expression and antiviral responses require protein deacetylase activity. *Proc Natl Acad Sci U S A*. 2004;101(26):9578-83.

68. Sakamoto S, Potla R, Larner AC. Histone deacetylase activity is required to recruit RNA polymerase II to the promoters of selected interferon-stimulated early response genes. *J Biol Chem*. 2004;279(39):40362-7.

69. Klampfer L, Huang J, Swaby LA, Augenlicht L. Requirement of histone deacetylase activity for signaling by STAT1. *J Biol Chem*. 2004;279(29):30358-68.

70. Wang Y, Fiskus W, Chong DG, Buckley KM, Natarajan K, Rao R, et al. Cotreatment with panobinostat and JAK2 inhibitor TG101209 attenuates JAK2V617F levels and signaling and exerts synergistic cytotoxic effects against human myeloproliferative neoplastic cells. *Blood*. 2009;114(24):5024-33.

71. Guerini V, Barbui V, Spinelli O, Salvi A, Dellacasa C, Carobbio A, et al. The histone deacetylase inhibitor ITF2357 selectively targets cells bearing mutated JAK2(V617F). *Leukemia*. 2008;22(4):740-7.

72. Savino AM, Sarno J, Trentin L, Vieri M, Fazio G, Bardini M, et al. The histone deacetylase inhibitor givinostat (ITF2357) exhibits potent anti-tumor activity against CRLF2-rearranged BCP-ALL. *Leukemia*. 2017.

73. Akahane K, Sanda T, Mansour MR, Radimerski T, DeAngelo DJ, Weinstock DM, et al. HSP90 inhibition leads to degradation of the TYK2 kinase and apoptotic cell death in T-cell acute lymphoblastic leukemia. *Leukemia*. 2016;30(1):219-28.

74. Piper PW, Millson SH. Mechanisms of Resistance to Hsp90 Inhibitor Drugs: A Complex Mosaic Emerges. *Pharmaceuticals (Basel)*. 2011;4(11):1400-22.

75. Mumin NH, Drobnitzky N, Patel A, Lourenco LM, Cahill FF, Jiang Y, et al. Overcoming acquired resistance to HSP90 inhibition by targeting JAK-STAT signalling in triple-negative breast cancer. *BMC Cancer*. 2019;19(1):102.

76. Robey RW, Chakraborty AR, Basseville A, Luchenko V, Bahr J, Zhan Z, et al. Histone deacetylase inhibitors: emerging mechanisms of resistance. *Mol Pharm*. 2011;8(6):2021-31.

77. Tambaro FP, Dell'aversana C, Carafa V, Nebbioso A, Radic B, Ferrara F, et al. Histone deacetylase inhibitors: clinical implications for hematological malignancies. *Clin Epigenetics*. 2010;1(1-2):25-44.

78. Scuto A, Kirschbaum M, Kowolik C, Kretzner L, Juhasz A, Atadja P, et al. The novel histone deacetylase inhibitor, LBH589, induces expression of DNA damage response genes and apoptosis in Ph- acute lymphoblastic leukemia cells. *Blood*. 2008;111(10):5093-100.

3.1 Supplementary Materials

Constitutive JAK/STAT signaling is the primary mechanism of resistance to JAKi in *TYK2*-rearranged acute lymphoblastic leukemia

Paniz Tavakoli Shirazi[1,2], Laura N Eadie[1,2], Susan L Heatley[1,2], John B Bruning[3] and Deborah L White[1,2,3,4]

1.Cancer Program, Precision Medicine Theme, South Australian Health & Medical Research Institute (SAHMRI), Adelaide, Australia

2.Faculty of Health and Medical Sciences, University of Adelaide, Adelaide, Australia

3. Faculty of Sciences, University of Adelaide, Adelaide, Australia

4. Australian Genomics Health Alliance (AGHA)

This PDF file include:

Supplementary Material and Methods

Supplementary Figure 1-6

Supplementary references

Supplementary Material and Methods:

PCR and Sanger sequencing. PCR was performed for the detection of possible mutations on the full-length fusion gene. cDNA was generated by Quantitect Reverse Transcription Kit (Qiagen, CAT#205313) from total RNA extracted from each line as described previously (Tavakoli *et al* (2020); under review). PCR was carried out using Phusion High-fidelity DNA Polymerase (New England Biolabs, CAT#M0530L) with following primers for: 1) full length fusion PCR; human MYB, 5'- CATGATGGCCCGAAGACC-3' (forward) and human TYK2, 5'- CGTCAGCACACGCTGAAC-3' (reverse) and 2) Sanger sequencing; human MYB, 5'-CTACAGCTCAACTCCCTGCC-3' (forward) and 5'-GCTGGCTGGCTTTTGAAGAC-3' (reverse) and human TYK2, 5'-CCAACCCAGAGGCCATCATT-3' (forward) and 5'-GCCAAAGTCCCCGATCTTGA-3' (reverse). Samples underwent denaturation for 30 sec at 98°C followed by 35 cycles of 10 sec at 98°C, 30 sec at 60°C, and 3 mins at 72°C and a final 10 mins extension at 72°C. PCR amplicons were agarose gel extracted using QIAquick Gel Extraction Kit (Qiagen, CAT#407137). Samples were submitted for Sanger sequencing at SA Pathology Flinders Sequencing Facility and/or Australian Genome Research Facility (AGRF) and analysed using the DNA variant analysis software Mutation Surveyor® (SoftGenetics) or cloud-based Benchling software.

Mutagenesis of *TYK2* p.R987Q. The p.R9887Q mutation was introduced into the p-Ruf-iG2-*MYB-TYK2* retroviral vector using Q5® Site-Directed Mutagenesis Kit (NEB, CAT# E0554S) according to manufacturer protocol. Retroviral particles of p-Ruf-iG2-*MYB-TYK2*$^{p.R9887Q}$ were packaged into HEK-293T cells using Lipofectamine™ 2000 (Thermo Fisher Scientific, USA) and the packaging vector pEQ-Eco (gift from Dr. Stephen Fitter and Professor Andrew Zannettino, The University of Adelaide). Ba/F3 pro-B cells were resuspended in viral supernatant and spinfected at 1800 rpm for 1 h using polybrene (4 μg/mL, Sigma-Aldrich, CAT#TR-1003). Cells harboring the *MYB-TYK2* fusion gene were selected by GFP using fluorescence activated cell sorting (FACS) 72 h post-transduction to generate stable cell lines.

Expression of the *MYB-TYK2* fusion and correct sequence was confirmed by RT-PCR and Sanger sequencing, respectively.

***In vitro* proliferation and inhibitor assays.** For growth analysis, cells were plated at $1x10^4$ per well in 24-well plates in triplicates. At each indicated time point, 25 μL of cells was transferred to black 384-well ViewPlates (PerkinElmer, CAT#6007460) and viability was assessed via luminescence-based CellTiter Glo® 2.0 Assay (Promega, CAT# G9242) as per manufacturer protocol. Results were normalized to day 0 readout. A media only control was used to ensure assay interaction with medium and evaluate background luminescence. For dose-response curves, cells were washed (x3), plated in duplicates at 3000 cells/well in black 384-well ViewPlates in the presence of increasing drug concentrations for 48 h prior to addition of CellTiter Glo reagent. Luminescence levels was read via VICTOR™ X Multilabel Plate Reader (PerkinElmer, Inc). For cell cycle analysis, $4x10^5$ cells were stained with CellTrace™ Violet reagent (Thermo Fisher Scientific, CAT#C34557) according to manufacturer's instructions. Cells were then plated at $1x10^5$ per well in 24 well-plates and analyzed by flow cytometry at indicated time points.

Cell Death assay. Cells were washed (3x) via centrifugation and plated at $1.5x10^5$ cells per well in 24-well plates in presence of indicated drug concentrations. After 48 h incubation at 37°C with 5% CO_2, 200 μL of cells were transferred to 96-well plates. Cells were then washed (1x) with HANK's Balanced Salt solution (Sigma-Aldrich, CAT#H9394) supplemented with 5 mM calcium chloride (Sigma-Aldrich, CAT#C1016) and 1% HEPES (Sigma-Aldrich, CAT#H0887) (binding buffer), stained with 2% Annexin V (BD Biosciences, CAT#556421) in 20 μL binding buffer and incubated for 1 h in the dark on ice. Cells were resuspended in 200 μL of binding buffer and analyzed on a BD FACSCanto II (BD Bioscience). All flow cytometry results were analyzed using FlowJo analysis software™ v10 (FlowJo, LLC).

Phosphoflow analyses. Cells were washed (3x) via centrifugation and resuspension in inhibitor free media with cell concentration adjusted to $5x10^5$ per tube. For evaluation of the effect of drug treatments, cells were resuspended in normal media with inhibitors at the indicated concentrations or DMSO for 1 h. Subsequently cells were fixed with 100 μL of 16% PFA/per 1 mL of sample, incubated for 10 min at room temperature and washed once in 1X PBS via centrifugation. Permeabilization was carried out by dropwise addition of ice-cold 80% methanol to cell pellet while vortexing at low speed (600 rpm) to allow resuspension. Samples were stored at -20°C overnight and the next day washed with phosphoflow buffer (1xPBS/1% BSA) prior to staining with pSTAT5 (pY694, #CAT612567), pSTAT3 (pY705, #CAT562072), pERK1/2 (pT202/pY204, CAT#612566), pAKT (pS473, CAT#560378), pSYK (pY348, CAT#558529) or the isotype controls IgG_1 (CAT#555749) and IgG_2 (CAT#559319) at concentrations recommended by the manufacturer. All antibodies were purchased from BD Biosciences. For global histone methylation and acetylation analysis, cells were stained with H3 (CAT#12230), H3K27me3 (CAT#12158) and H3K9ac (CAT#66070) purchased from Cell Signaling Technology. Cells were analyzed on a BD FACSCanto II (BD Bioscience). All flow cytometry results were analyzed using FlowJo analysis software™ v10 (FlowJo, LLC).

Western blotting. For total lysates, $1x10^6$ cells per cell line were lysed in NP-40 buffer containing 10 mM Tris-HCL (pH 7.4), 137 mM NaCl, 10% Glycerol and 1% NP-40 (Igepal™, Thermo Fisher Scientific, CAT#85124) supplemented with phosphatase and protease inhibitors (Complete mini EDTA-free protease inhibitors Cocktail, Roche, CAT# 04693132001). Lysates were pelleted, a sample of supernatant taken for protein quantification and to the remainder, addition of 1/3 volume of 4x loading buffer (0.25 M Tris-HCL (pH 6.8), 8% (v/w) SDS, 40% (v/v) glycerol, 20% (v/v) 2-mercaptoethanol and 0.05% (w/v) bromophenol blue) prior to boiling at 100°C for 10 mins. Protein quantification was determined by DC Protein Assay (Bio-Rad, CAT#500-0116) based on manufacturer's protocol. 70 μg of

total protein was separated by SDS-PAGE electrophoresis on Criterion™ TGX Precast gels (Bio-Rad, CAT# 5678084) with the Precision Plus Protein Kaleidoscope Standard (Bio-Rad, CAT#161-0375) used to determine protein size. Protein was transferred to LF-PVDF membrane (Bio-Rad, CAT#170-4275) via the Trans-Blot Turbo Transfer System (Bio-Rad Laboratories Inc., California, USA) using the midi blot and high molecular weight setting. The membrane was then incubated with Intercept Blocking Buffer (LI-COR, CAT#927-70001) for 1 h at room temperature, prior to antibody staining. Primary antibodies against TYK2 (CAT#14193), pTYK2 (CAT#68790), JAK2 (CAT#3230), pJAK2 (CAT#3771), JAK1 (CAT#3344), pJAK1 (CAT#3331), JAK3 (CAT#8863), HSP90 (CAT#4874) and GAPDH (CAT#2118) were purchased from Cell Signaling Technology. Membranes were probed overnight at 4°C, with primary antibodies diluted at 1:1000 in Intercept Blocking Buffer. The following day, membranes were washed 4x 5 mins in TBST and stained with donkey-anti-rabbit IRDye 800CW (1:10000; Li-Core, CAT#925-32213) for 1 h at room temperature. Membranes were washed and analysed on the Li-Cor Odyssey CLx Imaging System (Li-Cor Biosciences, Nebraska, USA). Immunoblot image analysis was performed using ImageStudio software version 5.2.5.

Computational modeling. The ICM Molsoft suite (79) was used to dock Cerdulatinib into the TYK2 structure. PDB 6DBM (80) with ligands removed was used as the starting model for docking. The TYK2 structure was prepared for docking by protonation, deletion of water molecules, and energy minimization by means of the ICM force field and distance dependent dielectric potential with an RMS gradient of 0.1. PocketFinder within ICM was used to define the ligand binding pocket and was consistent with previously published X-ray structures. Default settings within the ICM docking module were used with a rectangular box centered at the LBD with a grid spacing of 0.5Å. The top ranked docking for each ligand was chosen for interpretation as the conformations were very consistent.

Supplementary Figures

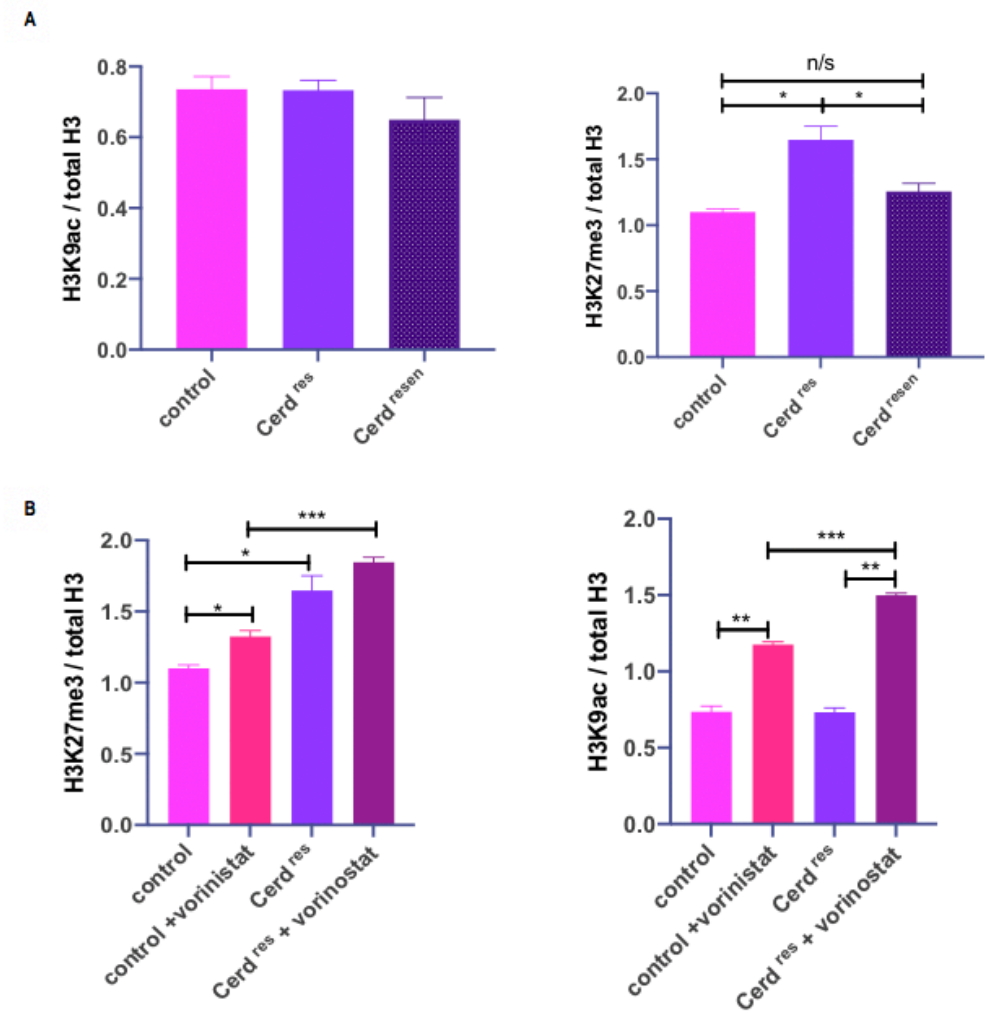

Supplementary Figure 1. Long-term cerdulatinib treatment resulted in increased H3K27me3 levels in cerd^{res} Ba/F3-*MYB-TYK2* cells. (A) Cerd^{res} Ba/F3-*MYB-TYK2*, cerd^{resen} Ba/F3-*MYB-TYK2* and control cells were assessed for levels of H3K27me3 and H3K9ac via flow cytometric analysis. (B) Flow cytometric analysis of H3K27me3 and H3K9ac levels in cerd^{res} Ba/F3-*MYB-TYK2* treated with vehicle or 1 μM vorinostat for a duration of 1 h. All MFI values are normalized to the total H3 of each line. Indicated error bars represent mean ±SD of 3 separate experiments. *p<0.05, **p<0.01, ***p<0.001.

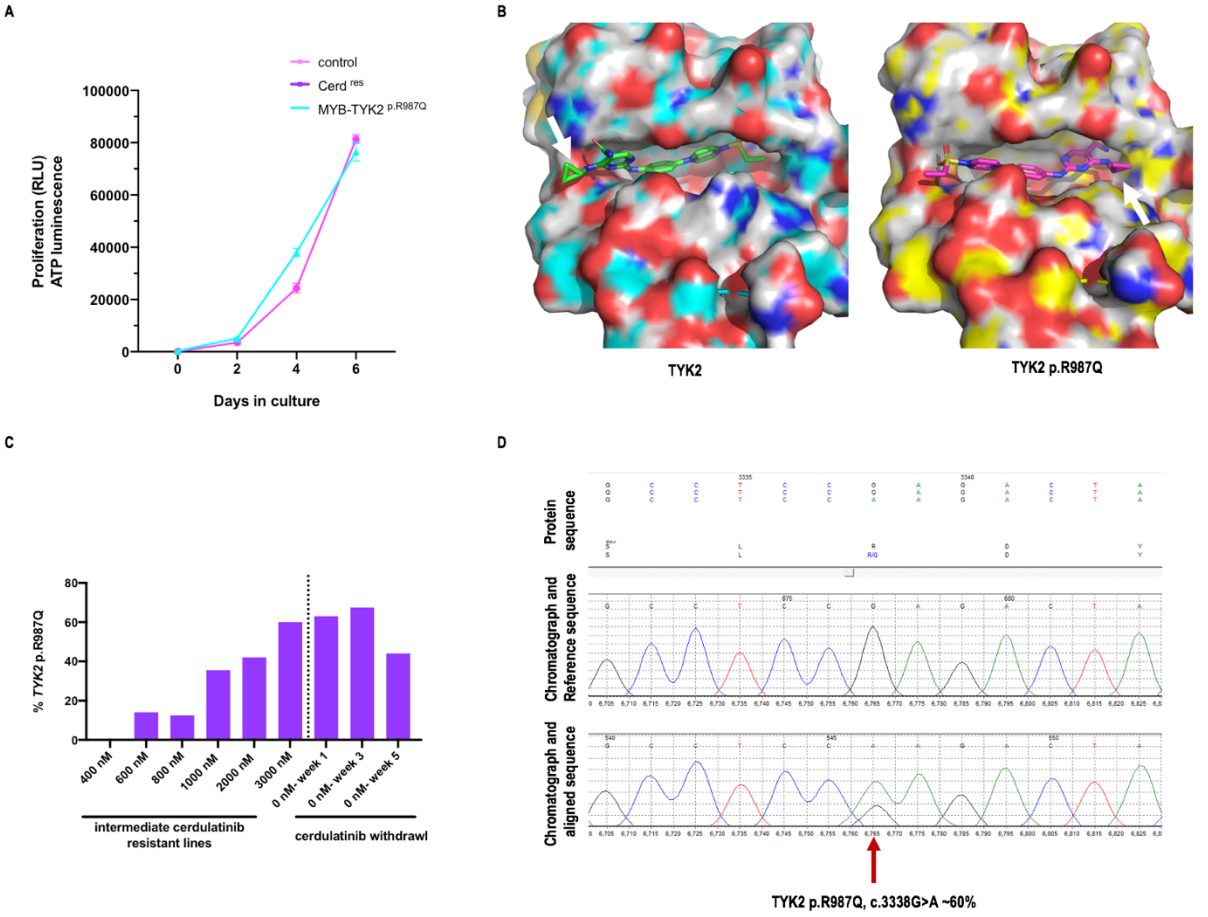

Supplementary Figure 2. Expression of the p.R987Q mutation did not result in persistent STAT5 activation in Ba/F3-*MYB-TYK2*$^{p.R987Q}$ cells nor alter the proliferation rate. (A) Proliferation rates of Ba/F3-*MYB-TYK2*$^{p.R987Q}$ and control cells determined by CellTiter Glo assay over a period of 6 days. (B) Drug binding domain surface/cavity changes induced by p.R9887Q mutation. The white arrow indicates the cyclopropane moiety of cerdulatinib on the left in wild type TYK2 and the right in TYK2 p.R987Q. Oxygen atoms are coloured red, nitrogen atoms coloured blue, and wild type carbon atoms coloured teal with mutant carbon atoms coloured yellow. (C) Level of p.R987Q mutation detected in different cerd^{res} Ba/F3-*MYB-TYK2* cell line intermediates. Approximate percent mutation was calculated by averaging the frequency of the identified mutation on the DNA chromatogram for forward and reverse primers over the *TYK2* kinase domain, using the DNA variant analysis software, Mutation Surveyor® (SoftGenetics). (D) Representative Sanger sequencing over the *MYB-TYK2* fusion gene isolated from cerd^{res} Ba/F3-*MYB-TYK2* cells confirming the presence of the p.R987Q mutation. The *MYB-TYK2* fusion gene was aligned against the individual NCBI reference sequences (*TYK2*, NM_003331 and *MYB*, NM_005375), assembled based on the breakpoint reported by Roberts *et.al.* (2014) {Roberts, 2014 #6}. Alignment was performed on Mutation Surveyor® (SoftGenetics). All statistical analyses were measured by paired student's t-test. All indicated error bars represent mean ±SD (n= at least 3 biological replicates). Abbreviation: RLU, relative luminescence unit.

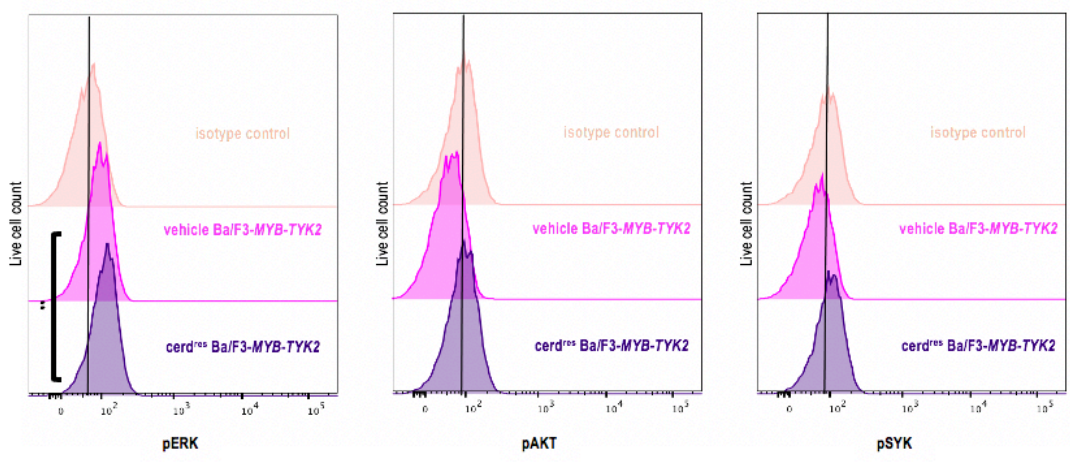

Supplementary Figure 3. No activation of AKT and B-cell receptor signalling was observed in Cerd^{res} Ba/F3-*MYB-TYK2* cells. (A) Representative histograms of phosphoflow cytometric analyses. Cerd^{res} Ba/F3-*MYB-TYK2* and control cells were assessed for phosphorylation levels of ERK, AKT and SYK. Three biological replicates were screened per condition.

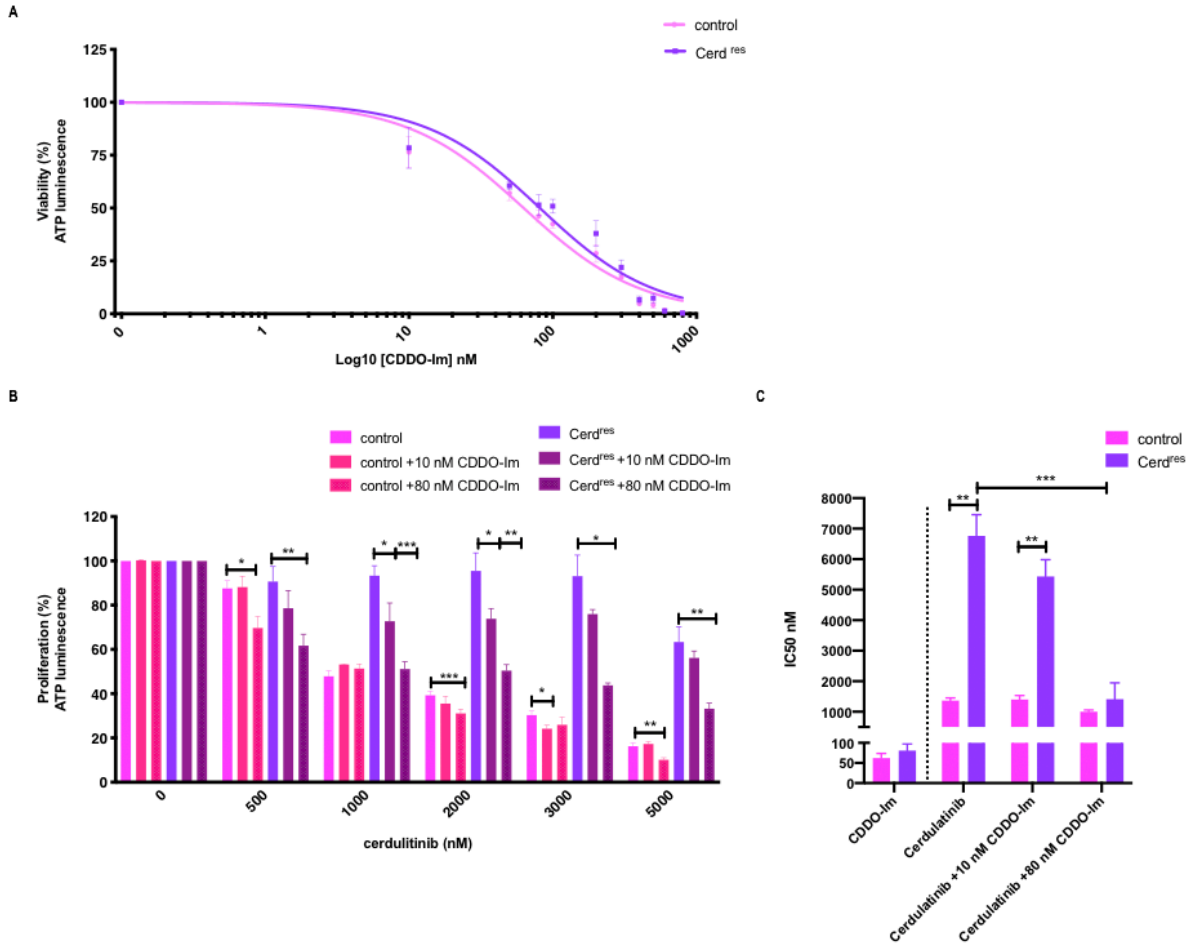

Supplementary Figure 4. Pharmacological inhibition of STAT5 and STAT3 results in increased sensitivity of cerd^{res} Ba/F3-*MYB-TYK2* cells to cerdulatinib. (A) Dose-response analysis displaying the percentage viability of cerd^{res} Ba/F3-*MYB-TYK2*, and control cells in response to increasing concentrations of CDDO-Im. (B) Percent viability of cerd^{res} Ba/F3-*MYB-TYK2* and control cells cultured with or without CDDO-Im, upon treatment with different cerdulatinib concentrations for 48 h. Viability was estimated relative to vehicle control via CellTiter Glo assay. (D) IC_{50} values for CDDO-im and cerdulatinib alone or in combination. All interactions were measured by un-paired student's t-test. Indicated error bars represent mean ±SD (n=3). *p<0.05, **p<0.01, ***p<0.001.

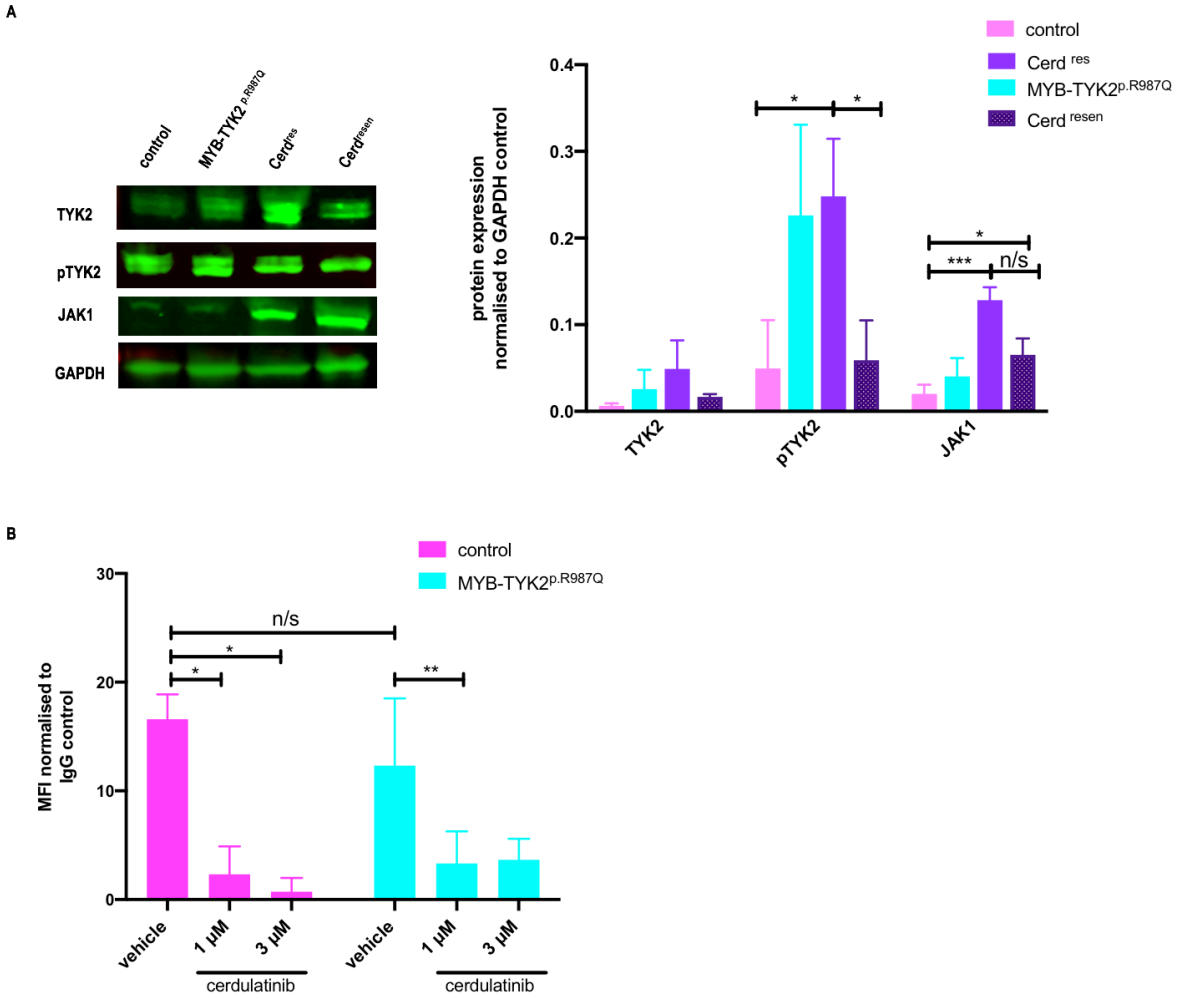

Supplementary Figure 5. Cerd^{res} Ba/F3-*MYB-TYK2* cells demonstrated a reversed JAK/STAT signalling profile, linked with decreased pTYK2 levels and its association to JAK1 upon cerdulatinib removal. (A) Western blot analysis of TYK2, pTYK2 and JAK1 protein levels in cerd^{res} Ba/F3-*MYB-TYK2*, Ba/F3-*MYB-TYK2*$^{p.R987Q}$, cerd^{resen} Ba/F3-*MYB-TYK2* and control cells. **(B)** Phosphoflow cytometric analyses of pSTAT5 levels in cerd^{res} Ba/F3-*MYB-TYK2*, Ba/F3-*MYB-TYK2*$^{p.R987Q}$ and control cells with or without treatment with cerdulatinib for 1 h. All interactions were measured by un-paired student's t-test. All indicated error bars represent mean ±SD of 3 biological replicates. *p<0.05, **p<0.01, ***p<0.001.

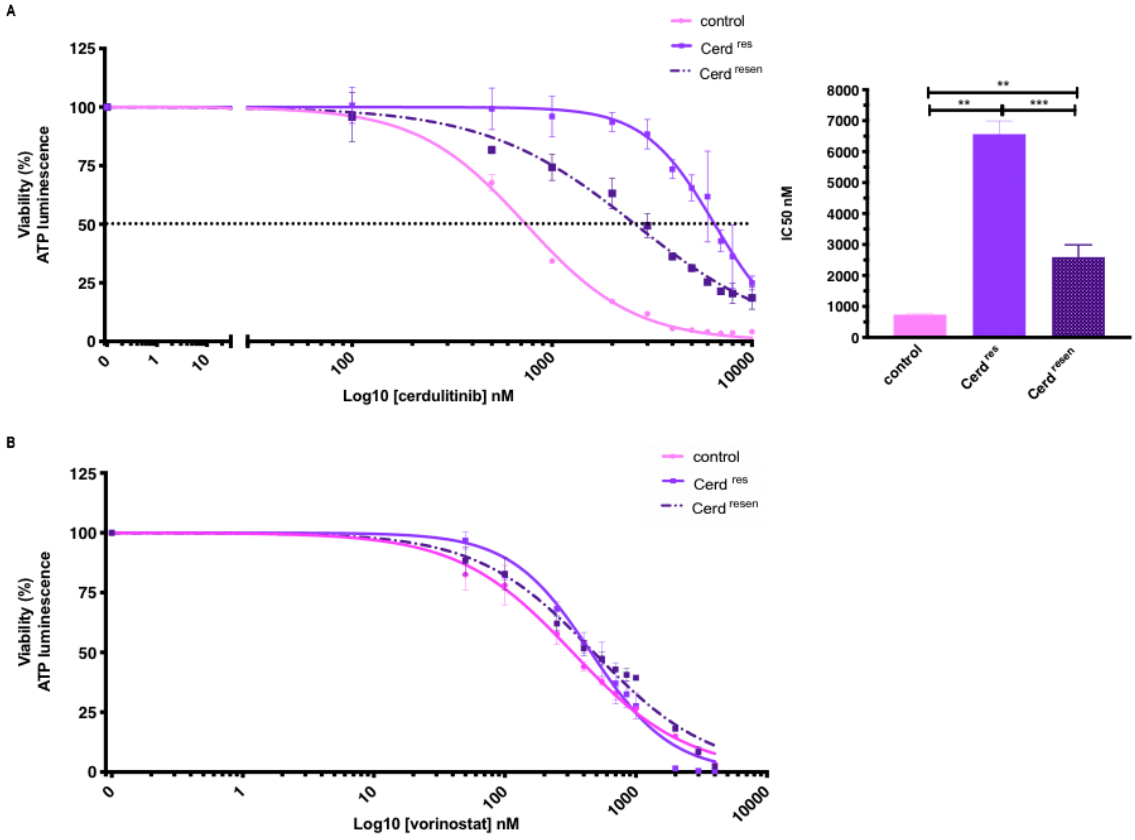

Supplementary Figure 6. Cerdulatinib withdrawal resulted in an IC_{50} decrease in cerd^{res} Ba/F3-MYB-TYK2 cells. (A) Percentage viability of cerd^{resen} Ba/F3-*MYB-TYK2* cells when grown in increasing concentrations of cerdulatinib for 48 h in comparison with resistant and control lines. The right panel indicates the IC_{50} values calculated by nonlinear regression analysis. (B) Dose-response analysis displaying the percentage viability of cerd^{res} Ba/F3-*MYB-TYK2*, cerd^{resen} Ba/F3-*MYB-TYK2* and control cells in response to increasing concentrations of vorinostat. All indicated error bars represent mean ±SD (n=3). **p<0.01, ***p<0.001.

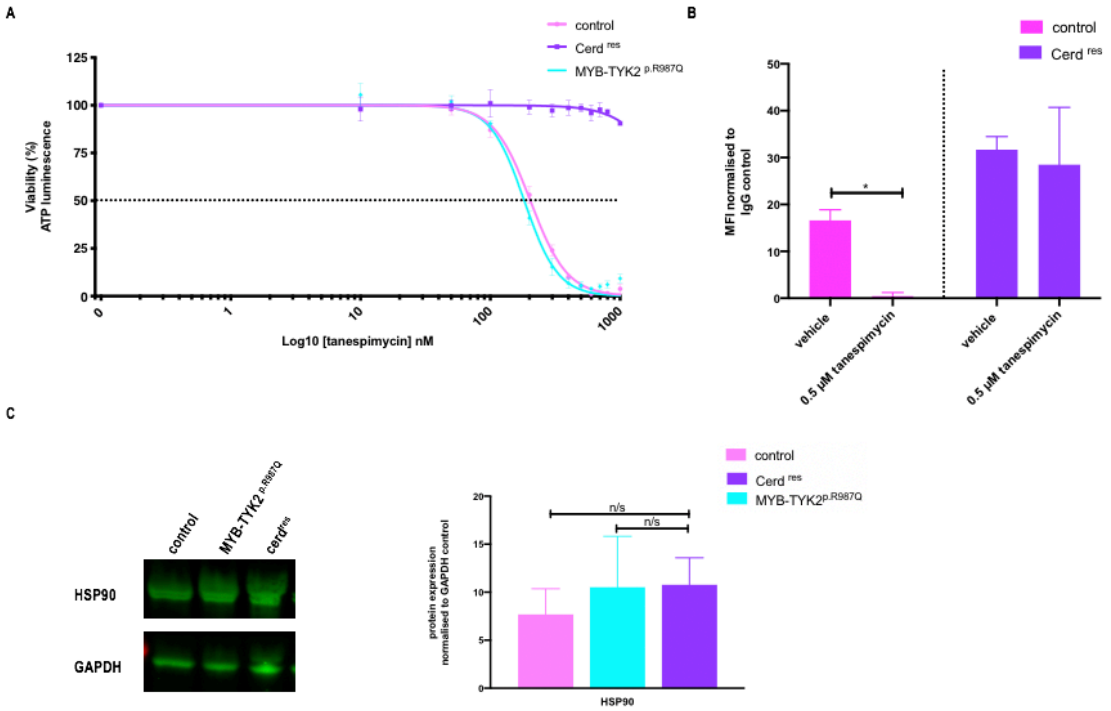

Supplementary Figure 7. Cerd^{res} Ba/F3-*MYB-TYK2* cells displayed cross-resistance to HSP90 inhibition. (A) Dose-response analysis displaying the percentage viability of cerd^{res} Ba/F3-*MYB-TYK2*, Ba/F3-*MYB-TYK2*$^{p.R987Q}$ and control cells in response to increasing concentrations of tanespimycin. (B) pSTAT5 levels in cerd^{res} Ba/F3-*MYB-TYK2* and control cells following 1 h incubation with or without 0.5 µM tanespimycin. Interactions as measured by un-paired student's t-test (C) Western blot analysis for indicated lines when probed for HSP90 and GAPDH loading control (n=3). All indicated error bars represent mean ±SD of 3 biological replicates. *p<0.05.

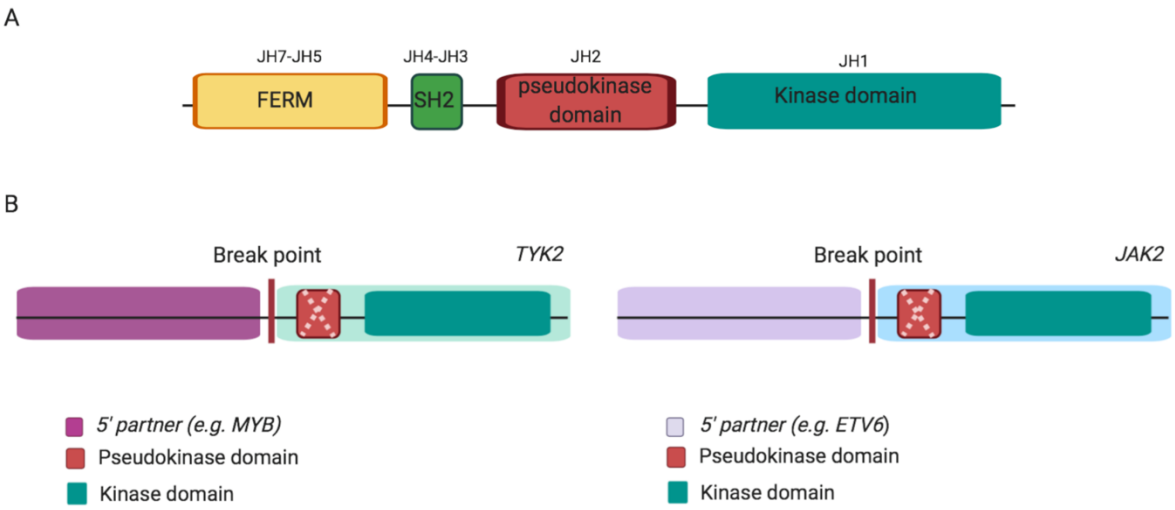

Supplementary Figure 8. Schematic structure of wild type JAK protein, JAK2 and TYK2 alterations in HR ALL. (A) Wild type Jak, each JAK protein consists of four domains including FERM, SH2, pseudokinase and kinase. (B) *TYK2* and *JAK2* alterations, *JAK*-class fusions exhibit an intact kinase domain with a disrupted pseudokinase or without (as indicated by crossed dashed lines) fused to variable 5' partner genes. Abbreviation: JH, Jak homology domain.

References:

79. Abagyan R, Totrov M. Biased probability Monte Carlo conformational searches and electrostatic calculations for peptides and proteins. *J Mol Biol*. 1994;235(3):983-1002.

80. Fensome A, Ambler CM, Arnold E, Banker ME, Brown MF, Chrencik J, et al. Dual Inhibition of TYK2 and JAK1 for the Treatment of Autoimmune Diseases: Discovery of ((S)-2,2-Difluorocyclopropyl)((1 R,5 S)-3-(2-((1-methyl-1 H-pyrazol-4-yl)amino)pyrimidin-4-yl)-3,8-diazabicyclo[3.2.1]octan-8-yl)methanone (PF-06700841). *J Med Chem*. 2018;61(19):8597-612.

4. Discussion and future direction

4.1 Introduction

The use of next generation sequencing (NGS) and greater characterisation of the genomic and transcriptomic profile of high-risk acute lymphoblastic leukaemia (HR-ALL) subtypes, led to the identification of novel lesions and classification of new subtypes. Due to the diverse genomic landscape of ALL, patients harbouring specific alterations have better survival outcomes when treated with a precision medicine approach. The pre-requisite to align effective targeted therapeutic regimens with patients however, relies on a detailed understanding of the underlying biology and molecular consequences of each alteration through robust *in vitro* and *in vivo* modelling.

An increasing number of *TYK2* gain of function mutations and rearrangements have been identified in High-Risk ALL (15, 111, 119, 120), yet our current understanding of Tyk2 function is limited. The consequences of constitutive *TYK2* activation and the involvement of the mutant protein in carcinogenesis and leukaemogenesis, remains to be comprehensively understood. The Tyk2 protein plays a fundamental role in activation of JAK/STAT signalling and/or crosstalk with other signalling pathways and if oncogenic, these pathways provide multiple avenues for targeted therapeutics (chapter 1, Figure 1-5). Hence, broad screening of small molecule inhibitors (SMIs) is of benefit when investigating targetability of *TYK2* alterations including the *MYB-TYK2* fusion gene. Moreover, as resistance to SMIs often occurs in the clinic (chapter 1, section 1.6) (181, 209, 210, 215, 216), identification of possible modes of resistance and alternative therapeutics to overcome potential resistance is prudent when investigating *TYK2*-rearranged disease. The studies presented here 1) investigate the leukaemogenic potential of the *MYB-TYK2* fusion gene, 2) inform its therapeutic targetability and 3) predict long term effects of JAKi therapy and possible mechanisms of resistance.

4.2 Major findings

4.2.1 Expression of the MYB-TYK2 fusion gene induces B-ALL in vivo

To date, the evidence demonstrating *MYB-TYK2* as a leukaemic driver gene has been limited to *in vitro* data (65). However, *in vivo* results presented in chapter 2 demonstrated the leukaemogenic and driving potential of the *MYB-TYK2* fusion gene. Mice engrafted with cells harbouring *MYB-TYK2* developed B-ALL with an immunophenotype consistent with developmental arrest at the pro/pre-B cell stage. This is the first time that an *in vivo* association between a *TYK2* activating alteration and leukaemogenesis has been established, providing new insights into the oncogenic potential of Tyk2 constitutive activation. Furthermore, the *in vitro* experiments in this study, demonstrated the kinase activity of the Myb-Tyk2 fusion protein, that stimulates the downstream activation of JAK/STAT signalling via constitutive phosphorylation of Stat3 and Stat5. These results extend existing evidence in other haematological malignancies such as myeloproliferative neoplasms (MPN) (111, 113, 114, 116, 117, 120) indicating predominant stimulation of JAK/STAT signalling via *TYK2* activating alterations.

4.2.2 The HDACi, vorinostat and the JAKi, cerdulatinib are efficacious against MYB-TYK2-altered disease

High-throughput drug screening of 3088 small molecule inhibitors and cytotoxic agents and categorisation of hits, indicated the profound sensitivity of cells expressing the *MYB-TYK2* fusion gene to the HDACi drug class, including vorinostat. Further *in vitro* and pre-clinical experiments detailed in chapter 2 emphasised the robust effect of vorinostat against *MYB-TYK2*-rearranged ALL, in agreement with the growing evidence of HDACi efficacy in haematological malignancies (153, 161). In particular, the efficacy of multiple HDACi was recently established in *in vitro* and *in vivo* ALL models with constitutive activation of JAK/STAT signalling (i.e. *CRLF2*-rearranged ALL) (199, 200). Although, the exact mechanism by which chromatin modifiers interact with STATs (and JAK/STAT signalling) in normal and malignant cells remains unclear and is not within the scope of this study. In the model of *MYB-TYK2*-altered disease presented here, vorinostat treatment resulted in attenuation of the activity of JAK/STAT

pathway downstream effector proteins, Stat5 and Stat3. The present analysis contradicts the association of HDACs only with transcriptionally repressed loci and further supports the mounting evidence suggesting the role of HDACs as activators of STAT-induced transcription (124, 152-154). Studies demonstrated that HDAC inhibition uniformly diminished the expression of STAT target genes in cytokine stimulated systems, whilst STAT activation and nuclear translocation was observed as either inhibited or unchanged in response to various cytokines (152, 155-159). Evidently, HDACi act through multiple mechanisms including induction of multiple pathways of apoptosis and cell death, proliferation arrest and interaction with proteins responsible for activation of transcription and signalling pathways (163). The observations reported here may be related to inherent differences in the function of HDACs with respect to cooperation with different STATs and receptor proteins. STATs activity and stability can be directly modulated by the changes in the acetylation level of the protein itself due to the regulatory effect of different HDACs on STATs proteins (160). Supporting this hypothesis, functional analyses indicated that deacetylation of the transcription activation sites of STAT target genes is required for recruitment of RNA polymerases and transcription machinery (152, 155-159). Thus, the data presented in this current study, combined with previous reports, indicate HDACi are a promising therapeutic option in disorders with overt STAT activation (152, 155-159).

Furthermore, the resultant activation of JAK/STAT signalling as a consequence of the *MYB-TYK2* fusion gene expression rationalises the use of JAKi against *MYB-TYK2* altered ALL. However, results obtained from the HTS screen, in agreement with Roberts *et al.* (2017) (65), indicated the limited sensitivity of cells harbouring the *MYB-TYK2* fusion gene to JAKi, including ruxolitinib, within a clinically achievable range. JAKi are often capable of targeting multiple JAK family proteins due to high sequence homology between individual JAK family proteins, particularly in the kinase (JH1) and drug binding domains (225, 226). However, while the selectivity and potency of these JAKi vary towards each JAK family of proteins and very few JAKi are reported to show selectivity in Tyk2 targeting (225, 226), cells expressing the *MYB-*

TYK2 fusion gene demonstrated sensitivity to cerdulatinib; a novel SYK/JAKi with established *in vitro* potency toward Tyk2 (227, 228).

Taken together, these pre-clinical studies demonstrated compelling evidence for the efficacy of both cerdulatinib and vorinostat against aggressive *MYB-TYK2*-induced B-ALL. These novel findings provide diverse therapeutic avenues that may be of benefit against other *TYK2* activating mutations and rearrangements reported in HR-ALL cases (i.e *SMARCA4-TYK2* and *ZNF340-TYK2*) (15, 111, 119, 120). Moreover, the demonstrated safety profiles of vorinostat (FDA approved for T-cell lymphoma) and cerdulatinib (Phase 1/2 Dose Escalation study (NCT01994382) for the treatment of Chronic Lymphocytic Leukaemia (229, 230)), emphasise the translational potential of this research for a better treatment outcome in patients with *TYK2*-rearranged ALL.

4.2.3 HDACi treatment can reverse the persistent JAK/STAT signalling in cerdulatinib resistant MYB-TYK2-altered disease

Despite the undeniable positive effect of JAKi treatment (i.e. ruxolitinib) in MPN and SMIs (i.e. ABLi) in chronic myeloid leukaemia (CML) and Ph-positive ALL, long term administration of these inhibitors has been associated with development of resistance in patients (181, 215, 216, 222, 231). Studies have identified the potential mechanisms of resistance to JAKi include kinase domain mutations in or near the ATP binding pocket (146, 217, 218) and persistent JAK/STAT signalling (219-221, 223). As the JAK family proteins such as Tyk2 and Jak2 exhibit highly conserved kinase domain sequences (225, 226), in this study it was hypothesised that following prolonged cerdulatinib exposure, development of similar resistance mechanisms may occur in the setting of *MYB-TYK2*-altered disease. Supporting this theory, continuous culture of cells expressing the *MYB-TYK2* fusion gene in the presence of increasing concentrations of cerdulatinib led to reduced drug sensitivity and the development of cerdulatinib-resistant (cerd^{res}) cells. Despite identification of a novel *TYK2* p.R987Q mutation in the cerd^{res} cells,

further investigations determined a minor effect of this mutation on induction of resistance in the *TYK2*-altered setting. This opposes previous *in vitro* studies demonstrating acquired kinase domain mutations as a mechanism of overt JAKi resistance in MPN cells harbouring *JAK2* p.V617F or p.R683G (146, 217, 218). To date, no secondary kinase domain mutations have been reported in MPN patients that developed resistance to ruxolitinib (222), limiting the clinical applicability of these *in vitro* findings. Conversely, data presented in chapter 3 suggest the secondary resistance mechanism that developed in the setting of *MYB-TYK2*-altered disease was due to persistent JAK/STAT signalling despite chronic Tyk2 suppression by cerdulatinib. The demonstrated increase in expression of Jak1 in cerd^{res} cells suggested persistent JAK/STAT signalling in these cells via transphosphorylation of the Myb-Tyk2 protein in co-operation with Jak1. These data are in agreement with previous studies that revealed a functional resistance mechanism in MPN cell lines and primary cells via persistent Jak2 signalling due to heterodimer formation of JAK family proteins with Jak2 (219-221, 223). The findings presented in Chapter 3 indicated that the cerd^{res} cells were equally sensitive to HDAC inhibition as vehicle treated cells, and HDACi treatment led to successful attenuation of JAK/STAT signalling. The retained sensitivity of Cerd^{res} cells to HDACi, may be explained by their high acetylation levels and/or the fact that HDACi treatment directly inhibits STATs activity and thus is capable of evading the effect of Myb-Tyk2/Jak1 co-operation in our JAKi resistant model. While previous studies suggested efficacy of HSP90 inhibition against JAKi resistant *JAK2* p.V617F cells (146, 219), the results here demonstrate HDACi as efficacious and alternative targeted therapeutics against *de novo* and JAKi-resistant *MYB-TYK2*-rearranged disease.

4.3 Limitations and future directions

4.3.1 Limitations of cerdulatinib and vorinostat incorporation into the treatment regimen of TYK2-rearranged ALL cases

Although, the efficacy and potency of both cerdulatinib and vorinostat against *MYB-TYK2*-induced B-ALL in the presented *in vivo* models was evident, even with only a short treatment period, this study was not

without limitations. In particular a survival benefit in the *MYB-TYK2* mouse model was not observed in treated mice. However, the lack of survival benefit may in part be explained by the fact that the secondary transplant animals demonstrated 1) a sudden and aggressive onset of disease (with ~36-fold increase in %GFP cells (1.2% vs 44.3%) in peripheral blood over 4 days) before treatment commencement and 2) infiltration into the central nervous system (CNS). In most pre-clinical studies for SMIs, treatment often commences at very early onset of the disease (1-5% leukaemic cells in the peripheral blood) (199, 232, 233). In addition, SMIs such as JAKi do not display the potential to penetrate the CNS as a single agent therapy (65, 234). Therefore, the significant anti-leukaemic effect of cerdulatinib and vorinostat within a short treatment window, despite the limitations outlined above, demonstrates promising clinical potential. Further research is warranted, in particular, assessment of inhibitor efficacy in combination with a chemotherapy backbone.

4.3.2 Co-binding and transphosphorylation of Jak1 and Tyk2 and increased JAKi insensitivity in cells

Although the findings here suggest an association between increased Jak1 expression and Tyk2 phosphorylation, and hence JAK/STAT persistent signalling in cerd^{res} cells, this interpretation should be regarded with caution, as these data require validation of Jak1 and Myb-Tyk2 co-interaction. Further experiments utilising techniques such as immunoprecipitation (IP) and FRET microscopy, are needed to capture possible binding of Jak1 to Myb-Tyk2 at the cytokine receptor site and membrane. In addition, whether the association of Jak1 and Myb-Tyk2 is the sole driver of JAKi resistance in the current model could be further explored. Accordingly, the insensitivity of cells to cerdulatinib could be validated in the setting of induced Jak1 overexpression via viral co-transduction of the cerdulatinib-naïve *MYB-TYK2* cells with a *JAK1* expression construct.

4.3.3 In vivo modelling of JAKi resistance in MYB-TYK2 mice and investigation of the pre-clinical efficacy of HDACi therapy against the resistance disease

Despite findings indicating the possibility of JAKi resistance development in the setting of *TYK2*-rearranged B-ALL, these results are limited to *in vitro* investigations. Therefore, to further elucidate whether similar JAKi resistance mechanisms occur in *TYK2*-rearranged patients, *in vivo* modelling of JAKi resistance may be of benefit. This can be achieved by long-term treatment of *MYB-TYK2* mice with cerdulatinib to investigate, firstly, the likelihood of relapse after the conclusion of therapy and secondly, whether resistance is likely through characterisation of minimal residual leukaemic cells. Residual leukaemic cells may provide a reservoir of resistant cells and can be assessed via candidate PCR, Jak1 protein expression, exome and mRNA sequencing to identify additional sequence mutations/alterations acquired in resistant cells in comparison to the primary engrafted material. In addition, the promising *in vitro* efficacy of HDACi such as vorinostat and panobinostat against cerd^{res} cells demonstrated here, warrants further investigation in *in vivo* models of either cerd^{res} cells harbouring the *MYB-TYK2* fusion gene or relapsed *MYB-TYK2* mice following JAKi therapy completion.

4.3.4 Final Conclusions

The findings of this thesis demonstrate, for the first time, the leukaemogenic potential of the *MYB-TYK2* fusion gene, resulting in an aggressive B-ALL, and provide insights into the driving potential of *TYK2* activating alterations. A high-throughput screening approach was used to identify potential inhibitors of *MYB-TYK2* disease which were subsequently evaluated *in vitro* and *in vivo*. Efficacious drugs included inhibitors already in clinical use in other malignancies, emphasising the translational potential of these results. In addition, modelling of cerdulatinib resistance *in vitro* recapitulated possible clinical scenarios of resistance that may arise due to continued JAKi exposure in *TYK2*-rearranged ALL cases and provides a rationale for the use of HDACi to treat patients with this resistance profile. These novel findings may be applicable against other *TYK2* activating mutations and rearrangements such as *SMARCA4-TYK2* and

ZNF340-TYK2 and ultimately may improve survival outcomes for patients with *MYB-TYK2*-altered disease.

References

1. Inaba H, Greaves M, Mullighan CG. Acute lymphoblastic leukaemia. *Lancet*. 2013;381(9881):1943-55.

2. Hunger SP, Mullighan CG. Acute Lymphoblastic Leukemia in Children. *N Engl J Med*. 2015;373(16):1541-52.

3. Pui CH, Robison LL, Look AT. Acute lymphoblastic leukaemia. *Lancet*. 2008;371(9617):1030-43.

4. Terwilliger T, Abdul-Hay M. Acute lymphoblastic leukemia: a comprehensive review and 2017 update. *Blood Cancer J*. 2017;7(6):e577.

5. Aifantis I, Raetz E, Buonamici S. Molecular pathogenesis of T-cell leukaemia and lymphoma. *Nat Rev Immunol*. 2008;8(5):380-90.

6. Alvarnas JC, Brown PA, Aoun P, Ballen KK, Barta SK, Borate U, et al. Acute Lymphoblastic Leukemia, Version 2.2015. *J Natl Compr Canc Netw*. 2015;13(10):1240-79.

7. Jabbour EJ, Faderl S, Kantarjian HM. Adult acute lymphoblastic leukemia. *Mayo Clin Proc*. 2005;80(11):1517-27.

8. Frishman-Levy L, Izraeli S. Advances in understanding the pathogenesis of CNS acute lymphoblastic leukaemia and potential for therapy. *Br J Haematol*. 2017;176(2):157-67.

9. Del Principe MI, Maurillo L, Buccisano F, Sconocchia G, Cefalo M, De Santis G, et al. Central nervous system involvement in adult acute lymphoblastic leukemia: diagnostic tools, prophylaxis, and therapy. *Mediterr J Hematol Infect Dis*. 2014;6(1):e2014075.

10. Lenk L, Alsadeq A, Schewe DM. Involvement of the central nervous system in acute lymphoblastic leukemia: opinions on molecular mechanisms and clinical implications based on recent data. *Cancer Metastasis Rev*. 2020;39(1):173-87.

11. Vanner RJ, Dobson SM, Grandal I, Gan O, McLeod J, Kennedy J, et al. Abstract 5173: Genetic profiling of central nervous system dissemination of B-acute lymphoblastic leukemia reveals clonal selection and therapeutic vulnerability. 2018;78(13 Supplement):5173-.

12. Ko RH, Ji L, Barnette P, Bostrom B, Hutchinson R, Raetz E, et al. Outcome of patients treated for relapsed or refractory acute lymphoblastic leukemia: a Therapeutic Advances in Childhood Leukemia Consortium study. *J Clin Oncol*. 2010;28(4):648-54.

13. Raetz EA, Bhatla T. Where do we stand in the treatment of relapsed acute lymphoblastic leukemia? *Hematology Am Soc Hematol Educ Program*. 2012;2012:129-36.

14. Larson S, Stock W. Progress in the treatment of adults with acute lymphoblastic leukemia. *Curr Opin Hematol*. 2008;15(4):400-7.

15. Roberts KG, Gu Z, Payne-Turner D, McCastlain K, Harvey RC, Chen IM, et al. High Frequency and Poor Outcome of Philadelphia Chromosome-Like Acute Lymphoblastic Leukemia in Adults. *J Clin Oncol*. 2017;35(4):394-401.

16. Fielding AK, Richards SM, Chopra R, Lazarus HM, Litzow MR, Buck G, et al. Outcome of 609 adults after relapse of acute lymphoblastic leukemia (ALL); an MRC UKALL12/ECOG 2993 study. *Blood*. 2007;109(3):944-50.

17. Chiaretti S, Zini G, Bassan R. Diagnosis and subclassification of acute lymphoblastic leukemia. *Mediterr J Hematol Infect Dis*. 2014;6(1):e2014073.

18. Abdul-Hamid G. Classification of Acute Leukemia, Acute Leukemia - The Scientist's Perspective and Challenge. *Mariastefania Antica, IntechOpen*. 2011:

.

19. Gokbuget N, Hoelzer D. Treatment of adult acute lymphoblastic leukemia. *Hematology Am Soc Hematol Educ Program*. 2006:133-41.

20. Ma X, Edmonson M, Yergeau D, Muzny DM, Hampton OA, Rusch M, et al. Rise and fall of subclones from diagnosis to relapse in pediatric B-acute lymphoblastic leukaemia. *Nat Commun*. 2015;6:6604.

21. Roberts KG, Mullighan CG. Genomics in acute lymphoblastic leukaemia: insights and treatment implications. *Nat Rev Clin Oncol*. 2015;12(6):344-57.

22. Liu Y, Easton J, Shao Y, Maciaszek J, Wang Z, Wilkinson MR, et al. The genomic landscape of pediatric and young adult T-lineage acute lymphoblastic leukemia. *Nat Genet*. 2017;49(8):1211-8.

23. Harrison CJ. Cytogenetics of paediatric and adolescent acute lymphoblastic leukaemia. *Br J Haematol*. 2009;144(2):147-56.

24. Roberts KG, Li Y, Payne-Turner D, Harvey RC, Yang YL, Pei D, et al. Targetable kinase-activating lesions in Ph-like acute lymphoblastic leukemia. *N Engl J Med*. 2014;371(11):1005-15.

25. Tasian SK, Hunger SP. Genomic characterization of paediatric acute lymphoblastic leukaemia: an opportunity for precision medicine therapeutics. *Br J Haematol*. 2017;176(6):867-82.

26. Tavakoli Shirazi P, Eadie LN, Heatley SL, Hughes TP, Yeung DT, White DL. The effect of co-occurring lesions on leukaemogenesis and drug response in T-ALL and ETP-ALL. *Br J Cancer*. 2020;122(4):455-64.

27. Chiaretti S, Gianfelici V, Ceglie G, Foa R. Genomic characterization of acute leukemias. *Med Princ Pract*. 2014;23(6):487-506.

28. Liu YF, Wang BY, Zhang WN, Huang JY, Li BS, Zhang M, et al. Genomic Profiling of Adult and Pediatric B-cell Acute Lymphoblastic Leukemia. *EBioMedicine*. 2016;8:173-83.

29. Chiaretti S, Li X, Gentleman R, Vitale A, Wang KS, Mandelli F, et al. Gene expression profiles of B-lineage adult acute lymphocytic leukemia reveal genetic patterns that identify lineage derivation and distinct mechanisms of transformation. *Clin Cancer Res*. 2005;11(20):7209-19.

30. Ross ME, Zhou X, Song G, Shurtleff SA, Girtman K, Williams WK, et al. Classification of pediatric acute lymphoblastic leukemia by gene expression profiling. *Blood*. 2003;102(8):2951-9.

31. Den Boer ML, van Slegtenhorst M, De Menezes RX, Cheok MH, Buijs-Gladdines JG, Peters ST, et al. A subtype of childhood acute lymphoblastic leukaemia with poor treatment outcome: a genome-wide classification study. *Lancet Oncol*. 2009;10(2):125-34.

32. Mullighan CG, Goorha S, Radtke I, Miller CB, Coustan-Smith E, Dalton JD, et al. Genome-wide analysis of genetic alterations in acute lymphoblastic leukaemia. *Nature*. 2007;446(7137):758-64.

33. Vora A, Goulden N, Wade R, Mitchell C, Hancock J, Hough R, et al. Treatment reduction for children and young adults with low-risk acute lymphoblastic leukaemia defined by minimal residual disease (UKALL 2003): a randomised controlled trial. *Lancet Oncol*. 2013;14(3):199-209.

34. Mullighan CG, Jeha S, Pei D, Payne-Turner D, Coustan-Smith E, Roberts KG, et al. Outcome of children with hypodiploid ALL treated with risk-directed therapy based on MRD levels. *Blood*. 2015;126(26):2896-9.

35. Mehta PA, Zhang MJ, Eapen M, He W, Seber A, Gibson B, et al. Transplantation Outcomes for Children with Hypodiploid Acute Lymphoblastic Leukemia. *Biol Blood Marrow Transplant*. 2015;21(7):1273-7.

36. Harrison CJ. Acute lymphoblastic leukemia. *Clin Lab Med*. 2011;31(4):631-47, ix.

37. Mullighan CG, Collins-Underwood JR, Phillips LA, Loudin MG, Liu W, Zhang J, et al. Rearrangement of CRLF2 in B-progenitor- and Down syndrome-associated acute lymphoblastic leukemia. *Nat Genet*. 2009;41(11):1243-6.

38. Mullighan CG, Zhang J, Harvey RC, Collins-Underwood JR, Schulman BA, Phillips LA, et al. JAK mutations in high-risk childhood acute lymphoblastic leukemia. *Proc Natl Acad Sci U S A*. 2009;106(23):9414-8.

39. Mullighan CG, Su X, Zhang J, Radtke I, Phillips LA, Miller CB, et al. Deletion of IKZF1 and prognosis in acute lymphoblastic leukemia. *N Engl J Med*. 2009;360(5):470-80.

40. Mullighan CG. Genomic characterization of childhood acute lymphoblastic leukemia. *Semin Hematol*. 2013;50(4):314-24.

41. Hunger SP, Mullighan CG. Redefining ALL classification: toward detecting high-risk ALL and implementing precision medicine. *Blood*. 2015;125(26):3977-87.

42. Bercovich D, Ganmore I, Scott LM, Wainreb G, Birger Y, Elimelech A, et al. Mutations of JAK2 in acute lymphoblastic leukaemias associated with Down's syndrome. *Lancet*. 2008;372(9648):1484-92.

43. Gaikwad A, Rye CL, Devidas M, Heerema NA, Carroll AJ, Izraeli S, et al. Prevalence and clinical correlates of JAK2 mutations in Down syndrome acute lymphoblastic leukaemia. *Br J Haematol*. 2009;144(6):930-2.

44. Reshmi SC, Harvey RC, Roberts KG, Stonerock E, Smith A, Jenkins H, et al. Targetable kinase gene fusions in high-risk B-ALL: a study from the Children's Oncology Group. *Blood*. 2017;129(25):3352-61.

45. Harvey RC, Mullighan CG, Chen IM, Wharton W, Mikhail FM, Carroll AJ, et al. Rearrangement of CRLF2 is associated with mutation of JAK kinases, alteration of IKZF1, Hispanic/Latino ethnicity, and a poor outcome in pediatric B-progenitor acute lymphoblastic leukemia. *Blood*. 2010;115(26):5312-21.

46. Russell LJ, Capasso M, Vater I, Akasaka T, Bernard OA, Calasanz MJ, et al. Deregulated expression of cytokine receptor gene, CRLF2, is involved in lymphoid transformation in B-cell precursor acute lymphoblastic leukemia. *Blood*. 2009;114(13):2688-98.

47. Yoda A, Yoda Y, Chiaretti S, Bar-Natan M, Mani K, Rodig SJ, et al. Functional screening identifies CRLF2 in precursor B-cell acute lymphoblastic leukemia. *Proc Natl Acad Sci U S A*. 2010;107(1):252-7.

48. Holmfeldt L, Wei L, Diaz-Flores E, Walsh M, Zhang J, Ding L, et al. The genomic landscape of hypodiploid acute lymphoblastic leukemia. *Nat Genet*. 2013;45(3):242-52.

49. Irving J, Matheson E, Minto L, Blair H, Case M, Halsey C, et al. Ras pathway mutations are prevalent in relapsed childhood acute lymphoblastic leukemia and confer sensitivity to MEK inhibition. *Blood*. 2014;124(23):3420-30.

50. Nikolaev SI, Garieri M, Santoni F, Falconnet E, Ribaux P, Guipponi M, et al. Frequent cases of RAS-mutated Down syndrome acute lymphoblastic leukaemia lack JAK2 mutations. *Nat Commun*. 2014;5:4654.

51. Paulsson K, Lilljebjorn H, Biloglav A, Olsson L, Rissler M, Castor A, et al. The genomic landscape of high hyperdiploid childhood acute lymphoblastic leukemia. *Nat Genet*. 2015;47(6):672-6.

52. Zhang J, Ding L, Holmfeldt L, Wu G, Heatley SL, Payne-Turner D, et al. The genetic basis of early T-cell precursor acute lymphoblastic leukaemia. *Nature*. 2012;481(7380):157-63.

53. Mullighan CG, Miller CB, Radtke I, Phillips LA, Dalton J, Ma J, et al. BCR-ABL1 lymphoblastic leukaemia is characterized by the deletion of Ikaros. *Nature*. 2008;453(7191):110-4.

54. Kuiper RP, Schoenmakers EF, van Reijmersdal SV, Hehir-Kwa JY, van Kessel AG, van Leeuwen FN, et al. High-resolution genomic profiling of childhood ALL reveals novel recurrent genetic lesions affecting pathways involved in lymphocyte differentiation and cell cycle progression. *Leukemia*. 2007;21(6):1258-66.

55. Shiraz P, Payne KJ, Muffly L. The Current Genomic and Molecular Landscape of Philadelphia-like Acute Lymphoblastic Leukemia. *Int J Mol Sci*. 2020;21(6).

56. Iacobucci I, Mullighan CG. Genetic Basis of Acute Lymphoblastic Leukemia. *J Clin Oncol*. 2017;35(9):975-83.

57. Heatley SL, Sadras T, Kok CH, Nievergall E, Quek K, Dang P, et al. High prevalence of relapse in children with Philadelphia-like acute lymphoblastic leukemia despite risk-adapted treatment. *Haematologica*. 2017;102(12):e490-e3.

58. Pui CH, Roberts KG, Yang JJ, Mullighan CG. Philadelphia Chromosome-like Acute Lymphoblastic Leukemia. *Clin Lymphoma Myeloma Leuk*. 2017;17(8):464-70.

59. He R, Geha RS. Thymic stromal lymphopoietin. *Ann N Y Acad Sci*. 2010;1183:13-24.

60. Roberts KG, Morin RD, Zhang J, Hirst M, Zhao Y, Su X, et al. Genetic alterations activating kinase and cytokine receptor signaling in high-risk acute lymphoblastic leukemia. *Cancer Cell*. 2012;22(2):153-66.

61. Shochat C, Tal N, Bandapalli OR, Palmi C, Ganmore I, te Kronnie G, et al. Gain-of-function mutations in interleukin-7 receptor-alpha (IL7R) in childhood acute lymphoblastic leukemias. *J Exp Med*. 2011;208(5):901-8.

62. Vesely C, Frech C, Eckert C, Cario G, Mecklenbrauker A, Zur Stadt U, et al. Genomic and transcriptional landscape of P2RY8-CRLF2-positive childhood acute lymphoblastic leukemia. *Leukemia*. 2017;31(7):1491-501.

63. Maude SL, Tasian SK, Vincent T, Hall JW, Sheen C, Roberts KG, et al. Targeting JAK1/2 and mTOR in murine xenograft models of Ph-like acute lymphoblastic leukemia. *Blood*. 2012;120(17):3510-8.

64. Waibel M, Solomon VS, Knight DA, Ralli RA, Kim SK, Banks KM, et al. Combined targeting of JAK2 and Bcl-2/Bcl-xL to cure mutant JAK2-driven malignancies and overcome acquired resistance to JAK2 inhibitors. *Cell Rep*. 2013;5(4):1047-59.

65. Roberts KG, Yang YL, Payne-Turner D, Lin W, Files JK, Dickerson K, et al. Oncogenic role and therapeutic targeting of ABL-class and JAK-STAT activating kinase alterations in Ph-like ALL. *Blood Adv*. 2017;1(20):1657-71.

66. Duhoux FP, Auger N, De Wilde S, Wittnebel S, Ameye G, Bahloula K, et al. The t(1;9)(p34;q34) fusing ABL1 with SFPQ, a pre-mRNA processing gene, is recurrent in acute lymphoblastic leukemias. *Leuk Res*. 2011;35(7):e114-7.

67. Lilljebjorn H, Agerstam H, Orsmark-Pietras C, Rissler M, Ehrencrona H, Nilsson L, et al. RNA-seq identifies clinically relevant fusion genes in leukemia including a novel MEF2D/CSF1R fusion responsive to imatinib. *Leukemia*. 2014;28(4):977-9.

68. Kobayashi K, Mitsui K, Ichikawa H, Nakabayashi K, Matsuoka M, Kojima Y, et al. ATF7IP as a novel PDGFRB fusion partner in acute lymphoblastic leukaemia in children. *Br J Haematol*. 2014;165(6):836-41.

69. Poitras JL, Dal Cin P, Aster JC, Deangelo DJ, Morton CC. Novel SSBP2-JAK2 fusion gene resulting from a t(5;9)(q14.1;p24.1) in pre-B acute lymphocytic leukemia. *Genes Chromosomes Cancer*. 2008;47(10):884-9.

70. Kawamura M, Taki T, Kaku H, Ohki K, Hayashi Y. Identification of SPAG9 as a novel JAK2 fusion partner gene in pediatric acute lymphoblastic leukemia with t(9;17)(p24;q21). *Genes Chromosomes Cancer*. 2015;54(7):401-8.

71. Yano M, Imamura T, Asai D, Kiyokawa N, Nakabayashi K, Matsumoto K, et al. Identification of novel kinase fusion transcripts in paediatric B cell precursor acute lymphoblastic leukaemia with IKZF1 deletion. *Br J Haematol*. 2015;171(5):813-7.

72. De Keersmaecker K, Rocnik JL, Bernad R, Lee BH, Leeman D, Gielen O, et al. Kinase activation and transformation by NUP214-ABL1 is dependent on the context of the nuclear pore. *Mol Cell*. 2008;31(1):134-42.

73. Boer JM, den Boer ML. BCR-ABL1-like acute lymphoblastic leukaemia: From bench to bedside. *Eur J Cancer*. 2017;82:203-18.

74. Roberts KG, Janke LJ, Zhao Y, Seth A, Ma J, Finkelstein D, et al. ETV6-NTRK3 induces aggressive acute lymphoblastic leukemia highly sensitive to selective TRK inhibition. *Blood*. 2018;132(8):861-5.

75. Iacobucci I, Li Y, Roberts KG, Dobson SM, Kim JC, Payne-Turner D, et al. Truncating Erythropoietin Receptor Rearrangements in Acute Lymphoblastic Leukemia. *Cancer Cell*. 2016;29(2):186-200.

76. Mayumi A, Tomii T, Imamura T, Kawamura M, Hosoi H. Leukemic Cell with a Novel Kinase Fusion Gene SPAG9-JAK2 Exhibits High Sensitivity to Ruxolitinib. *Blood*. 2019;134(Supplement_1):5044-.

77. Zhang G, Zhang Y, Wu J, Chen Y, Ma Z. Acute Lymphoblastic Leukemia Patient with Variant ATF7IP/PDGFRB Fusion and Favorable Response to Tyrosine Kinase Inhibitor Treatment: A Case Report. *Am J Case Rep*. 2017;18:1204-8.

78. Vanden Bempt M, Demeyer S, Mentens N, Geerdens E, De Bock CE, Wlodarska I, et al. Generation of the Fip1l1-Pdgfra fusion gene using CRISPR/Cas genome editing. *Leukemia*. 2016;30(9):1913-6.

79. Tomita O, Iijima K, Ishibashi T, Osumi T, Kobayashi K, Okita H, et al. Sensitivity of SNX2-ABL1 toward tyrosine kinase inhibitors distinct from that of BCR-ABL1. *Leuk Res*. 2014;38(3):361-70.

80. De Braekeleer E, Douet-Guilbert N, Guardiola P, Rowe D, Mustjoki S, Zamecnikova A, et al. Acute lymphoblastic leukemia associated with RCSD1-ABL1 novel fusion gene has a distinct gene expression profile from BCR-ABL1 fusion. *Leukemia*. 2013;27(6):1422-4.

81. De Braekeleer E, Douet-Guilbert N, Rowe D, Bown N, Morel F, Berthou C, et al. ABL1 fusion genes in hematological malignancies: a review. *Eur J Haematol*. 2011;86(5):361-71.

82. Lengline E, Beldjord K, Dombret H, Soulier J, Boissel N, Clappier E. Successful tyrosine kinase inhibitor therapy in a refractory B-cell precursor acute lymphoblastic leukemia with EBF1-PDGFRB fusion. *Haematologica*. 2013;98(11):e146-8.

83. Weston BW, Hayden MA, Roberts KG, Bowyer S, Hsu J, Fedoriw G, et al. Tyrosine kinase inhibitor therapy induces remission in a patient with refractory EBF1-PDGFRB-positive acute lymphoblastic leukemia. *J Clin Oncol*. 2013;31(25):e413-6.

84. Ihle JN, Gilliland DG. Jak2: normal function and role in hematopoietic disorders. *Curr Opin Genet Dev*. 2007;17(1):8-14.

85. Valentino L, Pierre J. JAK/STAT signal transduction: regulators and implication in hematological malignancies. *Biochem Pharmacol*. 2006;71(6):713-21.

86. Lacronique V, Boureux A, Valle VD, Poirel H, Quang CT, Mauchauffe M, et al. A TEL-JAK2 fusion protein with constitutive kinase activity in human leukemia. *Science*. 1997;278(5341):1309-12.

87. dos Santos NR, Ghysdael J. A transgenic mouse model for TEL-JAK2-induced B-cell lymphoma/leukemia. *Leukemia*. 2006;20(1):182-5.

88. Carron C, Cormier F, Janin A, Lacronique V, Giovannini M, Daniel MT, et al. TEL-JAK2 transgenic mice develop T-cell leukemia. *Blood*. 2000;95(12):3891-9.

89. Cuesta-Dominguez A, Ortega M, Ormazabal C, Santos-Roncero M, Galan-Diez M, Steegmann JL, et al. Transforming and tumorigenic activity of JAK2 by fusion to BCR: molecular mechanisms of action of a novel BCR-JAK2 tyrosine-kinase. *PLoS One*. 2012;7(2):e32451.

90. Ihle JN. Cytokine receptor signalling. *Nature*. 1995;377(6550):591-4.

91. Krolewski JJ, Lee R, Eddy R, Shows TB, Dalla-Favera R. Identification and chromosomal mapping of new human tyrosine kinase genes. *Oncogene*. 1990;5(3):277-82.

92. Velazquez L, Fellous M, Stark GR, Pellegrini S. A protein tyrosine kinase in the interferon alpha/beta signaling pathway. *Cell*. 1992;70(2):313-22.

93. Vogelstein B, Papadopoulos N, Velculescu VE, Zhou S, Diaz LA, Jr., Kinzler KW. Cancer genome landscapes. *Science*. 2013;339(6127):1546-58.

94. Hanahan D, Weinberg RA. Hallmarks of cancer: the next generation. *Cell*. 2011;144(5):646-74.

95. O'Shea JJ, Holland SM, Staudt LM. JAKs and STATs in immunity, immunodeficiency, and cancer. *N Engl J Med*. 2013;368(2):161-70.

96. Schwartz DM, Kanno Y, Villarino A, Ward M, Gadina M, O'Shea JJ. JAK inhibition as a therapeutic strategy for immune and inflammatory diseases. *Nat Rev Drug Discov*. 2017;17(1):78.

97. Strobl B, Stoiber D, Sexl V, Mueller M. Tyrosine kinase 2 (TYK2) in cytokine signalling and host immunity. *Front Biosci (Landmark Ed)*. 2011;16:3214-32.

98. Minegishi Y, Saito M, Morio T, Watanabe K, Agematsu K, Tsuchiya S, et al. Human tyrosine kinase 2 deficiency reveals its requisite roles in multiple cytokine signals involved in innate and acquired immunity. *Immunity*. 2006;25(5):745-55.

99. Kilic SS, Hacimustafaoglu M, Boisson-Dupuis S, Kreins AY, Grant AV, Abel L, et al. A patient with tyrosine kinase 2 deficiency without hyper-IgE syndrome. *J Pediatr*. 2012;160(6):1055-7.

100. Leitner NR, Witalisz-Siepracka A, Strobl B, Muller M. Tyrosine kinase 2 - Surveillant of tumours and bona fide oncogene. *Cytokine*. 2017;89:209-18.

101. Shimoda K, Kamesaki K, Numata A, Aoki K, Matsuda T, Oritani K, et al. Cutting edge: tyk2 is required for the induction and nuclear translocation of Daxx which regulates IFN-alpha-induced suppression of B lymphocyte formation. *J Immunol*. 2002;169(9):4707-11.

102. Ubel C, Mousset S, Trufa D, Sirbu H, Finotto S. Establishing the role of tyrosine kinase 2 in cancer. *Oncoimmunology*. 2013;2(1):e22840.

103. Gamero AM, Potla R, Wegrzyn J, Szelag M, Edling AE, Shimoda K, et al. Activation of Tyk2 and Stat3 is required for the apoptotic actions of interferon-beta in primary pro-B cells. *J Biol Chem*. 2006;281(24):16238-44.

104. Stoiber D, Kovacic B, Schuster C, Schellack C, Karaghiosoff M, Kreibich R, et al. TYK2 is a key regulator of the surveillance of B lymphoid tumors. *J Clin Invest*. 2004;114(11):1650-8.

105. Prchal-Murphy M, Witalisz-Siepracka A, Bednarik KT, Putz EM, Gotthardt D, Meissl K, et al. In vivo tumor surveillance by NK cells requires TYK2 but not TYK2 kinase activity. *Oncoimmunology*. 2015;4(11):e1047579.

106. Silver DL, Naora H, Liu J, Cheng W, Montell DJ. Activated signal transducer and activator of transcription (STAT) 3: localization in focal adhesions and function in ovarian cancer cell motility. *Cancer Res*. 2004;64(10):3550-8.

107. Ide H, Nakagawa T, Terado Y, Kamiyama Y, Muto S, Horie S. Tyk2 expression and its signaling enhances the invasiveness of prostate cancer cells. *Biochem Biophys Res Commun*. 2008;369(2):292-6.

108. Song XC, Fu G, Yang X, Jiang Z, Wang Y, Zhou GW. Protein expression profiling of breast cancer cells by dissociable antibody microarray (DAMA) staining. *Mol Cell Proteomics*. 2008;7(1):163-9.

109. Santos J, Mesquita D, Barros-Silva JD, Jeronimo C, Henrique R, Morais A, et al. Uncovering potential downstream targets of oncogenic GRPR overexpression in prostate carcinomas harboring ETS rearrangements. *Oncoscience*. 2015;2(5):497-507.

110. Prutsch N, Gurnhofer E, Suske T, Liang HC, Schlederer M, Roos S, et al. Dependency on the TYK2/STAT1/MCL1 axis in anaplastic large cell lymphoma. *Leukemia*. 2019;33(3):696-709.

111. Sanda T, Tyner JW, Gutierrez A, Ngo VN, Glover J, Chang BH, et al. TYK2-STAT1-BCL2 pathway dependence in T-cell acute lymphoblastic leukemia. *Cancer Discov*. 2013;3(5):564-77.

112. Vainchenker W, Constantinescu SN. JAK/STAT signaling in hematological malignancies. *Oncogene*. 2013;32(21):2601-13.

113. Velusamy T, Kiel MJ, Sahasrabuddhe AA, Rolland D, Dixon CA, Bailey NG, et al. A novel recurrent NPM1-TYK2 gene fusion in cutaneous CD30-positive lymphoproliferative disorders. *Blood*. 2014;124(25):3768-71.

114. Crescenzo R, Abate F, Lasorsa E, Tabbo F, Gaudiano M, Chiesa N, et al. Convergent mutations and kinase fusions lead to oncogenic STAT3 activation in anaplastic large cell lymphoma. *Cancer Cell*. 2015;27(4):516-32.

115. Tomasson MH, Xiang Z, Walgren R, Zhao Y, Kasai Y, Miner T, et al. Somatic mutations and germline sequence variants in the expressed tyrosine kinase genes of patients with de novo acute myeloid leukemia. *Blood*. 2008;111(9):4797-808.

116. Tron AE, Keeton EK, Ye M, Casas-Selves M, Chen H, Dillman KS, et al. Next-generation sequencing identifies a novel ELAVL1-TYK2 fusion gene in MOLM-16, an AML cell line highly sensitive to the PIM kinase inhibitor AZD1208. *Leuk Lymphoma*. 2016;57(12):2927-9.

117. Woss K, Simonovic N, Strobl B, Macho-Maschler S, Muller M. TYK2: An Upstream Kinase of STATs in Cancer. *Cancers (Basel)*. 2019;11(11).

118. Edmonson MN, Patel AN, Hedges DJ, Wang Z, Rampersaud E, Kesserwan CA, et al. Pediatric Cancer Variant Pathogenicity Information Exchange (PeCanPIE): a cloud-based platform for curating and classifying germline variants. *Genome Res*. 2019;29(9):1555-65.

119. Ma X, Liu Y, Liu Y, Alexandrov LB, Edmonson MN, Gawad C, et al. Pan-cancer genome and transcriptome analyses of 1,699 paediatric leukaemias and solid tumours. *Nature*. 2018;555(7696):371-6.

120. Waanders E, Scheijen B, Jongmans MC, Venselaar H, van Reijmersdal SV, van Dijk AH, et al. Germline activating TYK2 mutations in pediatric patients with two primary acute lymphoblastic leukemia occurrences. *Leukemia*. 2017;31(4):821-8.

121. Hammaren HM, Virtanen AT, Raivola J, Silvennoinen O. The regulation of JAKs in cytokine signaling and its breakdown in disease. *Cytokine*. 2019;118:48-63.

122. Kisseleva T, Bhattacharya S, Braunstein J, Schindler CW. Signaling through the JAK/STAT pathway, recent advances and future challenges. *Gene*. 2002;285(1-2):1-24.

123. Watowich SS, Wu H, Socolovsky M, Klingmuller U, Constantinescu SN, Lodish HF. Cytokine receptor signal transduction and the control of hematopoietic cell development. *Annu Rev Cell Dev Biol*. 1996;12:91-128.

124. Schindler C, Levy DE, Decker T. JAK-STAT signaling: from interferons to cytokines. *J Biol Chem*. 2007;282(28):20059-63.

125. Ghoreschi K, Laurence A, O'Shea JJ. Janus kinases in immune cell signaling. *Immunol Rev*. 2009;228(1):273-87.

126. Bacon CM, McVicar DW, Ortaldo JR, Rees RC, O'Shea JJ, Johnston JA. Interleukin 12 (IL-12) induces tyrosine phosphorylation of JAK2 and TYK2: differential use of Janus family tyrosine kinases by IL-2 and IL-12. *J Exp Med*. 1995;181(1):399-404.

127. Muller M, Briscoe J, Laxton C, Guschin D, Ziemiecki A, Silvennoinen O, et al. The protein tyrosine kinase JAK1 complements defects in interferon-alpha/beta and -gamma signal transduction. *Nature*. 1993;366(6451):129-35.

128. Staerk J, Kallin A, Demoulin JB, Vainchenker W, Constantinescu SN. JAK1 and Tyk2 activation by the homologous polycythemia vera JAK2 V617F mutation: cross-talk with IGF1 receptor. *J Biol Chem*. 2005;280(51):41893-9.

129. Shide K, Shimoda K, Kamezaki K, Kakumitsu H, Kumano T, Numata A, et al. Tyk2 mutation homologous to V617F Jak2 is not found in essential thrombocythaemia, although it induces constitutive signaling and growth factor independence. *Leuk Res*. 2007;31(8):1077-84.

130. Bousoik E, Montazeri Aliabadi H. "Do We Know Jack" About JAK? A Closer Look at JAK/STAT Signaling Pathway. *Front Oncol*. 2018;8:287.

131. Petkau G, Turner M. Signalling circuits that direct early B-cell development. *Biochem J*. 2019;476(5):769-78.

132. Greaves SA, Babolin C, Torres RM, Pelanda R. Ras, Erk, and PI3K signaling pathways in the central selection of B cells. 2017;198(1 Supplement):202.6-.6.

133. Nguyen MH, Ho JM, Beattie BK, Barber DL. TEL-JAK2 mediates constitutive activation of the phosphatidylinositol 3'-kinase/protein kinase B signaling pathway. *J Biol Chem*. 2001;276(35):32704-13.

134. Babon JJ, Lucet IS, Murphy JM, Nicola NA, Varghese LN. The molecular regulation of Janus kinase (JAK) activation. *Biochem J*. 2014;462(1):1-13.

135. Min X, Ungureanu D, Maxwell S, Hammaren H, Thibault S, Hillert EK, et al. Structural and Functional Characterization of the JH2 Pseudokinase Domain of JAK Family Tyrosine Kinase 2 (TYK2). *J Biol Chem*. 2015;290(45):27261-70.

136. Lupardus PJ, Ultsch M, Wallweber H, Bir Kohli P, Johnson AR, Eigenbrot C. Structure of the pseudokinase-kinase domains from protein kinase TYK2 reveals a mechanism for Janus kinase (JAK) autoinhibition. *Proc Natl Acad Sci U S A*. 2014;111(22):8025-30.

137. Babon JJ, Kershaw NJ, Murphy JM, Varghese LN, Laktyushin A, Young SN, et al. Suppression of cytokine signaling by SOCS3: characterization of the mode of inhibition and the basis of its specificity. *Immunity*. 2012;36(2):239-50.

138. Piganis RA, De Weerd NA, Gould JA, Schindler CW, Mansell A, Nicholson SE, et al. Suppressor of cytokine signaling (SOCS) 1 inhibits type I interferon (IFN) signaling via the interferon alpha receptor (IFNAR1)-associated tyrosine kinase Tyk2. *J Biol Chem*. 2011;286(39):33811-8.

139. Bollu LR, Mazumdar A, Savage MI, Brown PH. Molecular Pathways: Targeting Protein Tyrosine Phosphatases in Cancer. *Clin Cancer Res*. 2017;23(9):2136-42.

140. Myers MP, Andersen JN, Cheng A, Tremblay ML, Horvath CM, Parisien JP, et al. TYK2 and JAK2 are substrates of protein-tyrosine phosphatase 1B. *J Biol Chem*. 2001;276(51):47771-4.

141. Bocchini CE, Kasembeli MM, Roh SH, Tweardy DJ. Contribution of chaperones to STAT pathway signaling. *JAKSTAT*. 2014;3(3):e970459.

142. Taipale M, Jarosz DF, Lindquist S. HSP90 at the hub of protein homeostasis: emerging mechanistic insights. *Nat Rev Mol Cell Biol*. 2010;11(7):515-28.

143. Prodromou C. Mechanisms of Hsp90 regulation. *Biochem J*. 2016;473(16):2439-52.

144. Jaeger AM, Whitesell L. HSP90: Enabler of Cancer Adaptation. 2019;3(1):275-97.

145. Trepel J, Mollapour M, Giaccone G, Neckers L. Targeting the dynamic HSP90 complex in cancer. *Nat Rev Cancer*. 2010;10(8):537-49.

146. Weigert O, Lane AA, Bird L, Kopp N, Chapuy B, van Bodegom D, et al. Genetic resistance to JAK2 enzymatic inhibitors is overcome by HSP90 inhibition. *J Exp Med*. 2012;209(2):259-73.

147. Schoof N, von Bonin F, Trumper L, Kube D. HSP90 is essential for Jak-STAT signaling in classical Hodgkin lymphoma cells. *Cell Commun Signal*. 2009;7:17.

148. Kucine N, Marubayashi S, Bhagwat N, Papalexi E, Koppikar P, Sanchez Martin M, et al. Tumor-specific HSP90 inhibition as a therapeutic approach in JAK-mutant acute lymphoblastic leukemias. *Blood*. 2015;126(22):2479-83.

149. Taipale M, Krykbaeva I, Koeva M, Kayatekin C, Westover KD, Karras GI, et al. Quantitative analysis of HSP90-client interactions reveals principles of substrate recognition. *Cell*. 2012;150(5):987-1001.

150. Akahane K, Sanda T, Mansour MR, Radimerski T, DeAngelo DJ, Weinstock DM, et al. HSP90 inhibition leads to degradation of the TYK2 kinase and apoptotic cell death in T-cell acute lymphoblastic leukemia. *Leukemia*. 2016;30(1):219-28.

151. Kramer OH, Mahboobi S, Sellmer A. Drugging the HDAC6-HSP90 interplay in malignant cells. *Trends Pharmacol Sci*. 2014;35(10):501-9.

152. Nusinzon I, Horvath CM. Unexpected roles for deacetylation in interferon- and cytokine-induced transcription. *J Interferon Cytokine Res*. 2005;25(12):745-8.

153. Buchwald M, Kramer OH, Heinzel T. HDACi--targets beyond chromatin. *Cancer Lett*. 2009;280(2):160-7.

154. Wieczorek M, Ginter T, Brand P, Heinzel T, Kramer OH. Acetylation modulates the STAT signaling code. *Cytokine Growth Factor Rev*. 2012;23(6):293-305.

155. Rascle A, Johnston JA, Amati B. Deacetylase activity is required for recruitment of the basal transcription machinery and transactivation by STAT5. *Mol Cell Biol*. 2003;23(12):4162-73.

156. Nusinzon I, Horvath CM. Interferon-stimulated transcription and innate antiviral immunity require deacetylase activity and histone deacetylase 1. *Proc Natl Acad Sci U S A*. 2003;100(25):14742-7.

157. Chang HM, Paulson M, Holko M, Rice CM, Williams BR, Marie I, et al. Induction of interferon-stimulated gene expression and antiviral responses require protein deacetylase activity. *Proc Natl Acad Sci U S A*. 2004;101(26):9578-83.

158. Sakamoto S, Potla R, Larner AC. Histone deacetylase activity is required to recruit RNA polymerase II to the promoters of selected interferon-stimulated early response genes. *J Biol Chem*. 2004;279(39):40362-7.

159. Klampfer L, Huang J, Swaby LA, Augenlicht L. Requirement of histone deacetylase activity for signaling by STAT1. *J Biol Chem*. 2004;279(29):30358-68.

160. Zhuang S. Regulation of STAT signaling by acetylation. *Cell Signal*. 2013;25(9):1924-31.

161. Tambaro FP, Dell'aversana C, Carafa V, Nebbioso A, Radic B, Ferrara F, et al. Histone deacetylase inhibitors: clinical implications for hematological malignancies. *Clin Epigenetics*. 2010;1(1-2):25-44.

162. Chun P. Histone deacetylase inhibitors in hematological malignancies and solid tumors. *Arch Pharm Res*. 2015;38(6):933-49.

163. Xu WS, Parmigiani RB, Marks PA. Histone deacetylase inhibitors: molecular mechanisms of action. *Oncogene*. 2007;26(37):5541-52.

164. Pui CH, Evans WE. Treatment of acute lymphoblastic leukemia. *N Engl J Med*. 2006;354(2):166-78.

165. Lee JW, Cho B. Prognostic factors and treatment of pediatric acute lymphoblastic leukemia. *Korean J Pediatr*. 2017;60(5):129-37.

166. Poon LM, Hamdi A, Saliba R, Rondon G, Ledesma C, Kendrick M, et al. Outcomes of adults with acute lymphoblastic leukemia relapsing after allogeneic hematopoietic stem cell transplantation. *Biol Blood Marrow Transplant*. 2013;19(7):1059-64.

167. Mei L, Ontiveros EP, Griffiths EA, Thompson JE, Wang ES, Wetzler M. Pharmacogenetics predictive of response and toxicity in acute lymphoblastic leukemia therapy. *Blood Rev*. 2015;29(4):243-9.

168. Vrooman LM, Stevenson KE, Supko JG, O'Brien J, Dahlberg SE, Asselin BL, et al. Postinduction dexamethasone and individualized dosing of Escherichia Coli L-asparaginase each improve outcome of

children and adolescents with newly diagnosed acute lymphoblastic leukemia: results from a randomized study--Dana-Farber Cancer Institute ALL Consortium Protocol 00-01. *J Clin Oncol*. 2013;31(9):1202-10.

169. Goossens S, Van Vlierberghe P. Overcoming Steroid Resistance in T Cell Acute Lymphoblastic Leukemia. *PLoS Med*. 2016;13(12):e1002208.

170. Silverman LB. Balancing cure and long-term risks in acute lymphoblastic leukemia. *Hematology Am Soc Hematol Educ Program*. 2014;2014(1):190-7.

171. Pui CH, Cheng C, Leung W, Rai SN, Rivera GK, Sandlund JT, et al. Extended follow-up of long-term survivors of childhood acute lymphoblastic leukemia. *N Engl J Med*. 2003;349(7):640-9.

172. Friedman DL, Rovo A, Leisenring W, Locasciulli A, Flowers ME, Tichelli A, et al. Increased risk of breast cancer among survivors of allogeneic hematopoietic cell transplantation: a report from the FHCRC and the EBMT-Late Effect Working Party. *Blood*. 2008;111(2):939-44.

173. Rizzo JD, Curtis RE, Socie G, Sobocinski KA, Gilbert E, Landgren O, et al. Solid cancers after allogeneic hematopoietic cell transplantation. *Blood*. 2009;113(5):1175-83.

174. Sanders JE, Hoffmeister PA, Woolfrey AE, Carpenter PA, Storer BE, Storb RF, et al. Thyroid function following hematopoietic cell transplantation in children: 30 years' experience. *Blood*. 2009;113(2):306-8.

175. El Fakih R, Ahmed S, Alfraih F, Hanbali A. Hematopoietic cell transplantation for acute lymphoblastic leukemia in adult patients. *Hematol Oncol Stem Cell Ther*. 2017;10(4):252-8.

176. Li Y, Buijs-Gladdines JG, Cante-Barrett K, Stubbs AP, Vroegindeweij EM, Smits WK, et al. IL-7 Receptor Mutations and Steroid Resistance in Pediatric T cell Acute Lymphoblastic Leukemia: A Genome Sequencing Study. *PLoS Med*. 2016;13(12):e1002200.

177. Oshima K, Khiabanian H, da Silva-Almeida AC, Tzoneva G, Abate F, Ambesi-Impiombato A, et al. Mutational landscape, clonal evolution patterns, and role of RAS mutations in relapsed acute lymphoblastic leukemia. *Proc Natl Acad Sci U S A*. 2016;113(40):11306-11.

178. Daver N, Thomas D, Ravandi F, Cortes J, Garris R, Jabbour E, et al. Final report of a phase II study of imatinib mesylate with hyper-CVAD for the front-line treatment of adult patients with Philadelphia chromosome-positive acute lymphoblastic leukemia. *Haematologica*. 2015;100(5):653-61.

179. Thomas DA, Faderl S, Cortes J, O'Brien S, Giles FJ, Kornblau SM, et al. Treatment of Philadelphia chromosome-positive acute lymphocytic leukemia with hyper-CVAD and imatinib mesylate. *Blood*. 2004;103(12):4396-407.

180. O'Hare T, Corbin AS, Druker BJ. Targeted CML therapy: controlling drug resistance, seeking cure. *Curr Opin Genet Dev*. 2006;16(1):92-9.

181. Ottmann OG. Management of Philadelphia chromosome-positive acute lymphoblastic leukemia. *Leuk Suppl*. 2012;1(Suppl 2):S7-9.

182. Steelman LS, Pohnert SC, Shelton JG, Franklin RA, Bertrand FE, McCubrey JA. JAK/STAT, Raf/MEK/ERK, PI3K/Akt and BCR-ABL in cell cycle progression and leukemogenesis. *Leukemia*. 2004;18(2):189-218.

183. Leoni V, Biondi A. Tyrosine kinase inhibitors in BCR-ABL positive acute lymphoblastic leukemia. *Haematologica*. 2015;100(3):295-9.

184. Yeung DT, Moulton DJ, Heatley SL, Nievergall E, Dang P, Braley J, et al. Relapse of BCR-ABL1-like ALL mediated by the ABL1 kinase domain mutation T315I following initial response to dasatinib treatment. *Leukemia*. 2015;29(1):230-2.

185. Kobayashi K, Miyagawa N, Mitsui K, Matsuoka M, Kojima Y, Takahashi H, et al. TKI dasatinib monotherapy for a patient with Ph-like ALL bearing ATF7IP/PDGFRB translocation. *Pediatr Blood Cancer*. 2015;62(6):1058-60.

186. Harrison C, Kiladjian JJ, Al-Ali HK, Gisslinger H, Waltzman R, Stalbovskaya V, et al. JAK inhibition with ruxolitinib versus best available therapy for myelofibrosis. *N Engl J Med*. 2012;366(9):787-98.

187. Verstovsek S, Kantarjian H, Mesa RA, Pardanani AD, Cortes-Franco J, Thomas DA, et al. Safety and efficacy of INCB018424, a JAK1 and JAK2 inhibitor, in myelofibrosis. *N Engl J Med*. 2010;363(12):1117-27.

188. Verstovsek S, Mesa RA, Gotlib J, Levy RS, Gupta V, DiPersio JF, et al. A double-blind, placebo-controlled trial of ruxolitinib for myelofibrosis. *N Engl J Med*. 2012;366(9):799-807.

189. Mascarenhas J, Hoffman R. Ruxolitinib: the first FDA approved therapy for the treatment of myelofibrosis. *Clin Cancer Res*. 2012;18(11):3008-14.

190. Verstovsek S, Mesa RA, Gotlib J, Gupta V, DiPersio JF, Catalano JV, et al. Long-term treatment with ruxolitinib for patients with myelofibrosis: 5-year update from the randomized, double-blind, placebo-controlled, phase 3 COMFORT-I trial. *J Hematol Oncol*. 2017;10(1):55.

191. Harrison C, Vannucchi AM. Ruxolitinib: a potent and selective Janus kinase 1 and 2 inhibitor in patients with myelofibrosis. An update for clinicians. *Ther Adv Hematol*. 2012;3(6):341-54.

192. Suryani S, Bracken LS, Harvey RC, Sia KC, Carol H, Chen IM, et al. Evaluation of the in vitro and in vivo efficacy of the JAK inhibitor AZD1480 against JAK-mutated acute lymphoblastic leukemia. *Mol Cancer Ther*. 2015;14(2):364-74.

193. Wu SC, Li LS, Kopp N, Montero J, Chapuy B, Yoda A, et al. Activity of the Type II JAK2 Inhibitor CHZ868 in B Cell Acute Lymphoblastic Leukemia. *Cancer Cell*. 2015;28(1):29-41.

194. Akahane K, Li Z, Etchin J, Berezovskaya A, Gjini E, Masse CE, et al. Anti-leukaemic activity of the TYK2 selective inhibitor NDI-031301 in T-cell acute lymphoblastic leukaemia. *Br J Haematol*. 2017;177(2):271-82.

195. Maude SL, Dolai S, Delgado-Martin C, Vincent T, Robbins A, Selvanathan A, et al. Efficacy of JAK/STAT pathway inhibition in murine xenograft models of early T-cell precursor (ETP) acute lymphoblastic leukemia. *Blood*. 2015;125(11):1759-67.

196. Treanor LM, Zhou S, Janke L, Churchman ML, Ma Z, Lu T, et al. Interleukin-7 receptor mutants initiate early T cell precursor leukemia in murine thymocyte progenitors with multipotent potential. *J Exp Med*. 2014;211(4):701-13.

197. Kotb A, El Fakih R, Hanbali A, Hawsawi Y, Alfraih F, Hashmi S, et al. Philadelphia-like acute lymphoblastic leukemia: diagnostic dilemma and management perspectives. *Exp Hematol*. 2018;67:1-9.

198. Tasian SK, Teachey DT, Li Y, Shen F, Harvey RC, Chen IM, et al. Potent efficacy of combined PI3K/mTOR and JAK or ABL inhibition in murine xenograft models of Ph-like acute lymphoblastic leukemia. *Blood*. 2017;129(2):177-87.

199. Savino AM, Sarno J, Trentin L, Vieri M, Fazio G, Bardini M, et al. The histone deacetylase inhibitor givinostat (ITF2357) exhibits potent anti-tumor activity against CRLF2-rearranged BCP-ALL. *Leukemia*. 2017.

200. Scuto A, Kirschbaum M, Kowolik C, Kretzner L, Juhasz A, Atadja P, et al. The novel histone deacetylase inhibitor, LBH589, induces expression of DNA damage response genes and apoptosis in Ph- acute lymphoblastic leukemia cells. *Blood*. 2008;111(10):5093-100.

201. Ott CJ, Kopp N, Bird L, Paranal RM, Qi J, Bowman T, et al. BET bromodomain inhibition targets both c-Myc and IL7R in high-risk acute lymphoblastic leukemia. *Blood*. 2012;120(14):2843-52.

202. Jones D, Thomas D, Yin CC, O'Brien S, Cortes JE, Jabbour E, et al. Kinase domain point mutations in Philadelphia chromosome-positive acute lymphoblastic leukemia emerge after therapy with BCR-ABL kinase inhibitors. *Cancer*. 2008;113(5):985-94.

203. Branford S, Rudzki Z, Walsh S, Parkinson I, Grigg A, Szer J, et al. Detection of BCR-ABL mutations in patients with CML treated with imatinib is virtually always accompanied by clinical resistance, and mutations in the ATP phosphate-binding loop (P-loop) are associated with a poor prognosis. *Blood*. 2003;102(1):276-83.

204. Weisberg E, Griffin JD. Mechanism of resistance to the ABL tyrosine kinase inhibitor STI571 in BCR/ABL-transformed hematopoietic cell lines. *Blood*. 2000;95(11):3498-505.

205. Barnes DJ, Palaiologou D, Panousopoulou E, Schultheis B, Yong AS, Wong A, et al. Bcr-Abl expression levels determine the rate of development of resistance to imatinib mesylate in chronic myeloid leukemia. *Cancer Res*. 2005;65(19):8912-9.

206. Eadie LN, Hughes TP, White DL. Interaction of the efflux transporters ABCB1 and ABCG2 with imatinib, nilotinib, and dasatinib. *Clin Pharmacol Ther*. 2014;95(3):294-306.

207. Watkins DB, Hughes TP, White DL. OCT1 and imatinib transport in CML: is it clinically relevant? *Leukemia*. 2015;29(10):1960-9.

208. Thomas J, Wang L, Clark RE, Pirmohamed M. Active transport of imatinib into and out of cells: implications for drug resistance. *Blood*. 2004;104(12):3739-45.

209. Soverini S, Colarossi S, Gnani A, Castagnetti F, Rosti G, Bosi C, et al. Resistance to dasatinib in Philadelphia-positive leukemia patients and the presence or the selection of mutations at residues 315 and 317 in the BCR-ABL kinase domain. *Haematologica*. 2007;92(3):401-4.

210. Watanabe K, Minami Y, Ozawa Y, Miyamura K, Naoe T. T315I mutation in Ph-positive acute lymphoblastic leukemia is associated with a highly aggressive disease phenotype: three case reports. *Anticancer Res*. 2012;32(5):1779-83.

211. Vajpai N, Strauss A, Fendrich G, Cowan-Jacob SW, Manley PW, Grzesiek S, et al. Solution conformations and dynamics of ABL kinase-inhibitor complexes determined by NMR substantiate the different binding modes of imatinib/nilotinib and dasatinib. *J Biol Chem*. 2008;283(26):18292-302.

212. Sasaki K, Jabbour EJ, Ravandi F, Short NJ, Thomas DA, Garcia-Manero G, et al. Hyper-CVAD plus ponatinib versus hyper-CVAD plus dasatinib as frontline therapy for patients with Philadelphia chromosome-positive acute lymphoblastic leukemia: A propensity score analysis. *Cancer*. 2016;122(23):3650-6.

213. Thomas X, Heiblig M. Diagnostic and treatment of adult Philadelphia chromosome-positive acute lymphoblastic leukemia. *Int J Hematol Oncol*. 2016;5(2):77-90.

214. Westerweel PE, Te Boekhorst PAW, Levin MD, Cornelissen JJ. New Approaches and Treatment Combinations for the Management of Chronic Myeloid Leukemia. *Front Oncol*. 2019;9:665.

215. Verstovsek S, Mesa RA, Gotlib J, Levy RS, Gupta V, DiPersio JF, et al. Efficacy, safety, and survival with ruxolitinib in patients with myelofibrosis: results of a median 3-year follow-up of COMFORT-I. *Haematologica*. 2015;100(4):479-88.

216. Cervantes F, Vannucchi AM, Kiladjian JJ, Al-Ali HK, Sirulnik A, Stalbovskaya V, et al. Three-year efficacy, safety, and survival findings from COMFORT-II, a phase 3 study comparing ruxolitinib with best available therapy for myelofibrosis. *Blood*. 2013;122(25):4047-53.

217. Deshpande A, Reddy MM, Schade GO, Ray A, Chowdary TK, Griffin JD, et al. Kinase domain mutations confer resistance to novel inhibitors targeting JAK2V617F in myeloproliferative neoplasms. *Leukemia*. 2012;26(4):708-15.

218. Hornakova T, Springuel L, Devreux J, Dusa A, Constantinescu SN, Knoops L, et al. Oncogenic JAK1 and JAK2-activating mutations resistant to ATP-competitive inhibitors. *Haematologica*. 2011;96(6):845-53.

219. Koppikar P, Bhagwat N, Kilpivaara O, Manshouri T, Adli M, Hricik T, et al. Heterodimeric JAK-STAT activation as a mechanism of persistence to JAK2 inhibitor therapy. *Nature*. 2012;489(7414):155-9.

220. Meyer SC, Keller MD, Chiu S, Koppikar P, Guryanova OA, Rapaport F, et al. CHZ868, a Type II JAK2 Inhibitor, Reverses Type I JAK Inhibitor Persistence and Demonstrates Efficacy in Myeloproliferative Neoplasms. *Cancer Cell*. 2015;28(1):15-28.

221. Lim K-H, Chang Y-C, Chiang Y-H, Lin H-C, Huang L, Wang W-T, et al. Acquired Resistance to JAK Inhibitors in Calr-Mutated Myeloproliferative Neoplasms. *Blood*. 2019;134(Supplement_1):2970-.

222. Andreoli A, Verger E, Robin M, Raffoux E, Zini J-M, Rousselot P, et al. Clinical Resistance To Ruxolitinib Is More Frequent In Patients Without MPN-Associated Mutations and Is Rarely Due To Mutations In The JAK2 Kinase Drug-Binding Domain. *Blood*. 2013;122(21):1591-.

223. Meyer SC. Mechanisms of Resistance to JAK2 Inhibitors in Myeloproliferative Neoplasms. *Hematol Oncol Clin North Am*. 2017;31(4):627-42.

224. Andraos R, Qian Z, Bonenfant D, Rubert J, Vangrevelinghe E, Scheufler C, et al. Modulation of activation-loop phosphorylation by JAK inhibitors is binding mode dependent. *Cancer Discov*. 2012;2(6):512-23.

225. Gadina M, Johnson C, Schwartz D, Bonelli M, Hasni S, Kanno Y, et al. Translational and clinical advances in JAK-STAT biology: The present and future of jakinibs. *J Leukoc Biol*. 2018;104(3):499-514.

226. Vainchenker W, Leroy E, Gilles L, Marty C, Plo I, Constantinescu SN. JAK inhibitors for the treatment of myeloproliferative neoplasms and other disorders. *F1000Res*. 2018;7:82.

227. Coffey G, Betz A, DeGuzman F, Pak Y, Inagaki M, Baker DC, et al. The novel kinase inhibitor PRT062070 (Cerdulatinib) demonstrates efficacy in models of autoimmunity and B-cell cancer. *J Pharmacol Exp Ther*. 2014;351(3):538-48.

228. Ma J, Xing W, Coffey G, Dresser K, Lu K, Guo A, et al. Cerdulatinib, a novel dual SYK/JAK kinase inhibitor, has broad anti-tumor activity in both ABC and GCB types of diffuse large B cell lymphoma. *Oncotarget*. 2015;6(41):43881-96.

229. Coffey GP, Feng J, Betz A, Pandey A, Birrell M, Leeds JM, et al. Cerdulatinib Pharmacodynamics and Relationships to Tumor Response Following Oral Dosing in Patients with Relapsed/Refractory B-cell Malignancies. *Clin Cancer Res*. 2019;25(4):1174-84.

230. Flinn I, Hamlin PA, Strickland DK, Pandey A, Birrell M, Coffey G, et al. Phase 1 open-label dose escalation study of the dual SYK/JAK inhibitor cerdulatinib (PRT062070) in patients with relapsed/refractory B-cell malignancies: Safety profile and clinical activity. *Journal of Clinical Oncology*. 2015;33(15_suppl):8531-.

231. Patel AB, O'Hare T, Deininger MW. Mechanisms of Resistance to ABL Kinase Inhibition in Chronic Myeloid Leukemia and the Development of Next Generation ABL Kinase Inhibitors. *Hematol Oncol Clin North Am*. 2017;31(4):589-612.

232. Pardanani A, Hood J, Lasho T, Levine RL, Martin MB, Noronha G, et al. TG101209, a small molecule JAK2-selective kinase inhibitor potently inhibits myeloproliferative disorder-associated JAK2V617F and MPLW515L/K mutations. *Leukemia*. 2007;21(8):1658-68.

233. Ishikawa C, Senba M, Mori N. Anti-adult Tcell leukemia/lymphoma activity of cerdulatinib, a dual SYK/JAK kinase inhibitor. *Int J Oncol*. 2018;53(4):1681-90.

234. Ebadi M, Wasko J, Weisdorf DJ, Gordon PM, Rashidi A. Ruxolitinib combined with chemotherapy can eradicate chemorefractory central nervous system acute lymphoblastic leukaemia. *Br J Haematol*. 2019;187(1):e24-e7.

Appendix

Statement of Authorship

Title of Paper	*TYK2* activating alterations in acute lymphoblastic leukaemia: novel driver oncogenes with remarkable avenues for precision medicine?
Publication Status	☑ Published ☐ Accepted for Publication ☐ Submitted for Publication ☐ Unpublished and Unsubmitted work written in manuscript style
Publication Details	Tavakoli Shirazi P, Eadie LN, Heatley SL, White DL. TYK2 Activating Alterations in Acute Lymphoblastic Leukemia: Novel Driver Oncogenes with Potential Avenues for Precision Medicine? *Journal of Cancer Science and Clinical Therapeutics* 2021 5 201-19

Principal Author

Name of Principal Author (Candidate)	Paniz Tavakoli Shirazi
Contribution to the Paper	Conceived, designed, collected, interpreted/analysed data, wrote and revised manuscript
Overall percentage (%)	95%
Certification	This paper reports on original research I conducted during the period of my Higher Degree by Research candidature and is not subject to any obligations or contractual agreements with a third party that would constrain its inclusion in this thesis. I am the primary author of this paper.
Signature	Date 17/5/21

Co-Author Contributions

By signing the Statement of Authorship, each author certifies that:

i. the candidate's stated contribution to the publication is accurate (as detailed above);
ii. permission is granted for the candidate to include the publication in the thesis; and
iii. the sum of all co-author contributions is equal to 100% less the candidate's stated contribution.

Name of Co-Author	Laura Eadie
Contribution to the Paper	Supervised and critically revised the manuscript
Signature	Date 17/5/21

Name of Co-Author	Susan Heatley
Contribution to the Paper	Supervised and critically revised the manuscript
Signature	Date 17/5/21

Please cut and paste additional co-author panels here as required.

Name of Co-Author	Deborah White
Contribution to the Paper	Supervised and critically revised the manuscript
Signature	Date 17/5/21

TYK2 activating alterations in acute lymphoblastic leukemia: novel driver oncogenes with potential avenues for precision medicine?

Paniz Tavakoli Shirazi[1,2], Laura N Eadie[1,2], Susan L Heatley[1,2], Deborah L White[1,2,3,4,5]

1. Cancer Program, Precision Medicine Theme, South Australian Health & Medical Research Institute (SAHMRI), Adelaide, Australia

2. Faculty of Health and Medical Sciences, University of Adelaide, Adelaide, Australia

4. Faculty of Sciences, University of Adelaide, Adelaide, Australia

5. Australian Genomics Health Alliance (AGHA)

Corresponding author:

Prof. Deborah White (PhD. FFSc(RCPA)).

Director: Cancer Program SAHMRI.

Deputy Theme Leader: Precision Medicine SAHMRI.

NHMRC RD Wright Research Fellow

Beat Cancer Project Principal Research Fellow

Professor: The Faculty of Health and Medical Science, University of Adelaide.

Professor: School of Biological Sciences. The Faculty of Sciences, University of Adelaide.

Cancer Program. Precision Medicine Theme, South Australian Health & Medical Research Institute (SAHMRI), Adelaide, Australia

Phone: +61

E-mail:

Abstract:

Utilization of Next Generation Sequencing (NGS) and advances in genomic profiling have led to identification of new lesions in acute lymphoblastic leukemia (ALL) cases. *TYK2* alterations are among those that warrant an in-depth characterization of the underlying mechanisms that result in leukemogenesis, targetability potential and drug response. The current literature around the functional significance and clinical importance of these alterations in driving hematological cancer (in particular, leukemia) is limited. This review focuses on recent findings demonstrating the leukemogenic potential of *TYK2* alterations. Specifically, the molecular consequences of aberrant TYK2 levels are detailed and the effects of TYK2 deficiency or dysregulated activation are explored in carcinogenesis and leukemogenesis. In addition, the functional role of TYK2 in JAK/STAT signaling, possible cross talk to other cancer-related pathways and overarching avenues for pharmacological intervention in *TYK2*-altered ALL are also described.

Introduction:

Acute lymphoblastic leukemia (ALL) is a hematological malignancy most commonly occurring in children (1, 2). This disease is divided into two key groups: B-cell (B-ALL) and T-cell (T-ALL) lineage, which respectively account for 75-85% and 15-25% of cases depending on the age group (childhood- adult ALL) (3-6). Advances in the treatment of childhood ALL, by improvements in hematopoietic stem cell transplantation (SCT), CNS directed treatment and optimisation of chemotherapy regimens through risk stratification, have resulted in increases in 5-year event free survival rate from approximately 60% in the 1970s to 85% in the 1990s (5). However, relapsed or refractory ALL still occurs in approximately 20% of childhood cases, and for these patients, outcomes are poor (5, 7, 8). Therefore, this malignancy remains a leading cause of non-traumatic death in children. In addition, the outcome for adult patients remains extremely poor with an overall 5-year survival rate of approximately 40% and of these, nearly 7% experience a subsequent relapse (9-11). To overcome the limitations of current chemotherapy and treatment regimens (including SCT), the ultimate approach is personalised medicine that targets specific driver lesions and pathways in individuals. Precision medicine may ultimately improve outcome for these patients and decrease the risk of treatment failure by increasing the anti-leukemic efficacy of treatment and reducing drug associated toxicities. The targeting of *BCR-ABL1*+ leukaemias with ABL tyrosine kinase inhibitors (ABLi) are testament to this approach, and efficacy has also been demonstrated in patients with other *ABL1* and *PDGFRB* fusions (12-17).

ALL is a heterogenous disorder and based on the presence and functional consequence of the various lesions identified in leukemic cells, is divided into subtypes with diverse pathological and prognostic outcome (18, 19). Technologies such as gene expression profiling, single nucleotide polymorphism (SNP) analysis and next generation sequencing (NGS) have drastically improved our understanding of the genomic basis of ALL. Genome-wide profiling studies have enabled identification of novel alterations, refinement of genomic classification and definition of genetically high risk (HR) ALL subgroups. Notably,

HR ALL subtypes are characterized by alterations that activate cytokine receptor, tyrosine kinase and/or JAK/STAT signaling and are associated with poor outcome (10, 20-23). These subtypes are of clinical importance due to potential targetability by small molecule inhibitors (SMIs) (16, 19, 22, 24-30). *TYK2* gain of function alterations, with the potential to activate the JAK/STAT pathway have only recently been described in ALL. However, the functional role of alterations involving *TYK2* in leukemia development and targetability are not, to date, well understood.

Pathology of ALL

ALL is generally thought to be the result of deregulated transcription and maturation arrest of lymphoid lineage cells in the BM (3). This phenomenon is caused by the acquisition of initiating lesions, including gene translocations that confer self-renewal, differentiation arrest and epigenetic reprogramming of lymphoid progenitors (1). Accumulation of additional secondary mutations and genomic alterations, affecting multiple cellular pathways, then contribute to the clinical manifestation of the disease (1, 2). Perturbed pathways comprise those governing lymphoid development, cell cycle regulation, tumour suppression, transcriptional regulation, epigenetic modification, Janus family of tyrosine kinases (JAK)/signal transducer and activator of transcription (STAT) signaling, phosphatidylinositol 3-kinase (PI3K)/mammalian target of rapamycin (mTOR) and RAS signaling (Figure 1). In the case of *TYK2*-altered disease, perturbations in JAK/STAT, PI3K/mTOR, RAS and ERK have been reported (31-35). JAK/STAT is one of the most frequently mutated signaling pathways in cancer; recognised as one of the twelve core cancer pathways (36, 37). In ALL, *JAK* activating alterations are recurrent and account for approximately 10% of HR ALL, 25% of T-ALL cases and 20% of a HR subtype of B-ALL (also known as Ph-Like ALL) (22, 23, 38, 39).

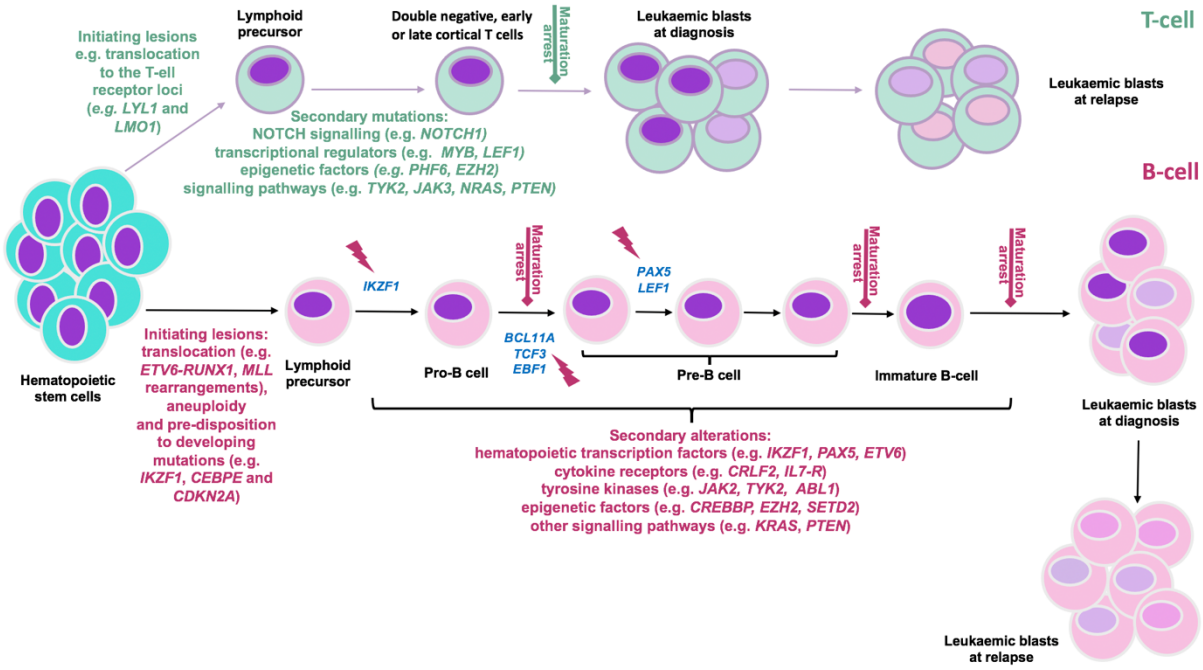

Figure 1. Predisposition and consequent development of ALL can be due to chronological acquisition of deleterious genomic alterations. The differentiation of hematopoietic cells into B- and T-lineage (represented in pink and green respectively) and their maturation is strictly regulated by transcription factors re-enforcing commitment to either fate. T-ALL initiation is mainly due to rearrangement of oncogenic transcription factors (e.g. *LYL1, LMO1)* into a position adjacent to T-cell receptor loci. In the B-ALL setting, changes in chromosome number (aneuploidy); acquisition of chromosomal rearrangements including translocations of genes that 1. control lymphoid development (e.g *ETV6, RUNX1*) 2. activate kinase signaling (e.g. *ABL1*) or oncogenes (e.g. *MYC*) 3. control epigenetic regulation (e.g. *MLL*(*KMT2A*)); and mutations in B-cell transcriptional regulator genes (e.g. *IKZF1, PAX5, EBF1, CEBPE*) and tumour suppressor genes (e.g, *CDKN2A/2B*) confer developmental arrest on lymphoid progenitors at various stages based on the altered genes (indicated by red flash). Subsequently, acquisition of additional co-operating events (as indicated) contribute to development of a genetically polyclonal disease. Selection or acquisition of further mutations can result in resistance to therapy and relapse. Adapted from (1, 2, 38).

TYK2 mediates cytokine signaling and activation of JAK/STAT pathway.

Four human JAKs comprising JAK1, JAK2, JAK3 and TYK2 have been reported and are associated with activation of type I and II cytokines including both interleukin (IL) and interferon (IFN) receptors (40, 41). TYK2 was the first member of the JAK family of tyrosine kinases to be described and linked to cytokine signaling and the downstream JAK/STAT pathway (Figure 2) (42, 43). Cytokine signaling is associated with cross-specificity in activation of overlapping JAKs and STATs (44). TYK2 mediated cytokine signaling has been demonstrated, including type I, II and III IFNs (e.g. IFNα, β and λ) and ILs (e.g IL-6, IL-10, IL-12, IL-22 and IL-23) (45, 46), but importantly the capability of TYK2 to activate all STAT proteins has also been defined (46). Apart from homo-dimerization of JAK family proteins, hetero-dimerization of these proteins can also lead to activation of the JAK/STAT pathway (45, 47). Various studies have reported TYK2 signaling upon dimerization with JAK1 and JAK2 in response to cytokines (Figure 2) (43, 45, 47-50) and the association of TYK2 with JAK1 and/or JAK2 has also been reported in hematological malignancies (32, 35, 51, 52). Here, constitutive TYK2 auto- and trans-phosphorylation due to activating *TYK2* genomic alterations predominantly results in activation of STAT1, 3 and 5 (31-34, 53). Therefore, dependent on the specific cell types, cytokines present and also the disease, multiple JAK and STAT family proteins can be activated in response to TYK2 perturbation.

TYK2 mediates crosstalk with other oncogenic signaling pathways.

JAK signaling and STAT family protein activation can interact with, and induce activation of, several other signaling pathways such as PI3K/mTOR and RAS (46, 54). RAS (family of small GTPases) and PI3K/mTOR signaling pathways are responsible for signal transmission from cytokine, B-cell receptors and tyrosine kinases (55). These signaling pathways are crucial for lineage commitment and development of B-cells in the bone marrow (55, 56). Crosstalk with other oncogenic pathways, has been demonstrated in the setting of B- and T-cell ALL. For example, the aberrant expression of the *ETV6*-

JAK2 fusion gene results in constitutive activation of RAS, PI3K and also NF-κB signaling pathways in the B-ALL setting (57). In T-ALL patients, 2 of 6 *TYK2* activating point mutations were reported to induce activation of extracellular signal-regulated kinase (ERK) signaling, in addition to JAK/STAT activation (33). In other hematological malignancies, activating mutations in *TYK2*, resulted in aberrant signaling through additional pathways such as PI3K/mTOR, RAS and also PIM (proto-oncogene serine/threonine-protein kinases) (34, 35). Taken together, these results demonstrate the capacity of the TYK2 protein to induce activation of additional oncogenic signaling pathways, depending on the specific cell type, mode of activation and disease context.

The interplay in regulation and stabilisation of TYK2 and STAT proteins.

The activity of JAK family proteins including TYK2 is negatively regulated by multiple intrinsic and extrinsic factors. The first intrinsic inhibitory feature includes the regulatory ability of the pseudokinase domain (JH2), to control the kinase domain activity (58-60). In addition, extrinsic negative regulation of the JAK/STAT pathway relies mainly on the SH2 domain-containing suppressors of cytokine signaling (SOCSs) proteins and proteases (e.g. protein tyrosine phosphatases PTPN1, PTPN6 and PTPN11) (45, 58). The SOCS family proteins promote ubiquitination and degradation of JAK family proteins while proteases dephosphorylate activated JAKs and cytokine receptors; both actions lead to attenuation of JAK/STAT signaling (58). Apart from the global role of these negative regulators, previous studies have demonstrated that deactivation of TYK2 signaling and acceleration of TYK2 protein degradation is largely due to direct protein-protein interaction of SOCS1/3, PTPN6 and PTPN1 with activated TYK2 (50, 61-64).

JAK and STAT family proteins are clients of heat shock proteins (HSP), in particular HSP90 (65). The HSP90 chaperone protein plays an important role in maturation, stabilisation, folding and function of JAK and STAT proteins (65-67). Interestingly, HSP90 is identified as the chaperone for various oncogenes

(68, 69). It promotes the functional stability of malignant cells that would otherwise be disrupted due to acquired alterations and increases their adaptability to environmental factors such as treatment (68, 69). This function of HSP90 is also vital in JAK/STAT dependent hematological malignancies and *CRLF2*-rearranged and *JAK2*- and *JAK1*-mutated B-ALL (65, 70-72). In these cases, inhibition of HSP90 by small molecule inhibitors (SMIs) or RNA interference resulted in attenuation of STATs phosphorylation and degradation of JAK proteins (70-72). Proteomic analysis further confirmed the direct interaction of HSP90 with TYK2 protein, enhancing its stability (46, 73). In addition, HSP90 inhibition resulted in TYK2 degradation and signal reduction in T-ALL cells harbouring wildtype and mutant *TYK2* (74).

HSP90 functions through association with several proteins and co-chaperones and is subject to multiple regulatory mechanisms (66, 67). One of these negative regulatory mechanisms involves acetylation of lysine residues on HSP90 that subsequently inhibits the binding of client and co-chaperone proteins leading to aggregation of JAK proteins (67, 75). Therefore, histone deacetylases (HDACs) including HDAC1, 6 and 10 play an important role in facilitating HSP90 activity (67, 75). Immunoprecipitation and western blot analysis, have demonstrated HDAC6 to be the main enzyme that stabilizes the HSP90 complex in multiple leukemia cell lines (76). Inhibition of HDAC6 in these cells resulted in degradation of driver oncogenes such as *BCR-ABL1,* mutated *FLT3* and subsequent reduction of their downstream signaling (76-78).

Moreover, STAT proteins interact with epigenetic co-factors such as histone acetyltransferases (HATs) and HDACs to modulate transcription of target genes (44). Historically, HDACs activity was believed to regulate transcriptional repression only, however, recent studies revealed that both HDACs and HATs can act as activators and/or repressors of STAT-mediated transcription (44, 79-81). HDAC mediated deacetylation of target gene transcriptional activation sites upon, STAT1, 2 and 5 binding to DNA, is essential to recruit the transcription machinery (e.g. RNA polymerase II) and initiate transcription (79, 82-

86). Hence, silencing of HDAC activity through SMIs or small interfering RNAs results in decreased STATs phosphorylation levels and expression of target genes (79, 82-86). However, this is not without conjecture as activation of STAT3 mediated transcription, for instance, is reported to be associated with either acetylation in response to IFN stimulation in the normal setting (87, 88) or deacetylation in B-cell lymphomas (89). It is important to note that the effect of acetylation/deacetylation on transcription can be cell type or condition specific. The exact mechanism by which chromatin modifiers interact with STATs in normal versus malignant cells remains unclear. However, the data highlighting a positive regulatory effect of HDAC is in agreement with the growing evidence of HDAC inhibitors (HDACi) efficacy in hematological malignancies and other cancers (80, 90).

The JAK/STAT signaling network is complex (Figure 2). The TYK2 protein can induce signaling redundancy, alternate signaling through other pathways and interact with positive or negative regulatory components. This interplay enables multiple therapeutic targets and emphasises the importance of careful analysis to find the appropriate inhibitors for each patient and disease context, discussed in further detail below.

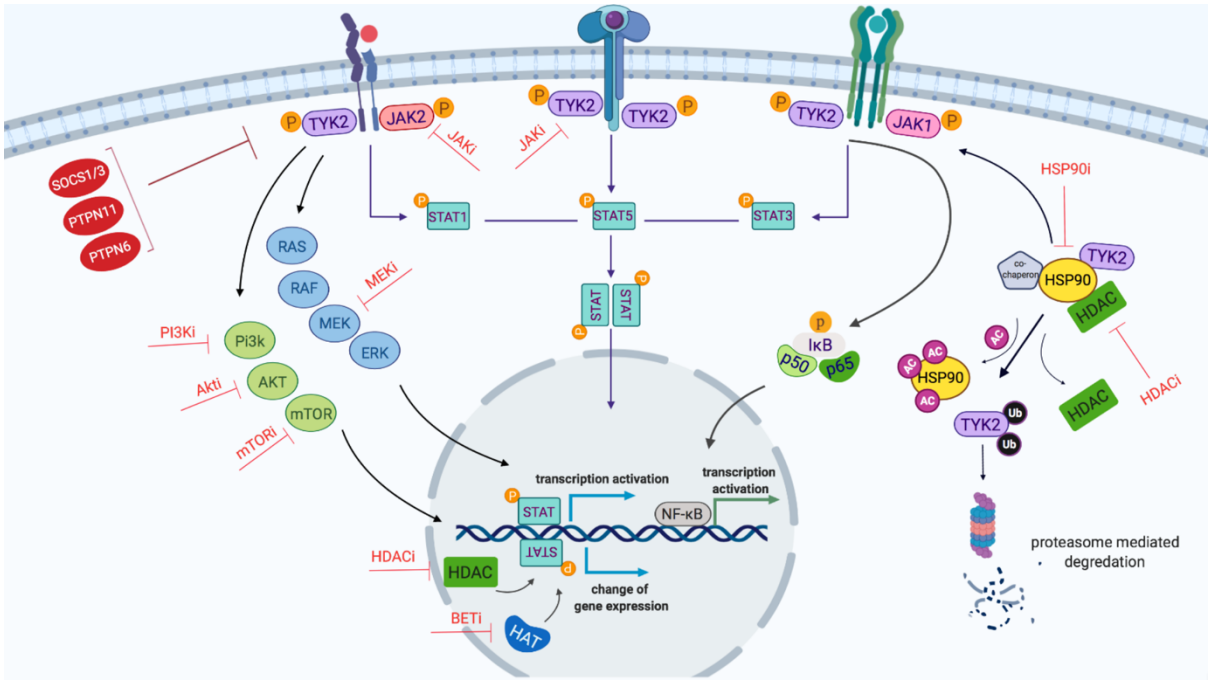

Figure 2. Schematic representation of TYK2-mediated JAK/STAT signaling network. Binding of cytokine to the cytokine receptor complex results in receptor dimerization, which consequently phosphorylates JAK proteins as the cytokine receptor itself lacks intrinsic biological activity. Activated JAKs induce the phosphorylation of STATs which, following dimerization, translocate into the nucleus and stimulate gene expression. STAT family proteins consist of seven members: STAT1-4, 5a, 5b and 6. STATs bind to the enhancer region of genes and by recruiting epigenetic modifiers (HDAC and HAT) to modulate the transcription of genes. JAKs activate other downstream signaling cascades including PI3K/mTOR, RAS and NF-κB. Furthermore, HSP90 and its co-chaperones such as HDAC proteins play an important role in facilitating signaling and JAK protein stabilisation. Red proteins (e.g SOCS1/3) are pathway regulators. Potential inhibitors of the proteins and pathways are indicated with red T-shaped lines. Abbreviations: AC, acetyl group; BET, Bromodomain and Extra-Terminal motif; HATs, histone acetyltransferases; HDAC, histone deacetylates; Ub, Ubiquitin; P, phosphorylation

Can aberrant TYK2 levels cause leukemia?

The involvement of JAK1-3 in inducing cancer have been intensively studied while TYK2 has primarily been studied in the setting of auto-immune and inflammatory diseases (91, 92). Impaired type I IFN and IL signaling due to TYK2 deficiency have been reported in several mouse models (93) but there is limited data in human cases (94, 95). Subsequent genome wide association analyses linked TYK2 deficiency with auto-immune and inflammatory diseases (50). Furthermore, *ex vivo* analysis on bone marrow cells

from wild type and TYK2 deficient mice, demonstrated a reduced inhibition of B-cell lymphopoiesis upon IFNα stimulation in TYK2 deficient cells (96). IFNα signaling can also inhibit B-cell differentiation and induce apoptosis in a normal setting (97). In addition, reduced STAT3 signaling and response to IFNβ-mediated apoptosis have been reported in TYK2 deficient pro-B cells (98). Collectively, these findings highlighted a possible role for TYK2 in the regulation of B-cell apoptosis that may be related to B-cell leukemia. Another study suggested an increased susceptibility of TYK2 deficient mice to the development of B-cell lymphoid leukemia/lymphoma and T-ALL induced by Abelson murine leukemia virus and *ETV6-JAK2* fusion gene, respectively (99). The increased incidence of disease in TYK2 deficient mice compared to wild type controls however, may be explained by the tumour surveillance properties of TYK2, as TYK2-deficient animals also demonstrated reduced cytotoxic activity of T- and natural killer cells (50, 99). Interestingly, the immunosurveillance properties of TYK2 are demonstrated to be independent of its canonical kinase activity. TYK2 deficient mice expressing kinase inactive TYK2 protein (harbouring *TYK2* p.K923E mutation) exhibited normal development of natural killer cells in bone marrow (100). The cytotoxic activity of these natural killer cells against a variety of tumour cells was also restored upon expression of kinase inactive TYK2 protein (107). These results highlight the potential benefit of TYK2 inhibitors (TYK2i) to treat cancers exhibiting higher TYK2 levels and would not lead to impairment of tumour surveillance.

TYK2 overexpression and activation has been demonstrated to be associated with oncogenesis in various cancer cell lines and patient samples (breast, prostate and ovarian cancer) (97, 101-104). For instance, a study by Ide *et al.* (2008) demonstrated increased invasiveness of prostate tumour cells as a result of increased TYK2 expression (102). Another study demonstrated invasion of malignant cells into the liver upon TYK2 protein expression using *in vivo* transgenic mouse models of B-cell lymphoma co-expressing the *c-MYC* oncogene (102). The significance of increased TYK2 expression in hematological malignancies was only recently highlighted in T-ALL (approximately 80% and 60% of lines and cases

screened in the cohort, respectively) and anaplastic large cell lymphoma (ALCL) (33, 105). *TYK2* gene knock down by small interfering RNA, resulted in impaired growth and increased cell apoptosis in more than 60% of patient derived T-ALL cells and cell lines (105). This observation was not reported in other *JAK* family genes and appeared specific to *TYK2* (105). In addition, *TYK2* deletion in mouse models of *NPM-ALK*-induced ALCL and human primary ALCL cells demonstrated prolonged survival in mouse models and reduced growth/increased apoptosis in primary cells (33). Data from both studies also demonstrated the dependency of T-ALL and ALCL cell lines and patient samples on TYK2 activation that leads to upregulation of STAT1/3 and consequently members of anti-apoptotic BCL2 family (33, 105).

***TYK2* alterations occur in ALL patients.**

Reports on gain of function or activating *TYK2* mutations and alterations in hematological malignancies have only recently emerged. In 2013, the first activating *TYK2* mutations (Table 1) were reported in T-ALL cell lines and were demonstrated to have transformative ability; enabling IL-3 dependent pro-B murine Ba/F3 cells harbouring these mutations cytokine independent growth (33). A year later, the first case of a *TYK2* fusion gene was reported in HR subtype of B-ALL (also termed Ph-like ALL; *MYB-TYK2*) (22). Subsequently, two more 5' partners for *TYK2* rearrangements in HR Ph-like ALL (*MYB, SMARCA4* and *ZNF340*) were reported (22, 26). *TYK2* rearrangements have variable 5' partners and breakpoints, yet retain an in-frame kinase domain (also known as JH1; Figure 3), potentially resulting in constitutive activation of the fusion protein. Each fusion may, or may not, contain a disrupted pseudokinase domain (termed JH2), responsible for auto-inhibition of JAK kinase domain (22, 40, 106). In addition, the fusions lack the FERM (four-point one, erzrin, radixin, moesin) and SH-like (Src-homology) domains, which are involved in protein and cytokine receptor binding, respectively (40, 107). Despite the diversity of the 5' partner, 5' genes commonly harbour a DNA binding domain and facilitate the dimerization and subsequent activation of TYK2 (22, 106).

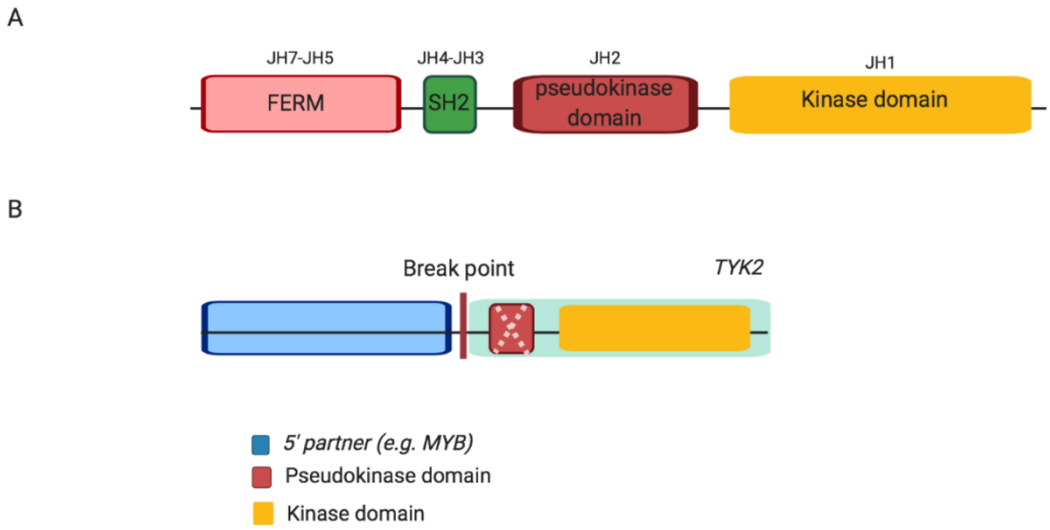

Figure 3. Schematic structure of wild type Jak protein, JAK2 and TYK2 alterations in Ph-like ALL. (A) Wild type Jak, each Jak protein consists of four domains including FERM, SH2, pseudokinase and kinase. (B) *TYK2* alterations, *JAK*-class fusions exhibit an intact kinase domain with either a disrupted or absent (as indicated by dashed cross) pseudokinase domain fused to variable 5' partner genes. Abbreviation: JH, Jak homology domain.

An *in vitro* study demonstrated the ability of the *MYB-TYK2* fusion gene to induce cytokine independent growth in pro-B murine Ba/F3 cells (26). Only recently, additional investigations by our group demonstrated the predominant activation of JAK/STAT signaling and constitutive phosphorylation of TYK2 due to the expression of MYB-TYK2 fusion protein (i (108). The leukemogenic ability of the *MYB-TYK2* fusion gene was also confirmed where the resultant gene fusion induced an aggressive B-ALL in mouse models (108). These findings provided evidence, for the first time, of the leukemogenic potential of *TYK2* fusion genes. Furthermore, *TYK2* alterations have been reported in other blood cancers including acute myeloid leukemia (AML), CD30-positive lymphoproliferative disorder (LPD) and ALCL (31, 32, 34, 109). *In vitro* analysis of *NPM1-TYK2* and *NFKB2-TYK2* fusion genes, detected only in LPD and ALCL patients respectively, demonstrated constitutive auto- and trans-phosphorylation of TYK2 and downstream activation of STAT family proteins (31, 32). However, the oncogenesis potential of these *TYK2* fusion genes in *in vivo* models is unknown. Table 1 highlights the key *TYK2* alterations and the current *in vitro* functional consequences in ALL.

Table 1. Key TYK2 mutations and rearrangements detected in ALL. Modified from Woss *et.al* (2019) (46) and St. Jude PeCan Data portal (110).

***TYK2* alterations**	**Disease**	**Known functional status**	**Domain**	**References**
TYK2 p.G271S	B-ALL	n.d. *	FERM	(111)
TYK2 p.W327R	B-ALL (Ph-Like)	n.d. *	FERM	(22)
TYK2 p.V678L	B-ALL	n.d. *	Pseudokinase (JH2)	(111)
TYK2 p.P760L	B-ALL	increased TYK2 autophosphorylation/ STATs activation	Pseudokinase (JH2)	(53)
TYK2 p.G909S	B-ALL	n.d.	Kinase (JH1)	(110)
TYK2 p.A1156V	B-ALL (Ph-like)	n.d. *	Kinase (JH1)	(110).
MYB-TYK2	B-ALL (Ph-like)	cytokine independent growth (*in vitro)* +STATs activation/ increased TYK2 autophosphorylation/ induced B-ALL in mouse models	Intact kinase (JH1)	(22, 26)
SMARCA4-TYK2	B-ALL (Ph-like)	n.d. *	Intact kinase (JH1)	(10)
ZNF340-TYK2	B-ALL (Ph-like)	n.d. *	Intact kinase (JH1)	(10)
TYK2 p.V15A	T-ALL	n.d.	FERM	(110)
TYK2 p.A35V	T-ALL	n.d.	FERM	(110)
TYK2 p.G36D	T-ALL	cytokine independent growth (*in vitro)*	FERM	(33)
TYK2 p.S47N	T-ALL	cytokine independent growth (*in vitro)*	FERM	(33)
TYK2 p.R425H	T-ALL	failed cytokine independent growth (*in vitro)*	FERM	(33)
TYK2 p.C192Y	T-ALL	n.d.	FERM	(110)
TYK2 p.R243W	T-ALL	n.d.	FERM	(110)

TYK2 p.R274H	T-ALL	n.d.	SH2	(110)
TYK2 p.A375V	T-ALL	n.d.	SH2	(110)
TYK2 p.P494S	T-ALL	n.d.	SH2	(110)
TYK2 p.V678L	T-ALL	n.d.	Pseudokinase (JH2)	(110)
TYK2 p.V731I	T-ALL	cytokine independent growth (*in vitro)*	Pseudokinase (JH2)	(33)
TYK2 p.G761V	T-ALL	increased TYK2 autophosphorylation/ STATs activation	Pseudokinase (JH2)	(53)
TYK2 p.G937A	T-ALL	n.d.	Kinase (JH1)	(110)
TYK2 p.E957D	T-ALL	cytokine independent growth (*in vitro)* / Weak STATs activation	Kinase (JH1)	(33, 53)
TYK2 p.M926V	T-ALL	no STATs activation	Kinase (JH1)	(53)
TYK2 p.Y955H	T-ALL	n.d.	Kinase (JH1)	(110)
TYK2 p.R1027H	T-ALL	cytokine independent growth (*in vitro)* /Weak STATs activation	Kinase (JH1)	(33)

* These alterations are speculated to be gain of function and activating mutations and rearrangements, since no functional analyses are available. +unpublished data (Tavakoli *et al*, 2021, under revision). Abbreviations: n.d.=no data

Targeted therapeutic possibilities for *TYK2*-altered disease

Currently, the lack of knowledge and efficient therapeutics targeting the *TYK2* oncogenic alterations, necessitate broader screening of SMIs. The subsequent JAK/STAT signaling activation due to *TYK2* alterations, provide a rational avenue for the use of JAKi against this HR subtype. Ruxolitinib was the first JAK1/2i approved for treatment of patients with myeloproliferative disorders such as myeloproliferative neoplasms (MPN), polycythemia vera (PV) and essential thrombocythemia (ET), the majority of whom harboured the activating *JAK2* p.V617F mutation (112-115). The significant improvement of symptoms and reduced splenomegaly, in addition to the good tolerability of ruxolitinib treatment (116, 117), accelerated the development and clinical use of JAKi as an anti-cancer drug. The efficacy of some

therapeutics against HR ALL harbouring JAK/STAT activating alterations has been demonstrated in *in vitro* and *in vivo* pre-clinical models and case studies (16, 19, 22, 24, 26-29). The sensitivity of cell lines harbouring *JAK2* fusions (i.e. *PAX5-JAK2* and *ATF7IP-JAK2*) to ruxolitinib *in vitro,* plus its efficacy in reducing leukemic burden in mouse models of *JAK2* rearranged ALL, has also been reported (26). In particular, a strong *in vitro* and *in vivo* anti-leukemic effect for NDI-031301 (TYK2-specific inhibitor) has been reported against TYK2-dependent T-ALL cell lines and primary cells (118). Similarly, our group identified the JAKi, cerdulatinib, as an efficacious therapeutic agent against cells harbouring the *MYB-TYK2* fusion gene, with significantly reduced cell proliferation and decreased tumour burden in mice (108).

The protein-protein interactions and co-operation of TYK2 with HDACs and HSPs to activate JAK/STAT signaling and possible cross talk of JAK/STAT signaling to other pathways due to *TYK2* alterations, provide an alternative kinase independent and even more attractive therapeutic targets (46, 73, 79). Thus far, the sensitivity of the *MYB-TYK2* fusion gene has been established to the HDACi, vorinostat and the HSP90i, tanespimycin *in vitro*; anti-leukemic effects of vorinostat were also demonstrated in pre-clinical *in vivo* models of *MYB-TYK2* altered disease (119). In addition to *TYK2*-altered cases, various SMIs (PI3K/mTORi, MEK1/2i, HSP90i and BETi) have demonstrated promising *in vitro* and *in vivo* efficacy against *CRLF2*-rearranged ALL cases exhibiting JAK/STAT hyperactivation (25, 30, 120-122). The use of HDACi such as vorinostat alone or in combination with a chemotherapy backbone has been approved for treatment of T-cell lymphoma and demonstrated activity against other hematological malignancies such as AML (123, 124). Interestingly, HDACi demonstrated efficacy in clinical trials for *JAK* mutated MPN and PV cases (125-127). Recently, studies have also demonstrated HDACi efficacy in inducing apoptosis in cells and engraftment reduction of leukemic cells in *in vitro* and *in vivo* models of B-ALL (B-ALL cell lines and xenograft models of *KMT2A*-rearranged ALL and *CRLF2*-rearranged ALL), respectively (122, 128, 129).

Taken together, these findings highlight the potential benefit of therapies targeted to specific genomic alterations that may improve the response to treatment and subsequent outcomes in patients. Currently, there is an unmet need to widely investigate the efficacy of SMIs on other HR ALL subtypes including *TYK2* alterations. The data so far, supports the further exploration of the efficacy of TYK2i, HDACi and HSP90i in larger cohort of cases with *TYK2*-altered disease. Furthermore, the efficacy of these SMIs in combination and/or as an addition to the chemotherapeutic backbone regimen requires future investigation. In the era of precision medicine, it is essential to understand the activated pathways of each underlying genomic alteration in individual patients. In addition, it is crucial to identify therapeutics that specifically target activated pathways, such as those in *TYK-2* altered disease. This will be achieved through robust pre-clinical models to test novel therapies and facilitate more genomic alteration-specific clinical trials.

Future prospects

Utilization of NGS technology has led to the identification of a growing number of *TYK2* alterations in ALL cases (10, 33, 53, 111). Given the well-established role of TYK2 in JAK/STAT signaling and its potential kinase-dependent oncogenic consequence, it is essential to inform effective targeted therapeutics for ALL cases harbouring *TYK2* gain of function mutations and/or rearrangements. The prerequisite for identifying effective targeted therapies, however, relies on robust *in vitro* and *in vivo* modelling of each alteration. Aside from the recent study by our group investigating the oncogenic potential of the *MYB*-TYK2 fusion gene in *in vivo* models, the significance of other *TYK2* alterations (e.g. pseudokinase or FERM mutated *TYK2* cases) as a driver oncogene in leukemogenesis is unknown. It is not clear whether all *TYK2* alterations are capable of inducing disease and activating similar pathways downstream of each specific alteration. Thus, future research should focus on the comprehensive characterization of the functional and prognostic consequence of these alterations and TYK2 activation in each setting as well

as to their therapeutic targetability. This approach will consequently elucidate a clear picture of the leukemogenic role, clinical importance and therapeutic targetability of *TYK2* alterations in ALL.

References:

1. Inaba H, Greaves M, Mullighan CG. Acute lymphoblastic leukaemia. *Lancet*. 2013;381(9881):1943-55.

2. Hunger SP, Mullighan CG. Acute Lymphoblastic Leukemia in Children. *N Engl J Med*. 2015;373(16):1541-52.

3. Jabbour EJ, Faderl S, Kantarjian HM. Adult acute lymphoblastic leukemia. *Mayo Clin Proc*. 2005;80(11):1517-27.

4. Pui CH, Robison LL, Look AT. Acute lymphoblastic leukaemia. *Lancet*. 2008;371(9617):1030-43.

5. Terwilliger T, Abdul-Hay M. Acute lymphoblastic leukemia: a comprehensive review and 2017 update. *Blood Cancer J*. 2017;7(6):e577.

6. Aifantis I, Raetz E, Buonamici S. Molecular pathogenesis of T-cell leukaemia and lymphoma. *Nat Rev Immunol*. 2008;8(5):380-90.

7. Ko RH, Ji L, Barnette P, Bostrom B, Hutchinson R, Raetz E, et al. Outcome of patients treated for relapsed or refractory acute lymphoblastic leukemia: a Therapeutic Advances in Childhood Leukemia Consortium study. *J Clin Oncol*. 2010;28(4):648-54.

8. Raetz EA, Bhatla T. Where do we stand in the treatment of relapsed acute lymphoblastic leukemia? *Hematology Am Soc Hematol Educ Program*. 2012;2012:129-36.

9. Larson S, Stock W. Progress in the treatment of adults with acute lymphoblastic leukemia. *Curr Opin Hematol*. 2008;15(4):400-7.

10. Roberts KG, Gu Z, Payne-Turner D, McCastlain K, Harvey RC, Chen IM, et al. High Frequency and Poor Outcome of Philadelphia Chromosome-Like Acute Lymphoblastic Leukemia in Adults. *J Clin Oncol*. 2017;35(4):394-401.

11. Fielding AK, Richards SM, Chopra R, Lazarus HM, Litzow MR, Buck G, et al. Outcome of 609 adults after relapse of acute lymphoblastic leukemia (ALL); an MRC UKALL12/ECOG 2993 study. *Blood*. 2007;109(3):944-50.

12. Daver N, Thomas D, Ravandi F, Cortes J, Garris R, Jabbour E, et al. Final report of a phase II study of imatinib mesylate with hyper-CVAD for the front-line treatment of adult patients with Philadelphia chromosome-positive acute lymphoblastic leukemia. *Haematologica*. 2015;100(5):653-61.

13. Thomas DA, Faderl S, Cortes J, O'Brien S, Giles FJ, Kornblau SM, et al. Treatment of Philadelphia chromosome-positive acute lymphocytic leukemia with hyper-CVAD and imatinib mesylate. *Blood*. 2004;103(12):4396-407.

14. Ottmann OG. Management of Philadelphia chromosome-positive acute lymphoblastic leukemia. *Leuk Suppl*. 2012;1(Suppl 2):S7-9.

15. Yeung DT, Moulton DJ, Heatley SL, Nievergall E, Dang P, Braley J, et al. Relapse of BCR-ABL1-like ALL mediated by the ABL1 kinase domain mutation T315I following initial response to dasatinib treatment. *Leukemia*. 2015;29(1):230-2.

16. Weston BW, Hayden MA, Roberts KG, Bowyer S, Hsu J, Fedoriw G, et al. Tyrosine kinase inhibitor therapy induces remission in a patient with refractory EBF1-PDGFRB-positive acute lymphoblastic leukemia. *J Clin Oncol*. 2013;31(25):e413-6.

17. Kobayashi K, Miyagawa N, Mitsui K, Matsuoka M, Kojima Y, Takahashi H, et al. TKI dasatinib monotherapy for a patient with Ph-like ALL bearing ATF7IP/PDGFRB translocation. *Pediatr Blood Cancer*. 2015;62(6):1058-60.

18. Tasian SK, Hunger SP. Genomic characterization of paediatric acute lymphoblastic leukaemia: an opportunity for precision medicine therapeutics. *Br J Haematol*. 2017;176(6):867-82.

19. Roberts KG, Mullighan CG. Genomics in acute lymphoblastic leukaemia: insights and treatment implications. *Nat Rev Clin Oncol*. 2015;12(6):344-57.

20. Roberts KG, Morin RD, Zhang J, Hirst M, Zhao Y, Su X, et al. Genetic alterations activating kinase and cytokine receptor signaling in high-risk acute lymphoblastic leukemia. *Cancer Cell*. 2012;22(2):153-66.

21. Reshmi SC, Harvey RC, Roberts KG, Stonerock E, Smith A, Jenkins H, et al. Targetable kinase gene fusions in high-risk B-ALL: a study from the Children's Oncology Group. *Blood*. 2017;129(25):3352-61.

22. Roberts KG, Li Y, Payne-Turner D, Harvey RC, Yang YL, Pei D, et al. Targetable kinase-activating lesions in Ph-like acute lymphoblastic leukemia. *N Engl J Med*. 2014;371(11):1005-15.

23. Mullighan CG, Zhang J, Harvey RC, Collins-Underwood JR, Schulman BA, Phillips LA, et al. JAK mutations in high-risk childhood acute lymphoblastic leukemia. *Proc Natl Acad Sci U S A*. 2009;106(23):9414-8.

24. Lengline E, Beldjord K, Dombret H, Soulier J, Boissel N, Clappier E. Successful tyrosine kinase inhibitor therapy in a refractory B-cell precursor acute lymphoblastic leukemia with EBF1-PDGFRB fusion. *Haematologica*. 2013;98(11):e146-8.

25. Maude SL, Tasian SK, Vincent T, Hall JW, Sheen C, Roberts KG, et al. Targeting JAK1/2 and mTOR in murine xenograft models of Ph-like acute lymphoblastic leukemia. *Blood*. 2012;120(17):3510-8.

26. Roberts KG, Yang YL, Payne-Turner D, Lin W, Files JK, Dickerson K, et al. Oncogenic role and therapeutic targeting of ABL-class and JAK-STAT activating kinase alterations in Ph-like ALL. *Blood Adv*. 2017;1(20):1657-71.

27. Iacobucci I, Li Y, Roberts KG, Dobson SM, Kim JC, Payne-Turner D, et al. Truncating Erythropoietin Receptor Rearrangements in Acute Lymphoblastic Leukemia. *Cancer Cell*. 2016;29(2):186-200.

28. Maude SL, Dolai S, Delgado-Martin C, Vincent T, Robbins A, Selvanathan A, et al. Efficacy of JAK/STAT pathway inhibition in murine xenograft models of early T-cell precursor (ETP) acute lymphoblastic leukemia. *Blood*. 2015;125(11):1759-67.

29. Treanor LM, Zhou S, Janke L, Churchman ML, Ma Z, Lu T, et al. Interleukin-7 receptor mutants initiate early T cell precursor leukemia in murine thymocyte progenitors with multipotent potential. *J Exp Med*. 2014;211(4):701-13.

30. Tasian SK, Teachey DT, Li Y, Shen F, Harvey RC, Chen IM, et al. Potent efficacy of combined PI3K/mTOR and JAK or ABL inhibition in murine xenograft models of Ph-like acute lymphoblastic leukemia. *Blood*. 2017;129(2):177-87.

31. Velusamy T, Kiel MJ, Sahasrabuddhe AA, Rolland D, Dixon CA, Bailey NG, et al. A novel recurrent NPM1-TYK2 gene fusion in cutaneous CD30-positive lymphoproliferative disorders. *Blood*. 2014;124(25):3768-71.

32. Crescenzo R, Abate F, Lasorsa E, Tabbo F, Gaudiano M, Chiesa N, et al. Convergent mutations and kinase fusions lead to oncogenic STAT3 activation in anaplastic large cell lymphoma. *Cancer Cell*. 2015;27(4):516-32.

33. Sanda T, Tyner JW, Gutierrez A, Ngo VN, Glover J, Chang BH, et al. TYK2-STAT1-BCL2 pathway dependence in T-cell acute lymphoblastic leukemia. *Cancer Discov*. 2013;3(5):564-77.

34. Tron AE, Keeton EK, Ye M, Casas-Selves M, Chen H, Dillman KS, et al. Next-generation sequencing identifies a novel ELAVL1-TYK2 fusion gene in MOLM-16, an AML cell line highly sensitive to the PIM kinase inhibitor AZD1208. *Leuk Lymphoma*. 2016;57(12):2927-9.

35. Staerk J, Kallin A, Demoulin JB, Vainchenker W, Constantinescu SN. JAK1 and Tyk2 activation by the homologous polycythemia vera JAK2 V617F mutation: cross-talk with IGF1 receptor. *J Biol Chem*. 2005;280(51):41893-9.

36. Vogelstein B, Papadopoulos N, Velculescu VE, Zhou S, Diaz LA, Jr., Kinzler KW. Cancer genome landscapes. *Science*. 2013;339(6127):1546-58.

37. Hanahan D, Weinberg RA. Hallmarks of cancer: the next generation. *Cell*. 2011;144(5):646-74.

38. Liu Y, Easton J, Shao Y, Maciaszek J, Wang Z, Wilkinson MR, et al. The genomic landscape of pediatric and young adult T-lineage acute lymphoblastic leukemia. *Nat Genet*. 2017;49(8):1211-8.

39. Tran TH, Loh ML. Ph-like acute lymphoblastic leukemia. *Hematology Am Soc Hematol Educ Program*. 2016;2016(1):561-6.

40. Ihle JN, Gilliland DG. Jak2: normal function and role in hematopoietic disorders. *Curr Opin Genet Dev*. 2007;17(1):8-14.

41. Ihle JN. Cytokine receptor signalling. *Nature*. 1995;377(6550):591-4.

42. Krolewski JJ, Lee R, Eddy R, Shows TB, Dalla-Favera R. Identification and chromosomal mapping of new human tyrosine kinase genes. *Oncogene*. 1990;5(3):277-82.

43. Velazquez L, Fellous M, Stark GR, Pellegrini S. A protein tyrosine kinase in the interferon alpha/beta signaling pathway. *Cell*. 1992;70(2):313-22.

44. Schindler C, Levy DE, Decker T. JAK-STAT signaling: from interferons to cytokines. *J Biol Chem*. 2007;282(28):20059-63.

45. Hammaren HM, Virtanen AT, Raivola J, Silvennoinen O. The regulation of JAKs in cytokine signaling and its breakdown in disease. *Cytokine*. 2019;118:48-63.

46. Woss K, Simonovic N, Strobl B, Macho-Maschler S, Muller M. TYK2: An Upstream Kinase of STATs in Cancer. *Cancers (Basel)*. 2019;11(11).

47. Ghoreschi K, Laurence A, O'Shea JJ. Janus kinases in immune cell signaling. *Immunol Rev*. 2009;228(1):273-87.

48. Bacon CM, McVicar DW, Ortaldo JR, Rees RC, O'Shea JJ, Johnston JA. Interleukin 12 (IL-12) induces tyrosine phosphorylation of JAK2 and TYK2: differential use of Janus family tyrosine kinases by IL-2 and IL-12. *J Exp Med*. 1995;181(1):399-404.

49. Muller M, Briscoe J, Laxton C, Guschin D, Ziemiecki A, Silvennoinen O, et al. The protein tyrosine kinase JAK1 complements defects in interferon-alpha/beta and -gamma signal transduction. *Nature*. 1993;366(6451):129-35.

50. Leitner NR, Witalisz-Siepracka A, Strobl B, Muller M. Tyrosine kinase 2 - Surveillant of tumours and bona fide oncogene. *Cytokine*. 2017;89:209-18.

51. Shide K, Shimoda K, Kamezaki K, Kakumitsu H, Kumano T, Numata A, et al. Tyk2 mutation homologous to V617F Jak2 is not found in essential thrombocythaemia, although it induces constitutive signaling and growth factor independence. *Leuk Res*. 2007;31(8):1077-84.

52. Bousoik E, Montazeri Aliabadi H. "Do We Know Jack" About JAK? A Closer Look at JAK/STAT Signaling Pathway. *Front Oncol*. 2018;8:287.

53. Waanders E, Scheijen B, Jongmans MC, Venselaar H, van Reijmersdal SV, van Dijk AH, et al. Germline activating TYK2 mutations in pediatric patients with two primary acute lymphoblastic leukemia occurrences. *Leukemia*. 2017;31(4):821-8.

54. Vainchenker W, Constantinescu SN. JAK/STAT signaling in hematological malignancies. *Oncogene*. 2013;32(21):2601-13.

55. Petkau G, Turner M. Signalling circuits that direct early B-cell development. *Biochem J*. 2019;476(5):769-78.

56. Greaves SA, Babolin C, Torres RM, Pelanda R. Ras, Erk, and PI3K signaling pathways in the central selection of B cells. 2017;198(1 Supplement):202.6-.6.

57. Nguyen MH, Ho JM, Beattie BK, Barber DL. TEL-JAK2 mediates constitutive activation of the phosphatidylinositol 3'-kinase/protein kinase B signaling pathway. *J Biol Chem*. 2001;276(35):32704-13.

58. Babon JJ, Lucet IS, Murphy JM, Nicola NA, Varghese LN. The molecular regulation of Janus kinase (JAK) activation. *Biochem J*. 2014;462(1):1-13.

59. Min X, Ungureanu D, Maxwell S, Hammaren H, Thibault S, Hillert EK, et al. Structural and Functional Characterization of the JH2 Pseudokinase Domain of JAK Family Tyrosine Kinase 2 (TYK2). *J Biol Chem*. 2015;290(45):27261-70.

60. Lupardus PJ, Ultsch M, Wallweber H, Bir Kohli P, Johnson AR, Eigenbrot C. Structure of the pseudokinase-kinase domains from protein kinase TYK2 reveals a mechanism for Janus kinase (JAK) autoinhibition. *Proc Natl Acad Sci U S A*. 2014;111(22):8025-30.

61. Babon JJ, Kershaw NJ, Murphy JM, Varghese LN, Laktyushin A, Young SN, et al. Suppression of cytokine signaling by SOCS3: characterization of the mode of inhibition and the basis of its specificity. *Immunity*. 2012;36(2):239-50.

62. Piganis RA, De Weerd NA, Gould JA, Schindler CW, Mansell A, Nicholson SE, et al. Suppressor of cytokine signaling (SOCS) 1 inhibits type I interferon (IFN) signaling via the interferon alpha receptor (IFNAR1)-associated tyrosine kinase Tyk2. *J Biol Chem*. 2011;286(39):33811-8.

63. Bollu LR, Mazumdar A, Savage MI, Brown PH. Molecular Pathways: Targeting Protein Tyrosine Phosphatases in Cancer. *Clin Cancer Res*. 2017;23(9):2136-42.

64. Myers MP, Andersen JN, Cheng A, Tremblay ML, Horvath CM, Parisien JP, et al. TYK2 and JAK2 are substrates of protein-tyrosine phosphatase 1B. *J Biol Chem*. 2001;276(51):47771-4.

65. Bocchini CE, Kasembeli MM, Roh SH, Tweardy DJ. Contribution of chaperones to STAT pathway signaling. *JAKSTAT*. 2014;3(3):e970459.

66. Taipale M, Jarosz DF, Lindquist S. HSP90 at the hub of protein homeostasis: emerging mechanistic insights. *Nat Rev Mol Cell Biol*. 2010;11(7):515-28.

67. Prodromou C. Mechanisms of Hsp90 regulation. *Biochem J*. 2016;473(16):2439-52.

68. Jaeger AM, Whitesell L. HSP90: Enabler of Cancer Adaptation. 2019;3(1):275-97.

69. Trepel J, Mollapour M, Giaccone G, Neckers L. Targeting the dynamic HSP90 complex in cancer. *Nat Rev Cancer*. 2010;10(8):537-49.

70. Weigert O, Lane AA, Bird L, Kopp N, Chapuy B, van Bodegom D, et al. Genetic resistance to JAK2 enzymatic inhibitors is overcome by HSP90 inhibition. *J Exp Med*. 2012;209(2):259-73.

71. Schoof N, von Bonin F, Trumper L, Kube D. HSP90 is essential for Jak-STAT signaling in classical Hodgkin lymphoma cells. *Cell Commun Signal*. 2009;7:17.

72. Kucine N, Marubayashi S, Bhagwat N, Papalexi E, Koppikar P, Sanchez Martin M, et al. Tumor-specific HSP90 inhibition as a therapeutic approach in JAK-mutant acute lymphoblastic leukemias. *Blood*. 2015;126(22):2479-83.

73. Taipale M, Krykbaeva I, Koeva M, Kayatekin C, Westover KD, Karras GI, et al. Quantitative analysis of HSP90-client interactions reveals principles of substrate recognition. *Cell*. 2012;150(5):987-1001.

74. Akahane K, Sanda T, Mansour MR, Radimerski T, DeAngelo DJ, Weinstock DM, et al. HSP90 inhibition leads to degradation of the TYK2 kinase and apoptotic cell death in T-cell acute lymphoblastic leukemia. *Leukemia*. 2016;30(1):219-28.

75. Kramer OH, Mahboobi S, Sellmer A. Drugging the HDAC6-HSP90 interplay in malignant cells. *Trends Pharmacol Sci*. 2014;35(10):501-9.

76. Bali P, Pranpat M, Bradner J, Balasis M, Fiskus W, Guo F, et al. Inhibition of histone deacetylase 6 acetylates and disrupts the chaperone function of heat shock protein 90: a novel basis for antileukemia activity of histone deacetylase inhibitors. *J Biol Chem*. 2005;280(29):26729-34.

77. Nimmanapalli R, Fuino L, Bali P, Gasparetto M, Glozak M, Tao J, et al. Histone deacetylase inhibitor LAQ824 both lowers expression and promotes proteasomal degradation of Bcr-Abl and induces apoptosis of imatinib mesylate-sensitive or -refractory chronic myelogenous leukemia-blast crisis cells. *Cancer Res*. 2003;63(16):5126-35.

78. Bali P, George P, Cohen P, Tao J, Guo F, Sigua C, et al. Superior activity of the combination of histone deacetylase inhibitor LAQ824 and the FLT-3 kinase inhibitor PKC412 against human acute myelogenous leukemia cells with mutant FLT-3. *Clin Cancer Res*. 2004;10(15):4991-7.

79. Nusinzon I, Horvath CM. Unexpected roles for deacetylation in interferon- and cytokine-induced transcription. *J Interferon Cytokine Res*. 2005;25(12):745-8.

80. Buchwald M, Kramer OH, Heinzel T. HDACi--targets beyond chromatin. *Cancer Lett*. 2009;280(2):160-7.

81. Wieczorek M, Ginter T, Brand P, Heinzel T, Kramer OH. Acetylation modulates the STAT signaling code. *Cytokine Growth Factor Rev*. 2012;23(6):293-305.

82. Rascle A, Johnston JA, Amati B. Deacetylase activity is required for recruitment of the basal transcription machinery and transactivation by STAT5. *Mol Cell Biol*. 2003;23(12):4162-73.

83. Nusinzon I, Horvath CM. Interferon-stimulated transcription and innate antiviral immunity require deacetylase activity and histone deacetylase 1. *Proc Natl Acad Sci U S A*. 2003;100(25):14742-7.

84. Chang HM, Paulson M, Holko M, Rice CM, Williams BR, Marie I, et al. Induction of interferon-stimulated gene expression and antiviral responses require protein deacetylase activity. *Proc Natl Acad Sci U S A*. 2004;101(26):9578-83.

85. Sakamoto S, Potla R, Larner AC. Histone deacetylase activity is required to recruit RNA polymerase II to the promoters of selected interferon-stimulated early response genes. *J Biol Chem*. 2004;279(39):40362-7.

86. Klampfer L, Huang J, Swaby LA, Augenlicht L. Requirement of histone deacetylase activity for signaling by STAT1. *J Biol Chem*. 2004;279(29):30358-68.

87. Wang R, Cherukuri P, Luo J. Activation of Stat3 sequence-specific DNA binding and transcription by p300/CREB-binding protein-mediated acetylation. *J Biol Chem*. 2005;280(12):11528-34.

88. Yuan ZL, Guan YJ, Chatterjee D, Chin YE. Stat3 dimerization regulated by reversible acetylation of a single lysine residue. *Science*. 2005;307(5707):269-73.

89. Gupta M, Han JJ, Stenson M, Wellik L, Witzig TE. Regulation of STAT3 by histone deacetylase-3 in diffuse large B-cell lymphoma: implications for therapy. *Leukemia*. 2012;26(6):1356-64.

90. Tambaro FP, Dell'aversana C, Carafa V, Nebbioso A, Radic B, Ferrara F, et al. Histone deacetylase inhibitors: clinical implications for hematological malignancies. *Clin Epigenetics*. 2010;1(1-2):25-44.

91. O'Shea JJ, Holland SM, Staudt LM. JAKs and STATs in immunity, immunodeficiency, and cancer. *N Engl J Med*. 2013;368(2):161-70.

92. Schwartz DM, Kanno Y, Villarino A, Ward M, Gadina M, O'Shea JJ. JAK inhibition as a therapeutic strategy for immune and inflammatory diseases. *Nat Rev Drug Discov*. 2017;17(1):78.

93. Strobl B, Stoiber D, Sexl V, Mueller M. Tyrosine kinase 2 (TYK2) in cytokine signalling and host immunity. *Front Biosci (Landmark Ed)*. 2011;16:3214-32.

94. Minegishi Y, Saito M, Morio T, Watanabe K, Agematsu K, Tsuchiya S, et al. Human tyrosine kinase 2 deficiency reveals its requisite roles in multiple cytokine signals involved in innate and acquired immunity. *Immunity*. 2006;25(5):745-55.

95. Kilic SS, Hacimustafaoglu M, Boisson-Dupuis S, Kreins AY, Grant AV, Abel L, et al. A patient with tyrosine kinase 2 deficiency without hyper-IgE syndrome. *J Pediatr*. 2012;160(6):1055-7.

96. Shimoda K, Kamesaki K, Numata A, Aoki K, Matsuda T, Oritani K, et al. Cutting edge: tyk2 is required for the induction and nuclear translocation of Daxx which regulates IFN-alpha-induced suppression of B lymphocyte formation. *J Immunol*. 2002;169(9):4707-11.

97. Ubel C, Mousset S, Trufa D, Sirbu H, Finotto S. Establishing the role of tyrosine kinase 2 in cancer. *Oncoimmunology*. 2013;2(1):e22840.

98. Gamero AM, Potla R, Wegrzyn J, Szelag M, Edling AE, Shimoda K, et al. Activation of Tyk2 and Stat3 is required for the apoptotic actions of interferon-beta in primary pro-B cells. *J Biol Chem*. 2006;281(24):16238-44.

99. Stoiber D, Kovacic B, Schuster C, Schellack C, Karaghiosoff M, Kreibich R, et al. TYK2 is a key regulator of the surveillance of B lymphoid tumors. *J Clin Invest*. 2004;114(11):1650-8.

100. Prchal-Murphy M, Witalisz-Siepracka A, Bednarik KT, Putz EM, Gotthardt D, Meissl K, et al. In vivo tumor surveillance by NK cells requires TYK2 but not TYK2 kinase activity. *Oncoimmunology*. 2015;4(11):e1047579.

101. Silver DL, Naora H, Liu J, Cheng W, Montell DJ. Activated signal transducer and activator of transcription (STAT) 3: localization in focal adhesions and function in ovarian cancer cell motility. *Cancer Res*. 2004;64(10):3550-8.

102. Ide H, Nakagawa T, Terado Y, Kamiyama Y, Muto S, Horie S. Tyk2 expression and its signaling enhances the invasiveness of prostate cancer cells. *Biochem Biophys Res Commun*. 2008;369(2):292-6.

103. Song XC, Fu G, Yang X, Jiang Z, Wang Y, Zhou GW. Protein expression profiling of breast cancer cells by dissociable antibody microarray (DAMA) staining. *Mol Cell Proteomics*. 2008;7(1):163-9.

104. Santos J, Mesquita D, Barros-Silva JD, Jeronimo C, Henrique R, Morais A, et al. Uncovering potential downstream targets of oncogenic GRPR overexpression in prostate carcinomas harboring ETS rearrangements. *Oncoscience*. 2015;2(5):497-507.

105. Prutsch N, Gurnhofer E, Suske T, Liang HC, Schlederer M, Roos S, et al. Dependency on the TYK2/STAT1/MCL1 axis in anaplastic large cell lymphoma. *Leukemia*. 2019;33(3):696-709.

106. Poitras JL, Dal Cin P, Aster JC, Deangelo DJ, Morton CC. Novel SSBP2-JAK2 fusion gene resulting from a t(5;9)(q14.1;p24.1) in pre-B acute lymphocytic leukemia. *Genes Chromosomes Cancer*. 2008;47(10):884-9.

107. Valentino L, Pierre J. JAK/STAT signal transduction: regulators and implication in hematological malignancies. *Biochem Pharmacol*. 2006;71(6):713-21.

108. Tavakoli Shirazi P EL, Heatley S, Yeung D & White D. The *MYB-TYK2* gene fusion induces B-cell acute lymphoblastic leukaemia in in vitro and in vivo models and can be effectively targeted by the dual SYK/JAK inhibitor, cerdulatinib. . *HemaSphere*. 2020;4:p 136-7.

109. Tomasson MH, Xiang Z, Walgren R, Zhao Y, Kasai Y, Miner T, et al. Somatic mutations and germline sequence variants in the expressed tyrosine kinase genes of patients with de novo acute myeloid leukemia. *Blood*. 2008;111(9):4797-808.

110. Edmonson MN, Patel AN, Hedges DJ, Wang Z, Rampersaud E, Kesserwan CA, et al. Pediatric Cancer Variant Pathogenicity Information Exchange (PeCanPIE): a cloud-based platform for curating and classifying germline variants. *Genome Res*. 2019;29(9):1555-65.

111. Ma X, Liu Y, Liu Y, Alexandrov LB, Edmonson MN, Gawad C, et al. Pan-cancer genome and transcriptome analyses of 1,699 paediatric leukaemias and solid tumours. *Nature*. 2018;555(7696):371-6.

112. Harrison C, Kiladjian JJ, Al-Ali HK, Gisslinger H, Waltzman R, Stalbovskaya V, et al. JAK inhibition with ruxolitinib versus best available therapy for myelofibrosis. *N Engl J Med*. 2012;366(9):787-98.

113. Verstovsek S, Kantarjian H, Mesa RA, Pardanani AD, Cortes-Franco J, Thomas DA, et al. Safety and efficacy of INCB018424, a JAK1 and JAK2 inhibitor, in myelofibrosis. *N Engl J Med*. 2010;363(12):1117-27.

114. Verstovsek S, Mesa RA, Gotlib J, Levy RS, Gupta V, DiPersio JF, et al. A double-blind, placebo-controlled trial of ruxolitinib for myelofibrosis. *N Engl J Med*. 2012;366(9):799-807.

115. Mascarenhas J, Hoffman R. Ruxolitinib: the first FDA approved therapy for the treatment of myelofibrosis. *Clin Cancer Res*. 2012;18(11):3008-14.

116. Verstovsek S, Mesa RA, Gotlib J, Gupta V, DiPersio JF, Catalano JV, et al. Long-term treatment with ruxolitinib for patients with myelofibrosis: 5-year update from the randomized, double-blind, placebo-controlled, phase 3 COMFORT-I trial. *J Hematol Oncol*. 2017;10(1):55.

117. Harrison C, Vannucchi AM. Ruxolitinib: a potent and selective Janus kinase 1 and 2 inhibitor in patients with myelofibrosis. An update for clinicians. *Ther Adv Hematol*. 2012;3(6):341-54.

118. Akahane K, Li Z, Etchin J, Berezovskaya A, Gjini E, Masse CE, et al. Anti-leukaemic activity of the TYK2 selective inhibitor NDI-031301 in T-cell acute lymphoblastic leukaemia. *Br J Haematol*. 2017;177(2):271-82.

119. Tavakoli Shirazi P, Eadie LN, Heatley SL, François M, Hughes TP, Yeung DT, et al. Exploring the oncogenic and therapeutic target potential of the *MYB-TYK2* fusion gene in B-cell acute lymphoblastic leukemia . *Oncogene* 2021;under revision.

120. Suryani S, Bracken LS, Harvey RC, Sia KC, Carol H, Chen IM, et al. Evaluation of the in vitro and in vivo efficacy of the JAK inhibitor AZD1480 against JAK-mutated acute lymphoblastic leukemia. *Mol Cancer Ther*. 2015;14(2):364-74.

121. Ott CJ, Kopp N, Bird L, Paranal RM, Qi J, Bowman T, et al. BET bromodomain inhibition targets both c-Myc and IL7R in high-risk acute lymphoblastic leukemia. *Blood*. 2012;120(14):2843-52.

122. Savino AM, Sarno J, Trentin L, Vieri M, Fazio G, Bardini M, et al. The histone deacetylase inhibitor givinostat (ITF2357) exhibits potent anti-tumor activity against CRLF2-rearranged BCP-ALL. *Leukemia*. 2017.

123. Zhang Q, Wang S, Chen J, Yu Z. Histone Deacetylases (HDACs) Guided Novel Therapies for T-cell lymphomas. *Int J Med Sci*. 2019;16(3):424-42.

124. How J, Minden MD, Brian L, Chen EX, Brandwein J, Schuh AC, et al. A phase I trial of two sequence-specific schedules of decitabine and vorinostat in patients with acute myeloid leukemia. *Leuk Lymphoma*. 2015;56(10):2793-802.

125. Finazzi G, Vannucchi AM, Martinelli V, Ruggeri M, Nobile F, Specchia G, et al. A phase II study of Givinostat in combination with hydroxycarbamide in patients with polycythaemia vera unresponsive to hydroxycarbamide monotherapy. *Br J Haematol*. 2013;161(5):688-94.

126. Rambaldi A, Dellacasa CM, Finazzi G, Carobbio A, Ferrari ML, Guglielmelli P, et al. A pilot study of the Histone-Deacetylase inhibitor Givinostat in patients with JAK2V617F positive chronic myeloproliferative neoplasms. *Br J Haematol*. 2010;150(4):446-55.

127. Mascarenhas J, Lu M, Li T, Petersen B, Hochman T, Najfeld V, et al. A phase I study of panobinostat (LBH589) in patients with primary myelofibrosis (PMF) and post-polycythaemia vera/essential thrombocythaemia myelofibrosis (post-PV/ET MF). *Br J Haematol*. 2013;161(1):68-75.

128. Einsiedel HG, Kawan L, Eckert C, Witt O, Fichtner I, Henze G, et al. Histone deacetylase inhibitors have antitumor activity in two NOD/SCID mouse models of B-cell precursor childhood acute lymphoblastic leukemia. *Leukemia*. 2006;20(8):1435-6.

129. Stubbs MC, Kim W, Bariteau M, Davis T, Vempati S, Minehart J, et al. Selective Inhibition of HDAC1 and HDAC2 as a Potential Therapeutic Option for B-ALL. *Clin Cancer Res*. 2015;21(10):2348-58.